HIGH-PERFORMANCE COTTON HYDROGEL-BASED FLEXIBLE SUPERCAPACITORS CONSISTING OF GRAPHENE

BADAWI NUJUD MOHAMMED M

FACULTY OF SCIENCE
UNIVERSITI MALAYA
KUALA LUMPUR

2023

Universiti Malaya

HIGH-PERFORMANCE COTTON HYDROGEL-BASED FLEXIBLE SUPERCAPACITORS CONSISTING OF GRAPHENE

BADAWI NUJUD MOHAMMED M

THESIS SUBMITTED IN FULFILMENT OF THE REQUIREMENTS FOR THE DEGREE OF DOCTOR OF PHILOSOPHY

DEPARTMENT OF PHYSICS
FACULTY OF SCIENCE
UNIVERSITI MALAYA
KUALA LUMPUR

2023

Universiti Malaya

UNIVERSITI MALAYA
ORIGINAL LITERARY WORK DECLARATION

Name of Candidate: **Badawi Nujud Mohammed M** Matric No: **S2100459/1**

Name of Degree: **DOCTOR OF PHILOSOPHY**

Title of Project Paper/Research Report/Dissertation/Thesis ("this Work"):

High-Performance Cotton Hydrogel-Based Flexible Supercapacitors Consisting of Graphene

Field of Study: **Physics**

I do solemnly and sincerely declare that:

a) I am the sole author/write of this Work;

b) This Work is original;

c) Any use of any work in which copyright exists was done of fair dealing and for permitted purposes and any excerpt and extract from, or reference to or reproduction of any copyright work has been disclosed expressly and sufficiently and the title of the Work and its authorship have been acknowledged in this Work;

d) I do not have any actual knowledge nor I ought reasonably to know that the making of this work constitutes an infringement of any copyright work;

e) I hereby assign all and every rights in the copyright to this Work to the Universiti Malaya ("UM"), who henceforth shall be owner of the copyright in this Work and that any reproduction or use in any form or by any means whatsoever is prohibited without the written consent of UM having been first had and obtained.

f) I am fully aware that if in the course of making this Work, I have infringed any copyright whether intentionally or otherwise, I may be subjected to legal action or any other action as may be determined by UM.

Candidate's Signature Date: **30 July 2023**

Subscribed and solemnly declared before,

Witness's Signature Date: **30 July 2023**

Universiti Malaya

HIGH-PERFORMANCE COTTON HYDROGEL-BASED FLEXIBLE SUPERCAPACITORS CONSISTING OF GRAPHENE.

ABSTRACT

The effectiveness of the electrochemical process for supercapacitors has been enhanced by conductive cotton hydrogel with the incorporation of graphene and other ionic contents. The inherently soft nature of cotton mixed with hydrogel provides superior flexibility of the electrolyte, whichbenefits the devices in gaining high flexibility. Herein, it is reported the current research progress in the field of solid-state hydrogel electrolytes based on 3D pure cotton/graphene and present an overview of the future direction of the research. The ionic conductivity of CGH2 complex hydrogel significantly increased up to 13.9 x 10^{-3} S/cm at 25 °C due to the presence of graphene which provides a smooth path for the transport of charge carriers and polymer. Furthermore, electrochemical studies were performed by sandwiching the composite hydrogel electrolytes between symmetric cotton-coated graphene electrodes. The electrical conductivity of cotton with different concentrations of graphene was studied. Four-probe method was employedto examine the electrical characteristics of treated cotton electrodes, the graphene coated cotton samples with 17^{th} layers resulted in a surface resistance of 0.644 Ω/sq and retained their maximum resistance even after two months. Thermogravimetric analysis (TGA) and differential scanning calorimetry (DSC) analysis are crucial tools for examining the samples' thermal stability and material degradation pattern. TGA was used to evaluate the thermal stability of the pure cotton sample and the cotton that had been treated with graphene, and the mechanical properties of the composite cotton sample were evaluated by tensile strength test. The fabricated cotton-graphene electrode/ composite hydrogel electrolyte cotton- graphene electrode based symmetric supercapacitor attained the highest specific capacitance of 327 F/g at 3 mVs^{-1} which was measured by cyclic voltammetry measurement and from galvanostatic charge-dischargemeasurement, it is

Universiti Malaya

obtained a maximum value of 385.4 F/g at 100 mAg^{-1} current density. The instruments, namely X-ray diffractometer (XRD), Fourier-transform infrared (FTIR) spectroscopy, Raman spectroscopy, Field emission scanning electron microscope (FESEM) have been employed to study the properties of the electrodes and electrolyte, which showed good dispersion of electrode and hydrogel electrolytes samples obtained by dimethyl sulfoxide (DMSO) doping, which reduced the rippleof the cotton. The effectiveness of symmetric supercapacitors fabricated using composite hydrogel electrolytes has been confirmed by powering upa light- emitting diode (LED). Furthermore, the electrochemical analysis demonstrated that cotton- graphene-based hydrogel electrolyte is electrically stable and could beused for the design of next-generation supercapacitors.

Keywords: Supercapacitor; Graphene; resistance; conductive cotton; pure cotton; Hydrogels.

Universiti Malaya

SUPERKAPASITOR FLEKSIBEL YANG BERASASKAN HIDROGEL KAPAS BERPRESTATI TINGGIYANG TERDIRI DARIPADA GRAFIN

ABSTRAK

Keberkesanan proses elektokimia bagi superkapasitor telah dipertingkatkan oleh penggunaan hidrogel kapas yang bersifat konduktif dengan penggabungan grafin dan ion-ion yang lain. Sifat semulajadi kapas yang lembut dan dicampurkan pula dengan hidrogel dapat menyediakan elektrolit yang sangat fleksible dan memberi manfaat kepada fleksibiliti yang tinggi sebuah peranti. Di sini, karya ini melaporkan kemajuan penyelidikan semasa bagi elektrolit hidrogel keadaan pepejal berasaskan 3D kapas tulen/grafin dan membentangkan gambaran keseluruhan hala tuju masa depan penyelidikan ini. Kekonduksian ionik bagi CGH2 hidrogel kompleks telah meningkat dengan ketara sehingga 13.9 x 10^{-3} S /cm pada 25 °C, disebabkan oleh kehadiran graphene yang menyediakan laluan lancar untuk pengangkutan pembawa cas dan polimer. Tambahan lagi, kajian elektrokimia telah dilakukan dengan meletakkan hidrogel komposit di antara elektrod simetri yang berasaskan grafin bersalut kapas. Kajian mengenai kekonduksian elektrikal bagi kapas dengan berlainan kepekatan grafin telah di kaji. Kaedah “four-probe” telah digunakan untuk mengkaji ciri-ciri elektrik elektrod kapas yang dirawat, sampel kapas yang bersalut dengan grafin dengan kepekatan 168.36 % pada lapisan ketujuh belas telah menghasilkan rintangan permukaan 0.6444 Ω/sq dan mengekalkan rintangan maksimumnya walaupun setelah dua bulan. Analisis termogravimetri (TGA) dan DSC adalah kaedah yang penting untuk mengkaji kestabilan takat haba sampel dan juga corak degradasi bahan. Analisa termogravimetri TGA telah digunakan untuk menilai kestabilan haba sampel kapas tulen yang telah dirawat dengan grafin, dan ciri-ciri mekanikal sampel kapas telah dinilai dengan ujian kekuatan tegangan. Superkapasitor simetri yang berasaskan kapas- grafin/ elektrolit hidrogel komposit/ kapas- grafin elektrod mencapai kapasiti khusus yang tinggi iaitu 327 F/g pada 3 mVs^{-1}

Universiti Malaya

dalam teknik kitaran voltammetri dan teknik pelepasan caj galvanostatik menghasilkan nilai tinggi sebanyak 385.4 F/g pada ketumpatan semasa 100 mAg^{-1}. Peralatan seperti pembelauan sinar-X (XRD), transformasi empatier inframerah (FTIR), spektroskopi Raman dan mikroskop elektron pengimbasan emisi lapangan (FESEM) telah digunakan untuk mengkaji ciri-ciri elektrod dan elekrolit, yang memaparkan penyebaran yang baik oleh elektrod dan hidrogel elektrolit sampel diperoleh daripada doping dimethyl sulfoxide (DMSO), yang mengurangkan riak kapas. Ciri-ciri elektrolit hidrogel komposit bagi superkapasitor simetri telah disahkan dengan menghidupkan diod pemancar cahaya (LED). Tambahan pula, analisis elektrokimia menunjukkan bahawa elektrolit hidrogel berasaskan kapas-grafin adalah stabil secara elektrik dan boleh digunakan untuk reka bentuk generasi akan datang superkapasitor.

Kata kunci: Kapas; Kekonduksian; Superkapasitor; Grafin

Universiti Malaya

ACKNOWLEDGEMENTS

I would like to thank God for what he has given me of his bounty and his great knowledge and helped me in accomplishing this work.

I am grateful to all of those I have had the pleasure to work during my PhD research. Each of the members of my Dissertation Committee has provided me with extensive personal and professional guidance and taught me a great deal about scientific research.

First and foremost, I would like to express my utmost gratitude to my supervisors, Professor Dr. Ramesh T Subramaniam, Associate Professor Dr. Ramesh Kasi and Dr. Mrutunjaya Bhuyan from the Universiti Malaya, for offering me the opportunity to do my PhD study under their supervision. I would also like to thank them for their encouragement, assistance, and support in completing my study. Secondly, I would like to express my great gratitude to Professor Dr. Khalid Mujasam Batoo, Director of the Research Center at King Saud University, for his help, guidance, and patience and for providing knowledge to my research.

Besides, I would also like to thank The Saudi Cultural Attaché in Malaysia and the University of Hafr Al-Batin for providing the excellent lab environment and their financial support, and all other supports throughout my study. Last but not least, I would also like to give special thanks to my family as a whole for their continuous support and understanding in developing this research.

Universiti Malaya

TABLE OF CONTENTS

Universiti Malaya

Universiti Malaya

Universiti Malaya

Universiti Malaya

LIST OF FIGURES

Universiti Malaya

Universiti Malaya

University Malaya

LIST OF TABLES

Universiti Malaya

LIST OF SYMBOLS

T	:	Temperature	K
ρ(0)	:	Resistivity at temperature 0 K	Ω.cm
ρ(T)	:	Resistivity at temperature T (K)	Ω.cm
σ		Conductivity	S/cm
α		Thermal coefficient	0C\1
σ(t)	:	Conductivity at T (K)	S/cm
σ(0)		Conductivity at 0 K	S/cm
n	:	Number of electrons per unit volume	e/cm^3
e	:	Charge of an electron	C
γ	:	Dimensionality factor	dimensionless
KB	:	Boltzmann's Constant	m^2kg^2/s^2 K γ
ΔE	:	Change in energy	m
h	:	Planck's constant	J.s
I_{Max}	:	Maximum current	A
R(T)	:	Resistance at T (K)	Ω
R0	:	Resistance at infinite temperature	Ω

Universiti Malaya

T0	:	Energy barrier between localized states	K
N(EF)	:	Density of state at the Fermi level	$m^3\backslash 1$
TCR	:	Temperature coefficient of resistance	K/1
LII	:	Localization length in parallel direction	m
L⊥	:	Localization length in perpendicular direction	m
R	:	Resistance	Ω
t	:	Thickness	m
X	:	Reactance	Ω
F	:	Capacitance	farad
l	:	Length	m
e	:	Specific energy	J/kg
Rs	:	Sheet resistance	Ω /□
A	:	Area	m^2
W	:	Unit of power (watt)	$kg{\cdot}m^2{\cdot}s^{-3}$
PWR	:	Power-to-weight ratio	kW/kg
EDLCs	:	Electric Double-layer Capacitors	
AFC	:	Carbon fibre-cloth	

Universiti Malaya

CHAPTER 1: INTRODUCTION

1.1 Introduction

In recent years, smart wearable electronic textiles have become very popular as they make life safer, easier, healthier, and comfortable. Wearable technology deals with electronic devices that can be implanted in the body, worn as accessories, or incorporated into clothing. Smart textiles can sense and react according to the environment and stimuli. As textiles, they can sense and interact with the human body according to the changes in the environment and external stimuli (Yetisen A K et al., 2016). Due to the wireless revolution, smart wearable electronic fiber has seen significant advancements through wearable electronics innovation. The wearable textile can interact with the human body and monitor physiological information such as temperature, heart rate, activity monitoring, etc. Smart textiles along with solar cells, storage devices, sensors and actuators of various types (electronic, magnetic or mechanical) are part of this trend. Currently, electronic fabric is being integrated intowearable devices.

These electronic textiles act as electrodes (they record direct readings in electrocardiograms (ECG or EMG machines), in sensors and power sources, or as power and data cables. On the other hand, these components can be integrated into different types of wearable medical devices and used in healthcare applications (WangW et al., 2023). These devices can be inbuilt and embedded into the fabric or maybe attached externally which means that this intelligent tissue can be affected by externalfactors such as temperature and humidity, and if it merges with the skin, it may transmitvital information to the human body. Contemporary scientific research in textiles prefers to introduce different functionalities into the fabric material. However, for sensing, interactions and actions, these devices rely on electrical or electronic signals whereby, the precise electrical paths and signals are provided via an electrical circuit created on a fabric or a

Universiti Malaya

highly conductive filament.

Conductive textile materials can be used in many smart textile applications such as electrostatic discharge clothing, communications, heating textiles, and sensors. Conductive textiles that change their electrical and mechanical properties as a result of a physical variable, can be considered as sensors (Wang W et al., 2023). These fabric sensors can be designed to measure temperature, bio-voltage, radiation (infrared spectroscopy), sound (heart, lungs), ultrasound, biological, pressure (blood), chemical, movement (breathing), sweat and dour. Since traditional conductive materials have poor elasticity, conductive cotton is used in many applications of wearable, digital, and implantable electronic information in clothing along with several other applications.

Smart fabrics and wearable electronics have been developed to replace portable electronics. Where the tissue structure is 'intelligent', it can sense and respond to stimuli from the environment. The response of smart textiles is induced by chemical, thermal, magnetic, and electrical materials. "Textile electronics" is called smart textiles that combine electronics and textile structures. The production of electronic wearable cotton textiles using lightweight, flexible, cheap, and safe components, and high electrical conductivity fiber capable of withstanding the stresses associated withwearing and caring for the textiles is one of the major challenges. The main obstacle to metallic conductors is the lack of flexibility and excessive weight that must be overcome in the field of carbon-based electronic textiles. One of the disadvantages ofusing conventional metal conductors is that rigid and inelastic tissues cannot performtheir function when exposed to different environmental conditions or when subjectedto washing processes. Therefore, there is an urgent need to develop flexible and deformable conductive fabric and smart rubber that capture and transmit information and enable computing and assimilation of human body

Universiti Malaya

movement. In recent decades, multiple research methods have been pursued to meet this challenge using carbon materials and seersucker structures, as well as innovations in the field of particulate materials and fibers (Wang W et al., 2023).

In order to meet the trend of wearable electronics, and implantable electronic devices, flexible conductive materials are widely accepted. It also has broad application prospects in wearable devices, healthcare monitoring, and human- machine interface. The hierarchical nature of the various types of cotton textiles (such as fibers, knitted fabrics, threads etc.) makes them suitable for the manufacture of high-conductive and wearable smart cotton fabrics. To obtain high conductivity, some techniques depend on the use of a thick coating of metal or conductive ink. Theuse of conductive ink or metals makes the fabric uncomfortable and hard (Le T S Det al., 2019). On the other hand, the tissue achieves its porosity through these suggestive processes, making the fabric comfortable, having good thermal conductivity, fluid transferability and moisture absorption etc. The porosity of the fabric depends on the nature, quality and density of the threads (Yetisen A K et al., 2016). Some researchers have reported using various natural materials, such as cotton, to produce multifunctional devices, such as supercapacitors and stress sensors. Standard coating techniques such as dip coating, spray coating, electrophoretic deposition or the carbonization process can be adopted. However, the fabrication of highly conductive natural materials through an efficient strategy and its application in wearable electronics remains a challenge (Kursun Bahadir S et al., 2020).

Universiti Malaya

1.2 Electronic textiles

Smart electronic textiles, including conductive textiles, have gained great interest due to their broad applications in biomedical devices, sensing and actuation, data processing and communications, energy conversion and storage such as batteries, supercapacitors, and electromagnetic shielding. One of the most important features apart from ease of use of smart and wearable electronic textiles is electrical conductivity, lightweight, and high flexibility (Yetisen A K et al., 2016). 95% of cotton fiber consists of cellulose I (β-1,4-D-anhydroglycopyranose), which is the primary cell wall. The unique properties of cellulose fibers make them ideal for use in smart textiles due to their high absorption, low price, and low impurity content, aswell as their good mechanical properties. In the design of smart active materials that conduct electric current, cellulose fibers provide an ideal matrix (Wang W et al., 2023). Textiles are coated and printed to obtain a functional surface with different properties using different allotropes of carbon such as graphene (Le T S D et al., 2019), carbon black, carbon nanotubes (Kursun Bahadir S et al., 2020), and others to enhance textile conductivity, of which electrical conductivity is of great importance for smart textile application. Among the various textile materials, cotton is one of the most widely used materials for textiles and clothing. Cotton has unique elasticity andhigh breathability (Kursun Bahadir S et al., 2020). Cotton is a comfortable fabric andis more breathable when abraded compared to other fabrics. It has a chemical structure that consists of active hydroxyl groups, which makes cotton easy to adjust and hence, improves the adhesion and distribution of active substances on the fabric (Ho D H et al., 2019; Köhler A R ,2013).

On the other hand, graphene can meet most of the requirements for use inconductive fillers, ink, and coatings (Shaw R K et al., 2007) due to its high mobility (Htwe Y Z N and Mariatti M, 2022), mechanical durability (Siddiqua U H et al., 2017), and

Universiti Malaya

environmental stability. In addition to the possibility of production at a low cost, the oxygen-containing groups enhance the action of the treated tissues of both graphene and cotton to form hydrogen bonds with each other thus enhancing the adhesion. Some methods for manufacturing conductive fabrics have been reported, including layer-by-layer as well as a dip drying method (Su M et al., 2020). These arethe most frequently used processes in which graphene is absorbed on the surface of tissues by the action of capillaries, forming hydrogen bonds with the cloth (Zhu Y et al., 2010; Liu Y et al., 2018).

Increasing the layers/coatings of graphene on fabric leads to an increase in conduction or equivalently reduction in resistivity or resistance. Several researchers have contributed to this interesting and flourishing field of conducting fibers in recenttimes (Jee C E, Chow M K and Yeap S P, 2023), coated cotton fabric with graphene oxide (GO), which was then converted to graphene using a reducing agent $Na_2S_2O_4$. Itwas found that as the number of coatings of graphene was increased to up to 20, the surface resistance decreased by almost three orders of magnitude from 201.1 to 0.374kΩ cm^{-1}. When they used $C_6H_8O_6$ as a reducing agent, the results obtained were similar. The surface resistance was found to be reduced to 0.84 from 400.2 kΩ/sq as the number of coatings was increased to 20.

Xu J et al., 2021 prepared few-layer graphene (FLG) coated cotton cloth and measured its conductivity. It was observed that electrical conductivity increased (or surface resistivity decreased) from 1500 S m^{-1} to 7000 S m^{-1} when the amount of FLGwas changed from 3 wt.% to 6 wt.% in the composite.

Modified cotton fabrics were prepared by (Sivaranjana P et al., 2021) through xerogel

Universiti Malaya

coatings of Graphene or reduced graphene oxide (rGO). The graphene coating of 1.5 wt.% was found to result in the lowest surface and volume resistance of about 3.0×10^5 Ω and 1.7×10^4 Ω respectively.

Gouda M, 2012 used the interfacial trapping method to fuse fabric with FLG/graphite (though cotton was not used by them). The sheet resistance measured was the lowest at FLG loading of 10.7 wt.%, while at 2.5 wt.% it was four orders of magnitude higher.

The brush-coating-drying method was used by (Akram S, Javid A and Ashraf M, 2023) to prepare conductive textiles from cotton using graphite and solvents DMSO and dimethylformamide (DMF). The lowest value of sheet resistance obtainedby them was 0.47 k Ω /sq.

1.2.1 Cellulose

Cellulose is the most abundant renewable polymer resource available on the earth.For example, cotton (1011-1012 type) is made in a fairly pure form by using the process of photosynthesis while on the other hand, cellulose is combined with lignin and other sugars (hemicelluloses) in the cell wall of woody plants (Crawford R L et al., 1981). Wood is the most material source of cellulose, though besides cellulose, it also contains hemicellulose, lignin, and similar small amounts of extracts (Cellulose, Hemicellulose, Lignin and Extract) (Kulkarni P et al., 2022). Materials containing cellulose include agricultural residues, water, plants, herbs and other plant materials. It is noteworthy that commercial cellulose production focuses on very pure sources such as cotton or harvested sources such as wood.

Cellulose are polysaccharide polymers. The main industrial source of cellulose is vascular plants. Cotton is a source of textile manufacturing. Most paper products come

Universiti Malaya

from wood pulp, while textile fibers are generally not isolated from wood fibers. Cotton fibers are biological source of nearly pure cellulose, but are not used in food cellulose, however, they are being used for various cellulose derivatives, chemicals, pharmaceuticals, or in engineering usages, such as chromatography, explosives and paints. Some other sources of cellulose are hemp, jute, corn, rice, flasks, straw and wheat (Marchessault R H et al., 1987).

In a polysaccharide cellulose carbohydrate polymers consist of tens to hundreds to several thousand monosaccharide units (glucose) (Klemm D et al., 2005). Celluloseis a very important material. from which plants are made, and plants are the raw material often referred to as the first link in what is known as the food chain of all living organisms Besides, it is also the most abundant naturally occurring biopolymer (Peng H et al., 2020; Bochek A M et al., 2003). In various fibers such as cotton and plants, cellulose is the main component (Hattori K et al., 2002; Farrell R E et al., 2009). It consists of long chains of anhydro-D-glucopyranose units (AGU), with each cellulose molecule having three hydroxyl groups per AGU (except for the terminal ends) as shown in Figure 1.1.

Cellulose has various applications and uses in its different forms; which include wood for construction. paper products, pure cotton, linen and rayon for clothing, nitrocellulose for explosives, cellulose acetate for films etc. Cellulose is an excipientand since plant polysaccharides meet many expected requirements; pharmaceutical excipients have the advantages such as non-toxicity, stability, availability and regeneration on a large scale (Weiner M L et al., 2019). Cotton cellulose has a higher degree of polymerization and crystallinity. Crystallinity indicates that the fiber molecules are closely packed and parallel to one another.

Universiti Malaya

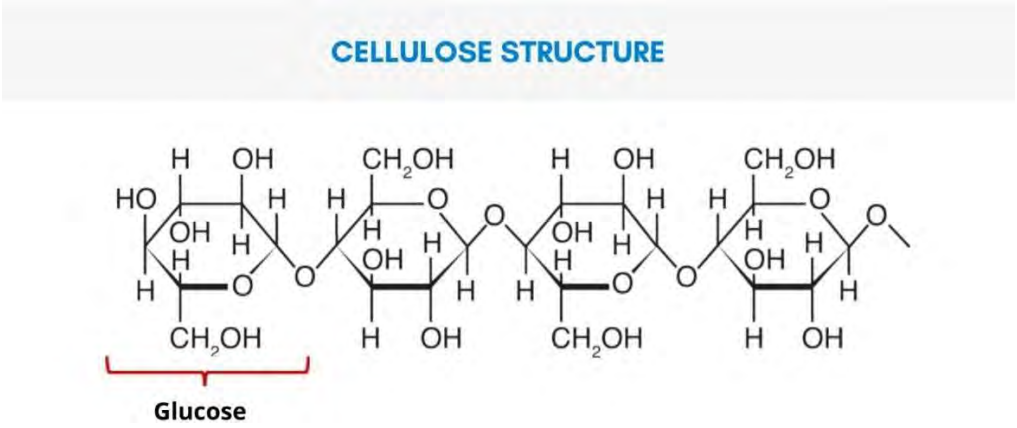

Figure 1.1: Chemical structure of cellulose.

On the other hand, cellulose is insoluble in water and the most common solvent (Bochek A M et al., 2003) due to the presence of strong intramolecular and intramolecular hydrogen bonds between individual chains (Peng H et al., 2020). Despite its poor solubility properties, cellulose is still used in a wide range of applications such as in composites, netting, upholstery, coatings, packaging, paper,etc. (WEINER M L et al., 2019). where a chemical modification of cellulose is done to improve the ability of the process and produce cellulose derivatives (cellulose) that can be manufactured on demand as per industrial applications (Argyropoulos D S et al., 2001). In general, cellulose is robust, repeatable and recyclable as well as biocompatible (Heinze Tet al., 2010).

Various sources of cellulose occur in natural and synthetic forms. Natural fibers are made from plant, animal and mineral sources. For example, natural fibers are classified according to their origin. vegetable fibers consist mainly of cellulose: such as cotton, flax and hemp (Shah J and Brown R M, 2005). As mentioned before, cellulose fibers are used in the manufacture of paper and cloth. These fibers are a subset of synthetic fibers, which are regenerated from natural cellulose (Balter M et al., 2009). Cellulosecomes from multiple sources like beech trees. Also, the bamboo fiber is cellulose fibermade from

Universiti Malaya

bamboo, sea cells are made from seaweed, and cane fiber is cellulose fibermade from sugar cane (Kvavadze E et al., 2009) (Figure 1.2).

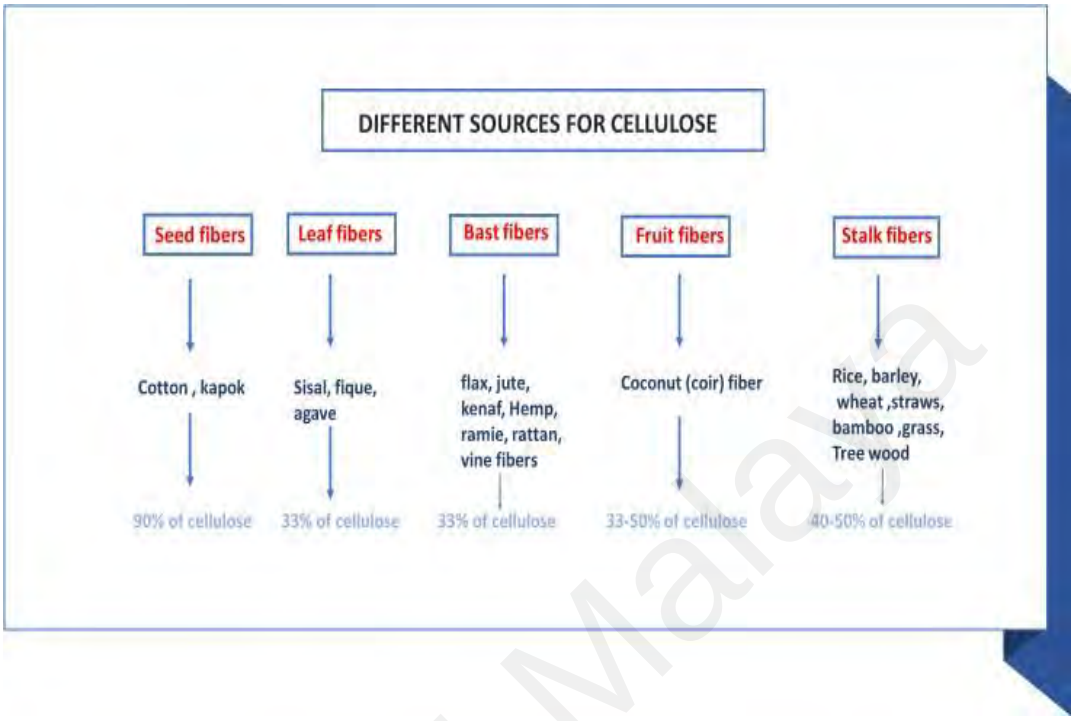

Figure 1.2 : Sources for cellulose.

1.2.2 Polymers

Polymers are macromolecules resulting from the chemical bonding of large numbers of smaller molecules or repeating units called monomers (Hao G P et al.,2014). The number of monomers within a polymer molecule often varies greatly, ascan the degree to which regularities appear in the order, relative orientation, and presence of monomers within the same polymer molecule (Shirakawa H et al., 1977). In order to adapt the properties of the material in synthetic and some natural polymers, the number of monomers can be precisely determined (Hao G P et al., 2014) (Figure 1.3).

Organic polymers play an important and essential role in living organisms in termsof providing essential structural materials and participating in vital life processes e.g.the hard parts of different plants are made of polymers. These materials are composedof

Universiti Malaya

cellulose, lignin and various resins. Cellulose is a polysaccharide polymer that includes sugar molecules. The lignin consists of a complex three-dimensional networkof polymers. Wood resins are polymers of a simple hydrocarbon, isoprene. Another familiar isoprene polymer is rubber (Hao G P et al., 2014).

Other natural polymers consist of proteins, such as polymers of amino acids, and nucleic acids, which are polymers of nucleotides and are composed of complex molecules of nitrogen-containing bases, sugars and phosphoric acid (Nakao Y et al., 1992). These nucleic acids carry genetic information in the cell. Starches are also an important source of dietary energy derived from plants, and they are natural glucose- containing polymers (Shirakawa H et al., 1977) (Figure 1.4).

Synthetic polymers are produced in different types of reactions (Review T and Mishra A K, 2018 ; Wichterle O and Lím D, 1960). By adding monomers one byone to the growing chain, Polyethylene can be composed by repeating ethylene monomers (Silva A K A et al., 2009; Ullah F et al., 2015). Many simple hydrocarbons,such as ethylene and propylene, can be converted into polymers, the process being a polymerization (Ward M A and Georgiou T K, 2011), which may contain up to 10,000 monomers connected in long coiled chains (Tanaka T et al., 1982). Polyethylene is amorphous and is, considered transparent. It is thermoplastic that is used for coatings, packaging, molded parts, and the manufacture of bottles and containers. Polypropylene is a crystalline and thermoplastic material, but it is harder than polyethylene. Its molecules may consist of 50,000 to 200,000 monomers (Abhishek Kumar Mishra,2018). They are used in the textile industry and to make molded objects. The chemical structure of polymers is depicted in (Figure 1.3) and (Figure 1.4) also gives brief details about some other polymers.

Universiti Malaya

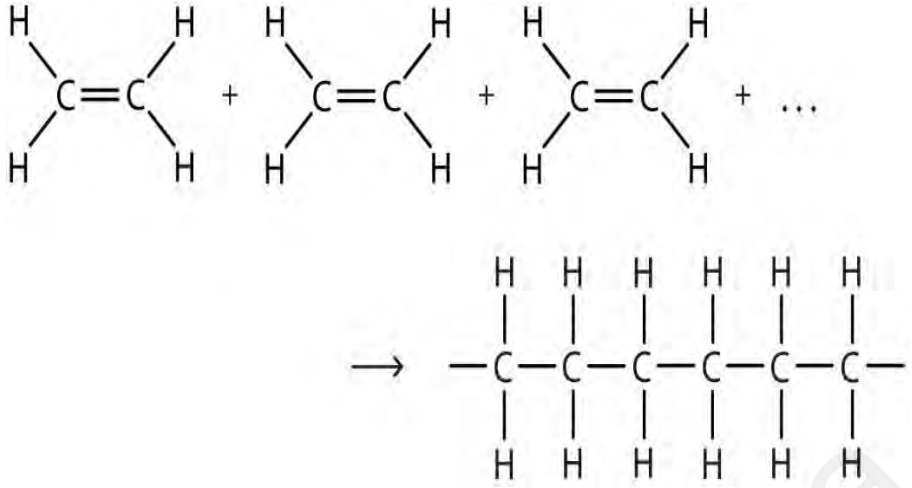

Figure 1.3 : Polymers chemical structure.

Example	Monomer	Polymer	Uses
Polyethylene	$CH_2{=}CH_2$	$-CH_2-CH_2-$	Most common polymer,bags, wire insulation,squeeze bottles
Polypropylene	$CH_2{=}CH(CH_3)$	$-CH_2-CH(CH_3)-$	Fibers, bottles, indoor-outdoor carpet
Polystyrene	$CH_2{=}CH(C_6H_5)$	$-CH_2-CH(C_6H_5)-$	Styrofoam, inexpensive molded objects: household items, toys
Polyvinyl chloride (PVC)	$CH_2{=}CH(Cl)$	$-CH_2-CH(Cl)-$	Synthetic leather, clear bottles, floor coverings, water pipe
Teflon	$CF_2{=}CF_2$	$-CF_2-CF_2-$	Non-stick surfaces, chemically resistant items
Polyacrylonitrile (Orlon, Acrilan)	$CH_2{=}CH(C{\equiv}N)$	$-CH_2-CH(C{\equiv}N)-$	Fiber used in sweaters, blankets, carpets

Figure 1.4 : Example of monomers and their addition polymers.

1.2.3 Hydrogel

The hydrogel is a three-dimensional network consisting of hydrophilic polymersthat can swell in water and retain a large amount of water while maintaining the structure due to the chemical or physical bonding of individual polymer chains. Classification of hydrogels depends on the respective polymers involved, the source of the polymers, the method of crosslinking, their response to stimuli, and their ionic charge etc. The polymers in hydrogels are natural, synthetic, or a mixture of natural and synthetic polymers. These

Universiti Malaya

polymers can form hydrogels such as homopolymer hydrogels, copolymer gels, block copolymer hydrogels, and terpene polymers (Wichterle O and Lím D, 1960). On the other hand, hydrogels can be prepared by crosslinking polymers; where crosslinking can be physical or chemical or both. Apartfrom this, hydrogels can be classified based on the ionic charge as cationic, anionic, and neutral hydrogels. The charges on the overall lattice depend on the polymer charge. Hydrogels were first discovered by (Wichterle O and Lím, 1960). For a hydrogel, water must make up at least 10% of the total weight (or volume) of a substance. This is the reason that hydrogels also have a degree of elasticity very similar to natural tissues due to their high water content. The hydrophilicity of the network is due to the presence of hydrophilic groups such as-OH, -NH_2, -COOH, CONH- $CONH_2$ and -SO3H (Ullah F et al., 2015).

Hydrogels undergo a bulk phase transition or gel-sol phase transition in responseto certain physical and chemical stimuli. Physical stimuli are temperature, light intensity, electric and magnetic fields, pressure, and solvent composition; while chemical or biochemical stimuli include ions, pH, and specific chemical structures. However, these conformational transformations can be reversed in most cases; Therefore, hydrogels are able to return to their initial and lip state after the reaction once the trigger is removed. The response of hydrogels to external stimuli is mainly determined by the nature of the monomer, charge density, suspended chains, and the degree of cross-linking. The magnitude of the response is also directly proportional to the applied external stimulus (Ward M A and Georgiou T K, 2011) (Figure 1.5).

Smart hydrogels are the subject of significant scientific research iridous fields including biomedicine and pharmacology, biotechnology, and separation science (Ward M A and Georgiou T K, 2011). There are four classes of hydrogels mostcommonly used

Universiti Malaya

which are pH-sensitive hydrogels (Tanaka T et al., 1982).

Temperature-sensitive hydrogels; Electro-sensitive hydrogels and Light-responsive hydrogels (Murdan S, 2003).

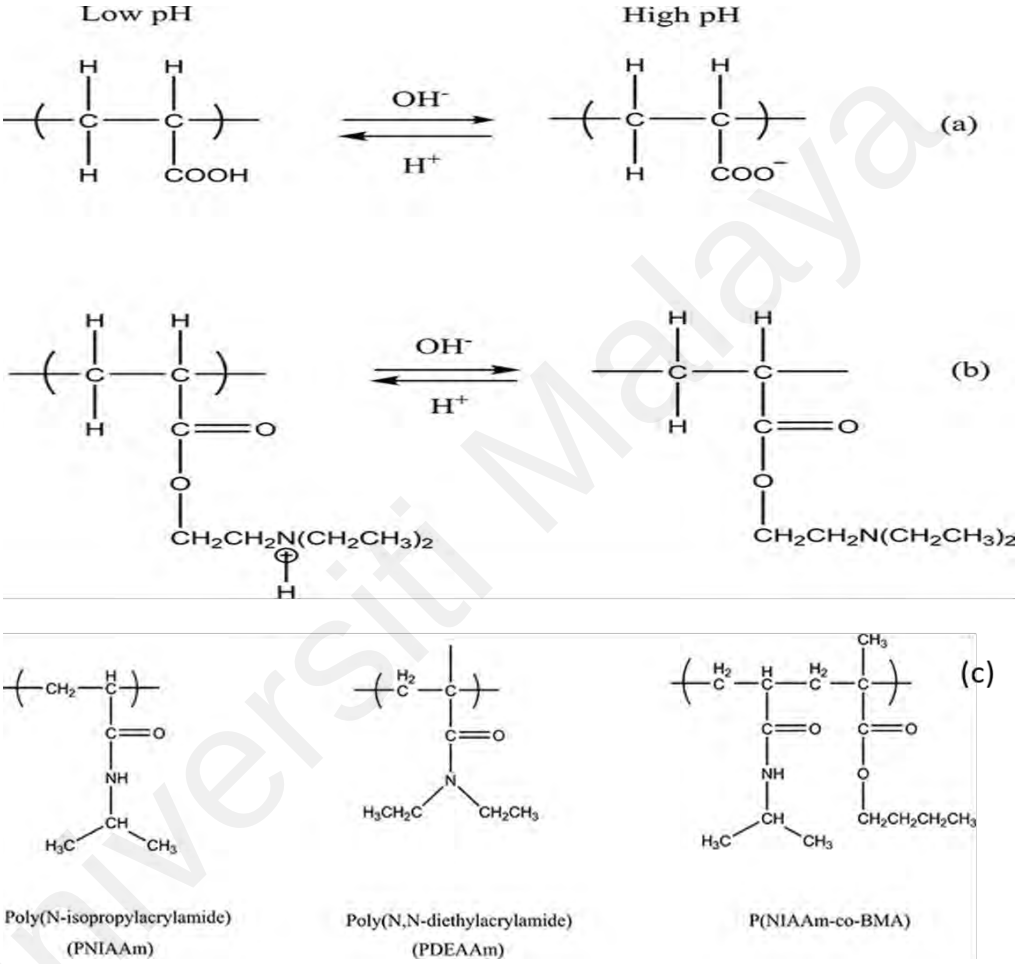

Figure 1.5 : pH-dependent ionization of polyelectrolytes. (a) poly(acrylic acid) and (b) poly(N,N'-diethylaminoethyl methacrylate) and (c) structures of some temperature-sensitive polymers.

Hydrogels are used in many fields due to their specific structures and compatibilitywith different conditions of use. Due to their higher water content, the enhancement inthe flexibility of hydrogels makes them suitable for many applications including industrial to

Universiti Malaya

biological (Fitzgerald M M et al., 2015). Due to their non-toxic nature inbiological environments, they are highly applicable in in medical sciences (FitzgeraldM M et al., 2015).

Figure 1.6 shows the main applications of hydrogel such as drug delivery (Fitzgerald M M et al., 2015); pH-sensitive hydrogels in drug delivery system(DDS) (Lee K Y and Mooney D J, 2001); temperature-sensitive hydrogels in DDS; dyes and heavy metal ions removal; scaffolds in tissue engineering (Zhao Yet al., 2013); contact lenses; pH-sensors; biosensors ; injectable hydrogel for spinal cord regeneration (Shi Y et al., 2014) and hydrogel electrolytes for supercapacitor (Hao G P et al., 2014).

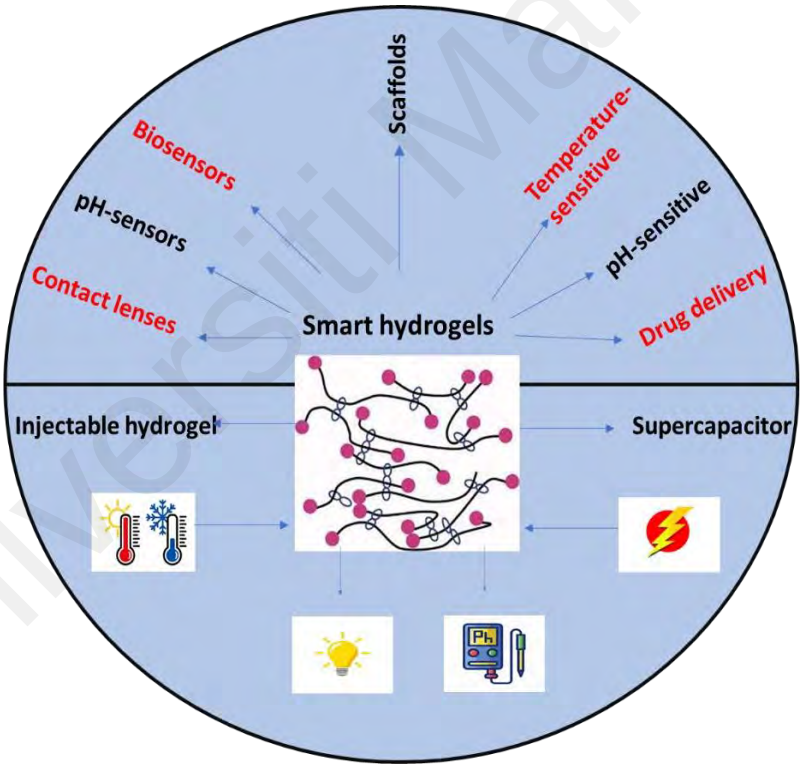

Figure 1.6 : A applications of hydrogel uses.

1.2.4 Graphene

Graphene is a two-dimensional form composed of crystalline carbon, which is a single layer of carbon atoms forming a honeycomb (hexagonal) network or several close layers

Universiti Malaya

(Figure 1.7) (Hao G P et al., 2014). The word graphene, when used without specifying the shape (eg, bilayer graphene, multilayer graphene), stands formonolayer graphene. Graphene is the original form of all graphite structures of carbon such as graphite, which is a three-dimensional crystal of relatively weak layers of graphene, or nanotubes, which are in the form of coils of graphene; and buckyballs, which are spherical particles made of graphene with pentagonal rings (Novoselov K S et al., 2019).

The theoretical study of graphene was initiated in 1947 by Physicist Philip R. Wallace. This was the first stage to understand the electronic structure of graphite (Geim A K and Novoselov K S, 2007). In 1986, the term graphene was introduced by chemists Hans-Peter Bohm, Ralph Seton, and Eberhard Stumpf. They named graphene as a combination of the word graphite, referring to carbon in its ordered crystalline form, and the suffix -'ene', referring to polycyclic aromatic hydrocarbons; in which the carbon atoms form hexagonal structures or six-sided configuration (Figure 1.8). In 2004, the Physicists Konstantin Novosel Vandre C and colleagues in University of Manchester, isolated monolayer graphene using the "sticky tape method" to remove the top layers from a sample of graphite and then apply the layers to a substrate material (Hass J, de Heer W A and Conrad E H, 2008). When the tape was removed, some graphene remained on the substrate in the form of a single layer. Upon studying the physical properties of graphene, it was shown that electrons have very high mobility in graphene, which means that graphene can be used in various electronic applications (Hass J, de Heer W A and Conrad E H, 2008). Versatile methods have been developed for the fabrication, growth or synthesis of graphene and its derivatives. In graphite, adjacent graphene layers are associated with weak van der Waals forces. Therefore, native graphene canbe obtained from the mechanical exfoliation of graphite using adhesive tapes (Lee GH et al., 2013).

Universiti Malaya

Graphene is a two-dimensional monolayer sheet of sp^2- hybridized carbon atoms, where the sp^2 carbon bonds are hybridized, with the in-plane C-C bond being one ofthe strongest in the material and outside the bond. This operates across an indeterminate network of electrons, which is responsible for the electronic conduction of graphene and provides the weak interaction between the graphene layers or between the graphene and the substrate. It has its exceptional physical properties, such as high electronic conductivity, excellent mechanical strength and good thermal stability (Figure 1.8) (Hass J, de Heer W A and Conrad E H, 2008).

Other forms of graphene-related materials are produced, such as graphene oxide, exfoliated graphite and reduced graphene. oxide. Promising properties combined with ease of processing and operation make graphene an ideal candidate for incorporation into a variety of functional materials (Geim A K and Novoselov K S, 2007). More importantly, graphene and its derivatives are widely used in a rangeof applications such as electronic devices, sensors, photonics, and clean energy (Figure 1 .9)(Lee G H et al., 2013).

The charge carriers in graphene behave as relativistic massless particles or Dirac fermions (Nair R R et al., 2008). This behaviour led to the existence of extraordinary phenomena in graphene. Graphene is more like a two-dimensional zero-gap conductor with little overlap between the valence and conduction bands. Here, the effect of the dipole electric field is so strong that it allows measurement of charge carrier concentrations of up to 1013 cm^2 with room-temperature mobility for 10,000 cm^2 (Novoselov K S et al., 2004). Using the electric field effect, the unusual quantum half-integer Hall effect (QHE) for both, electron carriers and holesin graphene was studied through chemical potential modulation. with absorption of 2.3% towards visible light

Universiti Malaya

(Nair R R et al., 2008). The thermal conductivity, (k) is measured with a value of 5000 W mK^{-1} for a single-layer laminate at a temperature of air is 25 W $m^{2}\cdot$ K (Balandin A A et al., 2008). Graphene also possesses excellent mechanical strength. The intrinsic mechanical properties of the free- standing monolayer graphene films were measured by nano-indentation in an atomicforce microscope (Park S et al., 2008). Graphene has a refractive resistance of 42 Nm and Young's modulus of 1.0 TPa , indicating that it is one of the strongest materials ever measured (Si Y and Samulski E T, 2008; Niyogi S et al., 2006).

Pure graphene is hydrophobic and has no solubility in most solvents. However, the processing of graphene compounds is primarily related to the dissolution of graphene. To improve the solubility of graphene, different functional groups are attached to the carbon backbone through chemical modification, (Li D et al., 2008) covalent, (Alexandrov G N et al., 2014; Zhang L et al., 2010) or non-covalent functional. It is impossible to disperse the hydrophobic graphene sheets directly in water without dispersion aids. Due to the presence of oxygen-containing groups, thechemically modified graphene could form a homogeneous aqueous suspension by controlling the reduction of graphene oxide (GO) with hydrazine and dialysis while maintaining the solution pH at about 10 by the addition of ammonia (Lin Y et al., 2010). However, the solubility of the resulting rGO in water is very limited, with a value of 0.5 mg/mL. Besides water, many organic solvents can be used, such as ethanol, dimethyl sulfoxide (DMSO), acetone and tetrahydrofuran (THF) (Zhu Y etal., 2009; Park S et al., 2009).

Universiti Malaya

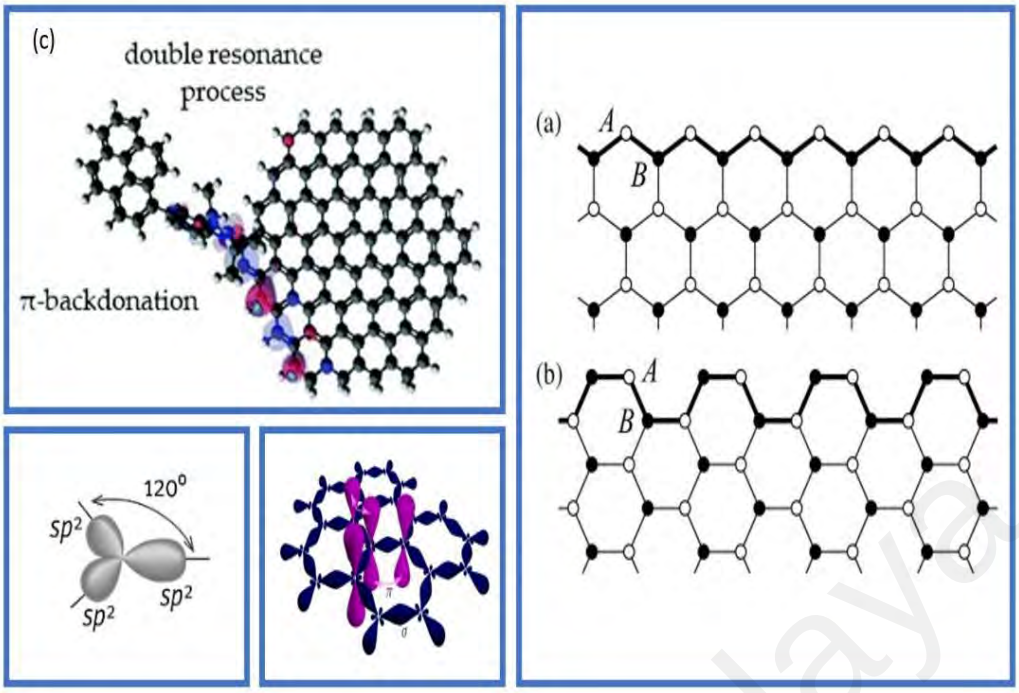

Figure 1.7 : (a) Zigzag and (b) armchair edge in graphene, (c) sp^2 hybridization in graphene.

Graphene is considered the strongest material in this world, as it can be used to enhance the strength of other materials. By adding a small amount of graphene to thematerials can be made stronger. Graphene-reinforced composite materials can be used in many applications such as aerospace, portable devices, and Energy storage (batteries and supercapacitors), Since graphene is the world's thinnest material, it hasa high value in the ratio of surface area to volume (Boehm H P, 2010). This makes graphene a very promising material for use in batteries and supercapacitors.

Graphene enables batteries and supercapacitors (and even fuel cells) to store more energy and charge faster, too. Graphene is also the most heat conductive material (Figure 1.10). Due to its properties of being strong but light weight, it is suitable for making heat dissipation solutions, such as heat sinks or heat dissipation films or microelectronics such as LED lighting; as it makes them more efficient and long lasting, and in thermal chips for mobile devices and graphene-based thermal films.

Universiti Malaya

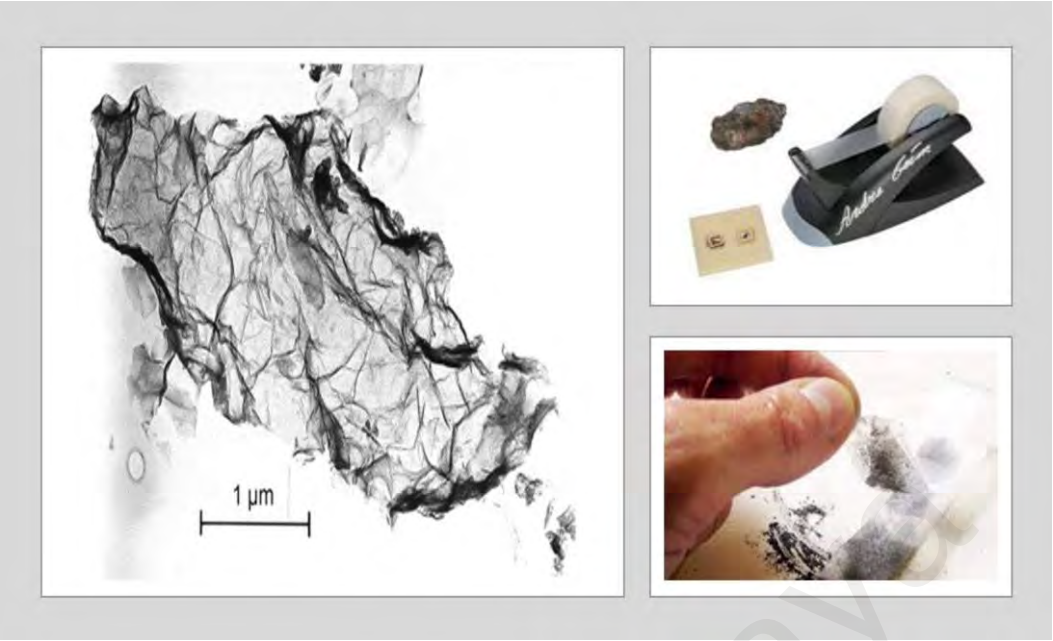

Figure 1.8 : Initial Introduction of Graphene by Chemist Hans.

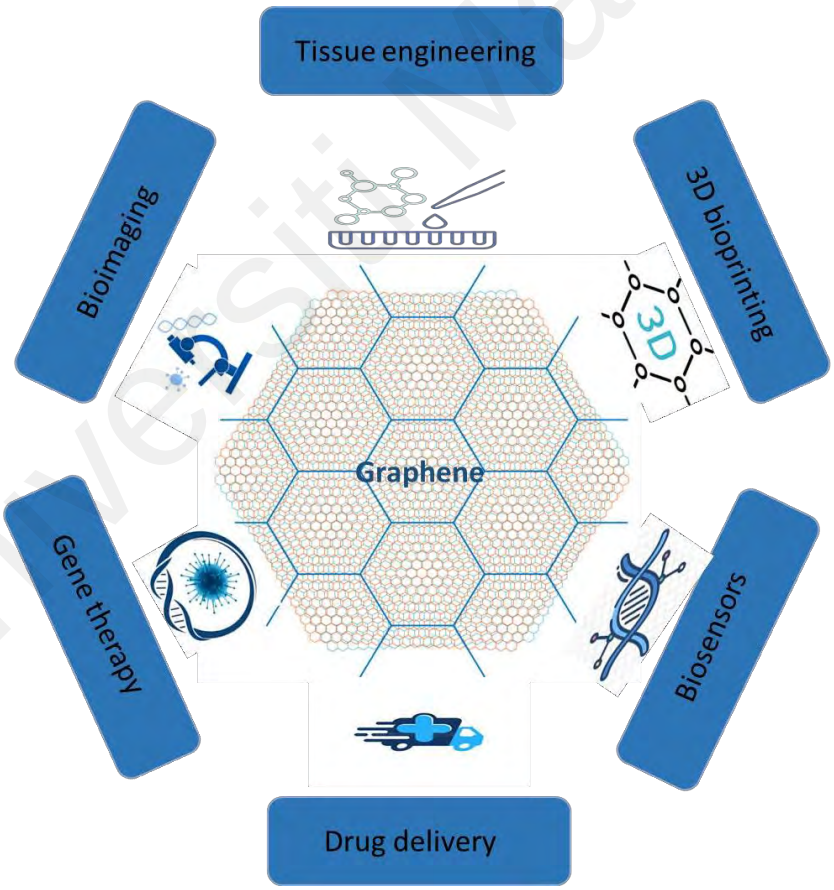

Figure 1.9: Applications of Graphene.

Universiti Malaya

Figure 1.10: (a) Graphene-enhanced composite materials applied in aerospace, mobile devices, building materials. (b)The advantages of graphene batteries.

1.3 Fundamentals of Supercapacitors

Electric double-layer capacitor (EDLC) and pseudocapacitive types of materials are categorized as supercapacitor electrode materials (Wang Z et al., 2020). Carbon-based substances like active carbon, template carbon, CNT, and graphene are examples of electrode materials for EDLCs (Wang Z et al., 2020; Dubey R and Guruviah V, 2019). Conducting polymers (CPs), metal oxides, nitrides, sulphides, and polymer composites are the main components of the pseudocapacitive type (Wang Z et al., 2020; Snook G A, Kao P and Best A S, 2011) supercapacitors. By electrostatically accumulating charge at the interface between the electrodes and the electrolyte, EDLCs store energy. The energy density and specific capacitance of pseudo capacitors are much higher than those of the EDLC type, in contrast, becausethey store energy through redox reactions at the surface (Gurunathan K et al., 1999).

Due to their dominating influence on modification, electrodes and electrolytes ina supercapacitor are crucial in determining the electrochemical behaviour and the effectiveness of the supercapacitor performance. This is apparent from the formulas for

Universiti Malaya

capacitance (F), specific capacitance(F/g), energy density (W h kg^{-1}), and power density (W kg^{-1}) calculated using the equations (1.1), (1.2), and (1.3),(1.4).

$$C = \mathrm{Q\ V}. \tag{1.1}$$

$$C = Q/(Vm) \tag{1.2}$$

$$[M^1 L^2 T^{-2}] \times [M^0 L^3 T^0]^{-1} = [M^1 L^{-1} T^{-2}] \tag{1.3}$$

Therefore, the energy density is dimensionally represented as

$$[M^1 L^{-1} T^{-2}].\ Pd = 0.1 \times E \times H \quad mW/cm \tag{1.4}$$

where *E* represents the permittivity of dielectric material in between the two electrodes. "*d*" represents the thickness of double layer near or at the electrode (m). "*V*" represents the potential difference (voltage) between the electrodes (V). *t* represents discharge time (h).*m* represents the active mass of the electrode (kg).

The aforementioned formulas make clear the elements that influence a supercapacitor's electrochemical performance. For instance, there are two ways to change a supercapacitor's capacitance or voltage in order to increase the energy densityof the device. The electrode's surface area, the type of dielectric material used, and thethickness of the double layer are all factors that affect capacitance and can improve itsuse.

1.4 Stretchable Supercapacitors

1.4.1 Hydrogel-Based Supercapacitors

Many stretchable devices use hydrogels, which are polymer networks with water in them, as ionic conductors (Rong Q, Lei W and Liu M, 2018). Excellent ionic conductivity, biocompatibility, toughness, and stretchability are all characteristics of hydrogels (Tang

Universiti Malaya

L et al., 2020). Supercapacitors perform noticeably better when stretchable electronic conductors made of carbon particles are combined with hydrogels (Wang Z et al., 2020). Stretchable supercapacitors can be made by using amethod introduced by Song C et al., 2021 , that involves coating ink on a hydrogel elastomer. A mixture of graphene flakes and carbon nanotube ink can be used to create supercapacitors (Song C et al., 2021). The percolating network of electrodes penetrated in the polymer matrix is permeated by a binary solvent composed of waterand diethylene glycol (Song C et al., 2021). The interpenetrating networks would provide high stretchability for supercapacitor. The printed supercapacitor exhibits low stretchability in the absence of a polymer network, with the percolating carbon network breaking under slight tensile strain. On the other hand, interpenetrating the percolating carbon network with a polymer chain would result in a larger strain valueunder repeated tensile strain. The imposed strain is accommodated without significantly affecting the electrical connection by sliding the graphene flakes to CNTs.

The larger dimensions of the carbon particles in comparison to the mesh size of the polymer chain are the cause of the entrapped carbon particles in the polymer networks (Song C et al., 2021). The tungsten electrodes and the percolating carbon/polymer network hold up well to repeated tensile deformation. Additionally,due to their high stiffness, the carbon particles' surface area is unaffected by the deformation. Because of this, the supercapacitor is stretchable and stress-resistant (Song C et al., 2021). After being uniaxially stretched to five times its original dimensions, the manufactured electrode exhibits no obvious damage and exhibits high reversibility. The supercapacitor's cyclic voltammetry (CV) curves, which were obtained at various stretching amplitudes, are identical, demonstrating the independence of the supercapacitor's capacitance from the mechanical stretch. For a total of 200 cycles, cyclic stretching was used with stretching

Universiti Malaya

amplitudes of 1.5, 2, 2.5, 3, 3.5, 4,4.5 and 5. After 1600 cycles, the supercapacitors still held 88.3% of their initial capacitance. By measuring the change in resistance of the electrode under stretching, the failure of the percolating network of carbons was examined. The findings demonstrate that tensile deformation causes the resistance to increase with stretching (Song C et al., 2021).

There were more articles about supercapacitors made of hydrogel. For instance, conducting polymer-based hydrogel composites were made using polypyrrole (PPy) and poly(vinyl alcohol)-H_2SO_4 hydrogel (CPH) hydrogel in the work of (Zang Let al.,2017). The cross-linked CPH film was interpenetrated with PPy during the vapor- phase polymerization process to create the composite hydrogels. The composites that were created had a stretchability of about 377%. Even after 10,000 cycles of folding tests, the capacitance was still present. Fang et al. also reported a graphene-based hydrogel supercapacitor that used phenylenediamine as the electrolyte (Fang J et al., 2018). By maintaining 98% of capacitance after 5000 cycles of charge-discharge testing, they demonstrated high stability.

Using only hydrogel materials, demonstrated a self-healing supercapacitor (ZouY et al., 2021) using a sandwich structure made of hydrogel electrodes made of polyaniline (PANI) and polyvinyl alcohol (PVA) offered a high stretchability of 633%. After a damage-healing process, the manufactured supercapacitor could restore the electrochemical performance by more than half of the initial values. Additionally, Yin et al., 2019 reported a conducting polymer-based deformable all- in-one hydrogel supercapacitor. At 110% compressive and tensile strains, the polypyrrole-polyvinyl alcohol/dilute sulphuric acid-polypyrrole (PHP) sandwiched device maintained $> 90\%$ of its initial capacitance while being 110% stretchable (Yinet al., 2019).

Universiti Malaya

1.5 Impact of energy research in Malaysia

Malaysia is highly dependent on non-renewable resources for energy generation for industrial, commercial and residential applications. The amount of these sources are depleting. Nuclear energy is also a non-renewable energy source where which involves fusion and fission reaction to generate heat, and eventually electricity. But the drawback of uranium is that it is difficult to handle and expensive to extract and process uranium into fuel for nuclear power plants.

On the other hand, renewable resources are now being considered to contribute to the energy supply. There are five main sources of renewable energy, solar energy fromthe sun, geothermal energy from the heat inside the earth, wind energy, biomass of plants, and hydropower from running water. They are called renewable energy sourcesbecause they are naturally renewable sources.

Malaysia has started introduce resources for the generation of electricity. Also, many policies are being implemented to combat carbon dioxide emissions and thus help avoid pollution which can contribute to global climate change.

1.6 Aims and objectives of the research

This research aims to fabricate the flexible supercapacitor -based cotton/ graphene as an electrode and electrolyte with excellent electrochemical performance.The objectives of this research are stated as below.

1. To formulate cotton/graphene electrode using a layering method and evaluate the performance.
2. To formulate cotton/graphene hydrogel electrolytes using hydrothermal method.

Universiti Malaya

3. To evaluate the electrochemical performance of the Electrode and electrolytes.
4. To investigate the fabricated cotton/graphene supercapacitor based on the optimized electrode and electrolytes.

1.7 Outlines of thesis

This thesis consists of 8 chapters. Chapter 1 explains the importance of energy and different type of supercapacitors, type of conductive polymers and components of supercapacitors and their properties. aims and objectives of this work are depicted. Chapter 2 presents the literature review on construction of solid state cotton fabric with the safety features of electrolytes/electrodes. Chapter 3 discusses the materials and methods. This study has investigated the morphological properties of *Gossypium herbaceum*, *Gossypium arboretum pima* and *Gossypium arboretum* fabric. These cottons were chosen because they are representative of the wide range of cotton fabrics available in the market. In this chapter, the preparation of electrolytes and electrodes are also explained in detail and the characterization methods are discussed. Chapter 4 illustrates the results obtained for the three different types of cotton materials to identify the best sample for further investigation. In Chapter 5, graphene (G) conductive cotton fabric (*Gossypium herbaceum*) was prepared layer by layer (LBL) coating of graphene treated at room temperature, first layer of graphene has been coated on cotton fabric using drop casting in the presence of sodium dodecylbenzene sulfonate (SDBS) as a dispersing agent and dimethyl sulfoxide (DMSO) to destabilize the ripple of the cotton fibers. Results obtained from scanning electron microscope (SEM), energy dispersive X-ray analysis (EDX), X-ray diffractogram (XRD), Fourier transform infrared spectroscopy (FTIR), thermogravimetric analysis (TGA), differential scanning calorimetry (DSC), and Electrochemical Impedance Spectroscopy (EIS). Chapter 6 solid-state hydrogel electrolytes preparation and characterization have been explained. Chapter 7 discusses

Universiti Malaya

the fabrication and characterization of the supercapacitors by using different hydrogel electrolyte and cotton/graphene electrode materials. Chapter 8 concludes the overall work and proposes the future progresses of this research on cotton for wearable flexible electronics.

Universiti Malaya

CHAPTER 2: LITERATURE REVIEW

2.1 Introduction

The worldwide environmental and energy issues have been exacerbated by accelerated industrialization and economic growth. Due to the properties of high energy density, excellent performance, and low self-discharge rate, lithium-ion batteries (LIBs) have been found inevitable in a variety of electronic applications during the last few decades. However, their extensive use is limited due to the presence of potentially hazardous liquid electrolytic components whereby. Lithium salts are dissolved in organic liquid solvents and Lithium ions are transported from anode to cathode in this liquid electrolyte and back again. Besides being susceptible to high temperatures and the production of lithium filaments at high currents, Li-ion batteries have several limitations and risk factors. The battery's internal structure may often be compromised by the formation of spiky dendrites; making them more susceptible to short circuits, fires, and other hazards in several applications. These dendrites are avoided in solid-state batteries with solid electrolytes, and non-toxic, flame-retardant materials may be used to make them. The solid-state battery (SSB) isone of the greatest options for the future generation of batteries since solid electrolytes have significantly greater thermal stability. It is possible to blend the advantages of both artificial ceramic electrolytes and natural polymer-based electrolytes into multi-phase solid-state electrolytic (SSEs) composites and Li-ion batteries in industrial applications are expected to benefit from alternatives like these.Several SSEs with high lithium-ion conductivity and chemo-mechanical stability have been developed in the past decades. However, all battery kinds and combinations do not guarantee their own safety and long-term viability. Sustainableenergy storage technology should concentrate on organically manufactured carbon batteries, thus discovering organic, cotton-based batteries that are economical and inexpensive, safer, more durable, and faster to recharge than the best lithium-ion

Universiti Malaya

power packs. Therefore, the construction of these cotton-based batteries will be a step closer to green, and economical options for energy sources.

Due to their affordability, quality, and superior electrochemical performance, cotton-based batteries are being considered for industrial applications. Sodium- related batteries, zinc/potassium-related batteries, and supercapacitors are among the battery chemistries examined in the current investigations, in addition to LIBs. A solvothermal technique has been used to manufacture a new and resilient fast-speed cathode made from cotton and treated with carbon (Zhu Y et al., 2020). $LiFePO_4$ hasbeen reported as a low-cost cathode material for high-performance LIBs, and it was found to be a promising candidate. Orthorhombic vanadium pentoxide (V_2O_5) HOMEs as cathode electrodes for LIBs have been examined and proven to be potential candidates (Xi Y et al., 2018). Regarding the anode materials, it has been discovered that even discarded cotton may be used for the manufacturing of valuableporosity carbon sources (Xiong J et al., 2018). This has the potential to be an excellent, low-cost, and durable anode for lithium-ion batteries (Zhou M et al., 2018). It also has the added benefits of improved rate capability and long-term spin- stability, which is a distinct advantage. On the basis of the work done by a number ofresearchers, discussions on the studies of sodium-ion batteries (SIBs) and potassium ion batteries (KIBs) were also explored in the context of understanding their electrochemical performance (Li Y et al., 2019; Liu W et al., 2012). In addition, the schematic representation of the manufacturing process for elastic sandwich structure (FSS) supercapacitors is examined which showcases outstanding spin and electrochemical stability (Yong S et al., 2013; Zhou W et al., 2022). In this study, itwas discovered that ammonia treatment of cotton fabric may make carbon cloth withhollow tubular fiber units and a large surface area. Carbon cloth-based organic electrolyte supercapacitors have thus been presented as a possible solution. For biomedical

Universiti Malaya

applications, LBL-assembled textiles with antibacterial and antifungal characteristics show tremendous potential (Li L et al., 2022). Due to its high conductivity and outstanding flexibility, a hub-type lithium-ion battery (Song H , Jeon S Y and Jeong Y, 2019), with a CNT-wrapped cotton filament and a nano mesh separator might also be useful.

For wearable electronic devices, the development of a flexible energy storage solution is essential. Supercapacitors manufactured from conventional polyester- cotton textiles may be a preferred storage device for smart sensor nodes. This study covers detailed research on these devices. Carbon nanotubes (CNTs) and/or pseudocapacitive materials are discovered to be the most commonly used materials in the production of flexible supercapacitor electrodes. Moreover, the large surface area and porous structure of these electrodes for supercapacitors benefit from CNTs'exceptional thermal and mechanical stability. The link between elastic moduli and Poisson's ratios is also being examined in light of Hertz contact theory. This aided inthe deciphering of electrolyte and electrode microstructure requirements.

Electron transmission may be facilitated by cotton's three-dimensional hierarchical porous structure. Electrodes based on CO_3O_4 structure, which has goodretention capacity and promising cyclic stability, have been explored in the current study. Research has also focused on the production of dendrites of cotton at the interfaces between electrolytes and the electrodes and the conditions that lead to higher internal resistance in the batteries. The interfacial resistance is claimed to bereduced by the fabrication of cotton cloth-based carbon tubes (DCTs) on the electrolyte surface (Wu T et al., 2018). Self-supported DCT in NIBs and cellulose nanographene (CNG) in Zn ion batteries have been explored to find out ways to havea high retention rate of capacity with a long cycle life (Zhang X et al.,

Universiti Malaya

2021). Studieshave also revealed that repeated cycles of Li coating/stripping on cotton fibers result in high performance because of the unique micro/nano hierarchical structure of the cotton fiber (Zhu R et al., 2020).

A thorough description of the nucleation and development of cotton dendrites within electrolytes has been presented in this article. Present review suggests that Carbon-based materials may be used as anode and reveals how cotton fabric's porosity structure operates. As a result of this investigations, it has also been foundhow wearable energy devices might be utilized in underwater systems.

2.2 Textile cotton fiber material

Cotton is an important textile fiber material. Most of the textile products, such as clothing materials and non-woven fabric are made of fibers and ventilation is provided through the pores formed by the fibers. Tissue porosity is defined as the ratio of the percentage of the volume of voids between textile fibers (when held in bulk), to the total packing volume (William WR J and Norman BB, 2004). The porosity of the cotton fiber assembly can be calculated using the following equation (2.1):

$$\varepsilon=[1-m/\rho V]x100 \tag{2.1}$$

Where ε is the porosity of fiber assembly (%), *m* is the mass of fiber assembly(g), ρ is the fiber density (g/cm³) and V is the volume of fiber assembly (cm³). The fiber volume V (g/cm^3) fraction for fiber aggregation V can be calculated as:

$$V_f = [\frac{\rho_m . W_f}{\rho_m . W_f + \rho_f . W_m}] \tag{2.2}$$

Universiti Malaya

Where V_f is the volume fraction of fibers, W_f is the weight of fibers, W_m is the weight of the matrix, ρ_f is the density of fibers, and ρ_m is the density of the matrix, respectively.

The cellulose found in cotton is the most abundant polymer on earth. For different variants and species, cotton fibers vary widely in overall morphology such as gyrus, cell wall thickness, cross-sectional shape etc., and also differ enormously in their finestructure in terms of fibrous direction, reflections, packing density of microfibers etc. (William WRJ and Norman BB, 2004; Gao J , Pan N and Yu WD, 2010).

Understanding the thermal degradation of cellulose is important for a wide range of fields, such as the generation of energy from biomass and flame improvement cellulose fiber inhibitors (Tugrul OR and Serin MM, 2012), (Igathinathane C et al., 2010) (AntalMJ, Varhegyi G and Jakab E, 1998).

2.3 Cotton Behaviors at Various Voltages

Using a technique known as multilayer electrostatic self-assembly, the researchersTian M et al., 2017 were able to create fabrics that had a variety of features, including those related to electrical protection and electromagnetic interference (EMI). In this instance, poly (4-sodium styrene sulfonate) (PSS) was deposited on the cotton fabric in the form of polyene. This was followed by a layer of the solution that was created with chitosan and graphene by mixing the solutions. A distinct "odd-even" regular pattern was shown on the cotton surface as a result of the alternating deposition of 10 layers of PSS and layers of chitosan and graphene. The stratified cotton's electrical conductivity reached 1.67 x 10^3 S/cm at its highest point (Figure 2.1). With a maximum SE value of 30.04 dB, this provides an exceptional level of protection against electromagnetic interference (EMI). When a voltage of 7V is applied to the fabric, the temperature of the cotton rises

Universiti Malaya

to the maximum steady-state value (δT_{max}) of 134 ˚C within eight minutes and displays excellent stability (Tian Met al., 2017). The fabric also possesses excellent electrical heating behavior, which can be seen in the fact that it shows excellent stability. By combining graphene nanoparticles with carbon black particles in a hybrid form, a straightforward technique has been developed (Souri H and Bhattacharyya D, 2018), that may be used for the industrial manufacturing of cotton textiles that are electrically conductive. In a high elastic elastomer, integrated conductive textiles are used as stress sensors as well as very elastic wearable warmers. The multifunctional tissues' electromechanical properties showed promising results as wearable stress sensors for monitoring human movement. In addition to this, it demonstrates the thermoelectric behavior of materials capable of functioning as stretchable and wearable heaters at a maximum temperature of 103 ˚C and a voltage of 20 V (Souri H and BhattacharyyaD, 2018). The feather-like electrochemical Ni-Co-S nanoflakes were placed on a flexible nickel-coated electrode that was produced as a substrate (Wang Z et al., 2020). Both the capacitance and the specific capacitance of the electrode are rather high. For use in wearable energy storage applications, the asymmetric supercapacitor cell has better electrochemical capabilities. This cell is constructed with Ni-Co-S as the cathode, active carbon as the positive electrode, and PVA/KOH as the electrolyte.The supercapacitor cell provides a high energy density of 48.9 W/h kg at 390 Wkg^{-1}, where four cells are connected in series, to operate the connected cells safely at a wide voltage window from 0V to 6.4 V due to the good electrochemical stability and consistency of the embedded cells (Paleo A J et al., 2018). The manufacture of composite flexible carbon electrodes was based on a top-down technique. Carbon nanofibers (CNFs) were coated by dipping them in cotton fabric, and then the CNFs were used to prepare the electrodes. After that, two distinct kinds of asymmetric supercapacitors (SCs) were assembled with these textile electrodes by using porous paper and Nafion-Na ion exchange membranes as spacers.

Universiti Malaya

This was done in order toimprove the electrochemical performance of the electrodes, which was accomplishedby adding additional layers of activated carbon and manganese oxide (MnO_2) materials. The performance of the carbon-based material showed a capacity of 138 and 134 F/g, as well as low self-discharge rates. In addition, this study was based on two techniques (spin and float) for the purpose of researching long-term durability testing. A solid-state hybrid device (Nafion membrane) has shown excellent results for energy storage applications (Kim H and Lee S, 2021). This device has exceptionally long endurance, with 10 thousand cycles, and an extra 270 hours at a constant voltage of 1.6V.

Researchers have investigated how the electrical characteristics of the cloth were affected by the relative humidity (Zhang X et al., 2018). The graphene/polymer composite has a flame retardant cotton fabric designed like a horseshoe coated on its surface. An aqueous sulfuric acid solution was used as the method for controlling therelative humidity (RH). Different RH conditions on the outside were used to store thesamples such as 25%, 35%, 45%, 55%, 65%, and 90%. It was found that the rate of weight change tends to rise owing to the increase in the amount of moisture absorbedby the cotton as a result of the impact of raising the relative humidity. This was because the quantity of moisture absorbed by the cotton increased. It was discovered that the rate of change in the surface resistance dropped from 25% to 55% relative humidity (RH), after which it began to rise up to 90 %. When a voltage between 5 V and 6 V was implemented to samples at various relative humidity conditions as shown in Figure 2.2, and the temperature was 50 °C with a RH condition up to 55%, it was observed that the surface temperature and current of samples at different RH conditions increased linearly with the increase in the applied voltage. Most appropriate results were obtained at a humidity condition of 55%, in which it recommended excellent electrical and electrical heating properties of the material as well as enhancing the electrical gain of electrical textiles for various electronic

Universiti Malaya

applications (Li Y et al., 2016). Also, the samples improved the electronic gain of electrical textiles for different electronic applications.

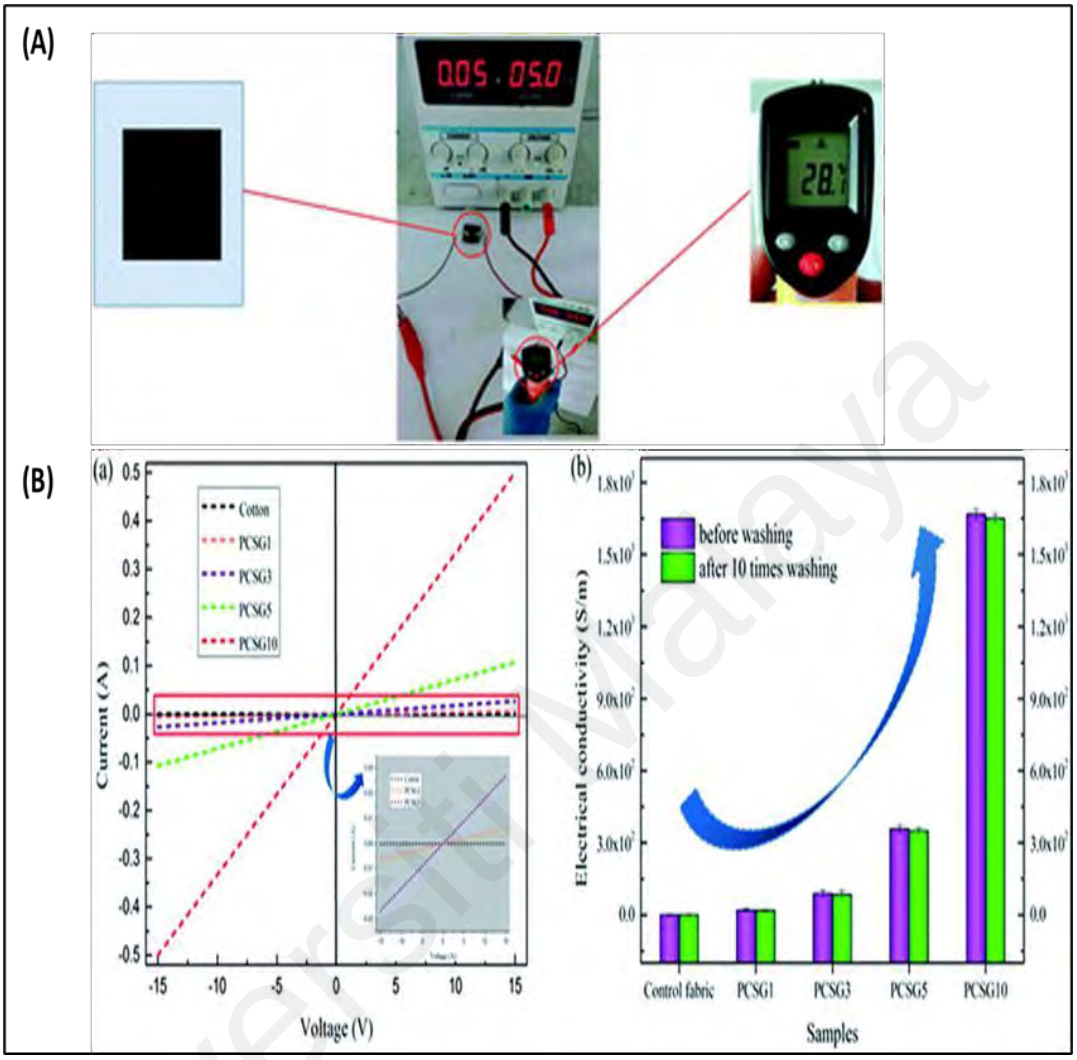

Figure 2.1 : (A) Schematic diagram of electro-heating measurement setup (Tian M et al., 2017), and (B) (a) Current vs. voltage curve, and (b) variation of surface electrical conductivity of PCSG fabrics and uncoated fabrics (Tian M et al., 2017).

University Malaya

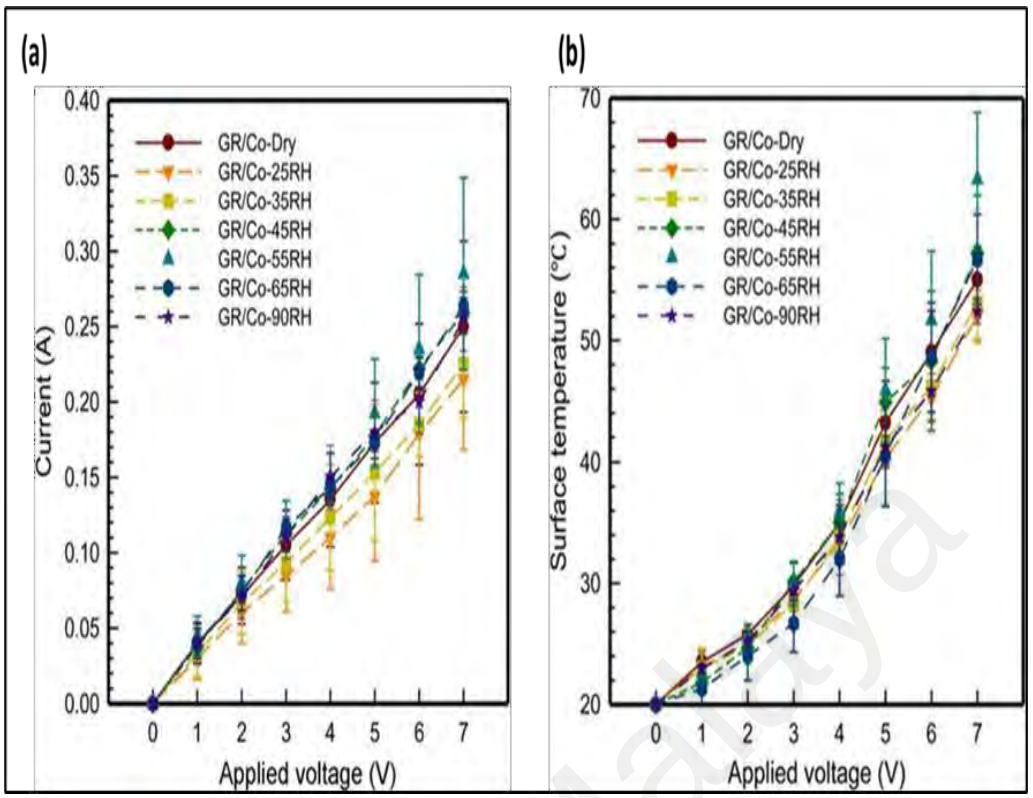

Figure 2.2 : (a) Current-Voltage (I-V) curve of graphene/PVDF-HFP composite coated on flame-retardant cotton fabric under various relative humidity conditions (Kim H and Lee S, 2021), (b) The relationship between applied voltage and surface temperature of graphene/PVDF-HFP composite (Xiong J et al., 2018).

2.4 Cotton Behaviors at Various Temperatures

Zhang H et al., 2018 looked into the foaming behaviour and thermal characteristicsof an attractive composite foam made of polylactide (PLA) and PLA/cotton fibers. Crystallization of PLA was profoundly influenced by the temperature, the amount of fiber present, and the CO_2 saturation pressure. Because of its high crystallinity and close-packed structure, low-pressure carbon dioxide formed non-uniform foam and a huge region that was not covered in foam at the same saturation temperature i.e., 140 ˚C. A homogeneous cell structure was formed as a result of the high carbon dioxide pressure, despite the fact that the cell sizes increased as the structure of the cell

Universiti Malaya

degraded. The action of the saturation pressure led to the formation of regular micro- cell formations in the middle temperature. Due to increased local pressures caused bythe fibers and the trans-crystals that surrounded the fibers, the morphology of the PLAcell was enhanced when low-content cotton fibers were included in the material (Zhang H et al., 2018). Natural cotton was used in the carbonization process which ledto the development of solid, hard carbon steel microtubes (HCTs) that were used as ananode (Liu W et al.,2012). Because of the differences in their microstructures and heterogeneous contents, the electrochemical performance of HCT is significantly affected by the carbonization temperature. HCTs that have been carbonized at a temperature of 1300˚C have the largest reversible capacity of 315 mAh/g and a good rate capability owing to the tubular structure of these HCTs. This study not only provides a new way for manufacturing carbon steel materials with a distinctive tubularmicrostructure by drawing inspiration from natural sources, but it also advances the basic knowledge of the process by which sodium is stored (Yong, S, Hillier N and Beeby S, 2021). In addition, conductive twill was made by drop-casting the material with a compound consisting of carbon black and polyaniline and then adding a polar solvent, dimethyl sulfoxide, to increase the conductivity (Soundharrajan V et al., 2020). This method was used to prepare the material. The method known as "dip and dry" was used in order to apply the composite carbon/polyaniline black on the surface of the cotton. After being treated with carbon black and polyaniline, the sheet resistance of the initial twill reduced to around 500 Ω/sq from its initial value of 3.57 x 10^{12} Ω/sq. The resistivity of the conductive cotton fabric was also evaluated as a function of temperature, ranging from 298 ˚C up to 573 ˚C. The investigation revealed that the conductive cotton fabric had a unique set of characteristics, one of which wasthe ability to switch between the properties of metals and semiconductors (Soundharrajan V et al., 2020).

A conductive cotton fabric containing a single-walled carbon nanotube (SWCNTs)was

Universiti Malaya

created by using a simple infusion method (Soundharrajan V et al., 2020). The surface functional groups that create a web on the cotton surface are responsible for the SWCNTs' increasingly strong binding to the cotton fibers. As a consequence, the fabric demonstrated increased electrical conductivity with a low plate resistance value (0.006Ω). It was discovered that the resistance of the conducting cotton fabric switched from the behaviour of a metal to that of a semiconductor at a temperature of around 75 ˚C, which resulted in a transition that was both stable and reversible (Han C G et al., 2017).

A graphene nanosheet/ poly(vinylidene fluoride-hexafluoropropylene) (PVDF- HFP) composite was used to generate an electro-heated fabric that was covered with a high concentration of graphene nanoparticles (GNP) (ranging from 32% by weight to 64% by weight). Electrodes were made out of silver-coated electrical leads with the purpose of increasing their flexibility. Crystallization and thermal stability were both increased by a graphene/PVDF-HFP nano-coated cotton fabric, which also contributed to an increase in content. As more graphene nanoplates were added to thePVDF-HFP complex solution, the resistance of the plates used in the samples steadily reduced. The sample had a sheet resistance of 44 Ω/sq after being coated with graphene/PVDF-HFP nanoparticles at a weight percentage of 64 grammes per square meter (64 GR/cotton). The graphene nanoplatelet/PVDF-HFP-coated cotton fabric's electrical heating performance was further improved with the higher content of graphene nanoplates (Figure 2.3). After applying 5 V to a 64 GR/cotton, it was discovered that the surface temperature was around 48 ˚C. This demonstrated that it could be utilized at a voltage that was < 10 V (Xu B et al., 2020).

Universiti Malaya

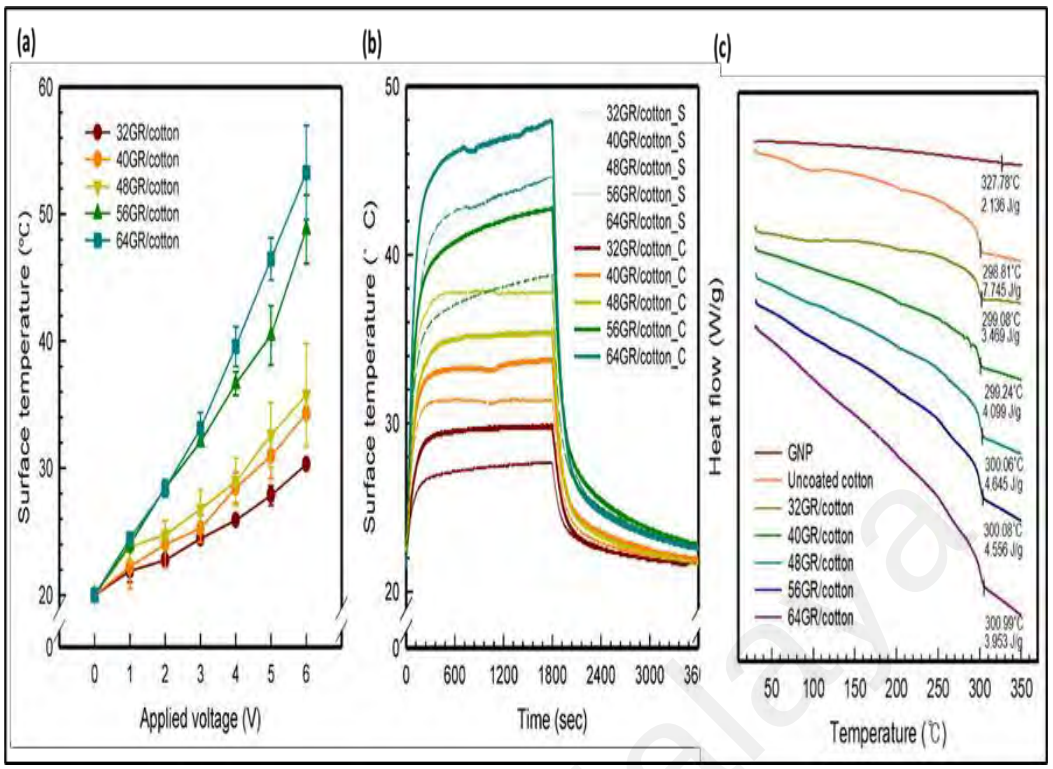

Figure 2.3 : (a) Variation of the surface temperature of GR/cotton coated with various high-content of graphene nanoplatelets (Xu B et al., 2020). (b) Time-dependent temperature of local area at 5 V (C) Differential scanning calorimetry (DSC) curve of GR/cotton (Song H, Jeon S Y and Jeong Y, 2019).

2.5 Design for Safe Cotton on the Cell Level

2.5.1 Cathode Materials

Cotton that had been processed with carbon $Na_4VMn_{0.9}Cu_{0.1}(PO_4)_3$ (NVMCP/C/CC) was the starting material for the copper cathode that was preparedby Yang C et al., 2018. The cathode preparation process was simple and quick.

Synchrotron XRD and GITT investigations utilizing DFT calculations indicated the stable structure of NVMCP/C/CC, as well as the reversible biphasic interaction that occurred when Na-ions were introduced or withdrawn from the system, this can be seen in Figure 2.4 . The superior electrochemical properties of the NVMCP/C/CC cathode at low (79 mA Hg^{-1} after 450 cycles at 1.5 °C) and high current rates (68 $mAHg^{-1}$ after 3000 cycles at 30°C) demonstrate that the combination of multiple attributes, such as the nano-

Universiti Malaya

dimensional architecture, uniform carbon coating, and copper doping, is advantageous for improving the electrochemical properties of NVMP cathodes (Yang C et al., 2018). In order to produce a $LiFePO_4$ cathode material, Xi Y et al., 2018 relied on the more traditional solvothermal technique. Theresults showed excellent cycle stability when a cotton fabric that had been soaked in 0.1M LiOH solutions was used in conjunction with $LiFePO_4$ as the cathode material for a lithium-ion battery. This resulted in a very low 7.8% capacity loss after 200 cycles when the temperature was set at 2 °C. This was due to the enhanced electronicconductivity and Li-ion diffusion processes. Electrochemical impedance spectroscopy (EIS), as shown in Figure 2.4 (A) and (B) has also shown this, thereby showing that low-cost twill $LiFePO_4$ composite is a viable cathode material for high-performance lithium-ion batteries (Xi Y et al., 2018). (Zhu Y et al., 2020) developed a high-load 3D fabric cathode for flexible, high-performance lithium-ion batteries by integrating hollow polyhedral structures (HoMSs) with conductive metallic twill.

This cathode is intended to be used in lithium-ion batteries. V_2O_5 HoMSs were employed as active materials using the chain molding process, in which they used conductive metallic textiles as current collectors and flexible substrates. This approach was used to produce the active materials. Because of the structure of the V_2O_5 HoMSs, which are able to successfully avoid volume change and absolve stress/stress during repeated insertion/extraction processes of lithium, as well as thetissue stream collector, which is a strong and durable metallic fabric, the excellentlyprepared textile devices demonstrated superior electrochemical performance and stability. Even after being subjected to 500 charge/discharge cycles, the capacitancedoes not lose its high value of 222.4 $mAHg^{-1}$ when subjected to a high mass load of 2.5 mg cm^2. It has been discovered that using V_2O_5HoMEs as the cathode electrodein conjunction with metallic fabric as the cathode electrode might result in very elastic lithium-ion batteries (Zhu Yet al., 2020).

Universiti Malaya

The charging-discharging curves are displayed flat after the battery has been energized for 25 cycles, and then again after a variety of bending cycles at an angle of 90 degrees, as shown in Figure 2.5 (e) . After being bent, the battery continues to function correctly, and the diminished capacity may be disregarded, presented in Figure 2.5(f). There was very little overlapbetween two of the curves (the 100 and the 200 bending cycles). With a voltage of 3V, the battery can power an LED bulb with a length of 1 meter regardless of whether it is horizontal or bent at an angle of 90 degrees or 180 degrees.

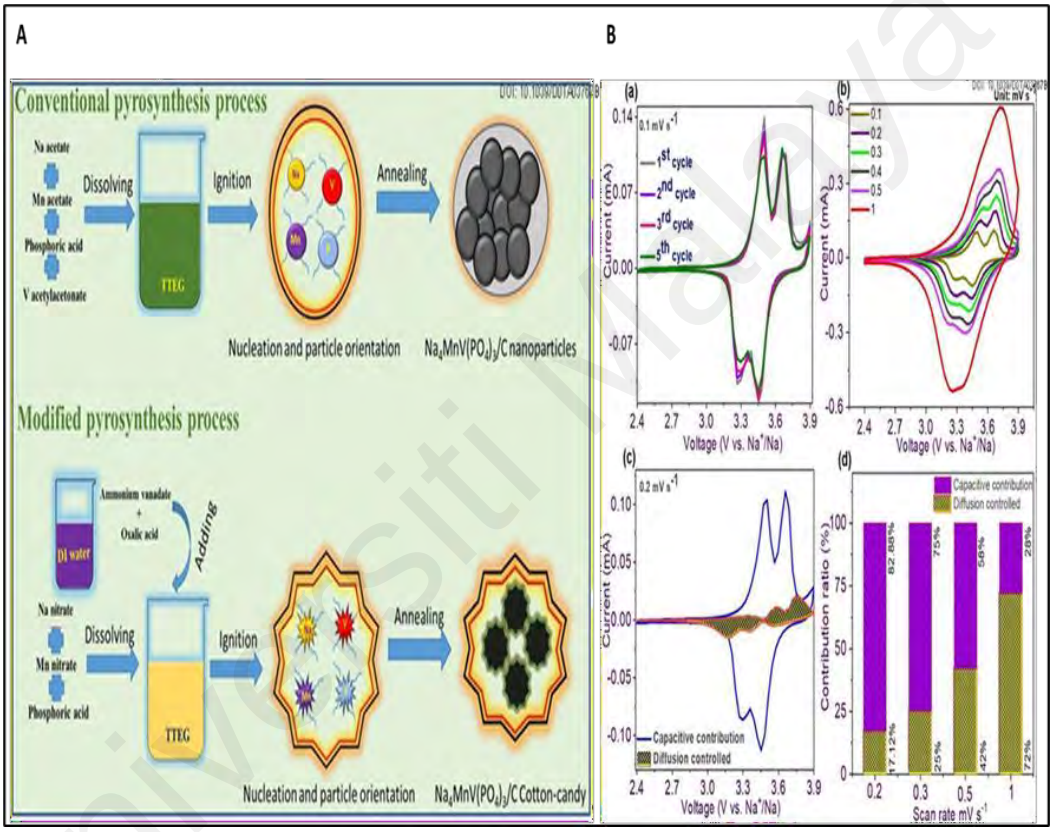

Figure 2.4 : (A) Comparison of conventional and modified-pyro-synthesis process (Li L et al., 2022). (B) (a) CV profile for NVMCP/C/CC at 0.1 mV s^{-1}, (b) multi- scan CV profile (c) the contribution ratio of the diffusion-limited capacities and capacitive capacities at 0.2 mV s^{-1} (d) bar chart for capacity contribution ratios(Wu T et al., 2018).

Universiti Malaya

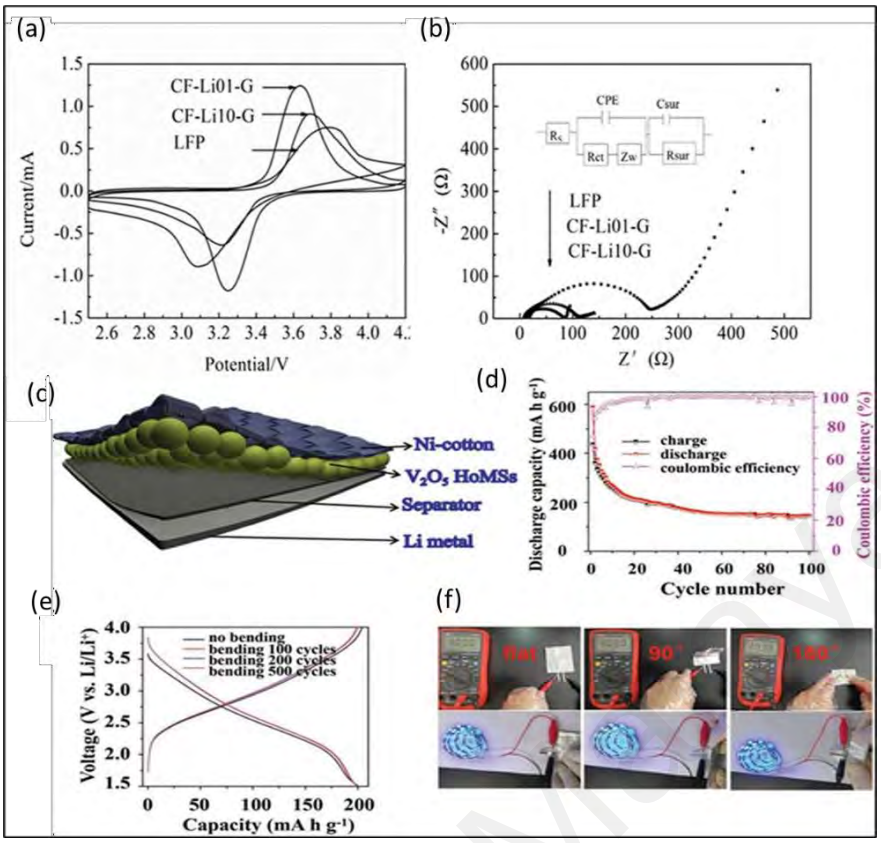

Figure 2.5 : (a) Typical cyclic voltammogram curves for the LFP, CF-Li01-G and CF-Li10-G electrodes (Zhu Y et al., 2020) and (Zhang X et al., 2021). (b) Electrochemical impedance spectra with corresponding equivalent circuit model (inset) for the LFP, CF-Li01-G and CF-Li10-G electrodes (Zhang, X et al., 2021). Electrochemical and mechanical performance of the flexible fabric battery, (c) Structure of the flexible battery, (d) Cycling stability of 3S-V_2O_5HoMSs/Ni- cotton at 100 mAg^{-1} (Zhang, X et al., 2021). (e) The charge and discharge curves of the flexible battery at 0, 100, 200, and 500 bending cycles. (f) 1 MLEDs were lit by the flexible battery after being bent at 0°, 90°, and 180° (Zhu R et al., 2020).

2.5.2 Anode Materials

As can be seen in Figure 2.6, Xiong J et al., 2018 developed a method to produce high-porosity carbon with large surface areas by making use of carbon sources that were produced from waste cotton. After undergoing heat treatment, carbon that was saturated with Sulphur and nitrogen was produced in the presence ofthiourea. This carbon was then put through testing to determine whether or not it is suitable for use as the anode in lithium-ion batteries. It was discovered that the synthesized S and N co-carbon exhibited

outstanding electrochemical performance when the S and N co-doping was used. This was accomplished by making use of both elements. It also gave a high reversible capacity of 1,101.1 $mAHg^{-1}$ after 150 cycles at 0.2 A/g and a high capacity of 531.2 $mAHg^{-1}$ even after 5000 cycles at 10.0A/g . Both of these capacities were achieved even after extensive cycling.

Additionally, it demonstrated a high capacity of 689 mAH $g^{-1}$when operating at 5.0 A/g. This improved lithium-storage performance of S, N-saturated carbon which makes it a viable low-cost and sustainable anode for high-performance lithium-ion batteries (Xiong J et al., 2018). The use of thiourea as a source of nitrogen and Sulphur allowed for the production of a N/S-adapted carbon. When these carbon compounds were investigated for use as anode materials for LIBs, the findings showed that they had higher rate capability and long-term spin stability (Xiong J et al., 2018). The preparation of Fe_3O_4/C compounds was accomplished by Liu X et al., 2019 by using cotton-assisted facile combustion in a vessel within a few minutes. According to the findings, the nanoparticles of well-dispersed Fe_3O_4 that were embedded in a carbon matrix generated from cotton exhibited outstanding electrochemical performance. The highest gravimetric and volumetric discharge capacities of 803 mAg and 948 $mAcm^3$, respectively, were attained after 300 cycles at a current of 0.4 A/g Fe_3O_4/C-8 (36.0% carbon). This was accomplished by using a current of 0.4 A /g. The presence of carbon causes a change in its buffer volume, which in turn prevents agglomeration. The great electrochemical performance that was achieved can be seen in Figure 2.7, which depicts Fe_3O_4 nanoparticles that were present throughout the process of introducing and extracting Li^+ ions. The simple andscalable Fe_3O_4/C compounds have great potential as anode materials that may be used in lithium-ion batteries (Liu X et al., 2019). They have outstanding electrochemical performance as well. According to the findings of the research carried

Universiti Malaya

out by He X et al, (2018), carbon and steel that were saturated with oxygen and Sulphur were produced by the surface hydrolysis of Sulphur derived from cotton.The researchers also discovered that simultaneous doping improved the rate at whichpotassium ions diffused through the material. This hydrolyzed carbon steel demonstrated strong reversibility (409 mAg^{-1} at 0.1 amp g^{-1}), superior rate capability (135 mA g^{-1} at 2 amp g^{-1}), and outstanding spinnability (about 120 mA g^{-1}) over 500 cycles at 2 A/g when it was employed as an anode for potassium-ion batteries (KIBs). According to the findings of the research, cotton solid carbon may function as an anode at a reasonable cost while maintaining excellent potassium storage characteristics (He X et al., 2018). New N/S-doped carbon nanosheets made from cotton utilized as the positive electrode in sodium-ion batteries have been reported by Dai P et al., 2020. These nanosheets were manufactured using cotton (SIBs).

According to the findings of electrochemical tests, the carbon anode outperforms conventional carbon-based main anodes in terms of processing capacity (482.1 mA gat 0.1 g), rate performance (375.6, 357.8, 340.5, 324.1 mA at 1.0, 2.0, 5.0, and 10.0 A/g, respectively), and rotational stability (351.1 mAg^{-1} g at 2.0 mAg^{-1} per 600 revolutions). Figure 2.8 shows that the outstanding Na^+ storage capability is due to defects, wide d-spacing, a barrier of Na^+ diffusion, and higher electronic conductivity of the co-combined N/S carbon nanoplates. The pseudo-storage behaviour of Na^+ also adds to the high-rate performance of the material. This study presents a roadmap for the low-cost manufacturing of high-performance carbon anode materials for SIB assemblies. Cotton fibers were used as a substrate, and the ionic liquid $[HMIm]N(CN)_2$ was used as a source of carbon and nitrogen. The discovery of nitrogen-coated cotton-derived carbon fibers (NC@CCFs) was made byDai P et al., 2020, and the preparation of these fibers was made by Liu X et al., 2019. The use of cotton resulted in significant enhancements to the

Universiti Malaya

structural steadiness of NC@CCFs. While the presence of nitrogen doping contributed to abundant active sites and increased lithium storage active sites in NC@CCFs; the highly conductive CCFs provided the conduction network for electron transport in NC@CCFs. Additionally, the highly conductive CCFs allowed for increased lithium storage active sites. In a lithium-ion battery, the NC@CCFs anode demonstrated outstanding cycle stability (614.25 mAh h^{-1} at 0.5 °C after 250 cycles), as well as rateperformance (Tarabella G et al., 2012). Also, He X et al., 2018 carried out the analysis of extremely turbulent cotton-derived carbon steel. According to the findings, a simple treatment consisting of soaking the cotton in hydrochloric acid before subjecting it to high-temperature carbonization has a significant impact on both the structure and the electrochemical characteristics of carbon steel. For the existence of the porous structure and the wide surface area, this carbon steel demonstrated excellent initial coulombic efficiency (73%), improved spin stability, and rate capacity (253 mAg^{-1} and 165 mAg^{-1} at 40 mA^{-1} and 4000 mA^{-1}, respectively). The electrochemical performance of the cell as a whole was significantly improved when carbon steel was included in the cathode material (Zheng C et al., 2012).

Universiti Malaya

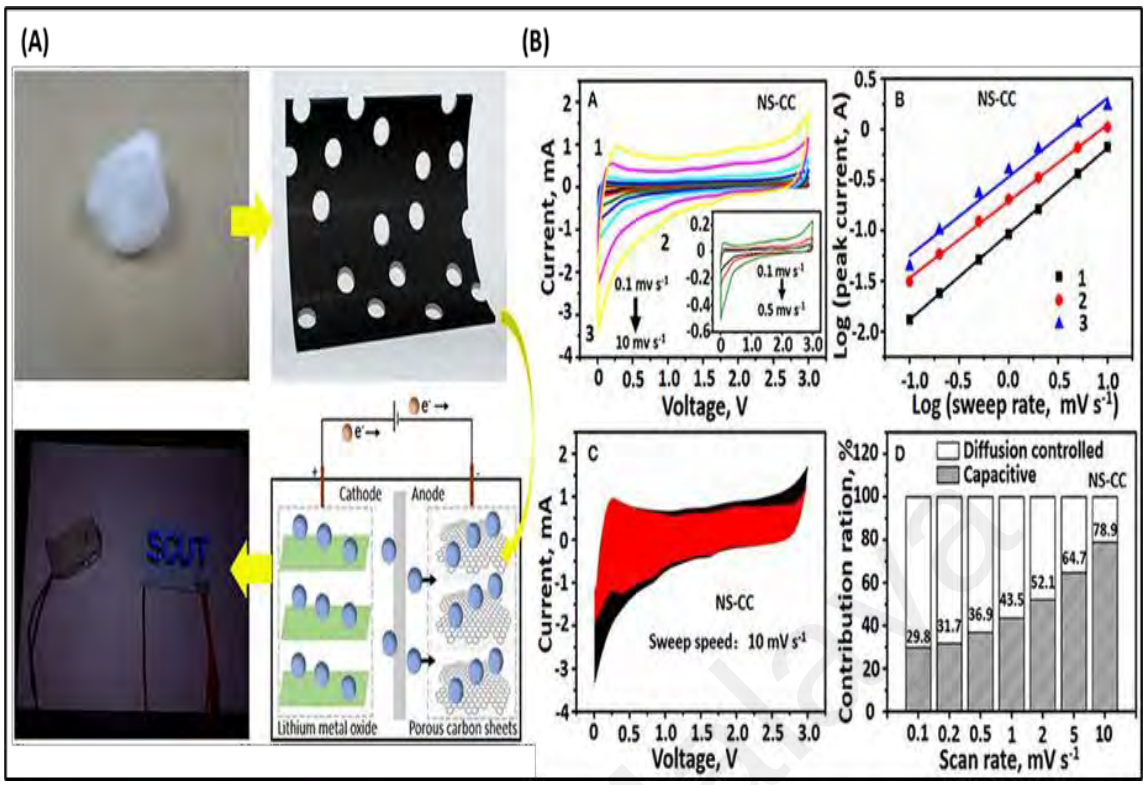

Figure 2.6 :(A) Schematic diagram of fabrication of porous carbon sheet anode form wasted cotton for Lithium-ion battery anode powering blue light emitting diode (LED)(Xiong J et al., 2018). (B) CV curves measured between 0.01 and 3.0 V. The b-value is determined by using the relationship between peak current and scan rate. CV curve with the pseudocapacitive fraction shown by red and diffusionshown by black at a scan rate of 10 mV s^{-1}. Bar chart showing the percentage of pseudocapacitive contribution at vs. scan of NS-CC (Tian M et al., 2017).

Universiti Malaya

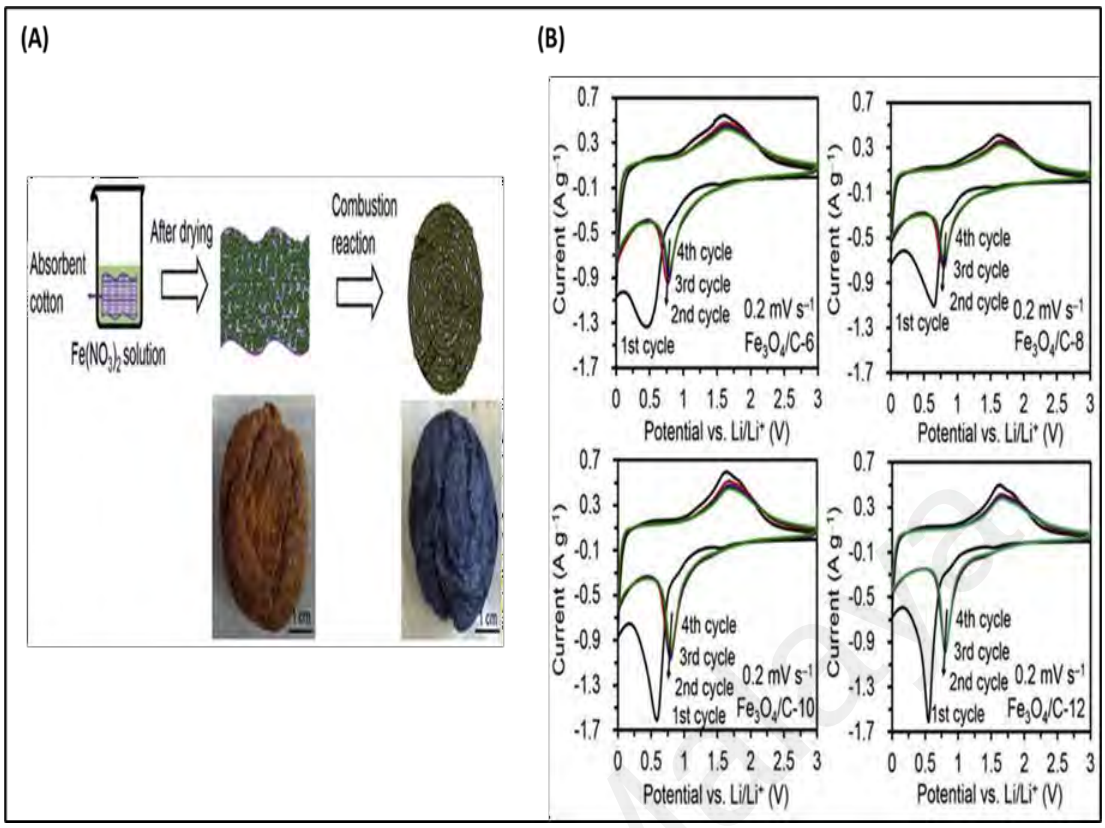

Figure 2.7 : (A) Schematic illustration for preparing Fe_3O_4/C composites, (B) CV curves of Fe_3O_4/C composites in the voltage range of 0 to 3.0 V at a scan rate of 0.2 mV s^{-1} (Liu X et al., 2019) and (Souri H and Bhattacharyya D, 2018).

Universiti Malaya

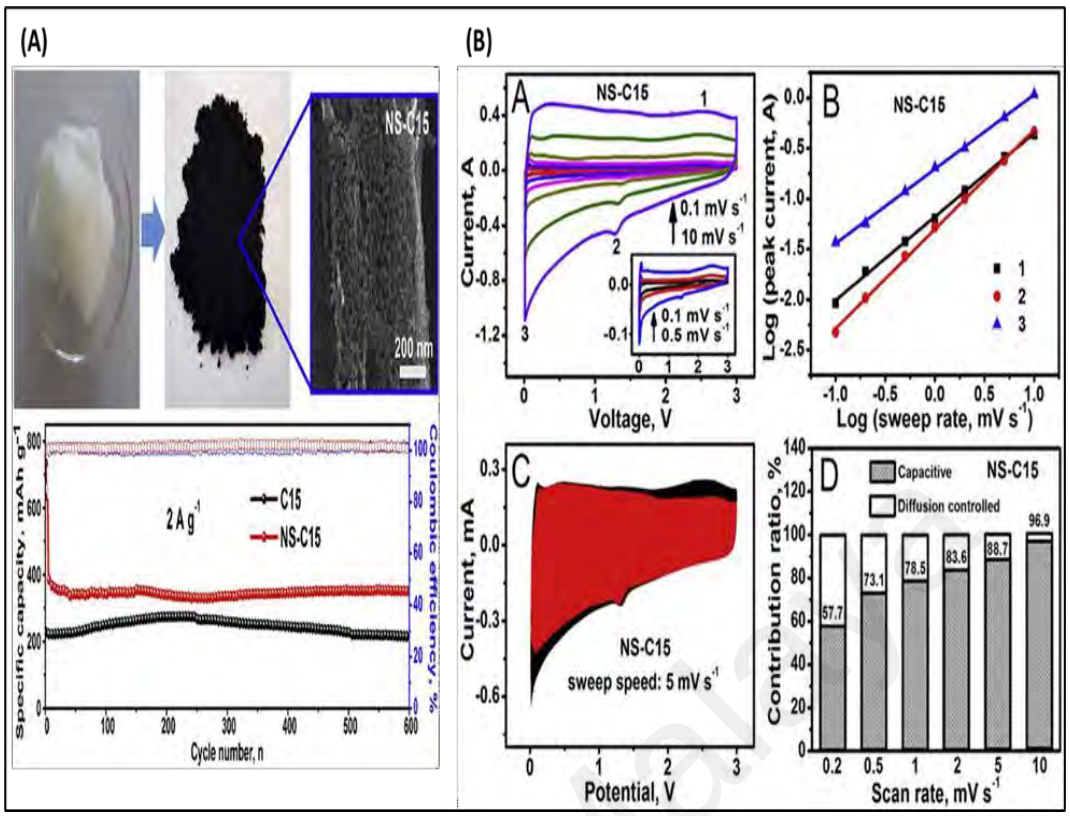

Figure 2.8 : (A) Schematic illustration of the TCR production of samples C0, C5, C10, C15 and NS-C15, (B)CV curves measured between 0.01 and 3.0 V at various scan rates from 0.1 to 10 mV s^{-1} (a), the b-value, (Yang C et al., 2018) (b) CV curve with the pseudocapacitive fraction, (c) percentage of pseudocapacitive contribution at versus scan rates (d) NS-C15(Yang C et al., 2018) and (Dai P et al., 2020).

2.5.3 Separator Materials

Screen printing was used to create a sandwich-shaped supercapacitor fabricated by Zhou M et al., 2018 in which poly (vinyl alcohol)/H_3PO_4 twill wasused as an electrolyte matrix, in addition to a separator and a support layer.

According to their findings, the device had a gravitational capacitance of 63.7 F/gand a current density of 1 A/g. After going through 2,000 charge and discharge cycles, it still had 85% of its original capacity. In addition to this, it was discovered that it could endure 100 times bending or twisting while maintaining a capacitance that was between 89.7 % - 93.3% of its original value. On a T-shirt, asquirrel-pattern supercapacitor was created by constructing a screen-printing mask. The capacitor consisted of three supercapacitors

Universiti Malaya

linked in series, and it was used to power red lighting as a demonstration of its effectiveness (Figure 2.9).

This study presents a straightforward approach for the fabrication of ultra-flexible fabric-based capacitors, which may have applications in intelligent textiles and wearable electronics (Zhou M et al., 2018).

A piece of graphene-coated cotton fabric was used as the foundation for the construction of a stiff, flexible, and symmetrical supercapacitor by Li Y et al., 2019. The materials for the flexible electrodes were prepared using the "dry coating" method, which does not have adverse effects on the environment. After that, the "two-step reduction" method for chemical and microwave reduction was utilized, which is an approach that is straightforward and user-friendly. After being packed and having its electrochemical performance examined, the supercapacitor was put together in theshape of a sandwich with a cotton separator in between the layers. The supercapacitorwith the flexible sandwich structure (FSS) demonstrated a high capacitance (464 F/g at 0.25 A/g), along with outstanding spin stability (91.6% capacitance retention after 1000 charge and discharge cycles) and excellent electrochemical stability. This supercapacitor as a gadget may be worn on the body (Li Y et al., 2019). Figure 2.10 presents the findings clearly. Reasonably good electrical conductivity, exceptional flexibility, and strong adhesion between GNSs and cotton fibers are the characteristicsof this material. A supercapacitor was created by using this GNSs-CC composite fabric as the electrode material and employing pure cotton CC as the separator in the creationof the device. This particular supercapacitor demonstrated a specific capacitance of 81.7 F/g (dipole system) in an aqueous electrolyte. This value is one of the highest values for GNSs-based supercapacitors, and the results were satisfactory in terms of how much capacity

Universiti Malaya

appeared in an ionic liquid or organic electrolyte. It was also possible to create an all-fabric supercapacitor by employing pure CC as a separator and GNSs-CC composite fabric as an electrode and current collector (Liu W et al., 2012). Using the dipping technique and a separator made of pure cotton, Yong S et al., 2013 constructed and characterized a super fabric capacitor. The results of their research showed that structured supercapacitors could achieve specific capacitances of 11.1 F/g, an areal capacity of 105 mF cm^{-2}, and maintain 95% of the initial capacitanceafter rotating the device more than 15,000 times (Yong S et al., 2013).

Zhou w et al., 2022 created a cellulose gel made from cotton and used it as a separator for aqueous zinc ion batteries (AZIBs). The gel was generated via surface filtering. The resulting separator has nanopores that are densely packed and uniformlydistributed across its whole, an abundance of hydroxyl groups, outstanding mechanicalcapabilities (with a strength of 29.2 MPa and a modulus of 4.16 MPa), and high ionicconductivity (56.95 mS cm^{-1}). When compared to the more usual fiber glass separator, this one was able to enhance the quantity of zinc ions transported, decrease the dissolving barrier for hydrated zinc ions, and speed up the kinetics of zinc precipitation. Additionally, it was able to lower the overvoltage of zinc production. Onthe other hand, the cellulose film separator is very effective and outstanding in its ability to prevent dendrites and undesirable interactions (Zhou w et al., 2022).

Universiti Malaya

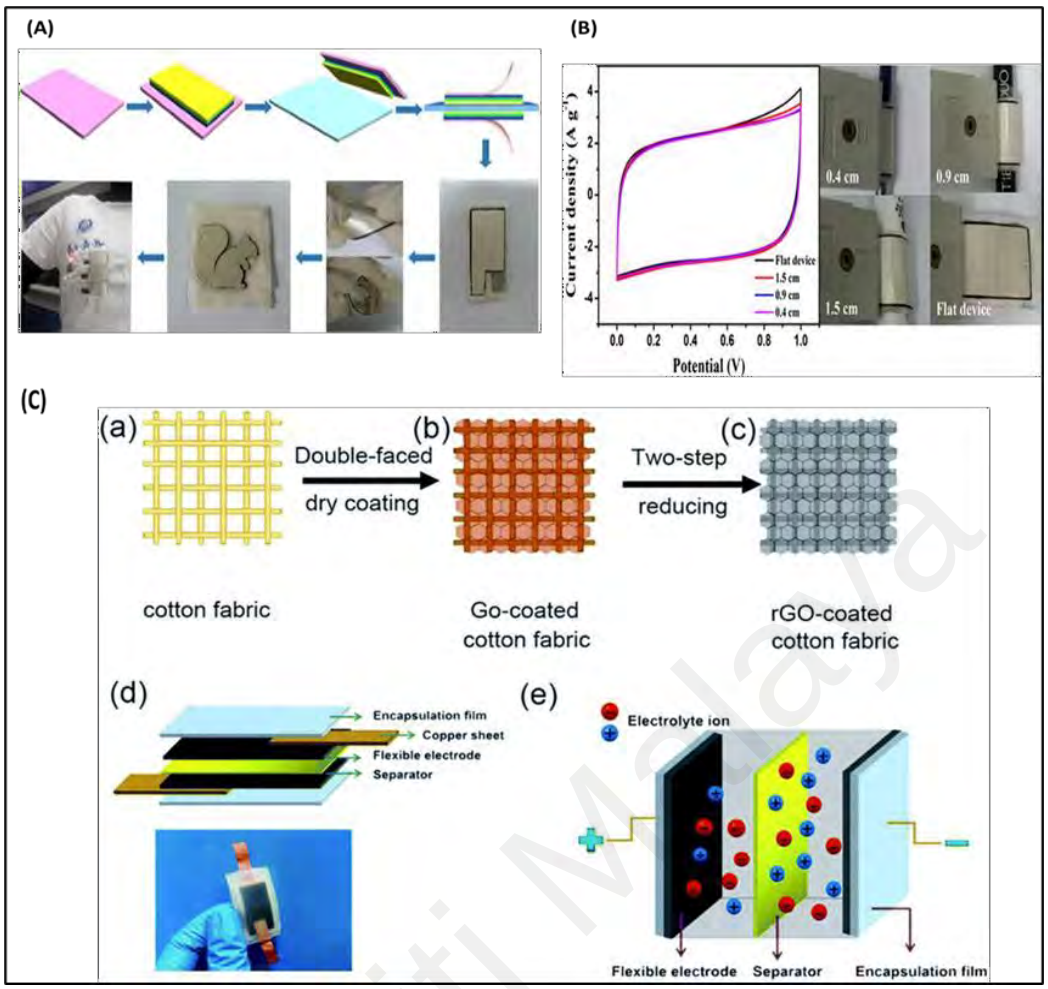

Figure 2.9 : (A) Schematic illustration of the supercapacitor fabrication process of the supercapacitor with a squirrel pattern (Zhou M et al., 2018), (B) CV curves of an prepared supercapacitor rolled on pens with different diameters (Li, Y et al., 2016). (C) (a-c) Schematic illustration of the fabrication process of rGO-coated cotton fabric (Li Y et al., 2016). (d) Schematic diagram of sandwich structure supercapacitor assembly and the FSS supercapacitor device. (e) Schematic diagram of the internal work of FSS supercapacitor (Zhang h et al., 2018).

Universiti Malaya

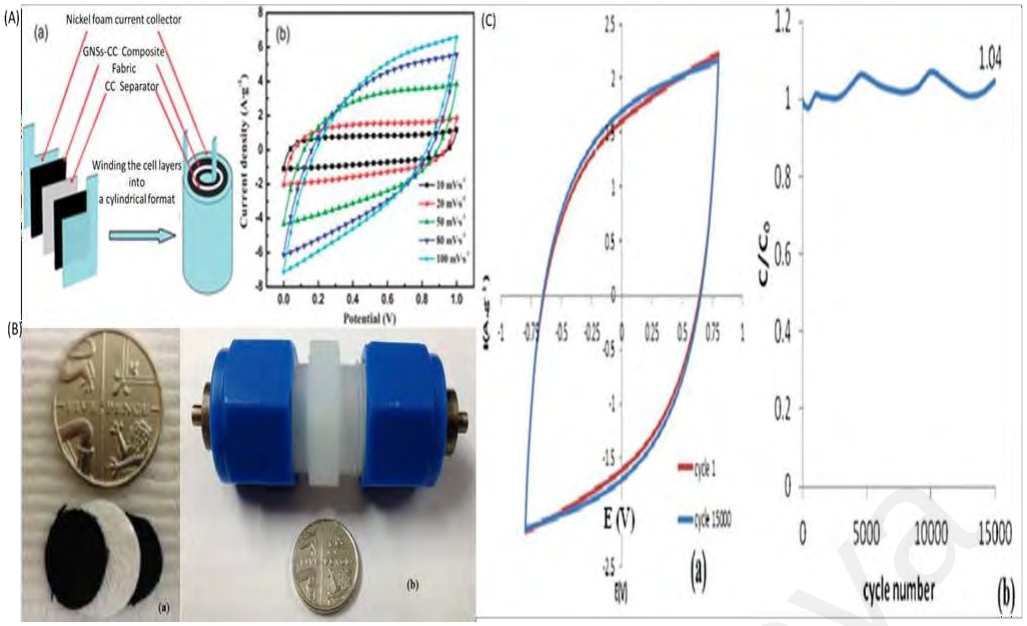

Figure 0.10 : (A) (a) A schematic diagram of the structure of an assembled symmetric supercapacitor (Liu W et al., 2012; Li Yet al., 2019), (b) CV curves ofthe assembled supercapacitor at various scan rates in 6 M KOH solution (Liu, W et al., 2012). (B) (a) Photograph of fabric supercapacitor before assembly, (b) Swagelok PFA tube fitting test ring and (C) (a) CV test of the device for 15000 cycles between +/- 0.8V at the scan rate of 200 mVs^{-1}, (b) stability of device over 15000 cycles (Yong S , Hillier N and Beeby S, 2021).

2.5.4 Electrolyte Materials

Treatment of cotton fabrics with ammonia results in the production of nitrogen-saturated activated carbon cloth with hollow tubular fiber units, high surface area, hierarchical porous structure, and useful surface functional groups, as stated in the research conducted by Dai P et al., 2020. This was accomplished by producing the nitrogen-saturated activated carbon cloth. According to the findings, the organic electrolyte supercapacitors that were based on carbon cloth exhibited a high specific capacitance (up to 215.9 F/g at 1 A/g), as well as an incredibly high-rate capacity (89 percent from 1 A/g to 200 A/g). Due to its low IR drop (0.23V at 100 A/g) and excellent spin stability (98 percent capacitance retention over 20,000 cycles) in N- doped activated carbon fabric, it has been demonstrated that it is resistant to the defectsthat are typically

Universiti Malaya

found in carbon fabrics. As a result, it is utilized in high-density energy storage devices with high levels of both energy and energy density (Zheng C et al., 2012; Tarabella G et al., 2012) (Figure 2.11(A)). Using a single natural cotton fiber doped with a conductive polymer poly (styrene sulfonate) (PEDOT: PSS) by soaking, Tarabella G et al., 2012 investigated its applications as a channel for an organic electrochemical transistor (OECT), in which it reacts directly with a liquid electrolyte in contact with the gate of an Ag wire. The gadget demonstrated current modulation that was both steady and repeatable (Wang Q J and Zhu D, 2013). Theseinvestigations have shown that treated cotton fibers are effective in the electrochemicalsensing of NaCl content in water. This is possible due to the fact that OECT formed with single-wire cotton fibers is a device that is simple and inexpensive (Zhou Q et al., 2015) (Figure 2.11 (B)).

On the other hand, poly (N, N-dimethyl-N-decyl ammonium ethyl methacrylate- co-methacrylamide) (PQDM) and poly (acrylic acid co-meth acrylamide) were two ofthe cationic and anionic N-halamine polymer precursors that were created by Li L et al., 2022 and laminated with cotton textiles using the layer-by-layer (LBL) assembly process. According to the findings, the textiles that had been treated with LBL had potent antibacterial activity and controlled biofilm formation against Gram-positive bacteria, Gram-negative bacteria, and fungus. The LBL-coated cotton textiles are compatible with cells, which is proof of the significant potential of LBL-assembled fabrics for future biomedical applications. This was shown by an in vitro cytocompatibility experiment directed against the cells of mouse fibroblasts. In addition, cotton that has been treated may be used to boost the product's antibacterial and antifungal characteristics. It is used in the formation of two-dimensional fibrous materials by polymeric N-halamine electrolytes (Figure 2.11(C)) (Li L et al., 2022).

A large number of electrolyte-reactive dyes were also developed. These dyes included

Universiti Malaya

one epoxy structure serving as the reactive group and two groups of quaternary ammonium salt functioning as the soluble components. Cotton was subjected to an electrolyte-free dying technique so that proton nuclear magnetic resonance and elemental analysis could be performed, as well as dye's qualities couldbe researched. According to the findings, electrolyte reactive dyes with these structureshave a high rate of both fixing and depletion on cotton, as well as excellent accumulation qualities Zheng C et al., 2012 observed that the stability features of thesedyes were extremely good. The ideal dyeing procedure for these colors was dyeing cotton fiber electrolytes at 60 ˚C with 20 g/L of sodium carbonate. The hub-type lithium-ion battery was invented by Song and colleagues (Song H , Jeon S Y and Jeong Y, 2019), and it consists of a cotton filament wrapped with carbon nanotubes (CNT) and a nanomesh separator. Because of its high conductivity, flexibility, and network structure, CNT film is used as an aggregate material. Cotton yarn not only acts as a reservoir for electrolytes but also provides a skeleton for the fiber itself. Cotton threads absorbed the electrolyte up to nine times their weight and grew up to 20% in diameter, which led to a strong contact between the components of the battery.In order to understand the function of cotton yarn, simulations were run that focused on the swelling behaviour of cotton yarn caused by the absorption of electrolytes. It was helpful to have the nano-mesh spacer there so that one could accommodate the internal deformation that took place while the battery was bent (Figure 2.12). According to the findings, this particular coaxial fiber battery maintained its performance even when subjected to bending or knotting situations. Additionally, it offered 144.82 MWh^3 of volumetric energy density while maintaining a CEC efficiency of almost 95%. Batteries made with flexible fibers have great potential as a power source for wearable electronic devices (Song H, Jeon S Y and Jeong Y, 2019).

Universiti Malaya

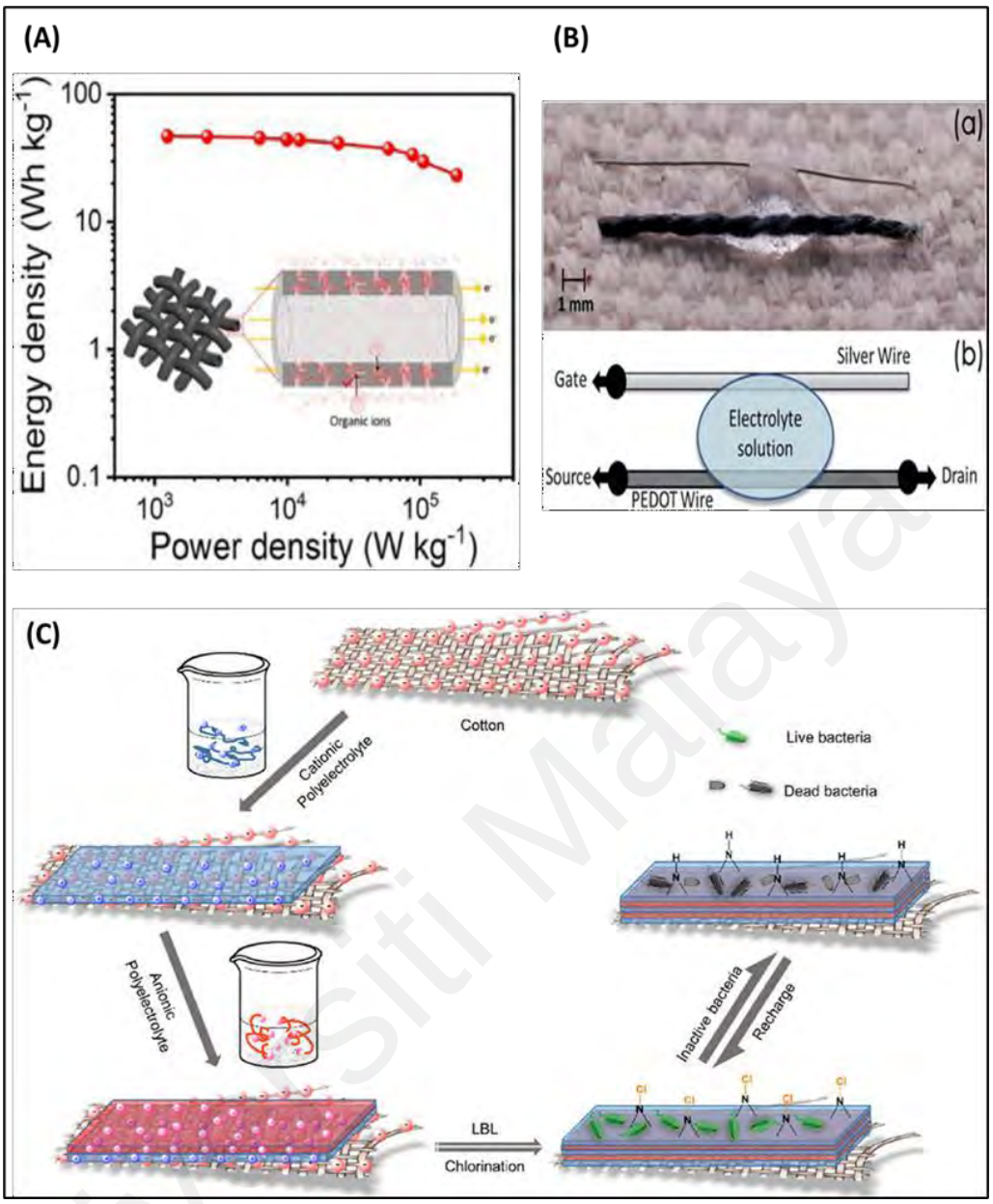

Figure 2.11 : (A) Ultrahigh-power-density supercapacitor in organic electrolyte (Tarabella G et al., 2012) and (Han C G et al., 2017). (B) (a) Organic electrochemical transistor based on a single cotton thread directly integrated into cloth, (b) Schematics of the cotton-OECT (Zhou Q et al., 2015). (C) Schematicillustration of the layer-by-layer technique and the rechargeable inactivationprocess (Yang C et al., 2018).

Universiti Malaya

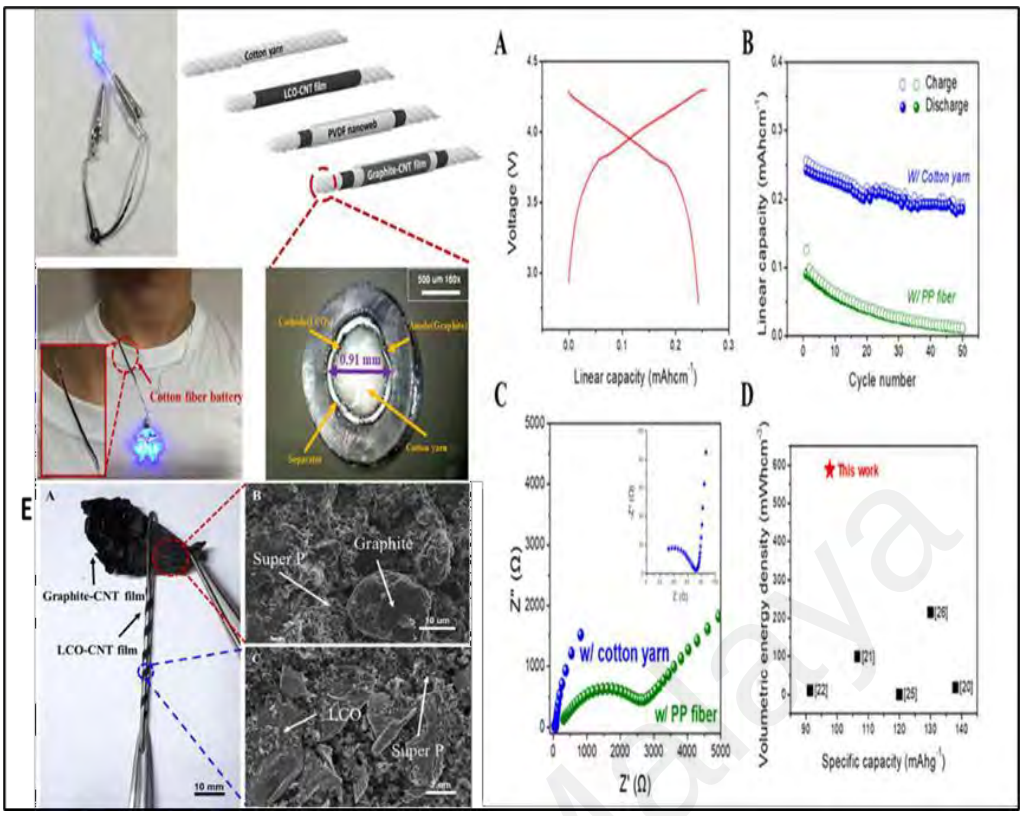

Figure 2.12 : (A) Voltage profiles of the C-FB battery at the 1st cycle (Song H, Jeon S Y and Jeong Y, 2019) . (B) Comparison of cycle performance of C-FB battery and PP-FB battery. (C) Nyquist plots of fiber batteries after 3 cycles in the frequency range from 100 kHz – 100 MHz. (D) Comparison of volumetric energy density and specific capacity with other reported fibre shape batteries. (E) (a) Photograph of the as-prepared graphite-CNT film electrode and the LCO-CNT film electrode, (b)SEM images of as-prepared graphite-CNT film electrode, and (c) LCO-CNT film electrode (He X et al., 2018).

2.5.5 Electrolyte and Electrode Microstructures

The form, size, and distribution of electrolytes, electronic conductors, and active materials are all influenced by hierarchically linked microstructures in order to achieve effective contact between the soft electrodes. electrons and electronic conductors as well as active materials. However, it is not possible to have close contact between theirregular particles owing to the stiffness of the materials. This is as per Hertz contact theory, which simply characterizes the interaction as two elastic spheres of radii R_1 and R_2 under the force (F) (Sun C et al., 2019). E_{eff} is the effective modulus between the sample and the indenter, which is defined as equation (2.5):

University of Malaya

$$\frac{1}{R_e} = \frac{R_1 \pm R_2}{R_1 R_2} \quad (2.3)$$

$$\frac{1}{E'} = \frac{(1-v_1^2)}{E_1} + \frac{(1-v_2^2)}{E_2} \quad (2.4)$$

$$E_{eff} = \frac{(1-v_1^2)}{E_1} + \frac{(1-v_2^2)}{E_2} \quad (2.5)$$

The circular contact region radius (r_0) can be calculated by the equation (2.6) :

$$r_0 = \left(\frac{R_1 R_2}{R_1 + R_2}\right)^{1/3} \frac{3F}{4} \left(1 - \frac{v_1^2}{E_1} + 1 - \frac{v_2^2}{E_2}\right) \quad (2.6)$$

in which E_1 and E_2 are the elastic moduli and υ_1 and υ_2 are the Poisson ratios.

Based on this equation, decreasing *R*, *υ* and *E,* and increasing *F* can result in larger effective contact areas for electrolyte/electrode interfaces.

In batteries, the quality and quantity of the electron and ion transport channels may be determined by the spatial distribution of electrolytes, electronic conductors, and active materials. In ideal distributions, there are generally two requirements thatneed to be satisfied: (i) the amount of active material is large enough to achieve a high energy density, and (ii) the electronic conductor and the electrolyte are connected in series with each other and in simultaneous contact with all of the activematerials. Cotton was turned into a self-contained, conductive, and electrically activefabric by the use of reduced graphene oxide (rGO) by Zhou Q et al., 2015. The flexible supercapacitor demonstrated high capacitance (87.53 $mFcm^{-2}$ at 2 mVs^{-1}), strong electrochemical stability, and outstanding cycle stability (89.82%capacitance retention after 1000 charge-discharge cycles) (90.5% capacitance retention after 100 bending cycles). In order to increase the performance of the supercapacitor, a multi-dimensional device-body and three-

Universiti Malaya

dimensional sandwiches have been constructed. The volumetric capacitance of the rGO/CCF-based dielectric supercapacitor (SIS) is 5.53 Fcm^{-3} with a current density of 0.0625 Acm^3 in an aqueous electrolyte. This is 1.67 and 4.28 orders of magnitude greater than the traditional (SS) and condensedsandwich construction. Figure 2.13(A) and (C) illustrates how the first high- performance electrode SIS supercapacitor paves the way for novel flexible storagedevice applications (Tarabella G et al., 2012).

Carbonization and electrodeposition of supercapacitors were all that was required to produce a flexible polypyrrole/twill carbon fiber (PPy/CCF) electrode, as stated bySun C et al., 2019 in their research work. According to the findings, the electrode displays a high specific capacitance of 3596 $mFcm^{-2}$ with a density of 2 $mAcm^{-2}$, which is almost nine times higher than that of pristine CCF (420 $mFcm^{-2}$). In addition, the electrode demonstrated good rate ability and high stability, retaining 96.5% of itscapacitance after 4000 cycles. The cotton-based CCF substrate has a three-dimensionalhierarchical porous structure, which serves to provide conductive pathways for the rapid transfer of electrons and a large accessible surface area for PPy loading. These excellent electrochemical properties can be attributed to the presence of the cotton- based CCF substrate. It was also noted that the hybrid electrodes exhibited increased electrode diffusion in addition to quick discharge. The built flexible supercapacitor has a high volumetric power of 1.18 mWh^3, which may be ascribed to a drop in capacitancein the bends (Guragain D et al., 2019). Figure 2.13 shows that this high volumetric power is due to a considerable rise in the horn-like substructure (E).

In the research work of Guragain D et al., 2019 a study was conducted on the simple synthesis of Co_3O_4 tubular microstructures utilizing molds, as well as their electrochemical performance as prospective electrode materials for supercapacitors.

Universiti Malaya

Cotton fibers act as a biomould to create the porous and tubular microstructures of Co_3O_4 in this material. The form and organization of cotton fibers are mirrored in thestructure of the compound Co_3O_4. The electrochemical performance of an electrode consisting of a tubular Co_3O_4 structure was investigated in a variety of different aqueous electrolytes such as 3 M KOH, NaOH, and LiOH. The capacitance performance of the Co_3O_4 tubular microstructure was 401 F/g at 1 A/g and 828 F/g at 2 mVs^{-1}. Additionally, the microstructure exhibited remarkable cycle stability, retaining around 80% of its capacity after 5000 cycles. The tubular Co_3O_4 microstructure also exhibited excellent electrochemical performance in 3M KOH electrolyte, with a maximum energy density of 5500 W kg^{-1} and an energy density thatexceeded 22 W kg^{-1}. Due to the fact that it has a wide surface area and holes of varyingsizes, it is able to facilitate redox reactions and the transportation of water ions very well. The surface synthesis process has the potential to be repurposed for use in a variety of fields, including chemical and electrical catalysis, sensor development, andfuel cell production (Babu K F et al., 2009). In order to create conductive textiles, Babu K F et al., 2009 conducted research on cotton fabrics that were treated chemically and also had a chemical coating applied to them. The polypyrrole-coated tissue was electrophoresed at room temperature for four hours using direct current electrolysis at a current density of 2 $mAcm^{-2}$. By using an electrochemical approach, the researchers were able to produce polypyrrole films that were thicker and had a spherical microstructure. The polypyrrole films exhibited a high conductivity, which ranged from 1.9 $x10^{-2}$ to 3.3 x 10^{-1} S/cm. Because of the rise in pyrrole content and the longer electrolysis process, the coated tissue exhibited a greater increase in both its weight absorption and its electrical conductivity. There were a number of additional physical and chemical characteristics of the polypyrrole films that were found to be qualitatively comparable when compared between the two processes (Hong X et al., 2019). In this method, cotton cloth is used to obtain a conductive carbon cloth from hollow carbon fibers

Universiti Malaya

by the acidification treatment method. The conductive cloth thenacts as a flexible substrate for the development of hierarchical SnO_2 nanoclusters through a process that involves a thermal solvent reaction and calcination. In the FCC-coated SnO_2 composite, also known as FCC@SnO_2, the oxygen-containing groups inthe carbon microfibers serve as several anchoring sites for the growth of SnO_2nanoparticles. Additionally, the carbon microfibers serve as conductive channels for the efficient movement of electrons and ions throughout the material. A self-contained electrode in a symmetric bipolar supercapacitor, the composite FCC@SnO_2 has a higher capacitance of 197.7 F/g or 1265.3 $mFcm^{-2}$ at 1 A/g, which is significantly higher than that of FCC 100.3 F/g or 411.2 $mFcm^{-2}$, while its capacity remains 95.5% even after cycling for 5000 cycles at 15 A/g (Figure 2 .14 (A)). The FCC@SnO_2 composite is easier to produce, costs less money, and has the potential to be employedin high-performance supercapacitors as flexible electrodes that can sustain themselves (Hong X et al., 2019).

During the hydrothermal and calcination processes, cotton-like NiO develops on the surface of naked nickel foam. On the other hand, extremely thin NiO nanoflakes form on the surface of graphene-coated nickel foam (Figure 2. 14(B)). After 5000 charge-discharge test cycles, the findings demonstrated a high specificity capacity of 1,782 F/g at 1 A/g and a retention capacity of 90.2% at 1 A/g. Graphene creates verymicro-nanoflakes, which result in massive pseudo capacity because of its wide surface area and plentiful porosity. Graphene catalysis has high electrical conductivity and great interfacial contact. Graphene also forms micro-nanoflakes.

According to the findings of Jinlong L et al., 2017, the one-of-a-kind microstructure feature boosts the inter-electron transfer in the electrode material and improves the diffusion of ions during the process of electrochemical reaction. An electro

Universiti Malaya

polymerization procedure was used by Sun D et al., 2020 to successfully create PPy backbone-like arrays of sea urchins on a cotton electrode. This was done to improve the cyclic stability of supercapacitors. The electrode is a cotton fabric (CF) that has been treated with PVA-co-PE nanofibers (NF) as a flexible (NF/CF) substrate. This kind of fabric is referred to as EPPy-PPy/NF/CF. Due to the super-cyclic stability of PPy forked arrays, the symmetric flexible solid-state EPPy-PPy/NF/CF supercapacitor has impressive cycling stability, with 100% retention after 10,000 cycles at a current density of 4 $mAcm^{-2}$. This is made possible by the ability to shorten ion transport pathways and countercharges, which in turn weakens the stress-induced damage to the PPy structure (Figure 2.15 (A)). There is a significant marketopportunity for the flexible supercapacitor to be used in handheld and wearable electronic devices (Sun D et al., 2020). Figure 2.15 shows that the carbon nanotubesCo_3O_4 were hydrothermally produced and then calcined from cotton, which served as both a bio-mold and a precursor. This research was conducted by Sun D et al., 2019. This achieves its distinctive tube shape and porous characteristics due to the use of octahedral Co_3O_4 nanocrystals with a highly exposed face (111) that are supported on porous carbon nanotubes. According to the findings, the specific capacitance of the biomaterials was measured to be 284.2 F/g at 1 A/g, which is 4.8 times higher than the value measured for virgin Co_3O_4 that had been created without cotton mold. The bio model has inherited both a hierarchically optimized microstructure and a highly specific surface (Sun D et al , 2019). A functional carbonated (FCC) PANI nanocomposite textile may be made using a process that involves vacuum infiltration, however, this approach needs further development. Permeable PANI can be created by soaking the fluid catalytic cracking in a PANI solution that is diluted with water and placing the mixture in a vacuum. A strawberry-like FCC@PANI nanocomposite will be formed after the solvent is removed. On the surface of the fibers, PANI nanoparticles will be incorporated into these nanocomposites. When PANI loading is as high as 28.1% of

Universiti Malaya

the total weight of the sample. This is a new technique which may effectively prevent the production and agglomeration of PANI nanofibers. The FCC@PANI compound, when used as electrodes in symmetric supercapacitors, shows a maximum capacitance of 350.8 F/g(1859.2 $mFcm^{-2}$) at 1 A/g and a high-capacity retention of 90.8% /10,000 cycles.

Additionally, the compound has an excellent rate of high-capacity retention (Sun D et al., 2019). Figure 2.15(C) is able to illustrates the goal achieved as a result of itslow internal resistance, quick electron/ion transport, and robust inter-bonding interaction. According to Hong X et al., 2021, the vacuum infiltration approach offers good potential for the preparation of large-scale composite carbon fabrics/PANI electrodes because of its simplicity of operation and scalability.

Universiti Malaya

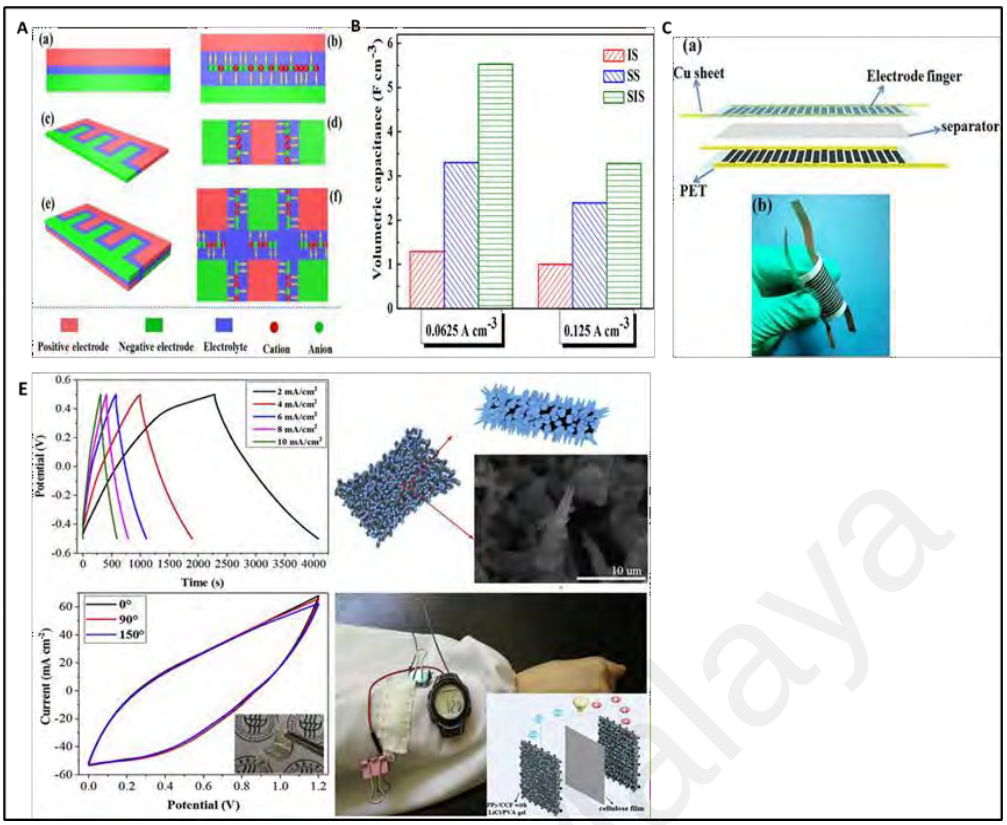

Figure 2.13 : (A) Diagrams of supercapacitors based on three types of device structures: (a) an SS supercapacitor and (b) the model of ions electrosorption shows that only the upper surface (or lower-surface) of the electrode is accessible to electrolyte ions; (c) an IS supercapacitor and (d) the model of ions electrosorption shows that only the electrode finger's two side-surfaces are accessible to electrolyte ions; (e) a SIS supercapacitor and (f) the model of ions electrosorption shows that each electrode finger's upper-surface (or lower-surface) and two side-surfaces are all accessible to electrolyte ions (Guragain D et al., 2019). (B)The volumetric capacitance values of the IS, SS and SIS supercapacitors obtained at different current densities; C20. (E) Flow diagram for the fabrication of electrode materials and all-solid-state (Zhou Q et al., 2015) and (Wang Q J and Zhu D, 2013).

University of Malaya

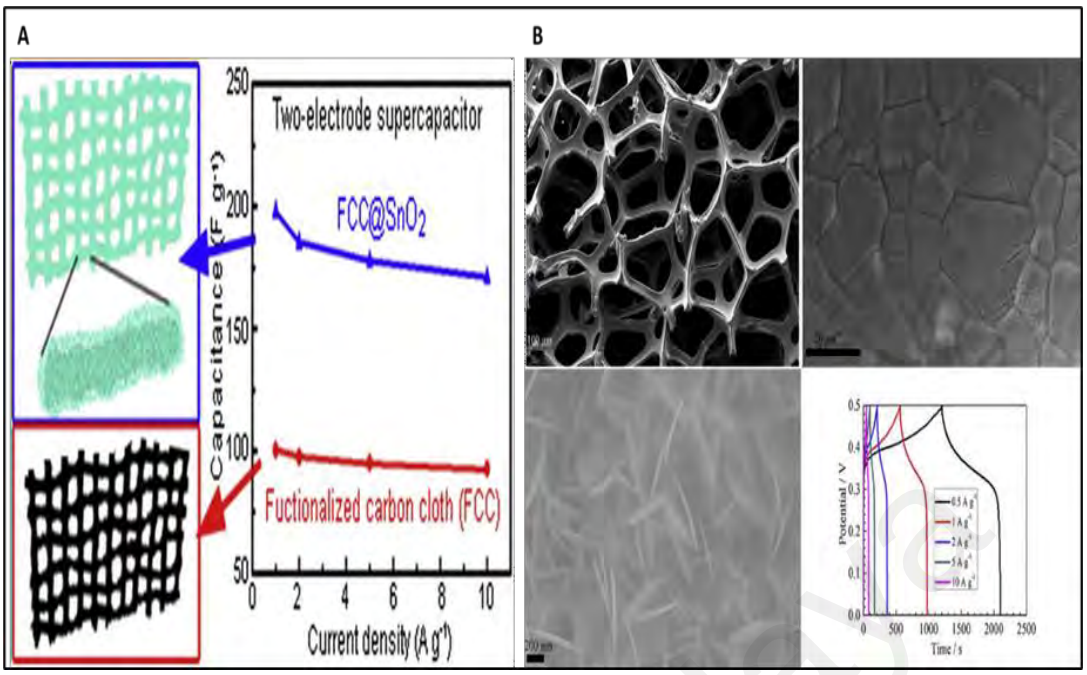

Figure 2.14 : (A) Acidified carbonized cotton cloth is acted as a freestanding flexible substrate (Hong X et al., 2019) and (Zhou Q et al., 2015). (B) The effect of graphene coated nickel foam on the microstructures of NiO (Jinlong L et al., 2017).

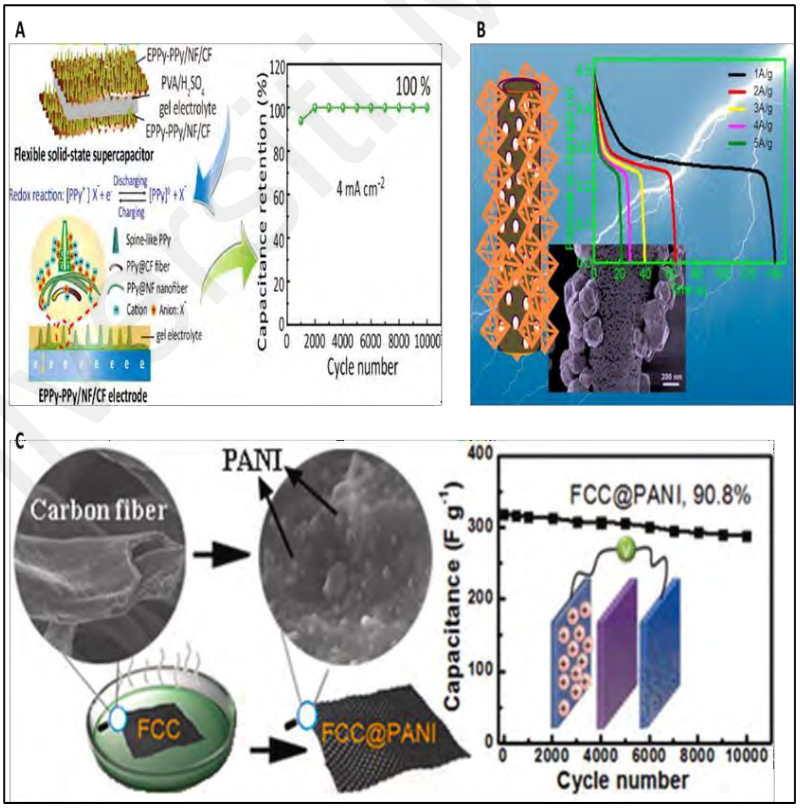

Figure 2.15 : (A) The construction of sea urchin spines-like polypyrrole arrays on cotton-based fabric electrode (Sun D et al., 2020) and (Hong X et al., 2019). (B) Biomorphic composite was prepared via a simple cotton-assisted hydrothermal route(Jinlong L et al., 2017). (C) Strawberry-like carbonized cotton cloth/Polyaniline nanocomposite (Jinlong L et al.,2017).

Universiti Malaya

2.6 Cotton Dendrite Formation at Electrolyte/ Electrode Interfaces

The electrolyte/electrode interfaces need a more sophisticated approach than that employed in liquid organic electrolyte batteries i.e. a solid-state connection. The poor electrolyte/electrode interfacial contact in these batteries may be attributed to stress cracking and poor electrolyte/electrode microstructures induced by various cyclic electrode diameters. Because the charge transfer area is reduced, this produces an increase in internal resistance, which in turn causes an increase in the batteries' internal resistance **(**Jinlong L et al., 2017).

The reduction in interfacial resistance that resulted from the addition of a layer of cotton cloth-derived carbon tubes (DCTs) to the surface of the solid Al_2O_3 (BASE) electrolyte is shown in Figure 2.16 (A) (Wu T et al., 2018). DCT-modified BASE by sodium results in the uniform and quick transport of Na^+ ions over the interface. This results in a considerable reduction in the interfacial resistance from 750 cm^{-2} to 150 cm^{-2} and demonstrates stable Na stripping/plating patterns at 58 degrees Celsius.

According to the findings, solid sodium batteries with a sodium anode, DCT-BASE, and $Na_3V_2(PO_4)_3$ (NVP) compound gel cathode, was successfully operated at 58 degrees Celsius that demonstrate a high level of efficiency and strong spinning performance. Furthermore, it has been shown that the self-supported DCT electrode material is capable of reversible, stable, and quick insertion and extraction of sodiumions in NIBs (Wu T et al., 2018). The fabrication of environmentally friendly electrodes employing a carbon cloth made from cotton and containing functional groups as a host for lithium precipitation has been the subject of research. Even at high current rates, the cotton-derived carbon cloth (C-400) containing Li^+ functionalgroups stimulate the production of a homogeneous and dense Li deposition in the host structure. This prevents Li deposition

Universiti Malaya

from occurring on the surface of the C-400. Additionally, the three-dimensional linked skeleton of the C-400 may maintainthe original size of the electrodes throughout the cycling process. Therefore, the C- 400 electrode is capable of providing a high areal capacitance of more than 10 $mAcm^{-2}$ without giving rise to the formation of Li dendrites. The results show that improvements have been made in the use of C-400 Li anode in lithium batteries with$LiNi_{0.8}Co_{0.15}Al_{0.05}O_2$ cathode and shown in Figure 2.16(B) in terms of retention capacity, voltage polarization, and rate capacity as compared to the bare Li anode(Meng J K et al., 2020).

Because water-induced corrosion cannot be meticulously regulated, the presence ofthe zinc metal anode in aqueous zinc ion batteries (AZIBs) inhibits dendrite formation.This results in a considerable loss in colic efficiency (CE) and a limited life for the battery. To find a solution to these issues, an innovative membrane called cellulose nano-graphene (CNG) that has dual functionalities, was developed. The findings of both experimental analysis and molecular dynamics modelling demonstrated that the presence of CNG film, which acts as a melting layer to block H_2O molecules from coming into contact with the zinc anode, inhibits the corrosion reaction that is produced by water. In order to get a redirected Zn precipitation parallel to the Zn (002) level, a deionization shock is generated at the same time by the CNG layer, which hasnegative surface charges. This shock is caused by the diffusion of cations and anions. In addition, the coating and stripping processes cause the flexible and tensile CNG film to absorb the zinc anode surface variation, which results in a high tensile force (8.54 N) and a significant piercing force (0.10 N). As a consequence of this, the cyclelife of the CNG/Zn CE anode is enhanced by 99.4% and is longer than that of the bareZn anode by about 5500 hours. This represents a difference of more than 27 times. Thecomplete MnO_2/graphene-CNG/Zn battery not only has a high discharge capacity (307mAh), but it also maintains 87.8% of its high capacity

Universiti Malaya

after 5000 cycles when the temperature is 5 ˚C (Zhang, X et al., 2021).

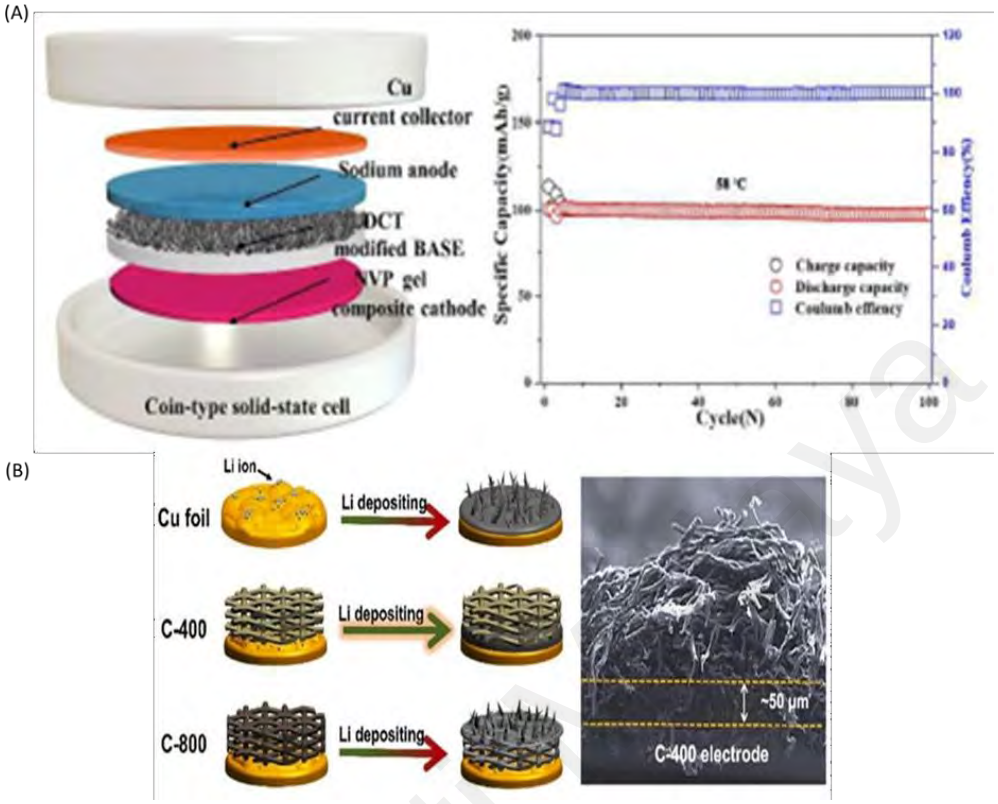

Figure 2.16 : (A) Electrochemical performance of full cells paired with NVP cathodes (Wu T et al., 2018) . (a) Schematic of the full cell structure (Zhou Q et al., 2015; Sun D et al., 2020). (B) Schematic diagrams of Li deposition on the bare Cu foil (a), C-400 electrode (b) and C-800 electro (Meng J K et al., 2020).

2.6.1 Cotton Dendrite Growth into Electrolytes

According to Wang T et al., 2020, a particular protein has been found that effectively inhibits and eliminates the formation of weak lithium dendrites. This enables cotton-containing lithium metal anodes to have a long-life cycle and high C- efficiency. The protein molecules function as "self-defense" agents, preventing the creation of lithium embryos and imitating to some extent, the abnormal natural immune response processes. After being mixed with the electrolyte, protein moleculesundergo a transformation in their spatial morphology and secondary structure, changing from a helical to a sheet-like configuration.

This causes them to spontaneously adsorb on the surface of highly absorbent lithium

metal anodes, particularly on the tips of lithium buds. Because of this, the electric field distribution around the tips of the lithium buds is effectively altered, which leads to the formation of a homogenous coating and the deamination of the Li-metal anodes. This enables to overcome the limited dispersion of protein in the ether-based electrolyte and achieve significantly improved cycling performance of more than 2,000 cycles in lithium-metal batteries (Wang T et al., 2020). This was made possible by the fact that one could overcome the limited dispersion of protein in the electrolyte. Cotton, glycerol, and tetraethyl orthosilicate may be combined in a hydrogel solution by following a process that is both simple and economical. This approach forms a complete hydrogel. According to the findings, the hydrogel solution has strong ionic conductivity, great mechanical characteristics, a very low freezing point, a good capacity to self-heal, high adhesion, and a good ability to withstand heat. When compared to aqueous electrolytes, the hydrogel has the ability to prevent zinc dendrites from developing and parasitic side reactions from occurringbetween temperatures of -40 ˚C and 60 ˚C. It is possible to create a flexible semi- solid Zn–MnO_2 battery by making use of this hydrogel electrolyte. This battery has an energy density in the range of -40 ˚C to 60 ˚C and has a high level of endurance under a variety of challenging settings and excellent durability when riding.

A Li-type composite Ag-NOCP@Li anode was constructed by Chen and colleagues (Chen M et al., 2021). This was accomplished by leaking Li into a three-dimensional carbon host that was coated with N, O, and Ag on cotton pads (Lu C et al., 2021). The host affinity of three-dimensional carbon for lithium may be improved by the insertion of numerous photophilic atoms. A superb Li^+ conductor and electronic insulator, in situ composite anode Li_3N ornamentation, is produced byinfiltration of molten lithium, which results in its generation. According to the findings, the locations containing thermal nitrogen are the ones responsible for the formation of Li_3N (Figure 2.17(A)). Li_3N with

favorable mechanical strength and an ultrafast Li^+ diffusion rate may significantly accelerate the kinetics of Li transport and reduction, hence preventing dendritic formation. This is because Li_3N has an ultrafast Li^+ diffusion rate. In addition to this, Ag-NOCP nanofibers have hierarchical pores and numerous micro channels across their interiors. It enables quick Li^+ diffusion and reduces scaling over extended cycles since the Ag- NOCP@Li electrode is able to maintain a constant cycle for 1400 hours at 1.0 mA cm^2/1.0 mA cm^2 despite the fact that it has a high current density. According to the findings, entire cells that make use of the Ag anode-NOCP@Li connected to a $LiFePO_4$ and $LiNi_{0.5}Co_{0.2}Mn_{0.3}O_2$ cathode have a long-term cyclic stability of up to 400 cycles when tested at temperatures of 0.5˚C and 1.0˚C (Huang X et al., 2019).A nickel (Ni) framework with a textured structure is produced as a current collector for a metallic Li anode by using a simple bio-mold method from cotton fiber with a one-of-a-kind micro-nano hierarchical structure that is suitable for Li assimilation, this is demonstrated in Figure 2.17(B). Due to the one-of-a-kind design of the structure, the test results demonstrated satisfactory performance after more than 200 cycles of repeated Li coating and stripping at a current density of 3 $mAcm^{-2}$. Zhu R et al., 2020 achieved a cross-linked and reversed Li metal anode by uniformly introducing more Ag_2S nanoparticles into the current collector. This resulted in the anode exhibiting low over potentials (24 mV at 1 $mAcm^{-2}$), high CE (98%), and excellent fast charge/discharge stability (up to 350 cycles at 10 $mAcm^{-2}$ in an identical cell).

Universiti Malaya

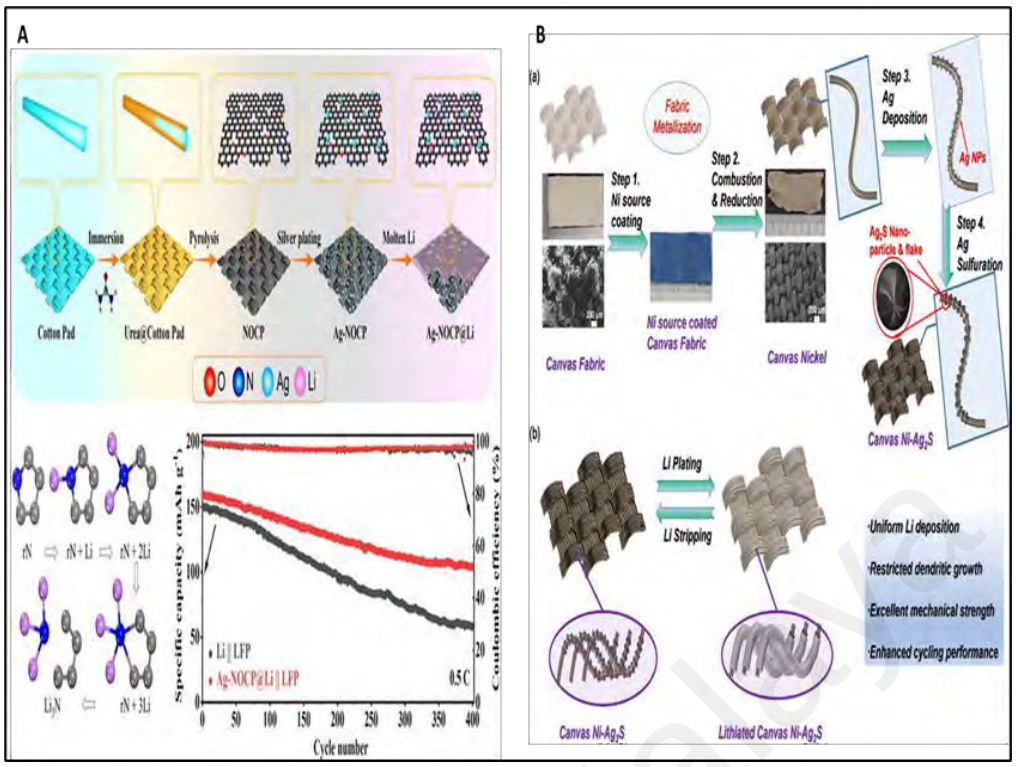

Figure 2.17 : (A) 3D lithophilic carbon host derived from cotton pad is designed for Li metal anode and Ionic conductive Li_3N (Lu C et al., 2021). (B) (a) Scheme of the preparation of Canvas-Ni and Canvas Ni-Ag_2S frameworks, (b) Graphical representation of the uniform electrodeposition behaviour (Huang X et al., 2019).

2.6.2 Cotton Dendrite Nucleation and Growth inside Electrolytes

It was possible to create a highly-stable, branchless Li metal anode using a three-dimensional (3D) conductive cotton scaffold containing rock-cut $NiCo_2O_4$ nanorods grown on nickel foam (LNCO/Ni). The lithium metal served as the anode in a device prepared by Wang Z et al., 2021. Large surface areas reduce the average electric current in electrodes, and a grained surface provided by the Li_2O coating on $NiCo_2O_4$nanorods makes it possible to perform stable Li lamination/stripping without the growth of lithium branches at current densities as high as the industry standard of 5 $mA.cm^{-2}$. High CE (98.7%), low hysteresis (16 mV), and stable cycle for more than 500 cycles (1000 hours) at 1 $mAcm^{-2}$ for the LNCO/Ni-Li anode have been shown. The anode was exposed to a current density of 1 $mAcm^{-2}$ to achieve these outcomes. To be more precise, no dendrite development or variations in electrode thickness wereobserved when a 20 m Ahg cm^{-2}

Universiti Malaya

extendable Li loading was applied to LNCO/Ni. Therewas no indication of the production of Li dendrites or the electrode's thickness changing. $LiFePO_4$ and LNCO/Ni-Li serve as the cathode and anode, respectively, ofthis cell, which has shown high-rate capability and CE of up to 99.6% for more than 160 cycles (Huang, X et al., 2019).

Utilizing a biologically-derived hollow carbon fiber fabric with hierarchical porosity, Wang Z et al., 2021 displayed the "outside-in" Li deposition behaviour in two phases. This is accomplished by using the term "outside-in". Due to the huge number of lithophile-compatible holes, the findings revealed that Li deposition occursfirst on the outer surface of the hollow carbon fibers. This occurs via deposition insidethe hollow carbon fibers as well as on the wall of the hollow carbon fibers. This mechanism occurs due to the pores in the woven carbon fiber, which act as a stable and robust host for uniform Li deposition, this mechanism is presented in Figure 2.18 (A). On the other hand, the composite Li anode demonstrates high coulombic efficiency for more than 500 cycles and high cycle stability for more than 1,400 hoursat a current density of 1 $mAcm^{-2}$. This study contributes to a new understanding of therole of the porosity structure in cotton fabric as well as its contribution to the design and synthesis of carbon-based materials that may serve as anode hosts (Wang Z et al., 2021).

On the other hand, in the hunt for batteries that are intrinsically safe, inexpensive,and kind to the environment, Zn-ion aqueous batteries (ZIBs) have showed considerable promise for flexible and wearable electronic devices. The fact that ZIB flexible instruments do not have an electrolyte that is both stable and permanent, presents a significant challenge for their usage in environments that are very severe. By combining a xanthan gum-polyacrylamide (XG-PAM) grafted copolymer with cellulose cotton nanofiber (CNF) using XG-PAM/CNF, researchers were able to produce a stable

Universiti Malaya

hydrogel electrolyte. This was described by Wang Z et al., 2021 in their research work . According to the findings, the XG-PAM/CNF hydrogel solutionthat was created. has excellent ionic conductivity (28.8 $mScm^{-1}$), strong ionic absorption, good adhesion, and high mechanical strength. Additionally, it demonstrates the influence that inhibition has on the development of dendrites. As can be seen in Figure 2.18 (B), the flexible ZIBs that were made using the XG– PAM/CNF hydrogel were able to obtain a high specific capacity of 237 $mAHg^{-1}$ and great rotational stability of 86.2% pretention over 1000 cycles at 4 °C. The bendable ZIBs are able to survive severe circumstances, such as folding, bending, pressing, soaking, cleaning, and even being used underwater. Therefore, the work presented here proposes a unique technique and application for the creation of energystorage devices that are dependable, durable, and wearable (Wang B et al., 2020). The use of these devices is in the context of an underwater rescue system.

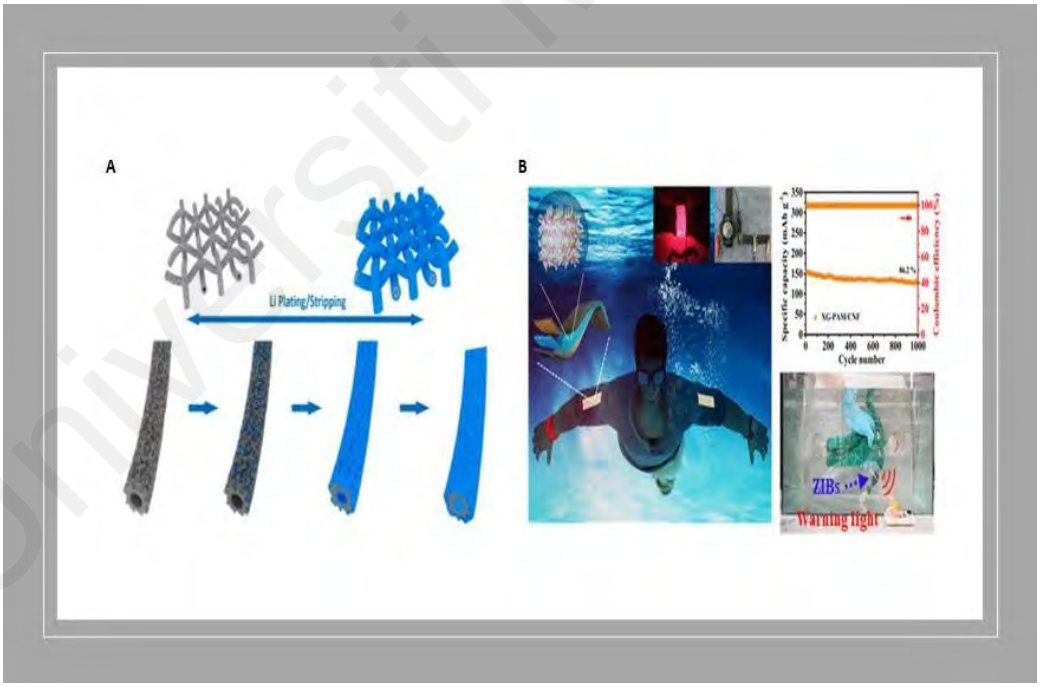

Figure 2.18 : (A) Naturally derived cotton textile for preparing three-dimensional porous lithium hosts (Wang Z et al., 2021). (B) Stable Hydrogel Electrolytes for Flexible and Submarine-Use Zn-Ion Batteries (Wang B et al., 2020).

2.6.3 State of charge estimation for lithium-ion battery

Lithium-ion batteries are used in all walks of life for many aspects related to the environment and resources. Accurate State of Charge (SOC) estimation ensures proper

Universiti Malaya

battery operation. Few methods have focused on the problem of SOC estimation in different circumstances.

The remaining useful life shows an extraordinary function in guiding the replacement of supercapacitors that reach the maximum service life, which is of greatimportance to the security and stability of the energy storage system. In order to estimate the residual life of the supercapacitors so as to ensure the reliability of the supercapacitor bank, a time convolutional network is used. The residual block can address the problems of gradient bursting and disappearing in a recurrent neural network. By using the early stop technique to avoid overfitting, Adam's algorithm improves parameter tuning of the temporal convolutional network. And using the capacitive dilution data set for supercapacitors to verify the stability and accuracy of the model prediction. The results show that the temporal convolutional network modelhas high accuracy in estimating the residual useful life of supercapacitors, as well as strong robustness (Liu C et al., 2022). The stability of the small signal of a network- connected virtual synchronous generator was studied by Lu S et al., 2022. Through small signal models, single-VSG and multi-VSG networked systems are made. Then the Eigen values were obtained by solving the state matrix, and the oscillatory modes of the system were analyzed by using the eigenvalue analysis method to analyze the effects of parameter changes, k, line resistance, the virtual moment of inertia, line inductance, and default damping coefficient on system stability. Virtual synchronous generator (VSG) technology is used to simulate the external characteristics of a synchronous generator (SG) providing some damping and inertia for power systems. On the other hand, it may simply cause low frequency oscillation of the power system. By Cui Z et al., 2022 a hybrid method based on CNN-BWGRU network has been demonstrated. The method improves the impact of battery information on the results by means of a "multi-moment input" structure and a bidirectional network. Whereas, a

Universiti Malaya

convolutional neural network (CNN) is used to learn the feature parameters in the input. With the Bi-Directional Weighted Repeater Unit (BWGRU), the performance of the network installation under different conditions such as low temperatures can beimproved by changing the weights. The network has generalizability, robustness, and estimation accuracy. SOC estimation is performed under various conditions to check the reasonableness of the network. The results showed that the proposed network method has higher accuracy and stability than other networks. Moreover, this methodcan overcome the effect of different initial SOC on the estimation results. Therefore, CNN-BWGRU provides an exemplary method for estimating a battery's SOC with thepotential to provide useful guidance for safe and stable battery operation in natural environments.

A machine learning and adaptive monitor method for battery SOC estimation have been devised by Shen H et al., 2022. Transformer neural network is used as input to predict SOC with current, voltage and temperature data sequences. An innovative Immersion and Stability I&I (Immersion and Invariance) adaptive controller is then applied to reduce transducer prediction vibrations. The Transformernetwork command has the advantage that it contains an overview of the entire input sequence and obtains more important information than other traditional neural networks. Furthermore, the adaptive controller I&I is qualified to correct potentiallearning fluctuations and ensure that the battery parameter estimation error is confined within a static manifold. The results demonstrate a high accuracy of SOCestimation compared to the common baseline method (Figure 2.19 (a)).

The state of health of the (SOH) is critical to the efficient use of lithium-ion batteries (LIBs). Through (Li et al, 2022) an electrochemical impedance spectroscopy (EIS)-based SOH estimation approach was used and proved to be effective. Two models for estimating SOH were made based on the ECM method, where various combinations of ECMs are

Universiti Malaya

imposed. Through EIS the ECM can be predicted, the results demonstrate that this improved approach ensures the validity ofthe ECM and improves the results of SOH estimation. By using a data-driven algorithm, a convolution neural network (CNN) proposes to process EIS data, extractkey points, and simplify the complexity of feature extraction all manually (Figure 2.19 (b)). The bi-directional long-term memory model (BiLSTM) was also used to estimate and calculate the sequential regression. They also proposed a particle swarming optimization (IPSO) algorithm that improves the model. By comparing theimproved model (IPSO-CNN-BiLSTM) with the conventional PSO-CNN-BiLSTM, CNN-BiLSTM and LSTM models, the results showed a prediction improvement of 13.6%, 93.75% and 94.8%, respectively. There are two methods for estimating SoH (state of health) by EIS (Solid Electrolyte Interphase) based on data-driven method, which are based on ECM method and deep learning (Table 2.1).

Universiti Malaya

Table 2.1 : Typical studies on predicting SOH based on EIS.

Method	Remarks	Ref.
model method	EIS Measurements for Determining the SoC and SoH of Li-Ion Batteries	(Mingant R et al., 2011)
model method	Prove the relationship between Rsei and SOH	(Xiong R et al., 2017)
model method	Prove the relationship between Rct , T and SOC	(Wang X et al., 2019)
model method	prove the relationship between Rct and SOH	(Zhang Q et al., 2022)
data-driven method	The measure is done to get the SOH of the lithium ion battery	(Wang, H et al., 2011)
data-driven method	EIS and CS-Elman model preparation	(Chang C et al., 2022)
data-driven method	Model design of EIS and RNNs	(Eddahech A et al., 2021)
data-driven method	EIS and CNN model preparation	(Pradyumna T et al., 2022)
model and data-driven method	Using ANN to estimate equivalent circuit parameters	(Li Y et al., 2020)

Universiti Malaya

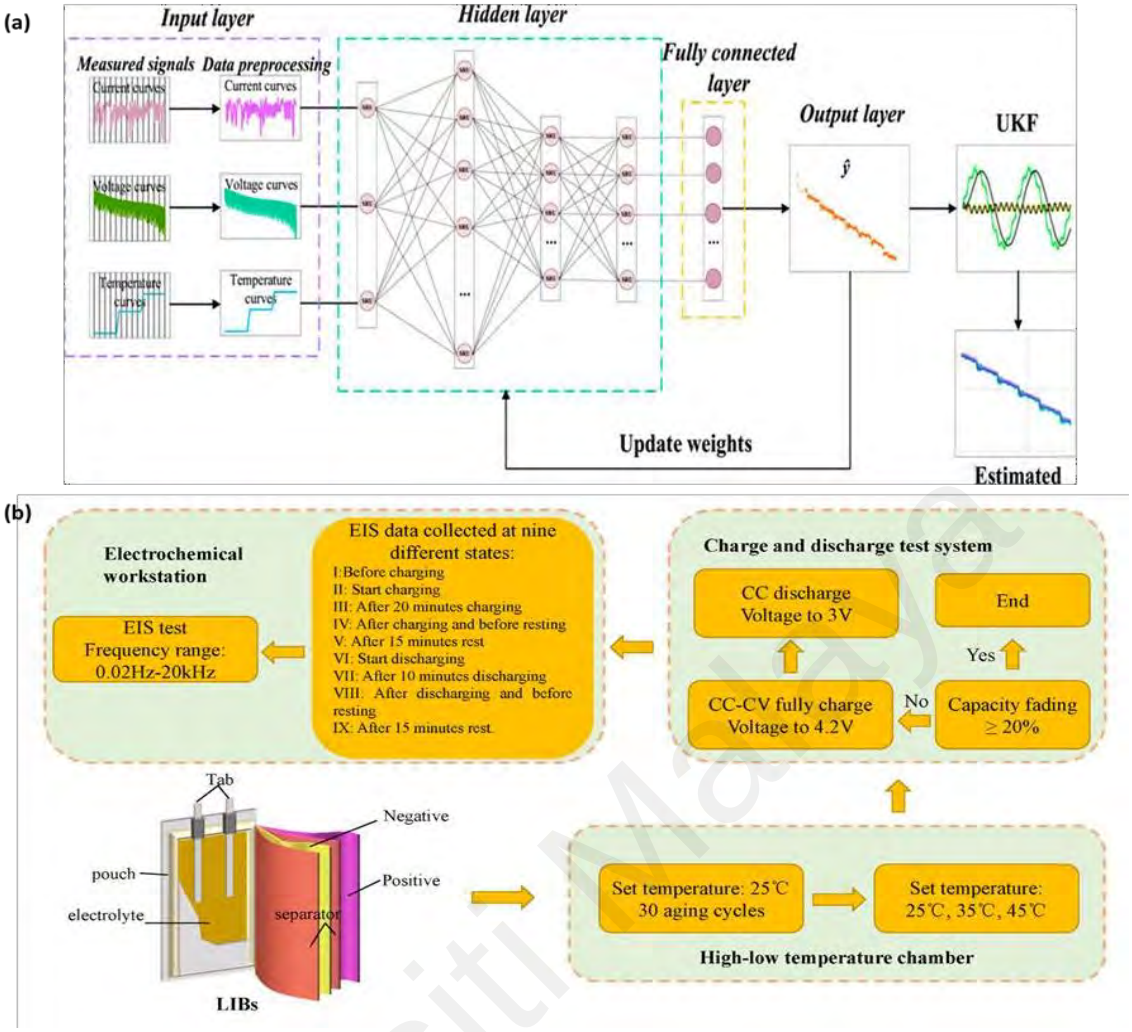

Figure 2.19 : (a) the structure for SOC estimation of the lithium-ion battery (ShenH et al., 2022). And (b)Aging and EIS impedance test diagram (Electrochemical K et al., 2022).

2.7 Advanced Battery Technologies for Energy Storage Devices

Energy storage technologies provide valuable advantages to improve energy quality stability as well as supply reliability.

Battery technologies have improved significantly to meet the challenges of practical electric vehicles and various applications. Currently, flywheel technologies are used in advanced and polluting uninterruptible power supplies.

Universiti Malaya

Capacitors are energy storage that is used in energy quality applications. Cotton- based flexible batteries are the main power source to enable flexible devices, which have other requirements, such as stretching, thinning, bending and torsion, to adapt tomechanical deformation under different working conditions.

Activated cotton twill (ACT) based porous tubular fibers, fused with NiS_2 nano-pots and wrapped with conductive graphene sheets (ACT/NiS_2-graphene) were produced through simple two-step heat treatment by Gao Z et al., 2015. The electrochemical performance of the ACT/NiS_2-graphene electrode was exceptional when used as a bond-free electrode; as it showed a high initial discharge capacity (~1710 mA g^{-1} at 0.01 °C), and the discharge capacity was maintained at 645 mA. g^{-1} at 1 °C after 100 cycles and excellent cyclic stability (it can recover discharge capacity to -1016 mAh after 400 cycles at 0.1 °C). According to the studies by Zhou W et al., 2014, porous core and veneer carbon mixtures were manufactured by an acid oxidation treatment. The results showed that the resulting porous core carbon parts had goodelectrochemical performance and excellent mechanical properties, with an estimated capacity of 20.4 F/g and a current density of 1 A/g based on the core device (0.41 Fcm^{-1}), as well as having good cyclic stability (~96% capacity retention) after 3000 charge-discharge cycles at 1 g^{-1}). Commercial pen ink was used as the active electrodematerial. As shown in Figure 2.20 (a), by simple dipping process, symmetric LM withNE scattering and strong adhesion on substrates can be achieved (Dai S et al., 2014).

On the other hand, carbon nanotube (CNT) filaments are one of the carbon-based filaments produced by dry and wet spinning, which has attracted great interest in thefield of energy storage due to its high electrical conductivity and excellent mechanical properties. Moreover, it is highly flexible, as studied by Dalton A B etal., 2003 by means

Universiti Malaya

of two twisted carbon nanotubes, a wire-shaped supercapacitor (WSS) was produced and shown to be woven into textiles. It is worth noting, that this is a big challenge for "Passive Infrared"

PIR wires and supercapacitors not only due to the high electrochemical performance but also due to the high extensibility, which is very important inelectronic textiles (Figure 2.20 (b)).

Pure cotton textiles can be used as a flexible backing for electroactive materials with excellent flexibility, high mechanical strength and low cost. Due to its high porosity, large surface area and presence of hydrophilic functional groups on the fibers, it is an ideal polar material for flexible supercapacitors after encapsulation by conductive carbon loading, (Jost K et al., 2011). The production of a carbon-treated elastomeric textile-based supercapacitor was reported by regular screen printing of porous carbon in cotton (Figure 2.20 (c)). The porous structure of cotton has the abilityto improve the diffusion of ions between the electrodes and the ions. The results showed that the electrodes achieved specific capacities of 85 F/g (0.43 F cm^{-2}) at 1, 200 and 1000^{th} cycles, respectively and excellent cyclic stability over 10,000 cycles.

Universiti Malaya

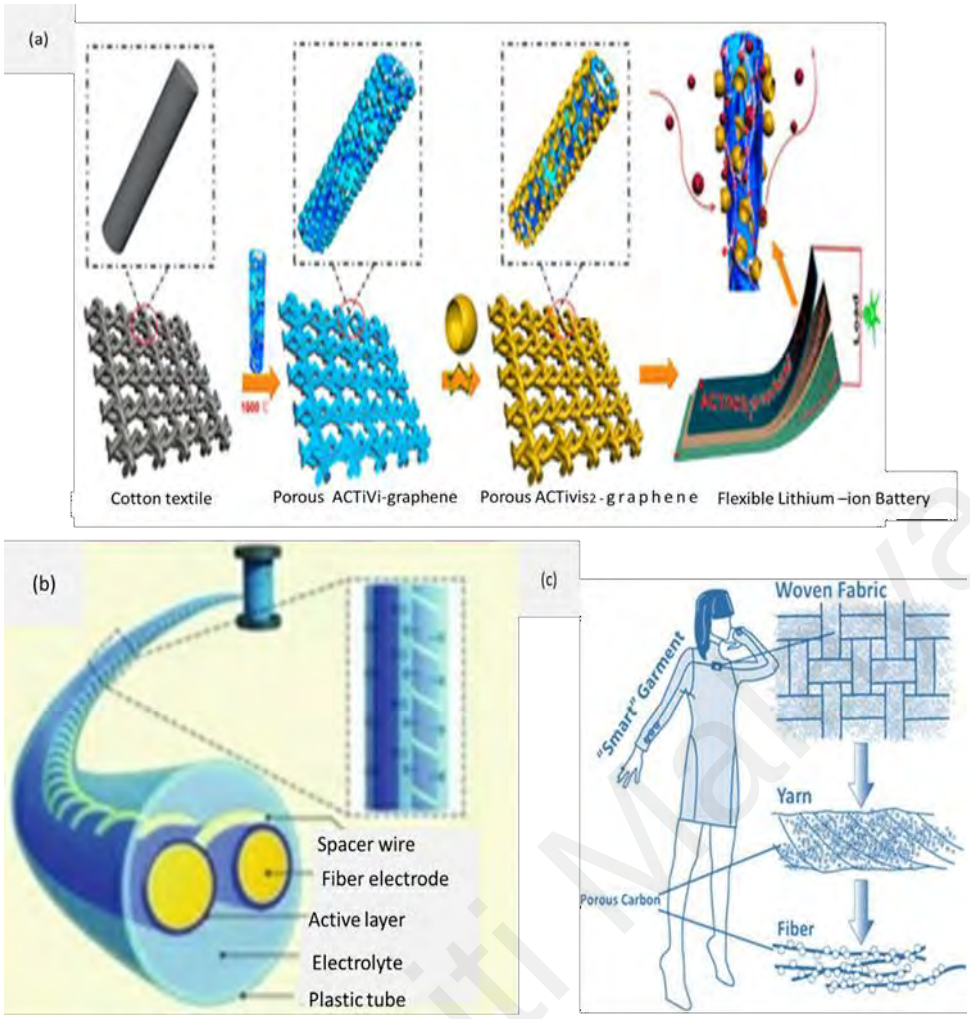

Figure 2.20 : (a) Cotton-Textile, Flexible Lithium-Ion Batteries (Gao Z et al., 2015) (b) Schematic diagram of the fiber supercapacitor (FSC) (Dai S et al., 2014) and Design concept of a porous textile supercapacitor integrated into a smart garment, demonstrating porous carbon impregnation from the weave, to the yarn, to the fibers (Jost K et al., 2011).

2.8 Carbon-based flexible electrodes for flexible supercapacitors

In recent years, there has been a significant progress in flexible supercapacitors,due to rapid growth of the flexible and wearable electronics market. Potassium-based electrochemical energy storage devices (KEES) have received great interest due to their low cost and easy availability of potassium resources (Xu Jie et al., 2021). Due to their excellent qualities, such as their abundance, light weight, and non-toxicity, carbon materials have been utilized extensively as electrode materials or substrates for flexible energy storage devices. In recent times, carbon materials (such as graphene, carbon nanotubes, and carbon nanofibers) have been used in flexible electrochemical potassium

Universiti Malaya

storage devices, including potassium ion batteries, K-S/Se batteries and hybrid potassium ion capacitors.

Xu Y and colleagues produced multichannel CNF by regulating the PMMA/PAN ratio. The fibers formed without the addition of poly (methyl methacrylate) (PMMA) showed a typical smooth surface of PAN-derived CNFs, compared with the polymorphs gradually formed with PMMA addition. (Xu Y et al., 2020) used poly (methyl methacrylate) (PMMA) in poly(acrylonitrile) (PAN) solution to synthesize porous multichannel carbon fibers, through electrospinning followed by carbonization. They were used as anode for Potassium-ion battery (PIB). It demonstrated high electrochemical ability to store potassium.

Controlling the morphology of CNFs made by electrospinning using template methods, Yang W et al., 2019 prepared pyrrolic/pyridinic-N-doped hollow knot-like carbon with hierarchical pores. The mono-dispersed nanospheres of ZnO were mixedwith PAN and N,N-dimethylformamide to make an electrospinning lead. Then, they were electro-spun into a fiber film, and high-temperature pyrolyzed under ammonia (NH_3) and argon (Ar) successively, where ZnO was removed, obtaining hollow, necklace-like carbon fibers. Both pyridine/pyrrolic-N super-doping, large specific surface area, and porosity facilitate (de)intercalation of K^+. This resulted in a high capacity of 293.5 mA h g^{-1} with a current density of 100 mA g^{-1} and an excellent ratecapability of 204.8 mA h g^{-1} at 2000 mA g^{-1} when used as an anode.

Yu Heng Lu et al., 2022 have created 3-dimensional continuous carbon nano networks using tetrakis (4-aminophenyl) methane as the crosslinking agent and polyacrolein-grafted graphene oxide molecular brushes as the building blocks. The

Universiti Malaya

developed materials have been found to have micro-meso-microporous structure. Thishas proven to obtain high surface area and a highly conductive N-doped carbon backbone. Also, large number of exposed active sites have been found and it leads to excellent charge/mass transfer ability.

Using an electrostatic self-assembly and vacuum filtration method, Li X et al., 2021 designed a hybrid membrane of $K_{0.5}V_2O_5$ nanobelt and CNT network. This film was used as cathode in PIBs and its properties were investigated. In K half-cell with potassium as the counter and a reference electrode, $K_{0.5}V_2O_5$/CNT film as cathode andhard carbon anode was tested. The results indicated good specific reversibility, while retaining the rate of performance.

Cheng zeng et al., 2022 fabricated free standing films of potassium titanate (KTO)/sodium titanate (NTO) nanosheets packed between graphene layers. Titanium Carbide (MXene) and rGO were used for the same. The film exhibited outstanding electrochemical performance when flexible KTO/rGO (or PTO/rGO) were used as electrodes. This was due to the unique sandwich packed structure, the short diffusion distance arising from thin Ti based nanosheets and better conductivity due to rGO. Observed reversible capacities for K and N ion batteries using KTO/rGO and NTO/rGO electrodes were 75 mA h g^{-1} at 2 A/g after 700 cycles and 72 mA h g^{-1} at 5 A/g after 10000 cycles, respectively.

Similarly, high-performance composite electrodes made of graphene and other materials, considering the issues of ionic conductivity of large-scale contrast transition metal phosphides, and poor electronic conductivity.

Universiti Malaya

Cheng Zeng et al., 2022 formed a flexible, porous, hierarchical PIB anode by encasing hollow FeP nanoparticles within a three-dimensional graphene framework (3DG/FeP). A reversible capacity of 323 mA h g^{-1} was achieved at 0.1 A /g.

Also, carbon sponge, carbon cloth and carbon foam have been used as highly flexible carbon materials to assemble the electrodes due to their high electrical conductivity, superior mechanical strength, scalability, commercial availability and lots of surfaces to hold the active ingredients. Qiu W et al., 2019 fabricated verticalgraphene doped with nitrogen and phosphorous (N, P-VG) on a carbon cloth uniformly (N, P-VG @CC). It exhibited a capacity of 344.3 mAh g^{-1} when used as abinder-free anode in flexible PIBs. The whole potassium ion battery fabricated on potassium Prussian blue//N, P-VG@CC had an energy density of 232.5 Wh kg^{-1}.

Self-supported VG nanosheet arrays were uniformly grown on a carbon cloth using microwave plasma-enhanced chemical vapor deposition. Then annealing was done in NH_3, mixed with PH_3 (resulting from the decomposition of NaH_2PO_2 H_2O), to dope with N and P. According to the results, N, P-VG @ CC had superior rotation performance and rate. Using N, P-VG@CC as the anode and potassium Prussian blueas the cathode, a flexible whole cell was also put together. It had a capacity decay after 150 cycles of 13.1% and a reversible capacity of 116.25 mAh g^{-1} at 50 mA g^{-1}. Maximum power density and energy density were 4000 W/Kg and 232.5 Wh Kg^{-1}.

Han J et al., 2019 prepared nitrogen-doped CoSb nanoparticles in carbon fibers, (CoSb@C nanofibers). In sodium ion batteries (SIBs) and PIBs, the capacity was measured as 708 mA h g^{-1} (after 200 cycles) and 449 mA h g^{-1} (after 160 cycles) respectively, at 100 mA g^{-1}, rGO/CNT hybrid papers were fabricated by Peng S et al.,

Universiti Malaya

2020 and it was found that electrochemical performance was greatly improved. This was due to a 3D conductive carbon network, where the CNTs made bridges between graphene layers, facilitating the movement of electrons and ions. Restocking was avoided and interlayer gaps in graphene were also increased, providing more space forthe storage of K^- ions. The weight ratio of CNTs was the controlling factor of the electrochemical performance. The findings demonstrated that all rGO/CNT hybrid papers had greater K storage capacity than pure rGO papers at various weight ratios (10%, 20%, and 30%). For rGO/CNT at 30%, 148 mA h g^{-1} capacity at 50 mA g^{-1} wasachieved after 200 cycles, where the starting reversible discharge capacity was 223 mA h g^{-1}.

On the other hand, potassium-ion capacitors having the advantages of the higher energy density of potassium-ion batteries and the higher output power ofsupercapacitors are receiving intense attention due to the abundant resources and record-low oxidation potential of potassium. Potassium ion batteries (PIBs) are a promising candidate in the field of energy storage devices due to the abundance of potassium and they have the advantage of high working voltage and low cost. Lang J et al., 2020 designed a flexible potassium-ion-based hybrid capacitor (PIHC) with a large surface area and structural porosity using the K-Sn alloy method on the Sn anodeand capacitive behaviour on an AC cathode. The results obtained by them for the manufactured Sn/|AC|PIHC had an energy density of 120 W h kg^{-1} and a power densityof 2850 W kg^{-1}. They were able to achieve long cycle stability with almost 100% capacity retention for 2000 cycles at the current density 3.0 A/g . According to Figure 2.21 (a), the Sn|AC|PIHC device has excellent flexibility and strong electrochemical stability, making it a potential candidate for wearable and flexible electronics applications in the future.

Anodes made up of graphite have an enormous capacity to store potassium, but their

Universiti Malaya

capacity soon declines due to large expansion and contraction within the layers(up to 60%) resulting from structural deterioration. Cao B et al., 2021 built a framework for integrated graphite nanostructure/MXene (GNFM) electrodes using Ti_3C_2Tx MXene nanosheets as a bifunctional electron/potassium-ion fast conductor. A 3D channel is created by the continuous MXene framework that rapidly transfers electron/potassium-ions, and provides the GNFM electrodes high structural stability(Figure 2.21(b)). Due to MXene, GNFM electrodes had an improved potassium storage performance over that of conventional polymer bonded electrodes even at higher loads. GNFM electrodes had outstanding cyclability in non-flammable electrolytes. These were used as electrodes to synthesize potassium ion capacitors having exceptional cyclability and high power and high energy density (113.1 W h kg^{-1} and 12.2 kW kg^{-1}, respectively).

Freestanding flexible porous carbon tube (FSF-PCTs) electrode material for PIHCs was used by Dong Wang et al., 2022 to develop symmetrical freestanding potassium-ion hybrid capacitors (SPIHCs). The SPIHCs produced a high energy density of 117.8 W h kg^{-1} and 8109.9 W kg^{-1} (at 39.2 W h kg^{-1}) respectively (at 450 W h kg^{-1}). A good cycle stability of 51 W h kg^{-1} at 1 A/g after 1500 cycles was alsodemonstrated. In addition, full charge was completed in one minute while discharge happened in fifteen minutes, showing fast charging and slow discharging. Systematiccharacterization analysis in half potassium ion batteries (PIBs) revealed that the K^+ storage method in the anode of FSF-PCTs is an associational effect of intercalation and surface capacitance, and the basis of operation of FSF-PCTs as a cathode is the adsorption behavior of $PF6^-$ on its surface (Figure 2.22 (a)).

On the other hand, future applications in flexible electronics could benefit from

Universiti Malaya

transparent flexible supercapacitors (TFSCs), which are an intriguing power source. But their energy density is too low to be useful for practical purposes. Ruijun Bai etal., 2021 reported a transparent, flexible micro-capacitor with potassium ions. Its energy density was much higher compared to TFSC (15.5 μWh cm^{-2}), due to the hybrid method of storage in the battery-supercapacitor, and amplified operating voltage (3V). To get high performance TFSCs, a composite anode was designed which was capable of accumulating energy by the mechanism of simultaneous and reversible absorption of potassium ions and electrons into itself. It also took care of the shortcomings in the functional and structural aspects, thereby creating a 3-D system for efficient diffusion of potassium ions and transport of electrons (Figure 2.22 (b)).

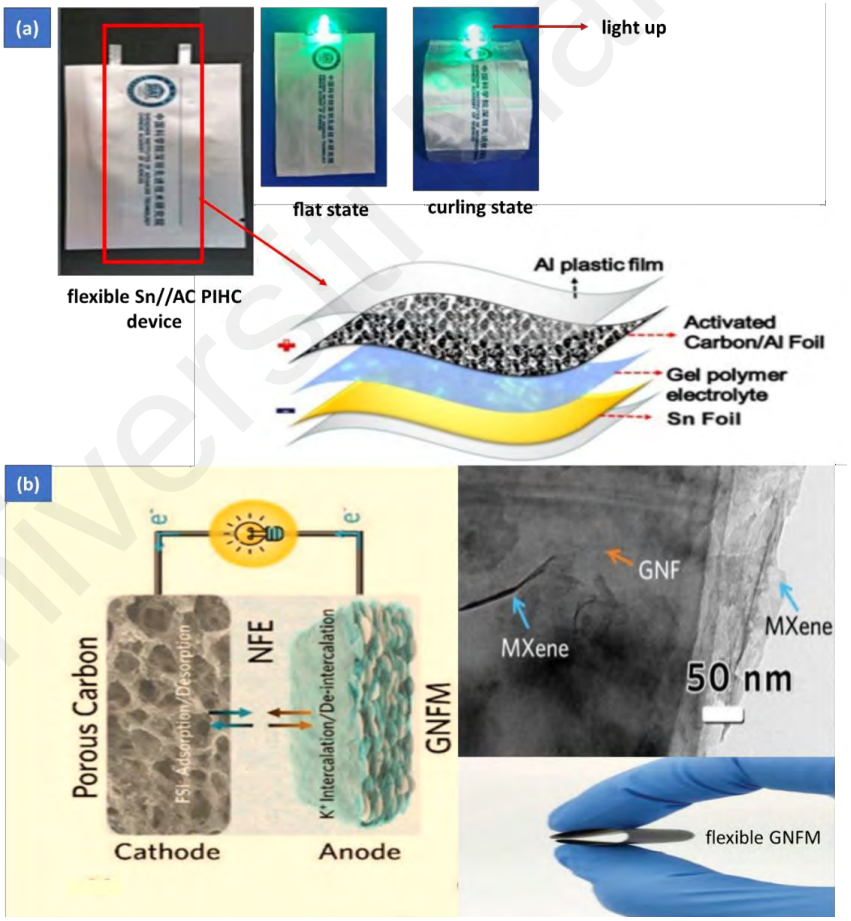

Figure 2.21: (a) Schematic structure of a flexible Sn AC PIHC device (Lang J etal., 2020). (b) NFE is used as the electrolyte, anode, and cathode in a schematic illustration for NFPICs and GNFM, along with porous carbon, HRTEM images, and SAED patterns for the GNFM (Cao B et al., 2021).

Graphite anodes have an enormous capacity to store potassium, however, theircapacity

University of Malaya

quickly fades due to the large expansion and contraction of the interlayer (i.e. up to 60%) resulting from structural degradation.

The 3D polymer gel electrolyte has a high porosity as the structure and high ionic conductivity were used to improve the structural stability of the Sn anode, which achieved good flexibility and long cycle stability with almost 100% capacity retention for 2000 cycles at the highest current density 3.0 A/g.

3D polymer gel electrolyte has high porosity structure and high ionic conductivitywere used to improve the structural stability of the Sn anode, which achieved good flexibility and long cycle stability with almost 100% capacity retention for 2000 cycles at the highest current density 3.0 A/g.

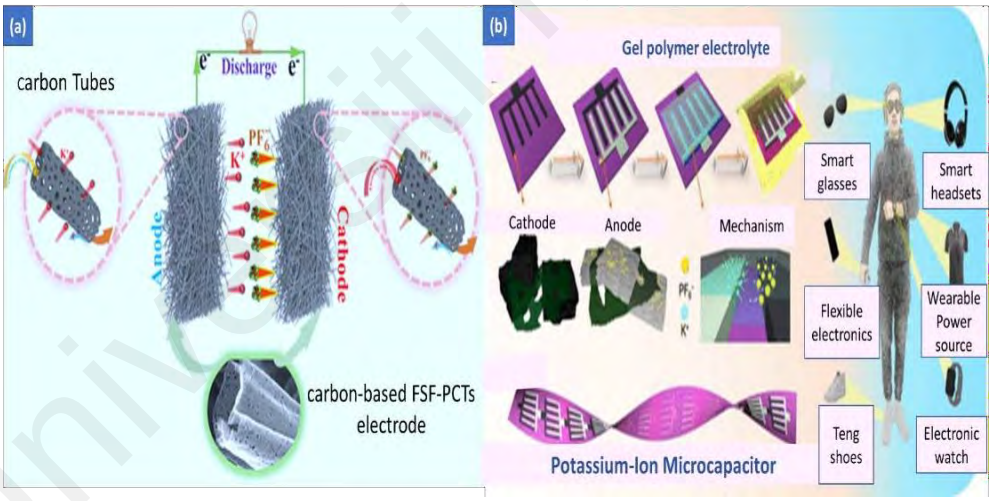

Figure 2.22 : (a) Symmetric Potassium-Ion Hybrid Capacitors with Flexible Electrodes (Dong Wang et al., 2021). (b) Multidimensional host composite anode for flexible potassium-ion-based microcapacitors (Ruijun Bai et al., 2021). On the other hand, potassium ion batteries (PIBs) are widely promising candidates in energy storage applications due to the advantages of abundant resources, high working voltage and low cost.

In recent years, much research is going on to develop new porous carbon materials,

University Malaya

having different formations and functionalities, depending on the polymer structure and availability of new innovative methods of synthesis. The use of porous carbon materials in energy storage is due to their proven structural stability and controllable physiochemical attributes, along with their large porosity and good conductivity. To produce high-performance porous carbon materials, it is very essential to use polymersas precursors, with adjustable physiochemical structures and other desired properties like carbonizability (Liu S et al., 2021).

Huang J et al., 2020 have used a class of molecular-scale porous carbonnanosheets (PCNs), silica, and various metal sulphides (MS/SiOx@PCNs) to create multifunctional coupled 2D porous carbon composites. These composites exhibited large conductivity and small ion diffusion length of porous carbon structure along withlarge storage capacity of sodium, due to MS NPs as well as stopping of polysulfides in SiO_x nanodomains. It was reported that Co_9S_8/SiO_x@PCNs had capacity retention of 94% at 10 A/g even after 5000 cycles, and large rate capability (Figure 2.23).

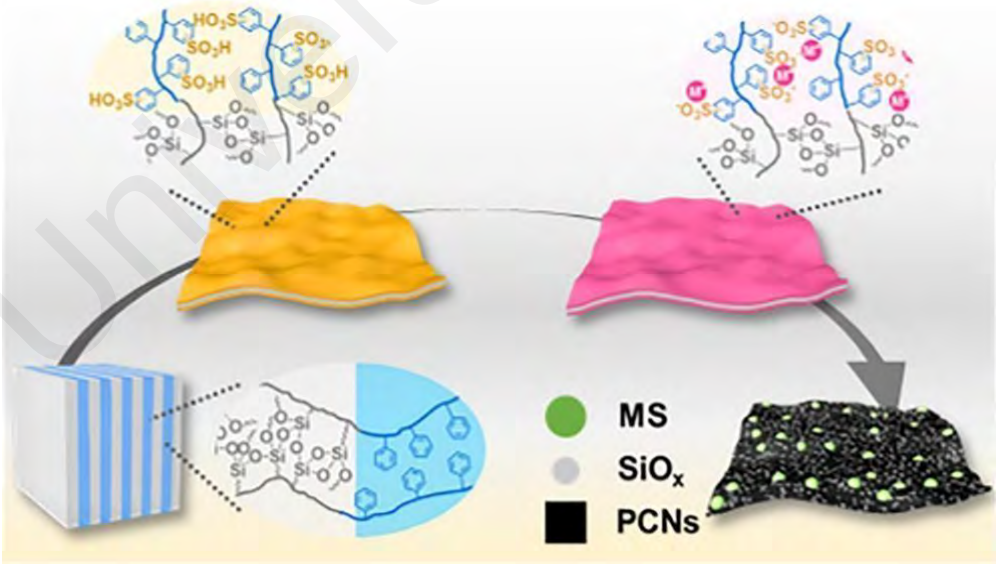

Figure 2.23 : Using Self-Assembled Block Copolymers to Carbonize in a Morphology-Persistent Way, an Illustration of the Synthesis of MS/SiOx@PCNs (Liu S et al., 2021).

Using chitosan and polyacrylic acid implanted Ti_3C_2 MXene, an ordered porouscarbon

aerogel containing TiO_2 NPs was prepared by Shi C et al., 2022. It was filtered, as a useful layer towards a sulfur cathode, in a polypropylene separator. With the altered separators, the Li-S batteries gave a large initial discharge (1439 mAh g^{-1} at 0.1 C) and exceptional rate capacity (502 mA h g^{-1} at 5 C).

2.9 Summary

To provide a brief summary, the current research demonstrates that the use of solid-state electrolytes to provide high safety, high energy density, and extended calendar lifespan may fundamentally solve the safety problem that is present in lithium-ion energy storage systems. In the creation of solid-state batteries (SSBs), itis important to note that, in addition to discover new electrolytes with high ionic conductivity, the scientific challenge of having an in-depth understanding that will lead to the development of controllable solid-state interfaces still needs to be overcome. Various research on cotton-based batteries is presented, along with an emphasis on the implications of and approaches for solid-state battery interfaces, such as electrolyte–electrode interfaces and particle interfaces. The focus has been given to cotton-based materials in energy storage devices.

Universiti Malaya

CHAPTER 3: METHODOLOGY

3.1 Introduction

This chapter provides an outline of the research materials and methods used in the study. It provides information about the materials used and the method of selecting the control sample, and how the samples were prepared and analyzed. It also describes the pure cotton samples and the sample that was chosen for further optimization for electrode and electrolytes. Electrode and electrolyte preparation based on cotton and graphene has been explained in details and the characterization analyses using different analytical method are discussed.

3.2 Materials

The materials/chemicals used in this research are listed in Table 3.1.

Table 3.1 : List of materials/chemicals and CAS No of chemicals used in this research.

Material / Chemical	CAS No.
Gossypium herbaceum	-
Gossypium arboretum pima	-
Gossypium aboretum fabric	-
Graphene (G) powder, C_6H_6.**Molecular Weight:** 12.01 g/mole	1034343-98-0
Sodium alginate, Alginic acid sodium salt	9005-38-3
Starch from wheat $(C_6H_{10}O_5)_n$	9005-25-8
Sodium dodecyl benzene sulfonate (SDBS)$CH_3(CH_2)_{11}OSO_3Na$. **Molecular Weight:** 288.38 g/mole.	30604-81-0
Dimethyl sulfoxide ((DMSO) $(CH_3)_2SO$. **Molecular Weight:** 78.13 g/mole	200-664-3-67-68-5
Sulfuric acid (H_2SO_4).**Molecular Weight:** 98.08 g/mole	7664-93-9
Potassium chloride (KCl). **Molecular Weight:** 74.55 g/mole	7447-40-7
Deionised (DI) water (H_2O). **Molecular Weight:** 18.02 g/mole	-

Universiti Malaya

3.2.1 Electrode Materials

Three different cotton samples such as Gossypium herbaceum, Gossypium arboretum pima and Gossypium aboretum were treated by opening and cleaning. The cotton samples were cut into a single-layer test specimen which was 35 mm longand 35 mm wide. The monolayer samples were then stacked layer by layer to make 10-layer test samples.

100 % pure cotton (Gossypium arboretum pima) was washed and dried with heat at100 °C for 30 minutes and turned into pure raw cotton; whereby the density of cottonfibers was found to be 1.15 g/cm, the average diameter of the cotton fibers was 15.3 μm, and the average length of the upper half of the cotton fibers was 25.5 mm. Distilledwater was used to wash and purify the sample.

Graphene was purchased with an initial flake size of 100 mesh from Sigma Aldrich. Dimethyl sulfoxide((DMSO)(assay 99.9%; Sigma Aldrich, UK)) was used as an additive for improving the conductivity of graphene. Sodium dodecyl benzene sulfonate (SDBS) was purchased from Sigma Aldrich, UK. Deionized water (DI) wasused as a solvent.

3.2.2 Electrolyte Materials

Cotton (100% pure natural; Gossypium arboretum pima) and graphene powder (G) are the major components of the electrolyte system. Raw materials such as sodium alginate powder (M_n = 357,475, M_n/M_w = 1.392, M/ G = 0.32), Starch fromwheat, dimethyl sulfoxide (DMSO), $(CH_3)_2$ SO(assay 99.9%), sulfuric acid (H_2SO_4) and potassium chloride solution(KCl) were purchased from Sigma Aldrich, UK. Deionized water (DI) was used as a solvent. The chemical formula of the materials used is shown in Figure 3.1.

Universiti Malaya

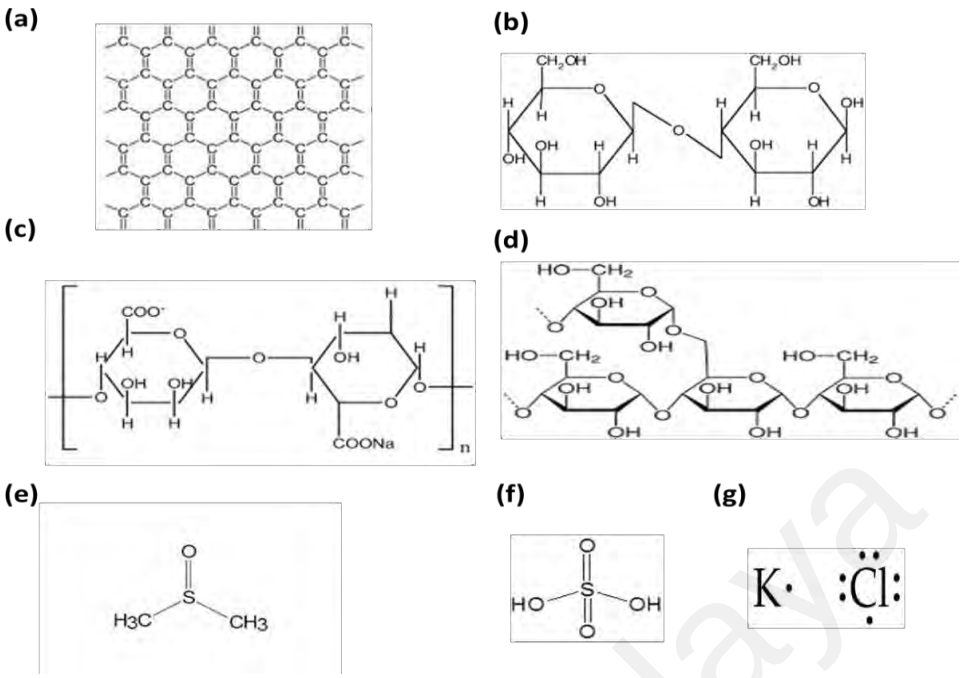

Figure 3.1 : The chemical formula for (a) Graphene (b) Cotton (c) Sodium alginate (d) Starch (e) Dimethyl sulfoxide DMSO (f) Sulfuric acid (H_2SO_4) and (g) Potassium chloride (KCl).

3.3 Cotton

Cotton is a plant fiber that comes from cotton plants of the Gossypium genus. While there are fifty different species present in this genus, only 3 of them are used in agricultural production (Gossypium arboreum, Gossypium arboretum pima, Gossypium arboretum). Cotton fibers are natural hollow fibers made of cellulose; which are soft, cool, breathable and highly absorbent and can hold water 24 to 27 times of their weight. Cotton fibers are strong, absorbent, and resistant to abrasion and can withstand hightemperatures while on the other hand, they are soft and comfortable. Due to the wrinkles of the cotton, the cotton fibers contain a variety of impurities that must beremoved. Table 3.2 gives a typical analysis of cotton fibers. A cotton wash, appropriate cleaning, and heat softening result in an absorbent fabric free of impurities that may adversely affect dyeing or printing (Abidi N , Cabrales L and Hequet E, 2010).

Universiti Malaya

Table 3.2 : Typical composition of greige cotton fibers.

Component	Percentage
Cellulose	94%
Proteins	1.3%
Pectin's	0.9%
Minerals	1.2%
Waxes	0.6%
Organic Acids	0.8%
Sugars	0.3%

3.3.1 Molecular orientation of the Cotton fibers

Cotton fiber molecular orientation is commonly examined using the birefringence index, $\Delta n = n_{\Pi} - n_{\perp}$, in which ($n_{\Pi}$) is the refractive index with the polarized light oscillating in a plane parallel to the fiber axis, and $n_{\pm}$ is the refractive index with the light oscillating in a plane perpendicular to the fiber axis (Abidi N, Hequet E and Cabrales L, 2010). A typical birefringence index of cotton may range from 0.04 to 0.09. Within a given fiber, this index increases from the tip (0 – 0.008) to the root ofthe fiber (above 0.04).

In relation to fiber friction, studies on synthetic fibers reveal that the higher the orientation, the more intimate the contact between fibers, and the higher the friction (Abidi N et al., 2008; Akerholm M, Hinterstoisser B and Salmen L, 2004).

With cotton fibers, such analysis will be difficult to replicate since orientation willbe directly associated with the growth rate of fibers (a difficult factor to control). In addition,

Universiti Malaya

cotton fibers of different levels of orientation will likely be different in manyother surface-related physical characteristics. Nevertheless, the assumption that higher cotton fiber orientation will result in higher inter-fiber friction seems to be reasonable (Khalid M Y et al., 2021).

3.3.2 Structure of cotton

Cotton fibers are single integrated cells that appear on the surface layer of cotton seeds. These cotton fibers consist of a stratum corneum, a primary wall, a secondary wall, and a central core or lumen Figure 3.2 which prepares the cuticle for the "outer"layer of cotton fibers. It consists of cotton wax . The cavity through is a hollow channelthat runs along the fiber and provides nutrients as the cotton grows and subsequently the lumen size varies greatly. Depending on the maturity of the fibers, mature fibers have a thick layer of cellulose in the secondary wall, resulting in a very small lumen; whereas immature fibers have a thin wall structure and large lumen (Hartzell M M and Hsieh Y L, 1998). The longitudinal width of the cotton fiber is a belt-like structure, and the surface of the cotton fiber is uneven, which increases the friction between thefibers, and can spin fine cotton threads with sufficient strength (Li Y and Hardin, 1997). Convolutions are cotton fibers and are partly responsible for many of cotton's unique properties. Cotton is soft, absorbent and strong. Its absorption comes from thefiber surface (which has a strong affinity for water), the fiber's microstructure (sponge-like), and the hydroxyl groups (-OH) in the molecule. Cotton fibers are fairly regular in width, varying from 12 to 20 microns in width. The cross-section of cotton fibers is generally kidney-shaped, and some are elliptical (Nevell T P and Zeronian S H, 1985).

Universiti Malaya

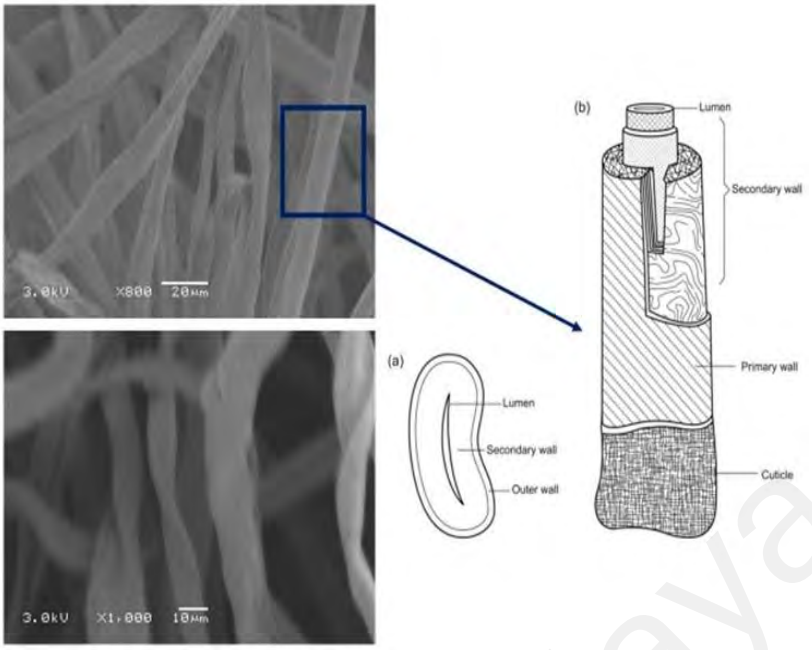

Figure 3.2 : Microstructure of cotton, (a) Cross-section of cotton, (b) vertical section of cotton.

3.3.3 Characterization

The structural properties were performed on a sample of pure cotton having 10 layers of fibers. The incident ray was kept perpendicular to eye level and the detectorarm was moved. The examination was carried on for two hours in the range of 5-50⁰, using a usual wavelength of CuKα equal to 1.541874 A˚.

Cotton is mainly composed of 95% of cellulose I (β-1,4-D- anhydroglycopyranose). The remaining 5% non-cellulose compounds are mainly found in the cuticle and primary cell wall. After washing and heat treatment, the impurities are removed, and the cellulose content of cotton fibers increases to morethan 99%. Whereby, the primary cell wall is formed.

Thermogravimetric analysis of cellulose cotton samples was performed using TGA. Curves were recorded between 150 and 600 °C with the following heating rates 4°C min^{-1} in a nitrogen flow at 20 ml min^{-1}. The mass of each sample was between 1 and 4 mg

Universiti Malaya

(Li Y and Hardin, 1997). The samples were fixed at 150 °C for 5 minutes beforethe start of the heating to get rid of the absorbed water. The baseline curves were alsosubtracted from the sample curves and this procedure was performed to exclude the effect of buoyancy on the results. Cotton is estimated to have a glass transition temperature of 220°C.

Differential scanning calorimetry (DSC) is often used to study polymers in whicha sample is heated along with a reference sample to study the transitional phase as theheat flows through it. When the sample undergoes a phase transition, a different amount of heat flows to the sample than to the reference. The difference in heat flow is plotted as a function of temperature (Hartzell M M and Hsieh Y L, 1998). The melting of a solid is endothermic. The extra heat flow to maintain the temperature appears as a peak on the plot. When the sample crystallizes, less heat flows to the sample. This appears as a dip in the plot. After a certain temperature, a polymer may undergo a glass transition with an increase in its heat capacity.

This is done by integrating the peaks corresponding to a given transition. It canbe seen that the transformation enthalpy can be expressed by the following equation (3.1):

$$\Delta H = KA \tag{3.1}$$

where ΔH is the transformation enthalpy, K is the caloric constant, and A is the area under the curve. The thermal constant varies from instrument to instrument and can be determined by analyzing a well-characterized sample with known enthalpies oftransition (Ruijun Bai et al., 2021).

By dividing heat flow ($\frac{q}{t}$) y the heating rate ($\frac{\Delta T}{t}$) one obtains the relation of heat supplied divided by the temperature increase, which is called heat capacity (Li Yand

Hardin I R, 1997; Ruijun Bai et al., 2021.

$$\left(\frac{q}{t}\right)\left(\frac{\Delta T}{t}\right) = \frac{q}{\Delta T} = Cp = Heat\ Capacity$$

FTIR was utilized to determine the functional group or chemical bonding presence in the cotton. FTIR spectra of pure cotton samples were recorded under environmentally controlled conditions using the FTIR Tool (Spotlight 400) in the frequency range 700 - 1800 cm^{-1} at 4 cm^{-1} resolution. The ATR-FTIR contains a crystalline compound with ZnSe-Diamond (single backscatter) that allows the collection of FTIR spectra directly on the cotton sample without any special prior preparation (Nevell T P and Zeronian S H, 1985). The 'pressure arm' of the tool wasused to apply constant pressure on cotton samples placed on top of a ZnSe-Diamondcrystal, so as to ensure a good contact between the cotton sample and the incident infrared beam, and to reduce the infrared beam (Azzouz B, ben Hassen M and Sakli F, 2008). Energy-dispersive X-ray spectroscopy measurement was performed on pure and cotton to determine the elemental composition and purity of the samples.

3.4 Preparation of graphene solution

The graphene solution was prepared in a beaker containing 1 g of graphene which was mixed with 50 ml deionized (DI) water for 30 min with the help of a sonicator at 50 °C until the mixture turned homogenous black solution. 1ml DMSO was added to the solution while gently stirring it at 45 °C for 5 minutes. 0.5 g of the anionic surfactant and a few drops of sodium dodecylbenzene sulfonate (SDBS) were added to the mixture to exfoliate the graphene. The surfactant acted as an exfoliant and stabilizer by binding it to the graphene surface, after which the solution was ready andapplied directly to the pure cotton. The procedure of graphene solution preparation is shown in Figure 3.3.

Universiti Malaya

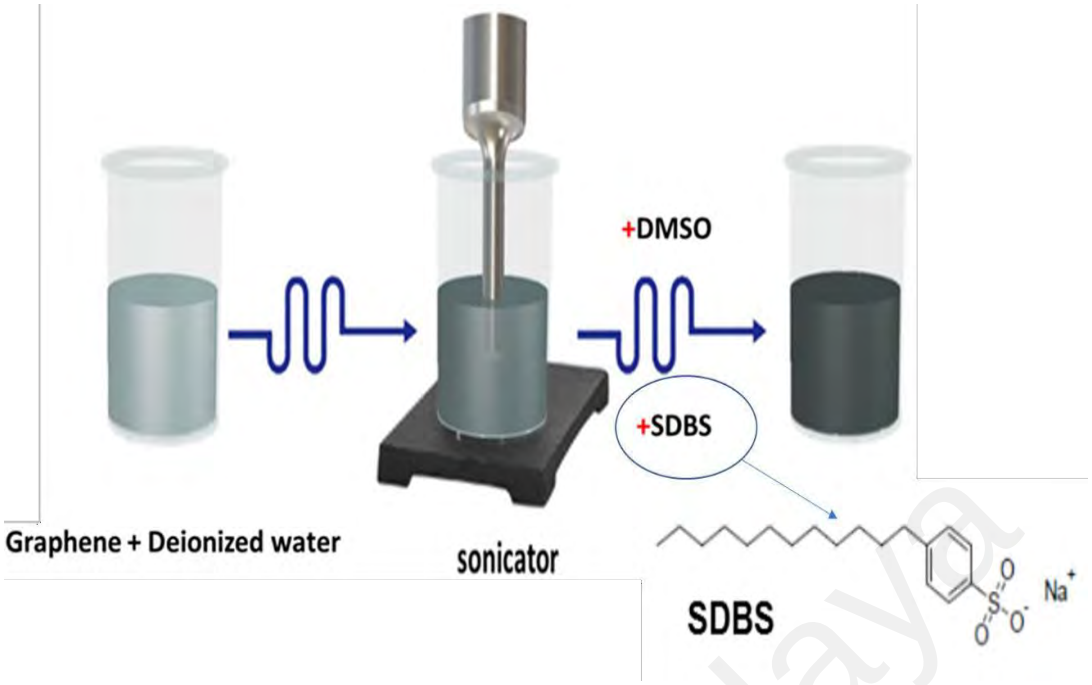

Figure 3.3 : Diagram of graphene solution preparation.

Water has a high surface tension of 72.8 mJ m^{-2} at room temperature. Hence, water alone cannot be used to exfoliate graphene. The range of 40-50 mJ m^{-2} is considered good for the same. Interfacial tension needs to be minimized between graphene and the solvent, which is achieved through the addition of DMSO. (DMSO has a surface tension of 42.9 mJ m^{-2} at room temperature). A binary mixture of water and DMSO, along with high temperature, helps to reduce surface tension (Sun F et al., 2019).

Surfactant is further added to water to reduce its surface tension. It is achievedwith the help of SDBS. The water/surfactant system helps in the exfoliation and stabilization of graphene. Water is also a good dispersion medium for graphene (Remadevi R et al., 2020).

3.4.1 Deposition of graphene on cotton

The prepared graphene solution was deposited on cotton cloth using a layering method. In this method, graphene was distributed on the cotton cloth layer by layer atroom

Universiti Malaya

temperature, first layer of graphene has been coated on cotton fabric using dropcasting then leave it for 25 minutes, followed by drying to obtain electrical resistancewith an effective area of 1 x 1 cm^2 for the cotton sample. The fabric was then dried inan oven at 100 ˚C for 1 h. Following the drying phase, the concentration of graphene in the conductive cotton after each layer was calculated using the following equation (3.2):

$$C(wt.\%) = (c_2\text{-}c_1/c_1)\ x100 \quad (3.2)$$

where c_2 is the weight of the conductive graphene cotton and c_1 is the weight of the pristine cotton (Remadevi R et al., 2020). To increase the concentration of graphene in the sample, the layer by layer - drying process was repeated until the sample reached saturation concentration at 18 layers, where the weight of pure cotton (Gossypium herbaceum) was 8.2 wt.% and after the first layer of graphene solutionthe weight become 10.7 wt.% to 188 wt.% on the 18^{th} layer, respectively. This is theconcentration for which the addition of more mixture leads to the formation of a layer on the surface of the sample.

Different concentrations of graphene have been applied to the cotton material to evaluate the effect on electrical conductivity. To calculate the amount of graphene loading, the cloth was weighed before it was dipped in graphene ink and after it had dried completely. To increase the concentration of graphene on the cotton sample, thetreated sample was left at room temperature for 25 minutes after each layer to ensure that the cotton was impregnated with the solution, and then dried in oven air for 1 hourat 100 °C. The electrical analysis has been carried out after each layer is ready.

Universiti Malaya

3.4.2 Characterization and Measurement

After the cotton was subjected to a layered manner-coating, the surface morphology of the pure cotton and graphene-coated cotton was studied using scanning electron microscopy (SEM, JEOL, JSM-6380LA). In addition, X-rayenergy dispersive analysis (EDX) was performed on graphene-treated fabric toensure the purity of the samples.

Fourier transform infrared spectroscopy (FTIR) was used to study the bonding between the various functional groups, the instrument used for FTIR was Perkin Elmer (Model: Spectrum Two, 114408), and the hydrogels materials were scanned at the wave number range of 4000 – 500 cm^{-1} at 4 cm^{-1} resolution. X-ray diffraction (XRD) analysis was performed for the structural investigation of the pure and coated cotton. A Analytical X-ray instrument with monochromatic X-ray Cu K_α of wavelength, λ = 1.541874 Å was used for the same. Scherrer's formula was used to estimate the size in the vertical direction (Yun Y et al., 2017; Roslan M et al., 2019).

$$D = \frac{K\lambda}{\beta \cos \theta} \tag{3.3}$$

where K = 0.98, λ is the X-ray wavelength, β is the full width at half maximum,and θ is the diffraction angle in radians.

Thermogravimetric analysis (TGA) and differential scanning calorimetry (DSC)were performed on pure and graphene solution-treated cotton fabrics using TGA 1000 and DSC 8000 instruments, respectively.

To study the electrical properties of the pure and treated cotton fibers, the four- probe method was used. The electrical resistances of the samples were calculated from I-V curves, at a temperature of 25 ˚C and relative humidity of 65%. The sheet resistance (R_s)

Universiti Malaya

after each layer, was calculated using the formula (equation 3.4):

$$R_s = R\frac{w}{d} \quad (3.4)$$

where R is the resistance, *w* is the width of the sample (2.5 cm) and *d* is the distance between the leads (0.35 cm) (Yun Y et al., 2017). The current was appliedusing a Keithley 2400 meter and the potential difference was measured using an HP34401A multimeter. Graphene-treated cotton fabrics can have unique electrical, andmechanical capabilities. Hence, these can be used in industry as an alternative to conductive wires.

3.4.3 Electrochemical Impedance Spectroscopy (EIS) Studies

The ionic conductivity of the graphene-treated cotton fibers(electrode) was measured using a Hioki 3532-50 LCR HiTESTER impedance spectroscopy over a frequency range of 10 to 10^6 Hz at a temperature of 25 °C. For this, the samples werekept in the sample holder. This holder is fitted with stainless steel electrodes as a blocking electrode (Yun Y et al., 2017). Bulk resistance was measured from the complex impedance cut-off of the hydrogel electrolyte.

The ionic conductivity of the treated cotton was calculated from the measured area of the stapled electrodes [A (cm^2)]. The mass resistance of the treated cotton ofthe composite was studied according to the equation (3.5) (Roslan M et al., 2019):

$$\sigma = 1 / (R_b \times A) \quad (3.5)$$

3.4.4 Mechanical testing

The uniaxial tensile tests were performed by Shimadzu AGS -X series equipped with a 500 N load cell, on pure and cotton samples treated with graphene with a thickness of 0.6 mm. The cross-sections of the pure cotton and graphene-treated cottonfibers were

Universiti Malaya

obtained by cutting along the radial direction. The sample strips were cut with a length of 0.6 cm, and a width of 0.6 cm. Tensile tests were performed at a junction speed of 2 mm /min until failure. From stress/strain analysis, the mechanical stability of the samples has been studied (Yun Y et al., 2017).

Stress is defined as the force per unit area and has units Nm^{-2} or Pa. The formulato calculate tensile stress is:

$$\sigma \text{ (stress)} = F/A \tag{3.6}$$

where σ is stress, F is force (in newton), and A is the cross-sectional area (cm^2) of the sample.

Strain is defined as extension per unit length. And, since it is a ratio of lengths, the strain has no units (Roslan M et al., 2019).

$$\varepsilon \text{ (strain)} = \Delta L/L_0 \quad ; \quad \Delta L = L\text{-}L_0$$

where L_0 is the original length (cm) of fiber being stretched, and L is the length (cm) after it has been stretched. (ΔL) is the difference between these two lengths.

3.5 Hydrogel electrolytes preparation

To prepare hydrogel, sodium alginate (2 g) and starch were added to 100 ml water solution in a beaker using the hydrothermal method. 0.8 g of cotton and 0.5 ml of DMSO were added to the prepared hydrogel and were stirred on a magnetic stirrer at 50 °C for 24 hrs. The solution was obtained after ultrasonic treatment for 5 mins underambient conditions. The graphene was then added to the above solution at 50 °C. The membranes were made with a simple solution casting method. Samples were then heated in an air

Universiti Malaya

oven at 60 °C for an hr. Once the oven was cooled down to room temperature, the corresponding cotton hydrogel was prepared by immersing themembranes in 4 ml KCl (4 mL of concentrated KCL :Molar mass KCl = 74.55 g / mol ,5 g of KCl is present in 100 g of Solution means5 g of KCl is present in 95 g of H_20) and 4 ml H_2SO_4 (4 mL of concentrated H_2SO_4: the density of sulfuric acid is 1.84 g/mL, Molar mass of H_2SO_4 = 98 ,the relationship is expressed as density ρ Density=Volume/ Mass, Mass=1.8×4, Mass =7.2 g, The percentage purity of H_2SO_4 is 95.28%)solution for 1 hr separately. The samples are coded as CGH1, CGH2, CGH3, and CGH4, respectively based on the cotton to graphene ratio, and the details are providedin (Table 3.3). The polymerization reaction was completed after 1 hr and the samples were freeze-dried before further characterization. Figure 3.4 presents the schematic diagram of 3D solid-state hydrogel electrolytes.

Table 3.3: Details of the samples with respect to the cotton to graphene ratio.

	system
CGH1	Cotton (0.8 g) + graphene (0.2 g) + 5 ml hydrogel solution +4 ml H_2SO_4.
CGH2	Cotton (0.8 g) + graphene (0.4 g) + 5 ml hydrogel solution + 4 ml H_2SO_4.
CGH3	Cotton (0.8 g) + graphene (0.2 g) + 5 ml hydrogel solution + 4 ml KCl .
CGH4	Cotton (0.8 g) + graphene (0.4 g) + 5 ml hydrogel solution +4 ml KCl .

University Malaya

Figure 3.4 : Preparation of 3D hydrogel electrolytes.

3.5.1 Characterization of hydrogel electrolytes

Structural characterization of the hydrogel electrolytes was performed through theX-ray diffraction technique using an Empyrean diffractometer with CuKα (λ =1.5406Å) radiation having a current of 30 mA and a voltage of 40 kV. The surface morphology was studied through field-emission scanning electron microscopy (FESEM, Quanta FEG 450) operating at an accelerating voltage of 5 kV. The samples were coated with gold before FESEM analysis**.** Fourier transformation infrared spectroscopy (FTIR) study was carried out using a Thermos Nicolet Avatar 380 FTIR spectrometer equipped with an attenuated total reflection (ATR) attachment with a germanium crystal in the frequency range from 4000 to 500 cm^{-1} with a spectral resolution of 1 cm^{-1}. This measurement was performed to reveal the complexity of the solid-state hydrogel electrolytes host, the presence of specific functional groups and the free ion, and to suggest conduction mechanisms (Kadir M et al., 2011; Yun Y et al., 2017). Electrochemical impedance spectroscopy (EIS)was performed by a Hioki 3532-50 LCR HiTESTER impedance spectroscopyinstrument in the frequency range of 50 Hz to 1 MHz. The ionic conductivity was calculated according

Universiti Malaya

to equation (3.7) (Denisa H et al., 2009):

$$\sigma = \frac{d}{RbS} \tag{3.7}$$

Where d is the thickness (cm) of the membrane, S is the surface or contact area (cm^2), and R_b *is* the bulk resistance (Ω).

The activation energy for ion transportation was calculated according to the equation(3.8) (Wang F et al, 2017):

$$\sigma = \sigma_0 \, e^{\frac{-Ea}{RT}} \tag{3.8}$$

Where (σ) is the ion conductivity, (σ_0) is the pre-exponential factor, R is the idealgas constant and T is the temperature.

The ionic conductivity also depends on several factors: the nature of the electrolyte added, the nature of the solvent used, its viscosity, the concentration of the electrolyte, the size of the ions produced, their dissolution, and the temperature**.**

3.6 Fabrication of flexible supercapacitors (SC)

Hydrogel electrolyte samples, CGH1, CGH2, CGH3, and CGH4 were cut into the size of 1.5 cm x 1.5 cm and used as the electrolyte.

Then, SC was assembled in a coin cell with two identical electrodes based on graphene-treated cotton. The fabricated supercapacitor will perform as an electric double-layer capacitor (EDLC) since the 2 electrodes are carbon-based and do not involve any faradaic reactions, and electrolyte based on cotton/graphene hydrogel (Wang K et al., 2016). All operations were performed at room temperature, on the fabricated

Universiti Malaya

supercapacitor based on two graphene treated cotton electrodes and graphene treated hydrogel electrolyte.

3.6.1 Characterization

The electrochemical performances of the fabricated supercapacitor were studied through an electrochemical workstation using a Gamry Interface 1000 at different scan rates. Cyclic voltammetry (CV) and galvanic charge/discharge (GCD) curves were recorded in the voltage in the range of 3-100 mVs^{-1} and current densities from 100 mA/g to 500 mA g^{-1}, respectively. Specific capacitance values (Cs) were calculated from the CV and GCD curves using equations (3.9) and (3.10) (Denisa H et al., 2009):

$$C = \frac{\int ivdv}{2\mu m \Delta V} \tag{3.9}$$

and

$$C = \frac{It}{m\Delta V} \tag{3.10}$$

Here, v represents the potential (V), μ represents the scan rate (V/s), m is the massof active materials (g), and ΔV is the potential window of discharge (0.5 V here). The quantities, I is the constant discharge current (A) and t is the discharge time (s).

The specific capacitance, power density and energy density were calculated basedon the galvanic charging-discharging curves using equations (3.11),(3.12) and (3.13) (Wang F et al, 2017, Stoller M D and Ruoff R S, 2010).

$$C = \frac{I\Delta t}{m\Delta V} \tag{3.11}$$

Universiti Malaya

$$E\ g = \frac{1}{2C\Delta V^2} \quad (3.12)$$

$$P\ g = \frac{Eg}{\Delta t} \quad (3.13)$$

Where C represents the specific capacitance (F/g), E_g is energy density ($Whkg^{-1}$), P_g is power density (Wkg^{-1}), ΔV is the potential window (here 1.6 V), I is discharge current (A), Δt is discharge time(s), m is the sum of the masses of the positive electrode and negative electrode (g).

The volumetric energy density could be estimated by using equations (3.14) and (3.15) (Stoller M D and Ruoff R S, 2010) :

$$E_v = E_g \text{ x } m/(2 \text{ cm x } 2 \text{ cm x } 0.05 \text{ cm}) \quad (3.14)$$

and

$$P_v = P_g \text{ x } m/(2 \text{ cm x } 2 \text{ cm x } 0.05 \text{ cm}) \quad (3.15)$$

The theoretical capacitance of the asymmetric full cell was calculated according to equation (3.16) (Stoller M D and Ruoff R S, 2010):

$$\frac{1}{C\tau} = \frac{1}{Cp} + \frac{1}{C\,\mathrm{N}} \quad (3.16)$$

Where C_T is the total capacitance of the cell, C_P is the capacitance of the positive dectrode C_N is the capacitance of the negative electrode.

Universiti Malaya

Cell capacitance is best determined from galvanostatic or constant current (CC) discharge curves using the equation (3.17) (Xiao Q et al, 2019):

Here dV/dt is calculated from the slope of the CC discharge curve. Galvanostatic discharge is the accepted measurement method for determining capacitance for packaged ultracapacitors in the ultracapacitor industry and correlates more closely tohow a load is typically applied to an ultracapacitor in the majority of applications (Xiao Q et al., 2019).

Universiti Malaya

CHAPTER 4: PREPARATION AND CHARACTERIZATION OF PURE COTTON BASED MATERIALS

4.1 Introduction

'Gossypium herbaceum', 'Gossypium arboretum pima' and 'Gossypium aboretum' fabrics are the purest form of cellulose, which is also the most abundant polymer available in nature. Approximately 94% of cotton fibers are cellulose. The non- cellulose materials are present on the outer layers while the secondary cell wall is purecellulose. Cotton can be considered white gold for the economy of many countries. Porosity is one of the most important characteristics of textile materials (cotton), as itensures comfort and ease of use. The internal porous structure of the cotton fiber assembly is complex and changeable, and the surface porosity is difficult to explain by the pore structure. Cotton samples are routinely analyzed using various analytical techniques such as x-ray diffraction to determine their crystal type(polymorph) and crystallinity. Fourier transform infrared spectroscopy (FTIR), thermogravimetric analysis (TGA), and (DSC) are also used for such studies. The advantage of using a FESEM and EDX microscope lies in the fact that it provides not only chemical composition information but also structural information.

4.2 Results and discussion

4.2.1 XRD Analysis

The degree of crystallinity and orientation as the microstructural parameter was measured by X-ray diffraction as shown in Figure 4.1. In general, fibers with highly oriented crystallinity are found stronger and more rigid. Usually, the crystallinity ofcotton ranges from 60% to 70%. The analysis was carried out for cellulose cotton crystals using CuK_{α} wavelength ($\lambda = 1.541874$Å). It can be seen that the pure cottondisplays square-like crystals (n = 0.1); being sharper at the (110) and ($\bar{I}10$) peaks near 14.9° and 16.7° of

Universiti Malaya

crystals with an ellipsoidal cross-section (Antal M J, Varhegyi G and Jakab E, 1998). However, the intensity of these two peaks decreasesas the value of n increases. The main peaks in all pure cotton are ($\bar{1}$10), (110), and (020). The original cotton samples show three main peaks for a single chain three- way unit cell Ia. It has Miller Indicators (100), (010), and (110) (which are Counterparts from ($\bar{1}$10) (110) and (020) are formed by interand intra-hydrogen bonding and they show a hydrogen-bonded network in cellulose) (Roslan M et al., 2019). The crest (200) is the "amorphous halo". The X-ray diffraction pattern of purecotton shows maxima at 2θ values of 14.9° and 22.77°. In this analysis, the amorphous content is represented by the height of the overlapping crest ($\bar{1}$10)/(110) (Abidi N et al., 2008). The cotton samples had the preferred orientation for the repression of (012) and (102) cellulose I peak located near 370 amorphous signal sites. The cotton samples have diffraction patterns with three major reflections at Millar indices -110, 110, and 200. The *Gossypium herbaceum and Gossypium arboretum pima s*amples exhibit sharply peaked X-ray patterns confirming the high stereoregularity of their segments whereas the peak of the X-ray pattern of the *Gossypium arboretum pima* sample is significantly broader.

The *Gossypium herbaceum* and *Gossypium arboretum* fabric samples are relatively unaffected by the treatment. However, the peak of the X-ray pattern of the Gauze sample at 002 is significantly sharper and the peaks at -110 and 110 are more pronounced, the higher Segal amorphous for control cotton was attributed to peak overlap. Despite differences in the shape of the samples no change in the detected XRD patterns, as shown in Figure 4.1. The XRD patterns show that the structured structure of the crystalline region on the remaining cellulose is not affected by hydrolysis based on the peak line width from the crystal plane 002 (Santos F et al., 2016).

Universiti Malaya

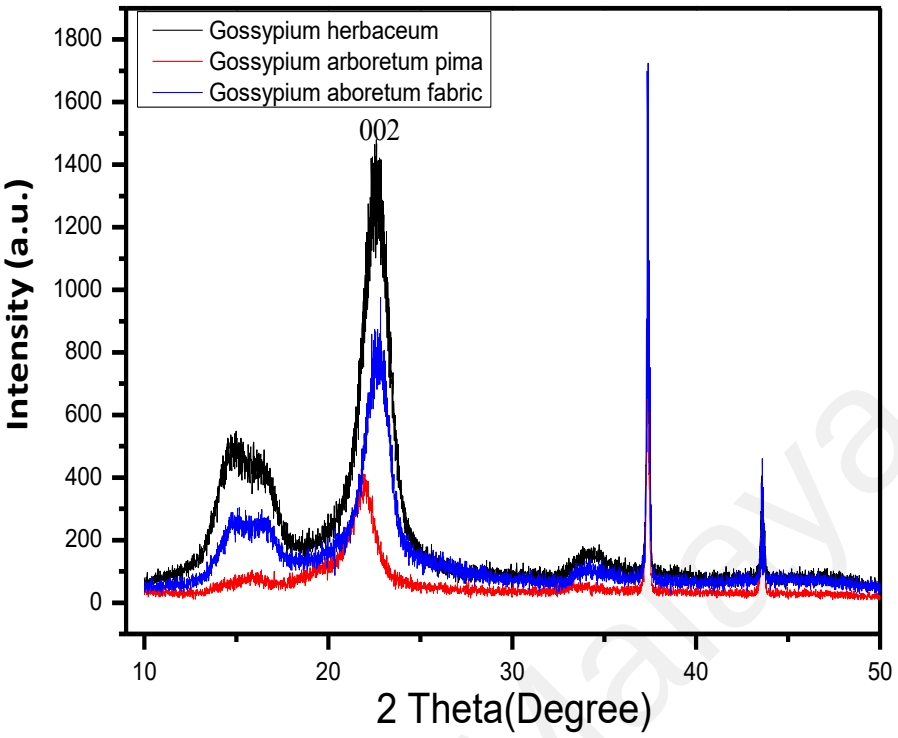

Figure 4.1:XRD peaks for cottons.

4.2.2 The TGA thermogram of cotton fiber

The TGA thermogram of cotton fiber is characterized by three regions for the *Gossypium herbaceum, Gossypium arboretum pima* and *Gossypium aboretum* fabric samples respectively (Figure 4.2). Region I located between 37 °C and 150 °C shows initial weight loss followed by a plateau region between 225 °C and 425 °C (region II) and region III located between 425 °C and 600 °C.

The amount of primary cell wall per unit mass is determined by measuring weightloss as a function of temperature because weight loss occurs in pure cotton fibers in a temperature range between 150 °C to 310 °C (Alexander K S, Riga AT and Haines P J, 2009). The depolymerization and thermal decomposition occur between 200 °C to280 °C, whereby, the initial decomposition releases carbon dioxide, and H_2O is formed by

Universiti Malaya

sequential random fission in low-order regions of cellulose followed by loosening of the broken chains and dehydration, with decarbonization of anhydrous glucose units. Volatile products include anhydrous glucose between 120 °C and 270 °C. TGAof cotton fibers is distinguished by three regions as shown in Figure.4.2. The first region is located between 10 °C and 100 °C which shows an initial weight loss. This is followed by a plateau region, between 225 °C and 425 °C which is the second regionand the third region located between 425 °C and 600 °C.

Cotton fibers consist essentially of 94 % cellulose I (β-1,4-d-anhydroglycopyranose). The remaining 5% no cellulosic compounds are located primarily in the cuticle and primary cell wall and contain wax, pectic substances, organic acids, sugars, and ash-producing organic salts (Pijpers MFJ and Mathot VBF, 2008). It is a noticeable difference from the beginning of decomposition temperatures for non-cellulosic materials such as waxes, pectin materials, acids, organic salts, and sugars. It has been reported that these materials have a lower decomposition temperature than the cellulose found in cotton (Abidi N, Cabrales L and Hequet EF, 2010). Therefore, pure cotton that are identical except for having different maturities have different quantities of primary cell wall per unit of mass. Consequently, the amount of the primary cell wall per unit mass is estimated by the measurement of the weight loss as a function of the temperature with TGA. The weight loss of cotton fibers occurs between 120 °C and 400 °C. This is attributed to cellulose decomposition between 250 °C and 350 °C. Below 200 °C, the weight lossis due to the loss of adsorbed water. Above 200 °C, thermal decomposition and depolymerization occur. Between 250 °C and 290 °C, primary volatile decomposition releases CO_2, CO, and H_2O consisting of random chain scission in the low-order regions of the cellulose followed by relaxation of the broken chains and dehydration, decarboxylation or decarbonylation of anhydro glucose units.

Universiti Malaya

As shown in Figure 4.2, the TGA thermograms of the cottons show that the *Gossypium herbaceum, Gossypium aboretum fabric* samples are thermally stable for temperatures below 422 °C and that the *Gossypium arboretum pima* is thermally stablefor temperature below 397°C. This behaviour is attributed to the high degree of polymerization and crystallinity of the cotton cellulose.

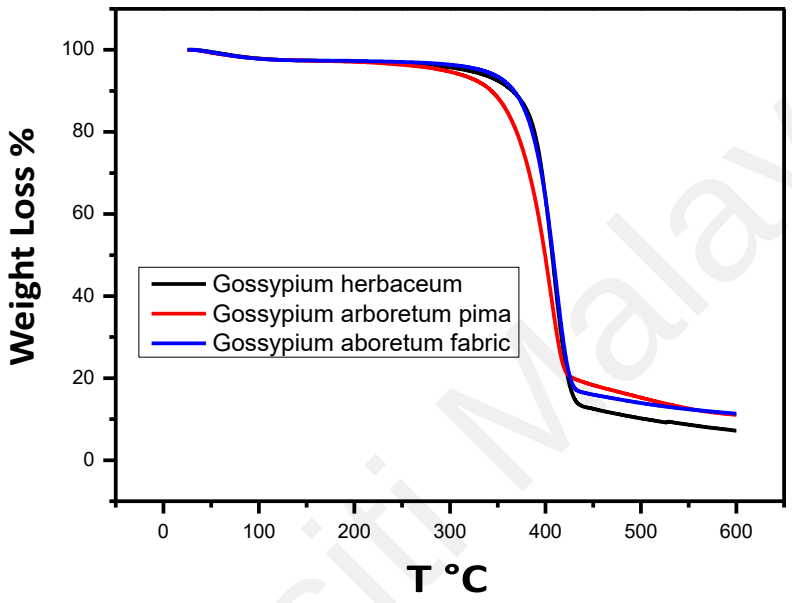

Figure 4.2: TG curves of cotton up to 600.

4.2.3 Differential Scanning Calorimetry (DSC): Analysis of cotton fiber

The results of the DSC investigations showed the processes of the glass transition temperature, crystallization and melting. The temperature indicates the initial temperature moving in for lower solubility and higher crystallization as shown in Figure 4.3. The first derivative of this thermogram (DTG) reveals three peaks at 55°C, 100°C, and 359°C for the *Gossypium herbaceum, Gossypium arboretum pima* and*Gossypium aboretum* fabric samples respectively. DSC analysis on the cotton shows peak characteristics with regard to the presence of water and heat of fusion of about 163 J/g (Abidi N, Cabrales L and Hequet EF, 2010).

Universiti Malaya

As an end process during melting, the additional heat flow appears as a large dip inthe DSC diagram (the cotton is heated after T_c, reaching another thermal transition, called melting). At 359 °C, the melting temperature of the cotton fibers T_m, is reached,and at that point, the cotton crystals begin to break down (melting). The onset of theirfree movement (which may be a disordered motion); is monitored on a DSC chart. Theheat that the cotton gives off while the crystallization process allows the temperature to reach at T_m. The latent heat of melting is the same as the latent heat of crystallization.When the cotton crystals melt, they absorb the heat to do so. Since this corresponds tothe melting temperature, the temperature of the cotton is not raised until all the crystalsin the fiber have melted (Liu W et al., 2012).

Thereafter, a considerable peak is observed when cotton reaches the crystallization temperature. Finally, a major dip occurs when the cotton reaches its melting temperature. On the other hand, the crystallization peak and the melting slope appear only for cotton fibers that can form crystals and dissolve. It may be noted that a completely amorphous cotton fiber will not show any crystallization or melting, however, cotton fibers with crystalline and amorphous domains will show all the features of the glass transition.

Melting and crystallization processes involve the release or absorption of heat where the glass transition temperature occurs with a change in the heat capacity of cotton. Since there is only a change in heat capacity and no change in latent heat in theglass transition; it pertains to a second-order transition while transitions in a cotton sample (melting and crystallization) are called first-order transitions, meaning therebythat they have a latent temperature (Tsuji W et al.,1992; Liu W et al.,2012).

Universiti Malaya

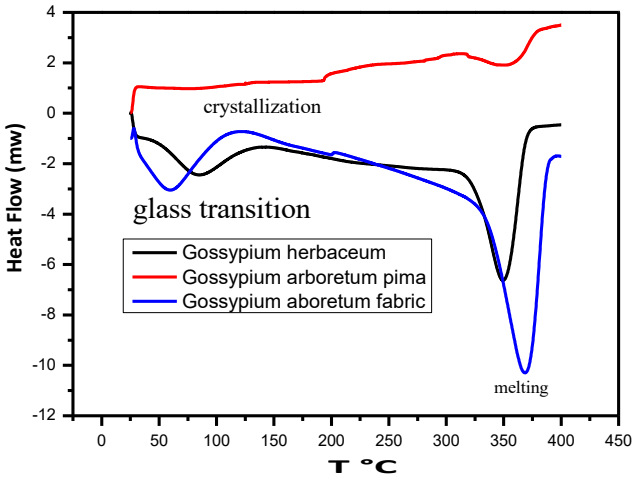

Figure 4.3 : Differential scanning calorimetry (DSC) curve of cotton.

4.2.4 FESEM

The *Gossypium herbaceum, Gossypium arboretum pima* and *Gossypium aboretum* fabric samples resembles a long, twisted, flattened tube with an irregular end that slightly tapers. The middle section of a cotton fiber is depicted in Figure 4.4, with convolutions visible. These are displayed in a SEM image more strikingly (Figure 4.4(b)). Ellis demonstrated that the formation of convolutions was a natural outcome of the collapse of a helical structure (Ellis J, 1995). Cotton fibers have the shape as depicted in Figure 4.4 in cross-section (Wang Z et al., 2021).

The bleached Gossypium herbaceum cotton has a ribbon shape with many twists along its length (Figure 4.4 (a)), the walls of *Gossypium arboretum pima* (Figure 4.4 (d)) and *Gossypium aboretum* fabric (Figure 4.4 (g)) slightly swollen and thicker.

The secondary cell wall makes up the majority of the fiber, with a thin cuticle and primary cell wall on the outside and a narrow, collapsed lumen in the center. This is deposited on the inside of the primary cell wall throughout the growth process in a series of daily growth rings, as depicted in Figure 4.4 (a) (Wang Z et al., 2021). A schematic

Universiti Malaya

representation of the different layers that make up the fiber is shown in Figure 4.4. The layers will be constructed from stacks of the lamellae mentioned in the previous section (Chen and Jakes, 2002). The fibrils in the primary wall are aligned in a basket-weave pattern. According to research on fibers two weeks post- anthesis (after flowering), the primary wall has a crystallinity index of 30 % and a fibril diameter of 2.98 nm, compared to 70 % and 4.22 nm for mature fibers at sevenweeks post-anthesis (Hosseini Ravandi, 2011).

Cotton fabric has large air spaces. Their surface tissue structure appears unevenly due to the large air voids in the structure which causes unevenness (Hequet E F et al.,2016). This microstructural property of the cotton was studied through a field emissionscanning electron microscope as shown in Figure 4.4.

Cotton fibers of all types have a ribbon-like shape with twists or swirls at regular intervals. The molecular chains are assembled in an extended and unfolded form into primary fibers that unite to form a microfiber. The fibers are 4-10 nm wide containing mismatched crystal masses with the same axial orientation of the cellulose chains, but having different orientations in the a and c axes. These fibers combine to form bundles (large fibers) of larger diameter due to physical fusion as a result of reduced free surface energy. They are interconnected and have a width of about 100 nm. Cotton ismainly frosted, only about one-third of the total molecules constitute the amorphous phase. The disorder is mainly due to the small crystal units being randomly packed. The cotton structure is considered paracrystalline.

Membrane shapes of pure cotton fabrics/fibers have also been studied. The cellulose

Universiti Malaya

fibers have high strength because the molecules are oriented parallel to eachother, and spiral around the fibers. The chiral angle is about 8^{0} or less in the bark fibers. Cotton fibers, on the other hand, have a spiral angle of roughly 20^{0} or more, which is why cotton stretches far better than bark fibers (Hequet E F et al., 2016).

The FESEM micrographs simply reveal that the surface of the pure cotton fiber is uneven. It shows that there are many deep grooves or slender concave grooves on the surface and slightly sharper at some local edges of the fibers. Furthermore, the images show that the surface is relatively smooth.

Figure 4.5 presents an optical image of the stack layer of the cotton fibers whileFigure 4.5 presents the EDX pattern for the fibers. The EDX pattern confirms the purity of the samples and rules out the presence of any unwanted or impurity element.

As shown in Figure 4.5, the spectra of the cotton samples demonstrated peaks located at 0.277 keV and 0.525 keV indicating the existence of carbon and oxygen respectively. More importantly, the spectrum of *Gossypium herbaceum* showed a peak at 1.739 keV indicating the presence of silica nanoparticles. The hydrophobic nature of silica may provide an explanation for the limited ability of the *Gossypium herbaceum* sample to absorb the polymer solution (Abidi N et al., 2008; Hequet EF et al., 2016).

Universiti Malaya

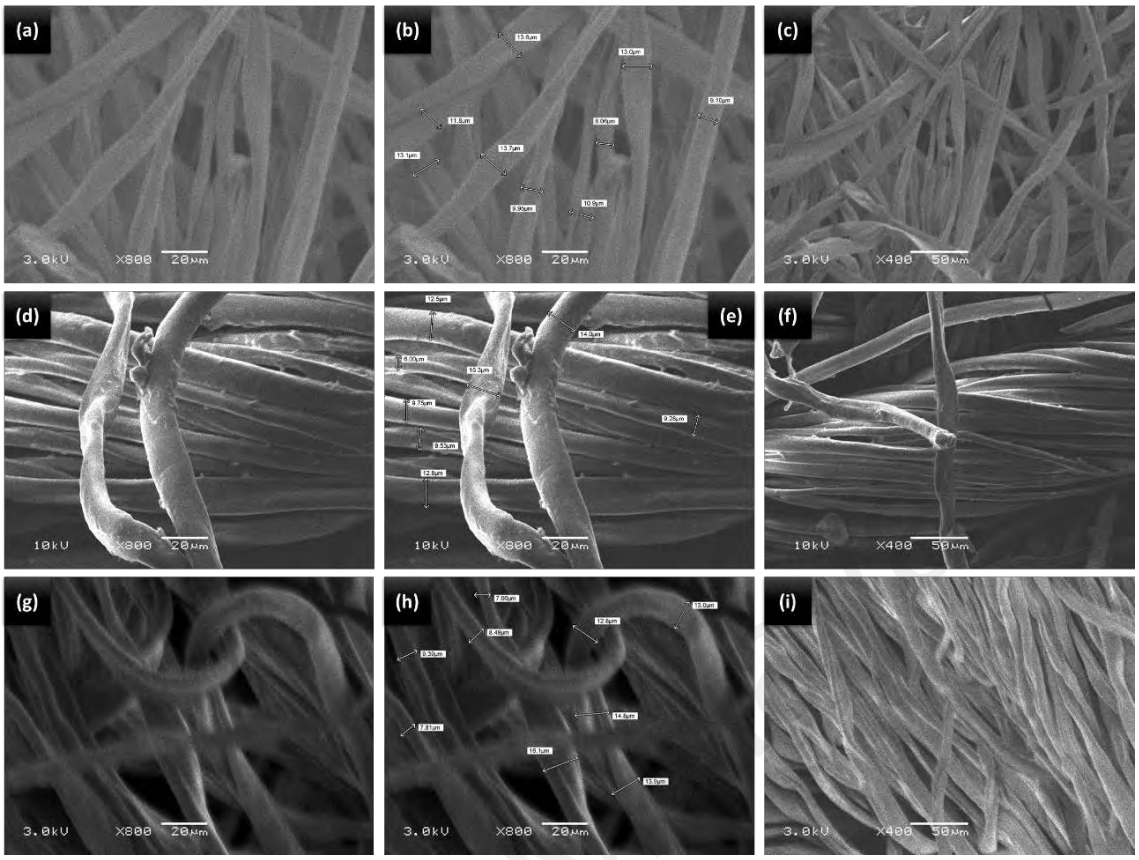

Figure 4.4 : FESEM images original microfibers(a ,b and c) Gossypium herbaceum, (d ,e and f) Gossypium arboretum pima and (g,h and i) Gossypiumaboretum fabric.

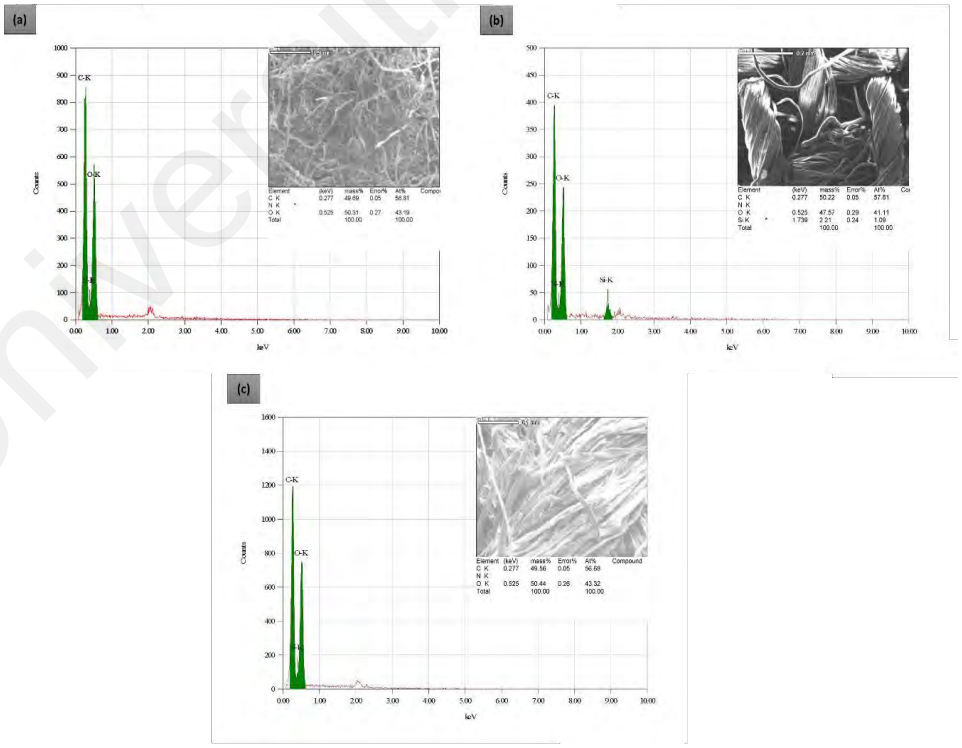

Figure 4.5 : EDX analysis of pure cotton(a) *Gossypium herbaceum*,(b) *Gossypium arboretum pima* and (c) *Gossypium aboretum* fabric.

University

4.2.5 Fourier transform infrared analysis

The chemical structure of the cotton is shown in Figure 4.6. Cellulose is an unbranched, natural polymer composed of repeating glucose units $(C_6H_{10}O_5)_n$, and is considered as the most profuse organic material and polysaccharide on Earth. This biodegradable polymer is mostly found in nature in the form of microfibrils in the cell walls of wood and plant, algae tissues, and membrane of epidermal cells of tunicate Cellulose is a carbohydrate polymer, where most of the composition of cotton is a methylated carboxyl group, which has long chains (Akerholm M, Hinterstoisser B and Salmen L, 2004). Although the fabric contains impurities such as wax and pectin; after washing with distilled water and heating, we note that the amount of these impurities is too small to appear in the spectrum.

Various chemical bond formation in the cotton was studied using FTIRspectroscopy as shown in Figure 4.7.

The absorption band at 1428 cm^{-1} is associated with the CH_2symmetric bending ofthe cellulose. The absorption bands at 1360 and 1315 cm^{-1} are relative to bending vibrations of the C-H and C-O groups, respectively, of the aromatic rings in cellulose polysaccharides (Morton W E and Hearle J W S, 2008). Intense peak vibrations observed at 1032 cm^{-1} are related to the (CO) and (OH) stretching vibrations of the polysaccharide in cellulose (Abdellatif KF et al., 2012). The peak at 894 cm^{-1} indicates the presence of β-glycosidic linkages between monosaccharides (AbdellatifKF et al., 2012).

It is known that two IR peaks around 750 and 710 cm^{-1} are characteristic for triclinic (Iα) and monoclinic unit (Iβ) allomorphs, respectively. The relative proportion of cellulose Iβ to Iα allomorph could be calculated by integrating the absorption bands near

Universiti Malaya

710 and 750 cm^{-1} and the percentage of Iβ could be obtained (Hequet E F et al., 2016). As we can see the FTIR spectra are identical in *Gossypium herbaceum, Gossypium arboretum pima* and *Gossypium aboretum* fabric, there is only a slight shift of the peak correlated with the valence vibrations ofthe OH groups.

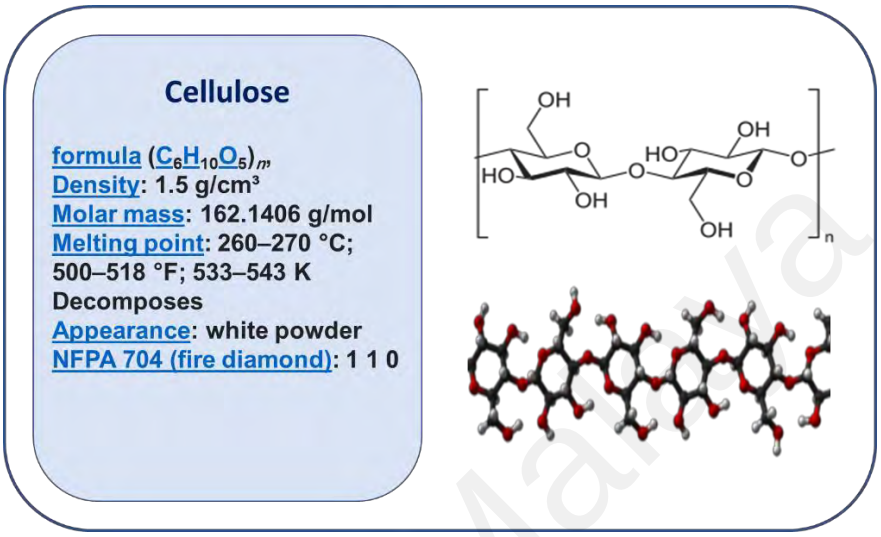

Figure 4.6 :Chemical structures of cellulose.

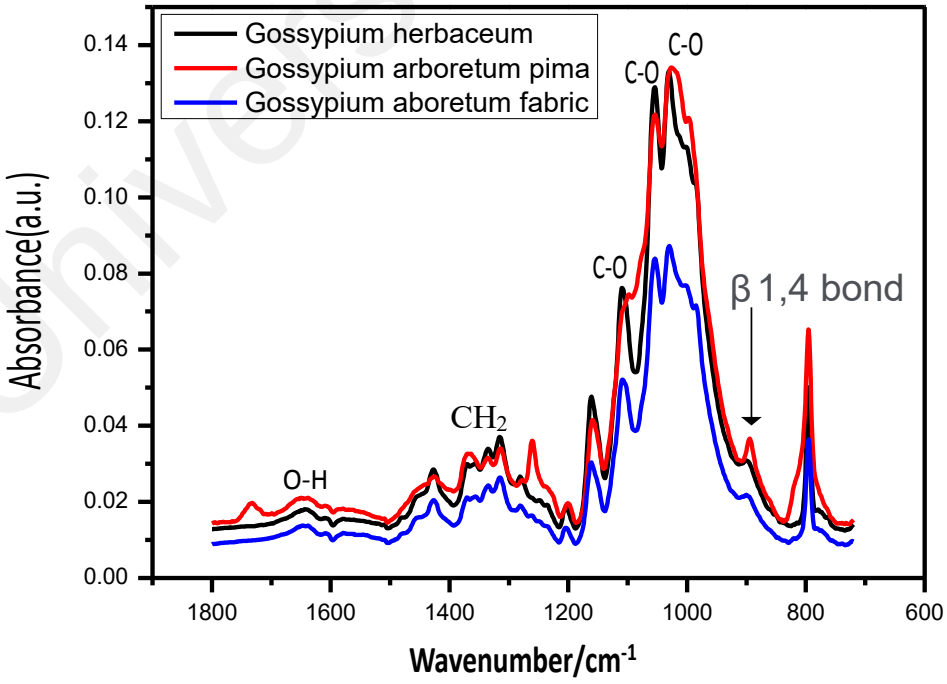

Figure 4.7 : FT-IR spectra of the pure cottons.

Universiti Malaya

4.3 Summary

Gossypium herbaceum, Gossypium arboretum pima and *Gossypium aboretum* fabrics are the purest form of cellulose, which is also the most abundant polymer available in nature. Approximately 94% of cotton fibers are cellulose. The non- cellulose materials are present on the outer layers while the secondary cell wall is purecellulose. Cotton can be considered white gold for the economy of many countries. Porosity is one of the most important characteristics of textile materials (cotton), as itensures comfort and ease of use. The internal porous structure of the cotton fiber assembly is complex and changeable, and the surface porosity is difficult to explain by the pore structure. Cotton samples are routinely analyzed using various analytical techniques such as X-ray diffraction to determine their crystal type (polymorph) and crystallinity, Fourier transform infrared spectroscopy (FTIR), thermogravimetric analysis (TGA), and differential scanning calorimetry (DSC). Crystallization analysisis important for practical reasons to provide information about the nature of amorphous cellulose. The control sample (*Gossypium herbaceum*) was selected from the best purecotton based on the results of SEM and TGA test, large exposed surface area and thermal stability, so it will be the control sample for the rest of the system in this research.

Universiti Malaya

CHAPTER 5: RESULTS AND DISCUSSION OF GRAPHENE COATED COTTON BASED ELECTRODE

5.1 Introduction

In the age of modern technology and information, wearable and smart electronic fabrics have been developed to replace portable electronics where the tissue structureis 'intelligent' in the sense that it can respond to the external sources of stimulation of the environment. Textile electronics pertain to "smart" textiles using the combination of electronics and textile structures. Major challenge lies in manufacturing the lightweight, flexible, affordable safe components, and fibers with strong electrical conductivity that can endure the production of electronic wearable cotton textiles (GaoD et al., 2022). Also, one of the biggest issues is the stress brought on by wearing such textiles and their maintenance, care. In the field of carbon-based electronic textiles, themain obstacle to use metallic conductors is the lack of flexibility and excessive weightthat must be overcome. One of the disadvantages of using conventional metal conductors as textiles is the occurrence of rigid and inelastic tissues which cannot perform their function when exposed to different environmental conditions or when subjected to washing processes (Badawi Nujud and Batoo K M, 2022). There is a need for developing smart fabrics to tune itself with respect to the body movement andconvert them into needful actions. Over the last few years, multiple research methodologies were developed to meet this challenge by using carbon materials and seersucker structures of particulate materials and fibres. The conductive cotton fabrichas been prepared by Layer by layer (LBL) coating of graphene and treated in the presence of sodium dodecylbenzene sulfonate (SDBS) as a dispersing agent and dimethyl sulfoxide (DMSO) to destabilize the ripple of the cotton fibers, which allows better incorporation of graphene on cotton fibers, at room temperature, first layer of graphene has been coated on cotton fabric using drop casting,

Universiti Malaya

followed by heating for1 hour at 100 °C. Experimental techniques like SEM, EDX, XRD, FTIR, TGA, and DSC were used to characterize the graphene-coated cotton fabric for structural,morphological and thermal properties. The conductivity of the materials was determined using a four-line probe and was monitored for two months to analyze the potential application of the coated material as smart wearable clothes and in designing modern electrical/electronic circuitry.

5.1.1 Graphene-coated cotton electrode material (fabric)

Graphene can form chemical bonds with cotton, making it a potential material for smart textiles. Here, the graphene-coating was performed on the cotton by a layering method where the chemical bonds of the graphene sheets on the surface of the fabric have fixed structures. Graphene with its hydroxyl, epoxy, and carboxylic functional groups makes it easily dispersible in water. Some specific functional groups present in graphene such as carboxylic acid, carbonyl moieties, C-OH, C-O-C as well as C-Ofacilitate the preparation of graphene-modified cotton fabrics. The graphene is absorbed into the cotton fabric layer by layer, and the resulting fabric is called cotton-graphene due to the bonding of the graphene sheets on cotton as depicted in Figure 5.1. Finally, the cotton is heated to activate the bonds between the graphene and cotton fibers to form a crosslinking network which includes graphene particles; hence, causing chemical cross-linking. As shown in Figure 5.1(c), after being treatedwith graphene, the color of cotton fabric changed from white to black, demonstrating that this material bonds with cotton via the electrons in the hydroxyl group in cellulose, breaking one of the C-O bonds in the graphene sheets (Gao D et al., 2022).

Universiti Malaya

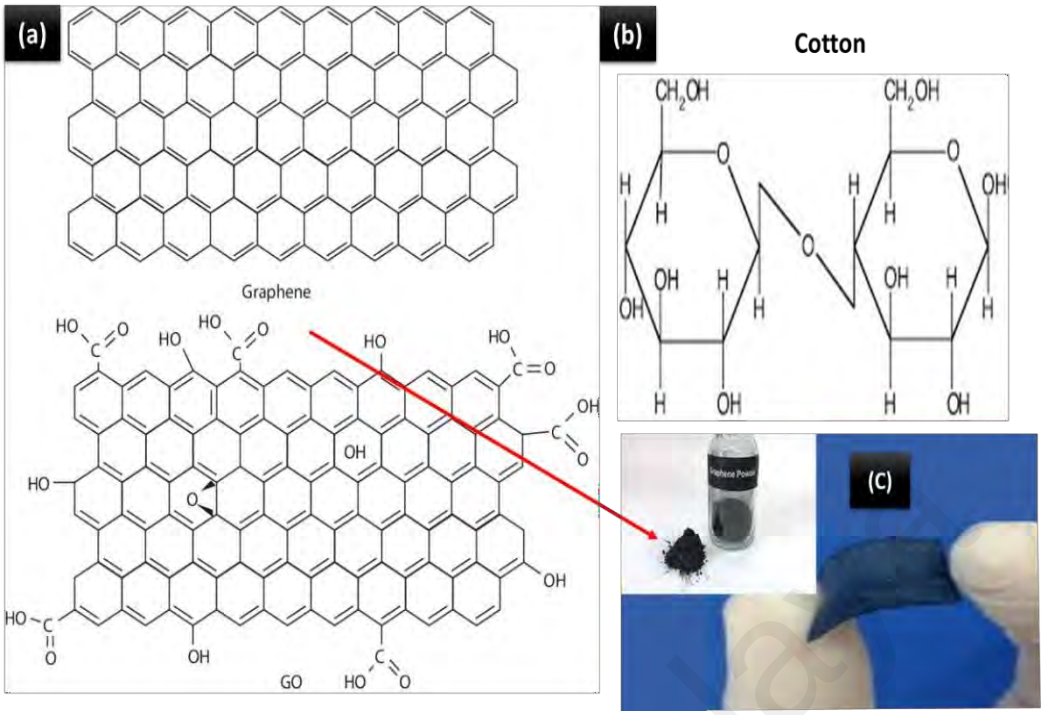

Figure 5.1 : The chemical structures of (a) graphene and (b) cotton and (c)cotton treated with graphene.

By incorporating graphene into cotton, agglomeration on the cotton surface is reduced to an optimal ratio, which is necessary to achieve desired properties. Due tothe strong interaction of bonds between graphene and cotton fabric, the electron transfer efficiency of cotton is greatly improved, and the graphene solution preparedwith DMSO and SDBS can reduce the stacking of cotton fiber, which makes it suitable for many potential applications including protective clothing, health monitoring, motion sensing, and sportswear.

5.2 Surface micro-morphology of the cotton fabrics

The surface morphology of the pure and treated cotton was studied by scanning electron microscopy (SEM) as shown in Figure 5.2. From the SEM images, it is clear that graphene affects the shape of the surfaces of the fibers. The surface of thecotton was found to be smooth before it was treated with graphene as in Figure 5.2 (a) & (b), while it turned rough after the treatment as depicted in Figure 5.2 (c) & (d).

Universiti Malaya

Due to the bonds between graphene and the cotton fiber, the electron transfer efficiency in the composite fibers is greatly improved (Figure 5.3) (Gao D et al., 2022). Graphene reduces the stacking of the textile fibers through the perfect distribution of the graphene on the cotton sample. It is observed that the graphene coating is well distributed on the cotton surface. Also, a decrease in cotton fiber ripple is observed due to the presence of DMSO with graphene. The dip-coating continued to form the layers, and a high concentration of coating was formed on thecotton fibers.

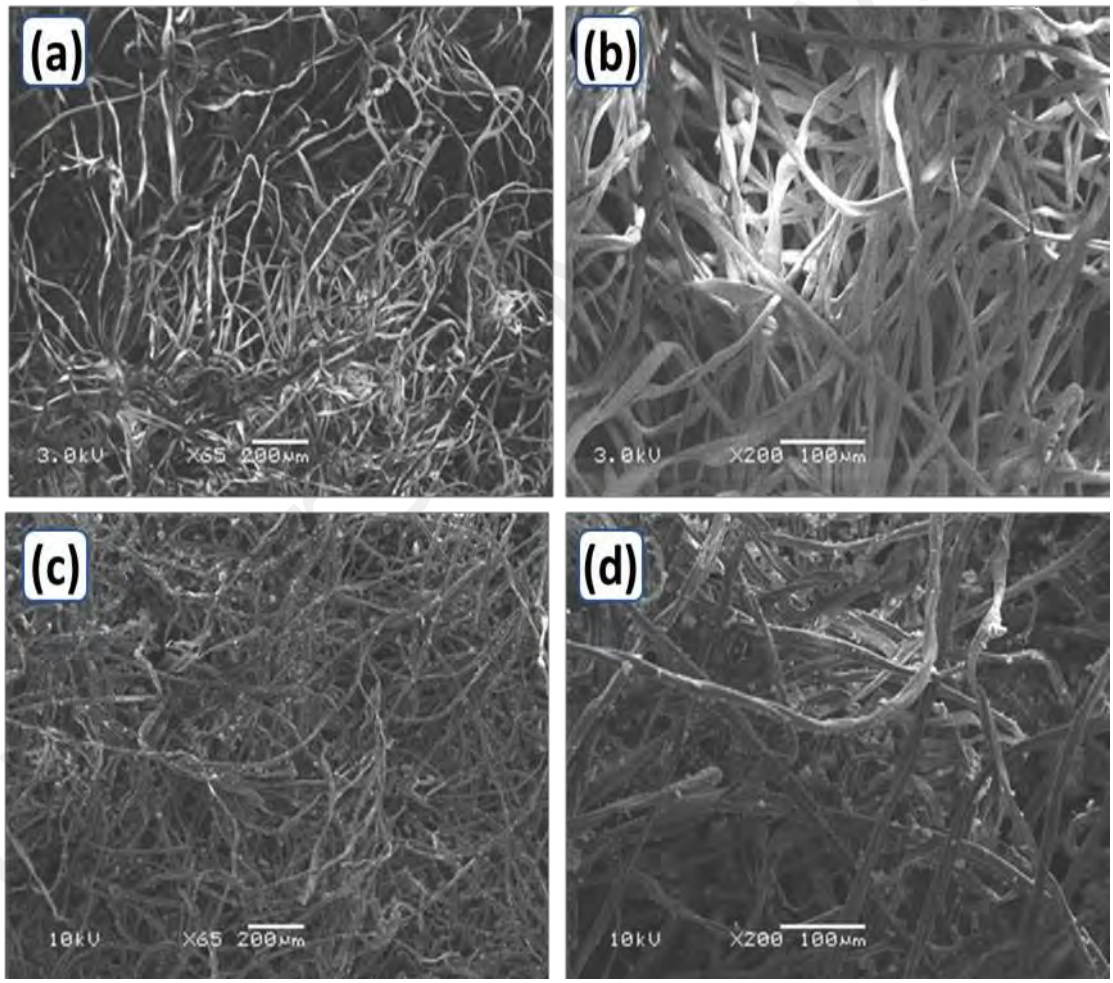

Figure 5.2 : Scanning electron microscopy images of pure cotton fiber: (a) & (b) before treatment; (c) & (d) after treatment.

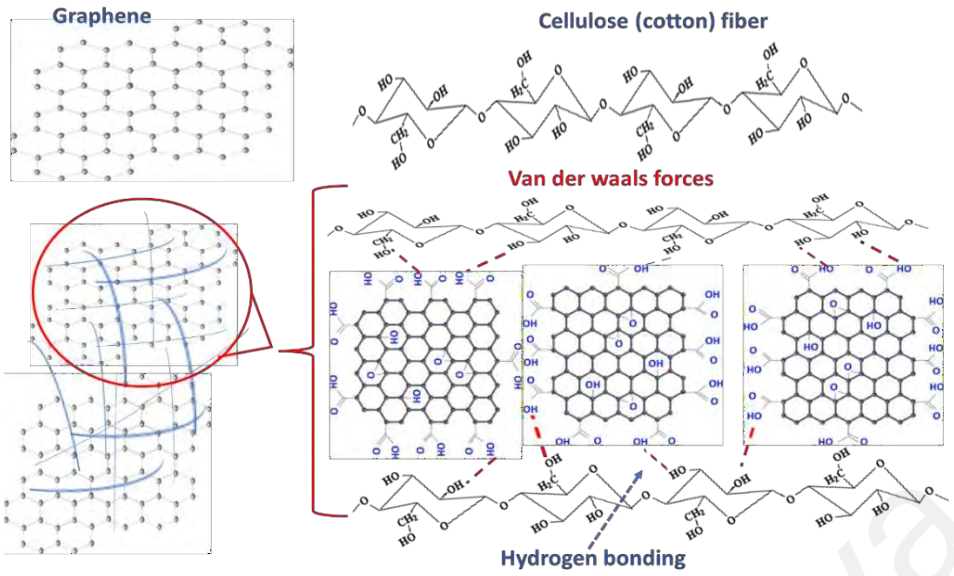

Figure 5.3 : Schematic representation of the formation of bonds between graphene and cellulose (cotton) fiber.

5.3 EDX Analysis

Energy-dispersive X-ray spectroscopy measurement was performed on pure and graphene-treated cotton to determine the elemental composition and purity of the samples. The spectra of the pure cotton samples showed peaks around 0.277 keV and 0.525 keV, indicating the presence of elements carbon and oxygen, respectively (Liu H et al., 2014), as shown in Figure 5.4 (a). Figure 5.4 (b) shows the EDX pattern of the graphene-treated cotton.

An additional peak, apart from carbon and oxygen peaks, is seen at 2.307 keV forthe element sulfur, which is due to the presence of graphene along with DMSO and SDBS.

Universiti Malaya

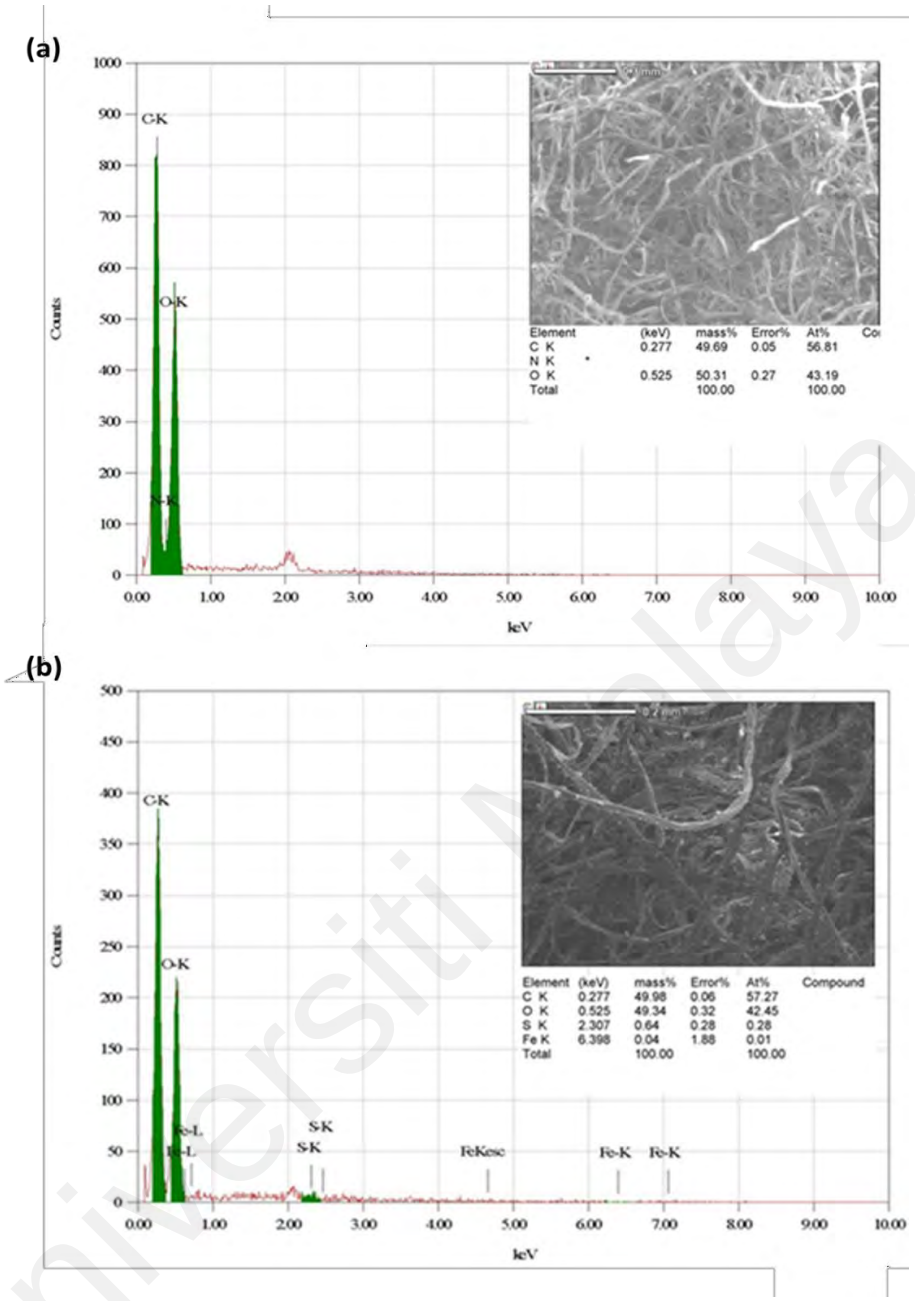

Figure 5.4 : (a) EDX pattern of the untreated contton and (b) EDX pattern of thegraphene-coated cotton.

5.4 FTIR characterizations of the graphene cotton fabric

Fourier transformation infrared (FTIR) spectroscopy was performed in the frequency range 700 - 1800 cm^{-1} for both pure cotton and graphene treated cotton (Figure 5.5). The peaks observed at 1300 cm^{-1}, 1320 cm^{-1}, 1120 cm^{-1}, and 1680 cm^{-1} are attributed to the C-OH bonding groups, C-O single bond stretch and C-H stretch. It is to be noted that the O-H bonds have much higher stretching frequenciesthan the corresponding bonds of

heavy atoms.

The spectrum of pure cotton shows major peaks at 1000, 1058, and 1300 cm^{-1} dueto OH, stretching of the C–H and C–O vibrational modes (Hequet E F et al., 2016; Zhu R et al., 2020). Weak signals are also observed at 900, 868, and 800 cm^{-1} which correspond to C-H vibrational modes, C-H bending (deformation stretching), and C- H vibrational modes. Further, the bands observed in pure cotton at 750 and 710 cm^{-1} are assigned to Iα and Iβ phases, while the cotton treated with graphene layers showed a strong band at 1730 cm^{-1} due to the C-O stretching vibrations and the signals at 1270, 1680 and 810 cm^{-1} are due to the symmetric and asymmetric stretching vibrations of the C–O bond, which are not present in the original cotton sample (Zhu R et al., 2020). In addition, peaks observed at 1400 and 1125 cm^{-1} correspond to the asymmetric and symmetric stretching vibrations of the C-H bond. Furthermore, medium bands are observed in the region from 1375-1280 cm^{-1} due to the C-H bending from the CH_2 group (Liu H et al., 2014). The peaks at 1730, 1680, and 1270 cm^{-1} indicate the presence of graphene in the grafted cotton fibers (Yazdanshenas M E and Shateri Khalilabad M, 2013). The results corroborate verywell with the X-ray data (López Barroso J et al., 2018).

Universiti Malaya

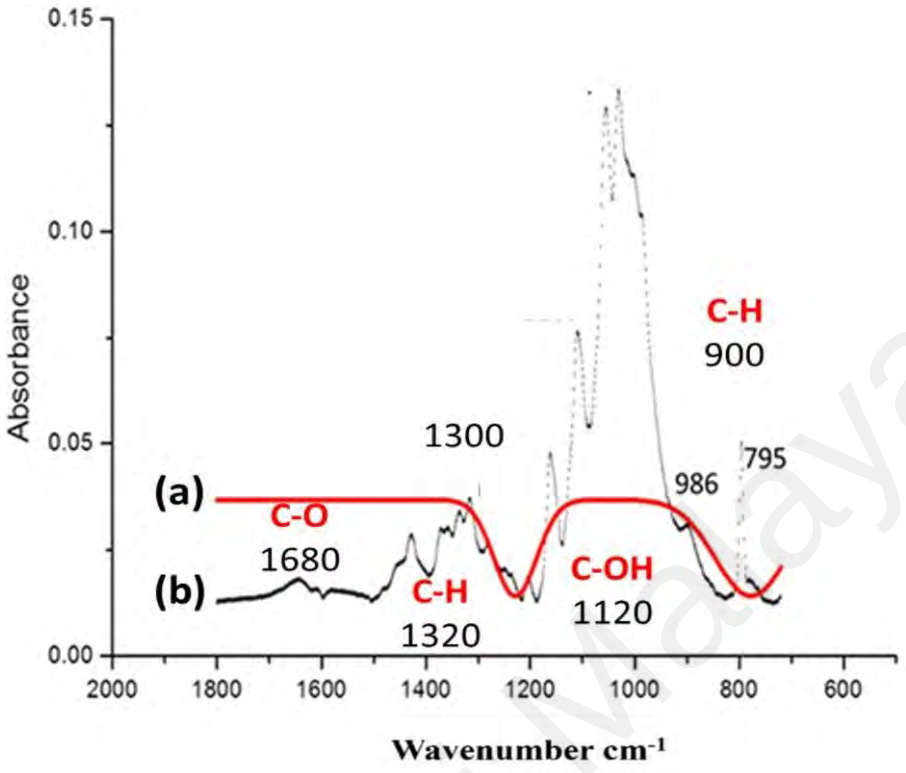

Figure 5.5 : FTIR spectra of (a) pure cotton thread strands and (b) the graphene-coated cotton.

5.5 X-ray Diffraction

Figure 5.6 presents the XRD pattern of the pure and treated cotton sample. XRD pattern reflects the changes in the characteristic diffraction peak after treatmentwith graphene. The main peaks observed and indexed for the pure cotton sample are (1-10), (110), and (020). The strong diffraction peaks at 2θ = 14.9°, 16.8°, 22.8°, and34.7° are characteristic peaks of cellulose crystalline form in cotton (López Barroso J et al., 2018). For the graphene-treated sample, a narrow, sharp peak is observed at 22.22º, with inter-crystalline spacing d = 0.399 nm, due to the presence of a typical graphene crystal structure.

Universiti Malaya

As observed from the high-intensity peak of the graphene-coated sample at layers 17th, the diffraction peak disappears and a new diffraction peak appears at 15.08º, withan inter-crystal spacing d value equal to 0.8945 nm, which indicates the introductionof oxygen functional groups. These oxygen-containing groups combine with water molecules and cotton fiber samples through hydrogen bonding with graphene, which has a hydrophilic property. For graphene-treated cotton, the XRD pattern was similarto that of pristine cotton with an additional peak at 26.6°.

The presence of diffraction peaks at 25.5° and 27.2° in the XRD pattern of graphene-treated cotton also confirms that the cotton fibers were completely covered with graphene sheets (Zhu R et al., 2020; Batoo K M , Badawi N M and Adil S F,2021).

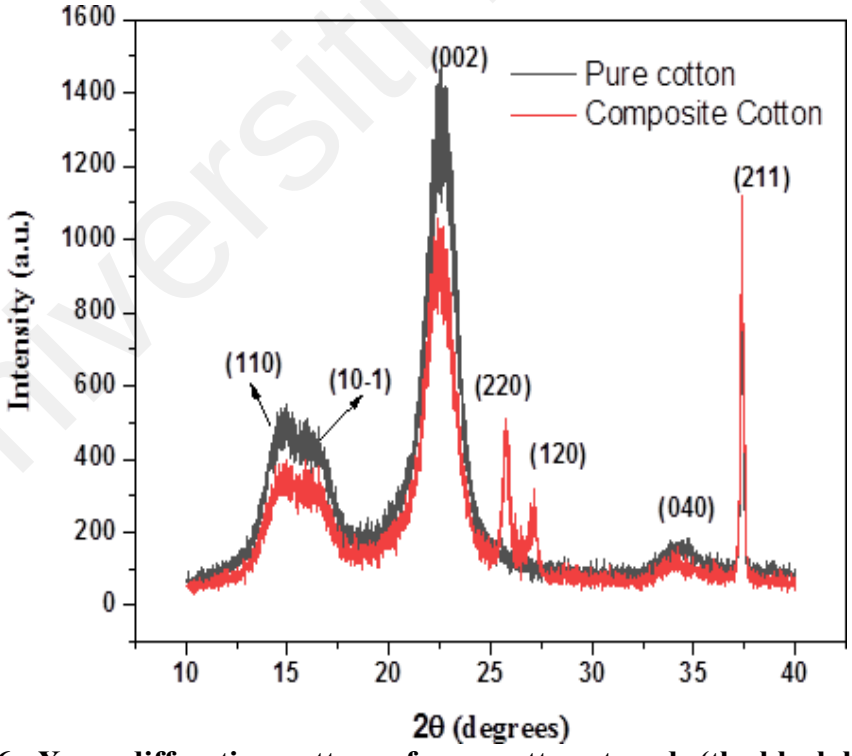

Figure 5.6 : X-ray diffraction pattern of pure cotton strands (the black line), and graphene-coated analogue (the red line).

Universiti Malaya

5.6 Thermal analyses (TGA & DSC)

TGA & DSC analyses are important tools to study the thermal stability and material degradation pattern of the samples. The thermal stability of the pure cotton sample and graphene treated cotton was examined using thermogravimetric analysis (TGA). TGA of control pure cotton exhibited a minor weight loss at 50.27 °C, probably due to the removal of moisture content. The onset of the melting peak arosegradually from 350 °C. After 380 °C, the major decomposition of the control peak started and it reached the peak melting point at 400 °C.

The thermogravimetric measurements were performed in the temperature range of25 - 600 °C as shown in Figure 5.7(a & b). The thermogram of pure cotton shown in Figure 5.7 (a) shows that the first stage of weight loss occurs in the temperature rangeof 100-300 ºC due to the presence of moisture and bound water molecules. The secondstage of weight loss is observed at 350 ºC due to the decomposition of the oxygen- containing functional groups, such as hydroxyl (–OH), and epoxy (C–O–C) which turninto molecules of gas like CO_2 and H_2O (Kabel K I et al., 2015). The thermal stabilityof graphene-coated cotton was analyzed which revealed the higher thermal stability and that decomposition of coated cotton occurred at higher temperatures.

Universiti Malaya

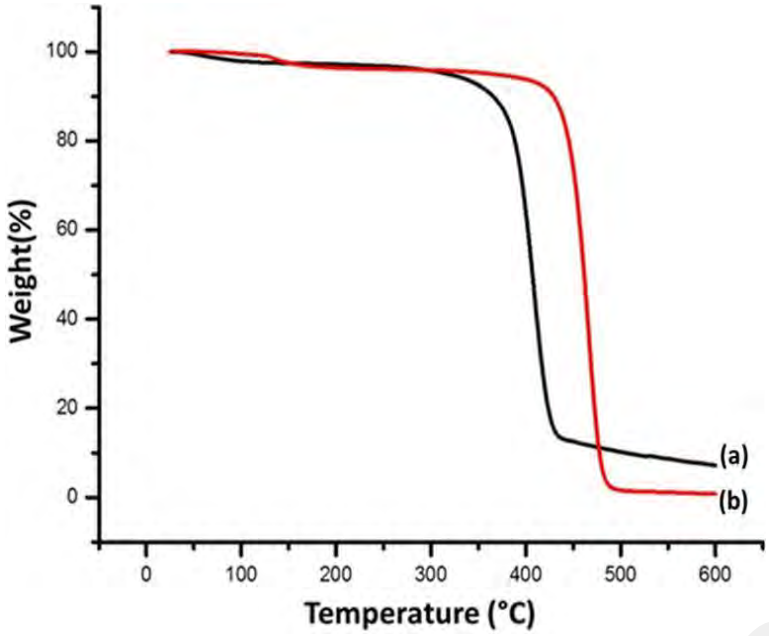

Figure 5.7 :TGA thermograms of (a) pure cotton strands and (b) graphene-coated samples.

In the TGA of graphene treated cotton, the small transition at 150.50ºC is due to the removal of moisture content. The onset of the melting peak arises at 430ºC and the corresponding peak melting transition is observed at 491.50ºC. The transition of graphene, which usually occurs around 200ºC, is not observed in the TGA curve of graphene treated cotton due to the lower weight fraction of graphene present in the cotton surface. The increase in the peak melting point is about 120ºC, which signifiesthe strong molecular level interaction between the graphene and the fabric, due to the(C–C) skeleton in the graphene nanostructures (López Barroso J et al., 2018). The treated cotton decomposes in two stages, the first stage (20 to 150 °C) in which the absorbed water molecules leave and the second stage (450 to 490 °C) in which the coated graphene starts to decompose.

In comparison, it is seen that the weight loss in the pure cotton sample issignificantly less than the graphene-coated cotton (Yazdanshenas M E and Shateri Khalilabad M,

Universiti Malaya

2013). This is because the amount of oxygen-containing functional groups in graphene fiber, such as hydroxyl (OH) and epoxy (C-O-C), is more in the coated sample than in the pure sample. Also, there is combustion of carbon present ingraphene that leads to loss in weight.

In the DSC analysis, it is noted that graphene-treated cotton fibers are flame retardant when the decomposition temperature is above 400°C. Also, it is observed that the pure cotton fiber is subjected to changes in the heat flow pattern when the temperature falls from 360 °C to 330 °C (Figure 5.8). The results indicate that the thermal stability of the graphene-treated cotton improves with the increase in graphene layers. It is demonstrated that, with the addition of graphene to cotton with17th layers, show an increase of glass-transition temperature (Zhu R et al., 2020).

Hence, graphene-treated cotton has better thermal stability and a higher decomposition temperature.

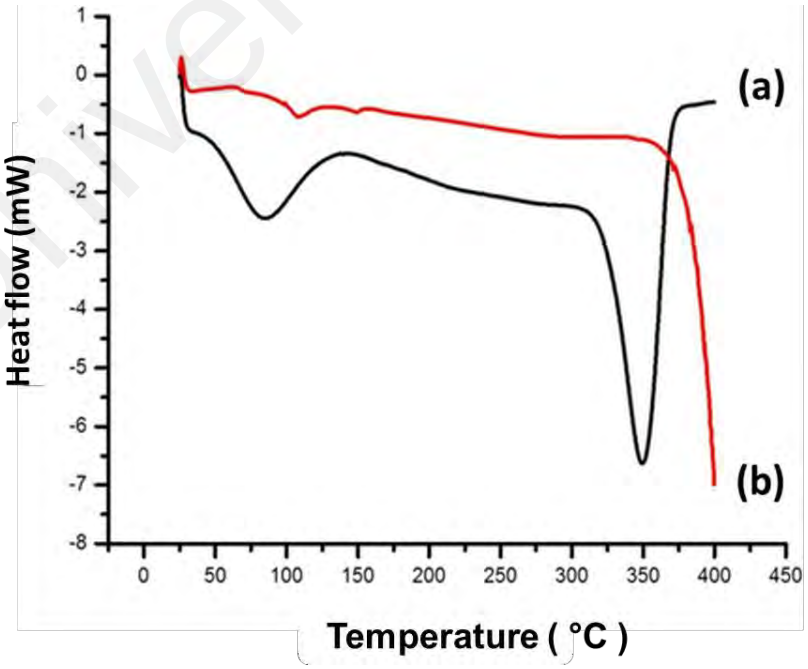

Figure 5.8 : DSC thermograms of the (a) pure cotton, and (b) graphene-coated samples.

Universiti Malaya

5.7 Electrical conductivity of the cotton fabrics

The four-probe method was used to investigate the effective resistance of graphene-treated cotton samples and to study the electrical properties of composite cotton. The pure cotton sample showed no electrical conductivity since it is an insulating material. Pristine cotton has an extremely high surface electrical resistance(~10^9 Ω/sq). However, after treatment with graphene, the surface resistance was found to be between (~370.8 Ω/sq at first layer to ~0.09 Ω/sq) at 17 layers as in Figure 5.9 (a) and listed in Table 5.1 (Yazdanshenas M E and Shateri Khalilabad M, 2013). The higher conductivity of graphene-treated cotton is attributed to the presence of co-activators (DMSO) which catalyze the morphological changes. It organizes the cotton fibers allowing greater penetration of graphene into the cotton fibers resulting in better charge transport. Moreover, it may be due to the effective chemical bonding between different functional groups of graphene and cotton (HongX et al., 2021). The high electrical conductivity of treated cotton also proves the efficiency of graphene. Considering the higher electrical properties of treated cotton,excellent potential applications of the material are expected in the fields like sensors,supercapacitors, the electronic industry, and smart clothing as wearable textiles (Alhashmi Alamer F , B N M and Alsalmi O, 2020). Moreover, both DMSO and SDBS also act as plasticizers that redirect cotton fibers in addition to stabilizing graphene at higher temperatures and allowing a regulated conduction mechanism deep inside by the improvement of bonds between cotton and graphene (Hu Z et al.,2017). Increasing the concentration of graphene layers increases the stability of graphene in the cotton sample and fills the spaces between the fibers and thus, enhances the electrical conductivity of the fabric, but at layer 18, the resistamce value begins to decline due to the beginning of the accumulation of grapheme, as it becomes difficult for the electron to move, thus affecting the electrical conductivity as listed in Table 5.1.

Universiti Malaya

The impregnation process also leads to isotropic electrical conduction throughout the cotton (Sun F et al., 2019). The nanoparticles behave like an electrical insulator that shows a plate resistance higher than 370.8 Ω corresponding to a sheet resistance of 2649.1 Ω/sq. Also, a sudden change in conductivity corresponds to an increase in the graphene concentration at 168.36 wt.%, where electro-filtration occurs leading to a surface resistance value around 0.0901 Ω. At this concentration, the composite sample behaves like an ohmic conductor and exhibits the lowest resistance value mentioned in Table 5.2. Improvements in the resistance value are of great importancefor practical purposes. A comparison of previously reported work on cotton/graphene-treated samples with the present work based on their method of preparation and electrical resistivity is presented in Table 5.3. Furthermore, the ionic conductivity of the graphene-treated cotton fibers at room temperature was determined (Remadevi R et al., 2020). Due to the presence of graphene, the electrode behaves like an ionic conductor, as it enhances ionic conduction and supports ionic diffusion through polymer networks along cellulose strands in pure cotton. The high porosity three-dimensional structure of the composite cotton and the graphene sheets increase its water-holding capacity due to the high absorbency of the cotton, leading to smoother pathways for ion transport. The electrolytic ions thus flow smoothly through the cotton around the charged groups, and hence, the ionic conductivity increases (Yun Y J et al., 2017).

Universiti Malaya

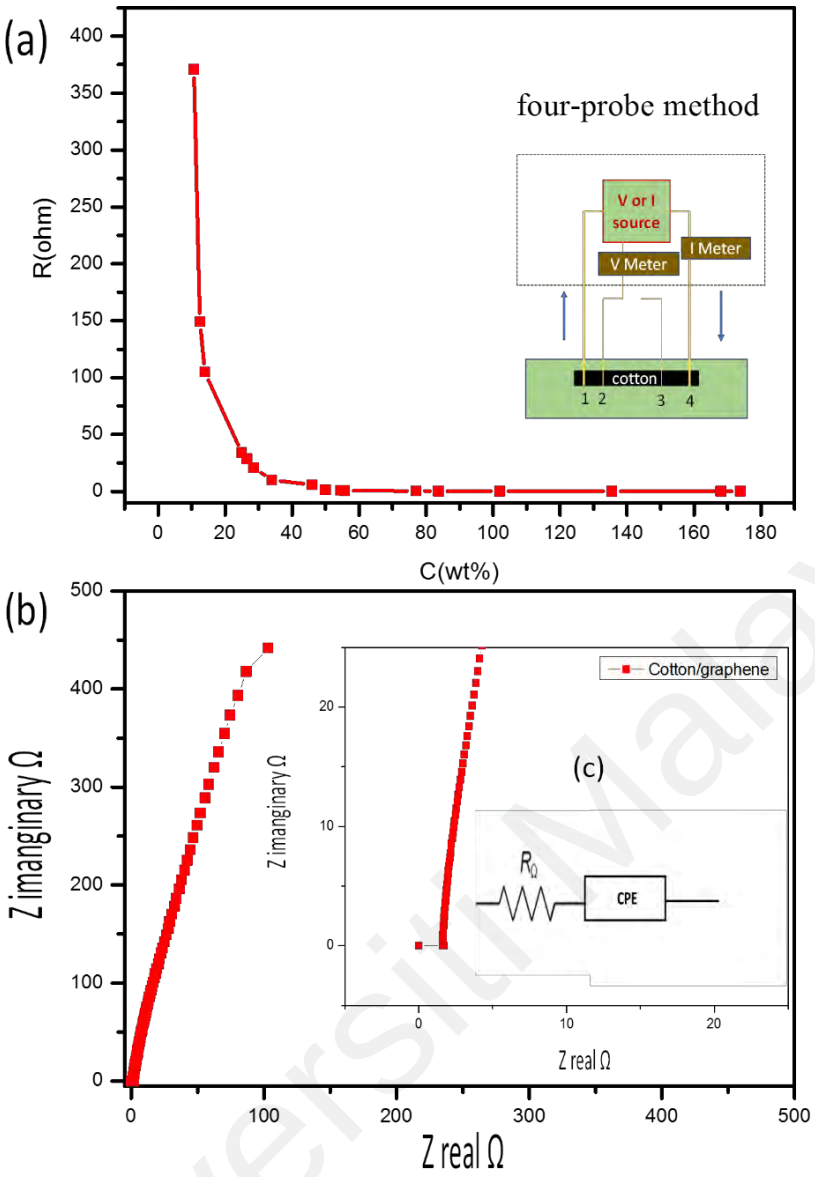

Figure 5.9 : (a) The sheet resistance of cotton fabric treated with different concentrations of graphene. (b) Nyquist plots of the cotton/graphene and (c) Electrical equivalent circuit used to fit the spectra of the graphene-treated cotton fibers at 17th layers.

University Malaya

The ionic conductivity of the graphene-treated cotton achieved at room temperature 9.2 x 10^{-2} S/cm (Figure 5.9 (b)). It is observed a straight line parallel to the imaginary axis (Makowski, T et al., 2018). Equivalent circuits reveal the extent towhich graphene covers cotton, which prevents electron transfer, the surface of the electrode that more complex equivalent circuits need to call modified electrodes, and can be graphene-treated cotton fibers the rate in the electrode resistance and charge separation represented by a second RC parallel group in series with the electrical circuits. Vertical straight lines appear for capacitors with angles less than 90° (Figure 5.9 (c)) (Bhattacharjee S et al., 2021).

To ascertain the electrical stability of the graphene-treated cotton fibers, the conductivity of coated cotton with graphene was measured in terms of bulk resistance using a four-probe technique over two months at room temperature, andthe results are shown in Figure 5.10. The treated samples demonstrated good electrical stability, as the electrical resistance values remained almost unchanged over the period of two months.

Universiti Malaya

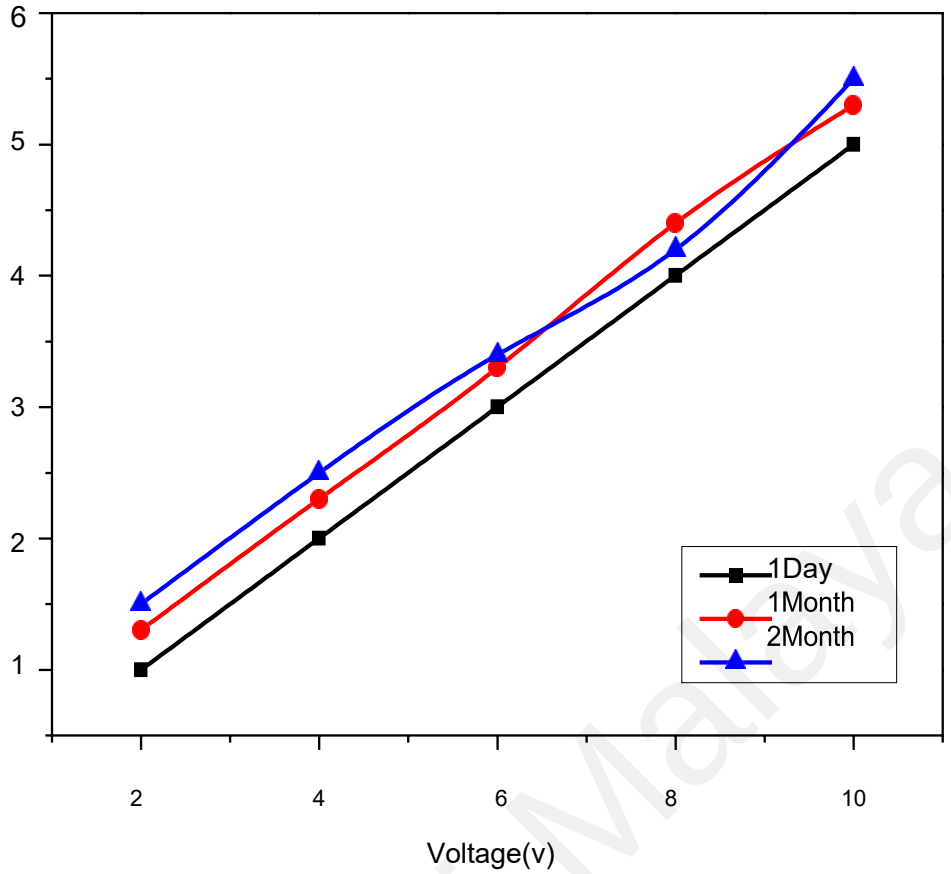

Figure 5.10 : I-V measurement on day 1, after 1 month, and 2 months.

Table 5.1 : The dependency of graphene-coated cotton fabric resistance and sheet.

Layer	C (wt. %)	R (Ω)	R_S (Ω/sq)
1	10.7	370.8	2649
2	12.5	149	1065.5
3	14	104.9	749.
4	25	34	243.6
5	26.5	28.8	206
6	28.6	20.9	149.5
7	34	10	72
8	46	5.89	42
9	50	1.50	10.7
10	54.6	1	10
11	55.8	0.66	4.7
12	77	0.4	3
13	83.7	0.19	2.9
14	102	0.17	2.5
15	135.5	0.15	2.06
16	173.8	0.1	1.8
17	186	0.09	0.6
18	188	0.155	2,067

Universiti Malaya

Table 5.2 : The sheet resistance of graphene cotton fabric at optimum concentration at 17 th layers .

C (wt %)	R (Ω)	Rs (Ω/sq)	log c	Log Rs
168.3	0.090	0.644	2.226	- 0.1909

Table 5.3 : Comparison of reported work on cotton/graphene with the presentwork.

Material	Method	Electrical property	Reference
Cotton cellulose coated with graphene	Dip-pad-dry	91.8 kΩ/sq	(Jain V K andChatterjee A, 2022)
Cotton fabric (SCF)/graphene oxide (rGO)	Dip coated	40 Ω/sq	(Tunakova Vet al., 2020)
Graphene oxide (RGO)coated-copper (Cu)/silver (Ag) nanoparticle incorporated cotton fabrics	Dip-coating approach	16.70 kΩ/sq	(Evseev Z Iet al., 2023)
Graphene oxide/ cotton/ sodium dithionite($Na_2S_2O_4$)	Dippingmethod	± 0.92 kΩ/ sq	(Sahito I Aet al., 2015)
knitted cotton fabrics/GO/ sodium nitrate/ H_2SO_4 and $KMnO_4$.	Dippingmethod	0.19 MΩ/sq	(Ganguly Set al., 2020)
rGO/ZnO coatedcotton	Simple spraying and drying process	8.4 10^{-2} S/cm	(Gan L et al.,2015)
Graphene / cottonfabric (HC-GCF)	Coatingmethod	7 Ω/ sq	(He S et al.,2019)
Graphene Oxide/Silver Nanoparticles/ CottonFabric	Dip-coating	~10^{-13} S/cm	(Gupta S etal., 2020)
Graphene nanoribbon/cotton fabric	Wet coating approach	~80 Ω 571.4 Ω/sq	(Zhao C etal., 2023)
Graphene oxide (GO) nanosheets/cotton fabric	Dip and dry method	10^{15} Ω/sq	(Knittel D and Schollmeyer E,2009)
Graphene/ pure cottonfabric	Dip-coating	0.0901Ω; ~0.644 Ω/sq	Presentwork

Universiti Malaya

The stability of the treated cotton sample was studied with a change in temperature from 25 °C to 100 °C as shown in Figure 5.11. The results indicate that the resistance of the graphene-treated cotton sample initially increased with increasing temperature. This shows that the samples exhibit metallic behavior, with the increase in temperature, the random motion of electrons increases, the number of conduction electrons decreases. As a result, the number of collisions of electrons with the positive ions increases in a cotton. Hence, the resistance of a cotton increases with increase in temperature. However, above 80 ºC, the resistance starts todecrease sharply with increasing temperature. Two reasons could be possible for this sharp increase in the current above 80 ºC. One, as the temperature increases, the DMSO solution evaporates, and the graphene sheets come closer to each other, thereby increasing the possibility of conduction. The structure of graphene is a two- dimensional plane, in which each carbon atom has three strong σ covalent bonds withnearest-neighbour carbon atoms and a weak van der Waals π bond in the perpendicular direction, ready to bond with other atoms (Evseev Z I et al., 2023).

Secondly, as the graphene planes and DMSO come close to each other, the π bonding happens between carbon and DMSO in the perpendicular direction (Jain V K and Chatterjee A, 2022). With an increase in temperature, DMSO evaporates between graphene planes, thus planes condense, and get closer to each other leading to charge transportation. It is seen that an increase in the graphene content reduces the surface resistance, while it increases the thermal stability of the composite cotton (Evseev Z I et al., 2023). To study the stability and thermal response, samples were kept for twomonths at 25°C and the relative humidity was around 65 %. It was observed that the sample retained its maximum resistance value of 0.6 Ω/sq over the period.

Universiti Malaya

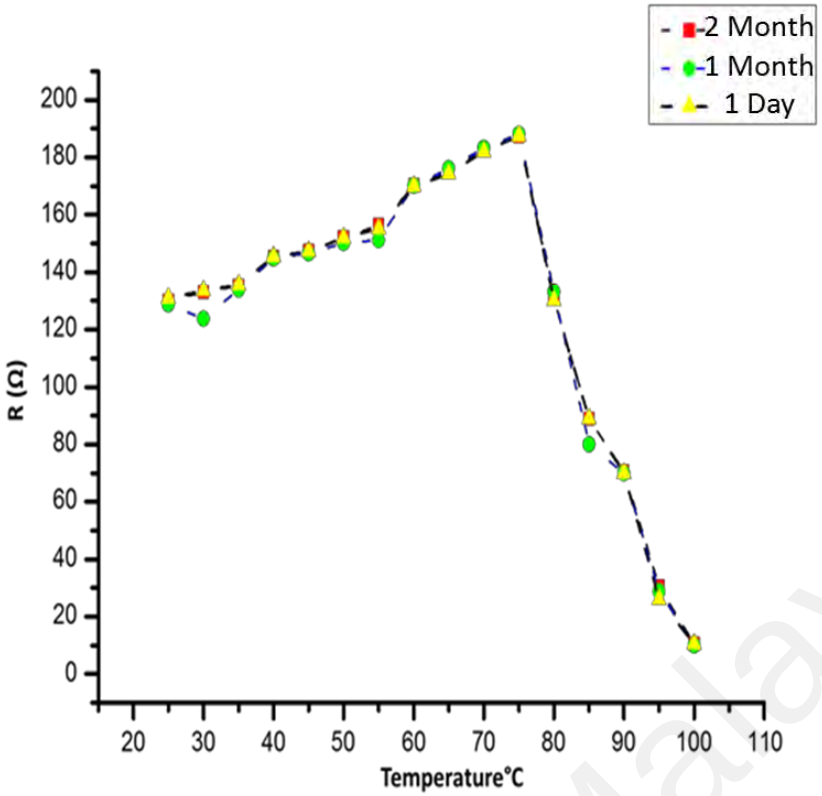

Figure 5.11 : Resistance variation with temperature from 25 °C to 100 °C, for coated cotton with optimum graphene concentration.

5.8 Mechanical Property – Tensile Test

The mechanical properties of the composite cotton sample were evaluated by a tensile strength test (Figure 5.12). In general, carbon-based materials often become hardened. It was observed that cotton impregnated with graphene had an increase in material hardness and strength. The treated sample shows three types of strengths: (1) yield strength, (2) ultimate strength, and (3) fracture strength.

Yield strength is the stress that the material can withstand without permanent deformation, (2) ultimate strength is the maximum stress that the material can withstand, and (3) fracture strength is the maximum value of strain where the material breaks. The measured strength and modulus of elasticity show that the processed cotton is 7 times higher than that of pure cotton (Evseev Z I et al., 2023).

Universiti Malaya

Compared with pure cotton fiber, the tensile strength of graphene-treated cotton is reduced by 67 %. Chemical regeneration reduces the tensile strength, modulus, and elongation of the treated cotton bundle by 13% (Tunakova V et al., 2020).

The stress coordinates on the stress-strain curve at the point of rupture after 7%for sample (1) and 13% for sample (2) at a stress rate of 0.006 per minute, respectively.

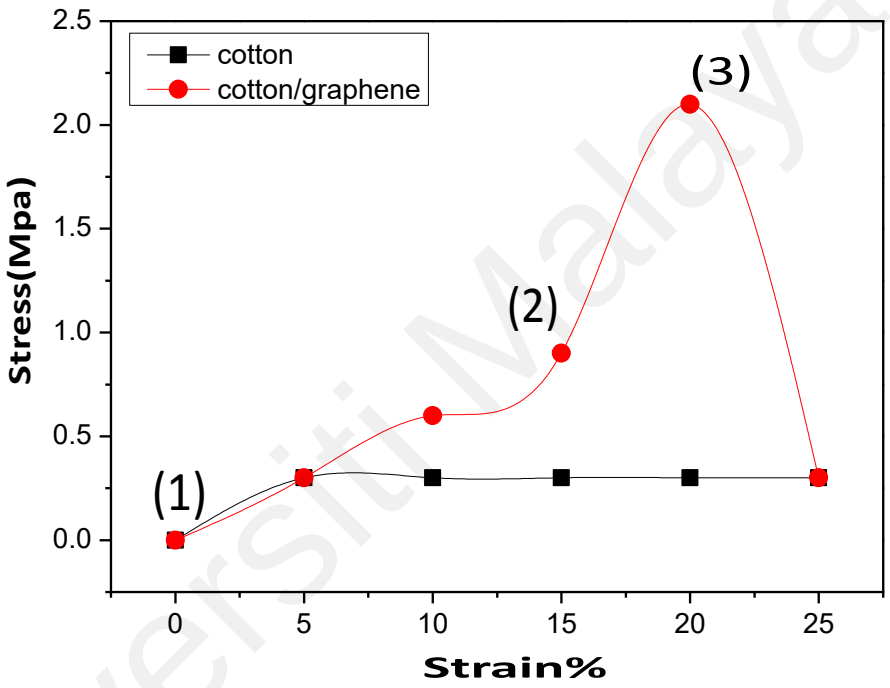

Figure 5.12 : Stress-strain curves of cotton /graphene textiles at 17th layers.

5.9 Proof of Concept

To verify the potential use of the composite cotton as an alternative to the conductive wires, an LED lamp was illuminated by powering the graphene-coated cotton in a series configuration to a DC power supply of 12 V. The lamp illuminatedwith no decrease in its intensity when tested for 35 minutes as shown in Figure 5.13.

Universiti Malaya

The experiment demonstrated the ability of the material to be used as an alternative to a conductive wire in a typical electrical system. The proof-of-concept and all ofthe studied results show that graphene-treated cotton fabric has promising applications such as mechanical sensors, actuators (Jain V K and Chatterjee A, 2022), electromagnetic shielding (Alhashmi Alamer F , B N M and Alsalmi O, 2020), flexible heating elements and supercapacitors (He S et al, 2019).

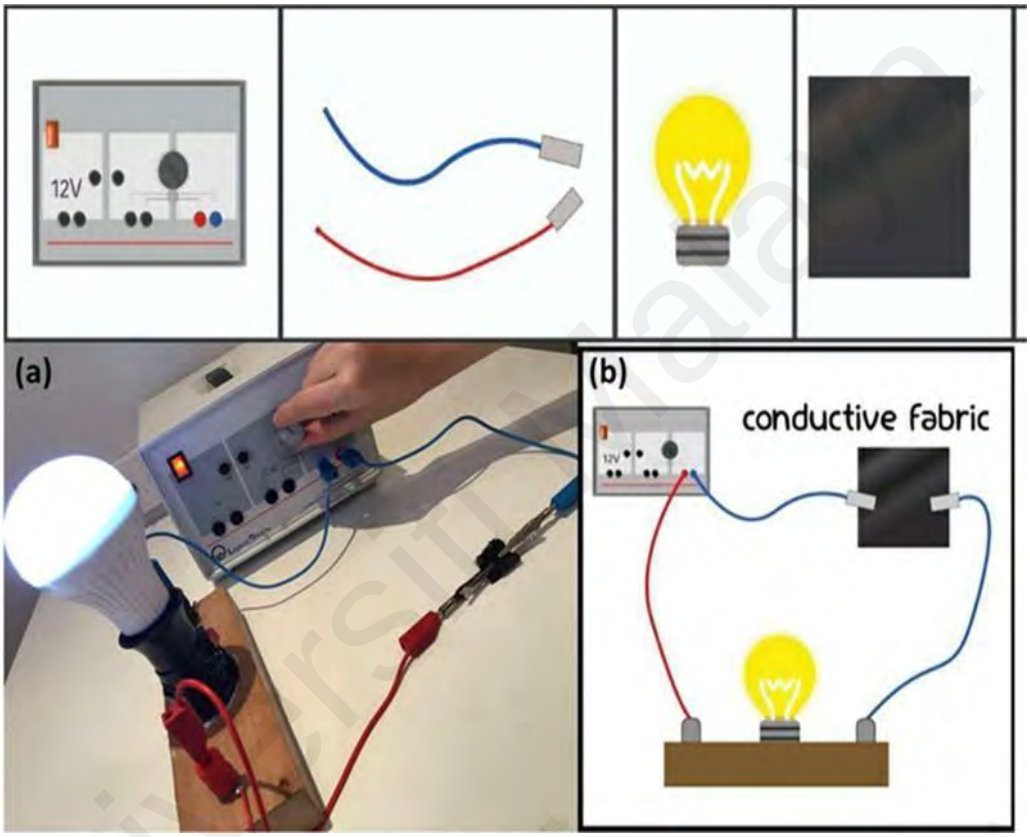

Figure 5.13 : (a) DC LED illuminated by conductive graphene-treated cotton fabric at 17 th layers , (b) circuit diagram.

5.10 Summary

Graphene-treated cotton was successfully prepared to convert cotton from an insulating material into a good electrical conductor using a layer by layer technique with a resistance of 0.644 Ω/sq. Graphene bonding was confirmed on the cotton surface by SEM, FTIR, and XRD while EDX testing ruled out the presence of any unwanted elements in the samples. Further, the cotton sample was tested by connectingit in series to a

12 V power supply and lighting a bulb. Due to the electrostatic attractionbetween the cotton substrate and the graphene particles, the coated sample exhibited significant thermal stability and electrical properties. The results demonstrate potentialcommercial benefits and technological advantages, especially in the design of electrical devices and smart conductive fabrics. However, the functioning of the surface effects in graphene networks is still debatable and further studies are warranted.

Universiti Malaya

CHAPTER 6: RESULTS AND DISCUSSION OF HYDROGEL ELECTROLYTE BASED ON GRAPHENETREAT COTTON/GRAPHENE FOR SUPERCAPACITORS

6.1 Introduction

Nowadays, flexible energy storage devices such as supercapacitors have received wide attention as they offer flexible and wearable electronics. Solid-state supercapacitors are new types of supercapacitors that can operate under successive expansion, bending, and torsion conditions. However, to obtain a flexible supercapacitor in the solid state with high electrochemical performance and super flexibility many challenges are encountered (Kasaw E, Haile A and Getnet M, 2020).The performance of the flexible supercapacitor (SCs) depends on the properties of the electrolyte materials, electrode materials, and device configuration (Wang K et al., 2016). Flexible Solid-State Supercapacitors (FSSSC) are characterized by fast chargeand discharge rates, high energy density, ease of manufacture, and low cost, and have promising applications as power sources for multifunctional portable and wearable electronic devices (You Y et al., 2020). The mechanical strength of the active electrodes and the electrolyte is what determines the configuration and flexibility of the devices, thus supercapacitors are expected to have excellent mechanical flexibilityand to achieve the absorption of significant levels of stress in rigorous real applications(Wu D Y and Shao J J, 2021). Carbon materials with variable and varied microstructures create great opportunities for the manufacture of high-performance flexible active electrolytes FSSSC. For example, graphene is a two-dimensional carbon material that has extraordinary physical properties, such as a large specific surface area, strong mechanical strength, high optical transparency, ultra-fast electronic mobility, and excellent thermal conductivity, therefore, it is an ideal active material for supercapacitors (S H Lee et al., 2011). However, owing to the p–p

Universiti Malaya

stacking interaction and van der Waals force, graphene is easy to agglomerate (X Wang et al., 2018).

Aqueous electrolytes have attracted a lot of attention due to several reasons. Aqueous electrolytes do not need the introduction of water and oxygen, such as organic electrolytes, which greatly reduces the cost. Also, it has low viscosity, low resistance, and high safety (Jia M et al., 2021). The smaller the resistance of ion transport, the lower the thermochemical temperature which can accelerate the chargestorage and the process thus improving device integrity. Importantly, compared to organic electrolytes, aqueous electrolytes have much smaller ion sizes and higher ionic conductivity, which gives them greater capacity, superior charge and discharge,and excellent power performance. On the other hand, strong acidic electrolytes such as H_2SO_4 and KCl with the lower H^+ generally have the highest ionic conductivity (0.8 S cm^{-1}) (Jia M et al., 2021).

Cellulose, the first and most abundant renewable biopolymer in nature, can be obtained mainly from plants, such as cotton, wood, bamboo, and grass. Cotton is aninexpensive natural product mainly based on cellulose and is widely used in appareland textiles in our daily life (X Wang et al., 2018). Although cotton is an insulator,it is directly converted into carbonated cotton when treated with a conductive material, to make it highly conductive while maintaining its flexibility, excellent mechanical properties, and structural compatibility, and with its improvement, the energy storage capacity of cotton-based supercapacitors (SC) becomes an importantfactor for practical applications (Kadir M et al., 2011).

Here the method of controllable fabrication of cotton-based and graphene-based tandem solid-state hydrogel electrolytes, and the electrochemical/mechanical

Universiti Malaya

performance of graphene-based flexible FSSSC (those based on cotton films and fibers) are associated with strategies commonly used to improve performance. The physical properties of the fabricator membranes and electrochemical performances of SCs have been marked (Sukor M et al., 2009).

6.2 X-ray diffraction (XRD) analysis

The prepared hydrogels were analyzed for the structural and phase formation through X-ray diffraction (XRD) as shown in the Figure 6.1. The XRD patterns of the CGH peaks were observed at 38°, 44°, 65° and 78°, which correspond to the crystal planes (111), (200), (220) and (311), respectively. A very strong peak was observed at 26.4° which is assigned to the plane (002) which indicates that the sample CGH2 is highly crystalline in nature. XRD pattern of graphene has a strongpeak at 2θ =25° and 27°.

The XRD results show the semi-crystalline nature of the hydrogels in the sample CGH4. In the sample CGH2 there is noticeable peak in the XRD pattern at 28°, 38°, 42° and 48°,complete dissociation may be due to soaking in H_2SO_4. This observation is consistent with the interaction between the hydrogel and the cotton/graphene confirming the amorphous nature of the samples CGH3 and CGH4 (Gürünlü B , Taşdelen Yücedağ Ç and Bayramoğlu M, 2020).

Universiti Malaya

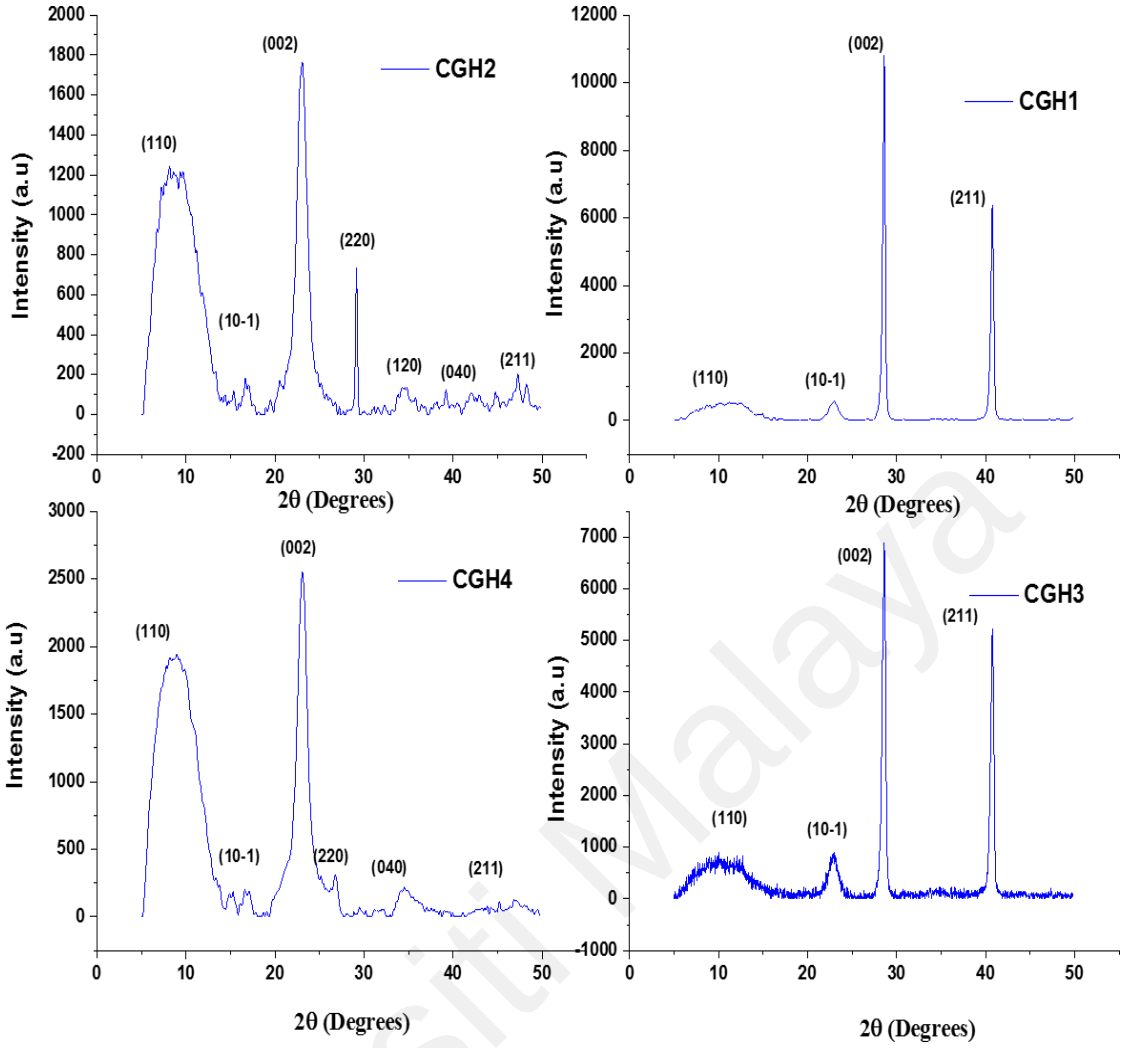

Figure 6.1 : XRD patterns of the samples CGH1,CGH3, CGH3 and CGH4, respectively.

6.3 FTIR analysis

Figure 6.2 shows the FTIR spectra of hydrogels based on 3D pure cotton graphene. The FTIR spectra of the CGH1 and CGH3 hydrogels show a weakabsorption band at 1700 cm $^{-1}$ due to the expansion vibration C = O (Ajalli N et al.,2022). The band observed at 1227 cm $^{-1}$ is due to C-O groups and also at the band 1045cm $^{-1}$, while the broadband observed at 1000 cm^{-1} could be due to C=C stretching vibrations in the carboxyl (Lin J et al., 2020).

Universiti Malaya

It is because there are still few oxygen-containing groups on the surfaces of CGH2, CGH4 in comparison to the FTIR spectra of samples treated with high concentrationsof graphene. Pure cotton shows peaks at 3500.55 cm^{-1}, corresponding to O–H stretching vibration and 1620.77cm^{-1}, 1402.33 cm^{-1} and 1360.11 cm^{-1} corresponds to C–H stretching vibration, O–H bending vibration and C-O stretching vibration (Lin Jet al., 2020). A peak of CGH2 is observed at 2870 cm^{-1} and 570 cm^{-1} can be attributedto the symmetry and asymmetry stretching vibrations of C-H. The hydrogel presents new peaks attributed to graphene (C = C) which causes an extended deformation at 1500 cm^{-1} (Riaz T et al., 2021). The group C = C results in an extended deformationat 1355cm^{-1} and C-H aromatic bends at 500 cm^{-1} (Bai, Y et al., 2020).

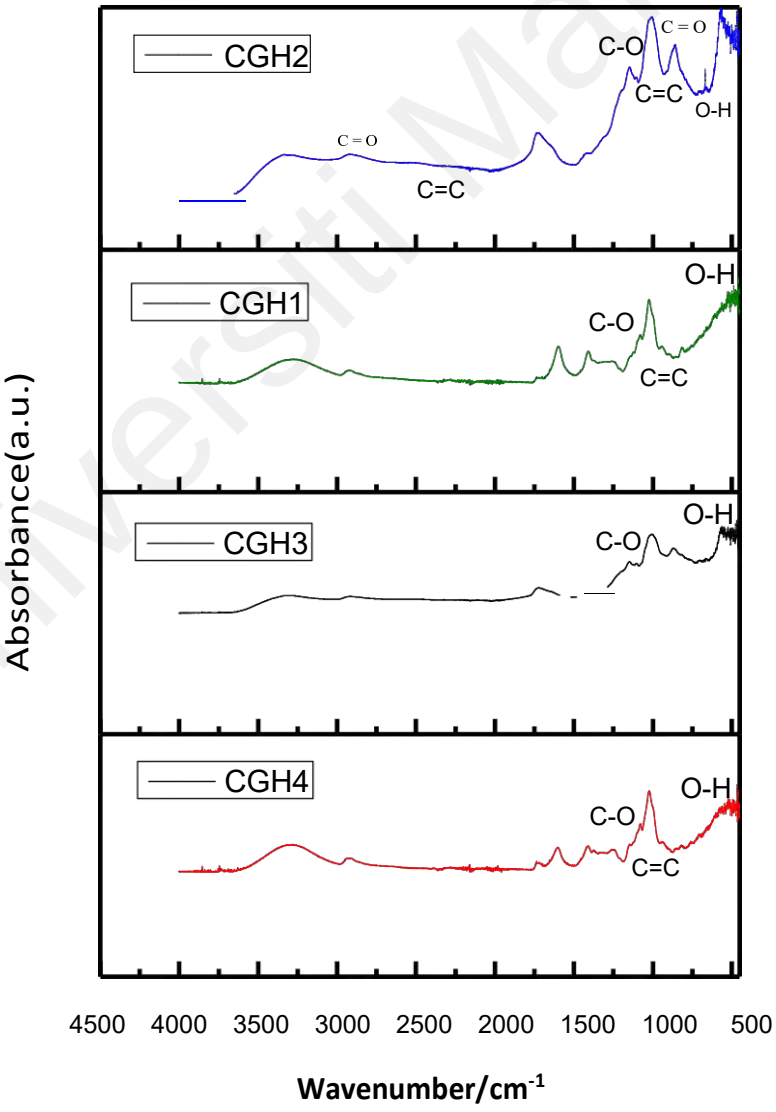

Figure 6.2 : FTIR Spectra of samples CGH1, CGH2, CGH3 and CGH4.

Universiti Malaya

6.4 Morphological studies

The surface morphology of the hydrogel electrolytes was examined by FESEM as shown in (Figures 6 .3 and 6.4). It is seen that the morphology of the samples CGH2 and CGH4 possess relatively higher graphene formation/composition ratios.

However, when graphene content is increased in the hydrogel, the pore distribution of samples CGH2 and CGH4 films becomes sparse and pore sizes also increase. Thismay be due to the phase separation between graphene and a compound hydrogel which can occur when the chain length and surface area increase due to the presence of graphene as indicated by the higher absorption due to the presence of cotton in thehydrogel formation (Wu X et al., 2020). As shown in Figure 6.3 (b,c) and Figure 6.4 (e,f)), the microstructures of the as-prepared samples CGH1, CGH2, CGH3 and CGH4 are characterized in different combinations, where the structure of the fiber bundle is destroyed, and the graphene rods are attached, forming a three-dimensionalnetwork structure based on a large number of pores, with almost having a uniform size and smooth surface (Simon P and Gogotsi Y, 2008). The 3D porous structure allows ions to be rapidly transferred from the electrolyte to the entire surface of the AC electrode where an electrical double layer can rapidly be formed (Conway B E and Pell W G, 2003).

The microstructure of the sample CGH2 can be seen in Figure 6.3 (d) which shows long fibers intertwined with each other forming a network structure with a largenumber of cavities with the hydrogel in which a large number of cavities contribute tothe high electrolyte liquid absorption (Larciprete R et al., 2009). Also, it is observedthat the membrane is a film consisting of a dense hydrogel evenly distributed over thesurface of the graphene-treated fibers. In addition, the cotton fiber bundle reveals a cross-linked structure that forms a three-dimensional network of cotton. It can be seen that

Universiti Malaya

crystallization of the sample occurs uniformly when immersed in H_2SO_4 (CGH1 and CGH2) while hydrogel clumps form on the surface when the sample is immersedin KCl (CGH3 and CGH4) (Figure 6.4(d & e)). Furthermore, the FESEM image of sample CGH2 is shown in (Figure 6.3 (d))**,** which shows that the obtained active hydrogel layers show a high homogeneous particle dispersion as the cotton/graphenefabric coats uniformly due to the H_2SO_4 treatment.

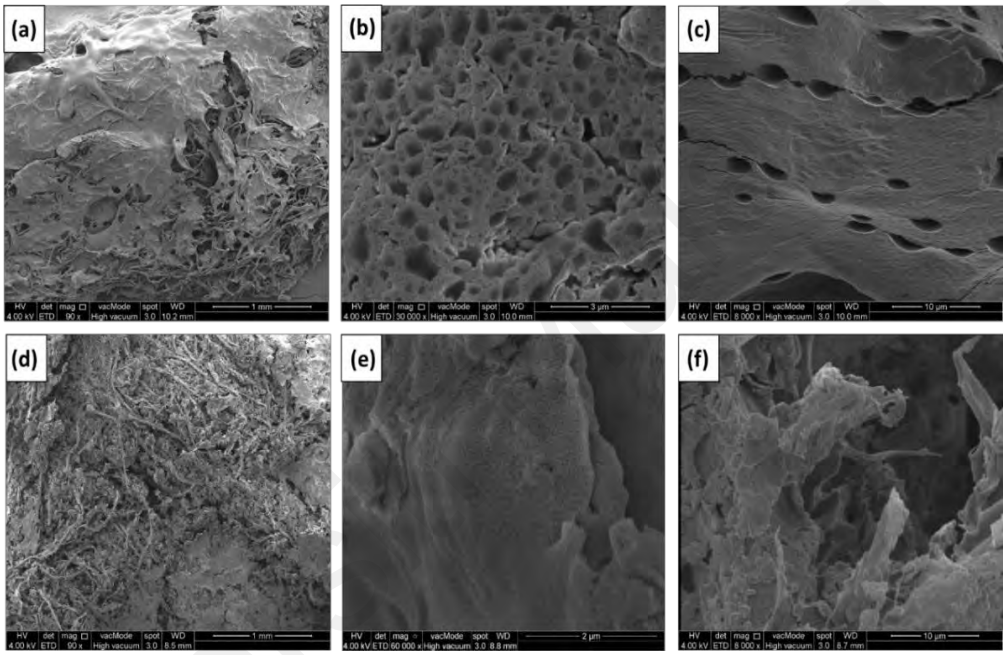

Figure 6.3 : SEM images: (a-c) of CGH1 and (d-f) of CGH2.

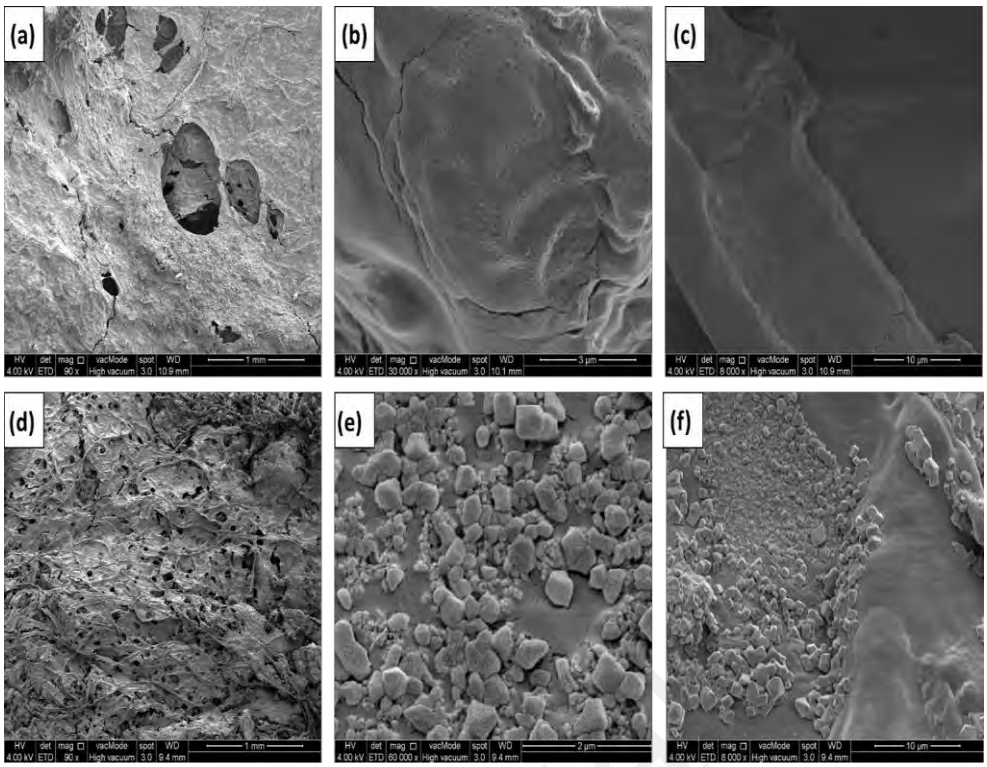

Figure 6.4 : SEM images (a-c) of CGH3 and (d-f) of CGH4.

6.5 Electrochemical impedance performance of hydrogel electrolytes

The ionic conductivity of the composite hydrogel electrolytes CGH1, CGH2, CGH3 and CGH4 were determined at room temperature. For all synthesized hydrogel electrolytes, graphene is the main component to make ionically conductive hydrogels. Adding H_2SO_4 and KCl greatly increases the conductivity, because water is an insulator (Lin J et al., 2020). 100% pure water doesn't conduct electricityvery well at all, when acid such as sulfuric acid (H_2SO_4) is added, the compounds separate into separate ions and having that small number of ions increases conductivity astronomically according to equations:

$H_2SO_4 + H_2O \rightleftharpoons HSO^{--} + H_3O^{++}$ $HSO_4 + H_2O \rightleftharpoons SO_4^{-2-2} + H_3O^+$

KCl which disassociates into ions in the water, so as it is introduced into water it dissociates completely into ions and dissolves in it, the polar water molecules are attracted by the charges on the K^+ and Cl^- ions. Furthermore, the addition of DMSOenhances ionic conductivity as it supports ionic diffusion through cotton networks asthe high-porosity 3D structure increases (Wu X et al., 2020).

Figure 6.5 shows the Nyquist plots for the hydrogel electrolyte which indicatesthe capacitive behavior with less resistance at high frequency and a steeper slope at low frequency for the prepared samples. In the Nyquist plot, the straight line at high frequency indicates the pure capacitive nature of the hydrogels due to the rapid transport of the charge carriers at room temperature (Lang J W et al., 2012). It is seen that the ion transfer is smooth for the charge carriers due to the available free space that is achieved through stretching. For cotton hydrogel samples CGH1, CGH2, CGH3 and CGH4, the maximum ionic conductivity of 11.5 x 10^{-3}, 13.9x10^{-3}, 10.9 x 10^{-3}, and 8.7 x 10^{-3} S/cm, respectively are achieved. This may be due to effectof ionic concentration on ionic conductivity, in electrolytes, the charge carriers are ions, which are atoms or molecules that have gained or lost electrons so they are electrically charged (Arof A K et al., 2014).

It can be seen that a higher value of impedance is noted for the sample CGH4, andthe resistance of the sample CGH increases when the chain length of the synthesized hydrogel increases (Deng F et al., 2015). The sample CGH4 exhibits the lowest ionicconductivity of 8.7 x 10^{-3} S/cm due to its low porosity and semi-crystalline structure due to the agglomeration of materials. When the hydrogel chain length increases, the ionic conductivity of the samples CGH3 and CGH4 gradually decreases due to their reduced porosity, while samples CGH2 and CGH1 have higher ionic conductivity of 13.9 x 10^{-3} S/cm and 11.5 x 10^{-3} S/cm, which is almost in agreement with the porosityand electrolyte

Universiti Malaya

absorption.

Cotton's higher water absorption potential leads to smoother ways of transporting ions across the polymer network. The ionic conductivity is increased through the electrolytic ion flow smoothly by the water molecules around the charged groups (Oh Y J et al., 2014).

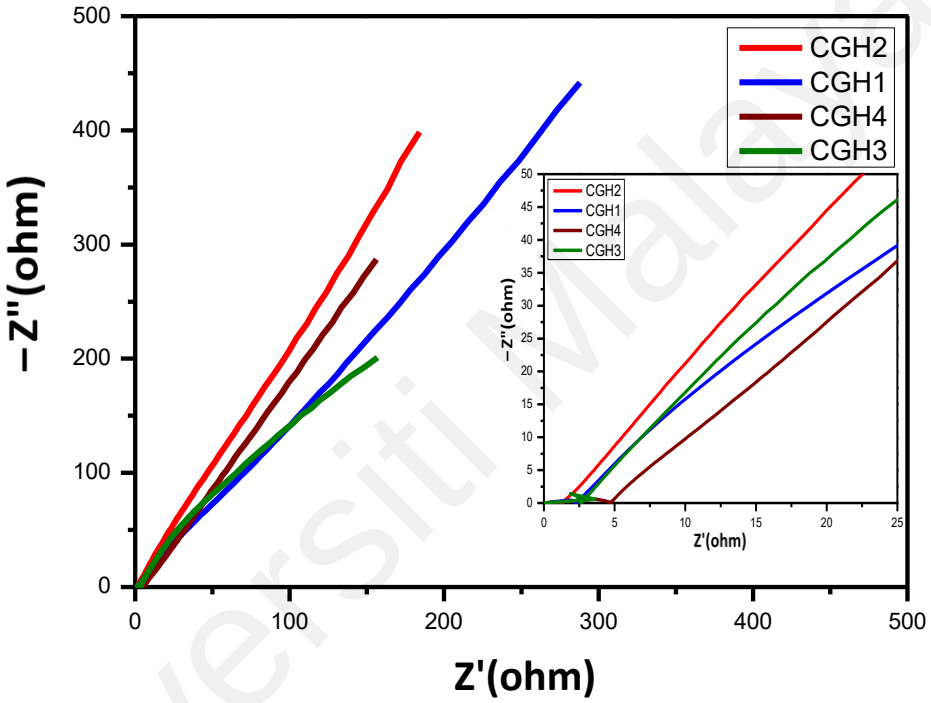

Figure 6.5 : Nyquist plots for the samples CGH1, CGH2, CGH3 and CGH4 at room temperature.

Universiti Malaya

CHAPTER 7: FLEXIBLE SUPERCAPACITOR - FABRICATION AND CHARACTERIZATION

7.1 Critical Performance of Supercapacitor

As a final part, this report concludes with some challenges and prospects for flexible graphene/cotton-based FSSSC as power systems for portable and wearableelectronics through LED lighting. Figure 7.1 shows a sandwich of 2 electrodes made of cotton/graphene, connected by a flexible hydrogel of cotton treated with graphene. After electrical conduction, the LED was lit (Tomiyasu, H et al., 2017).

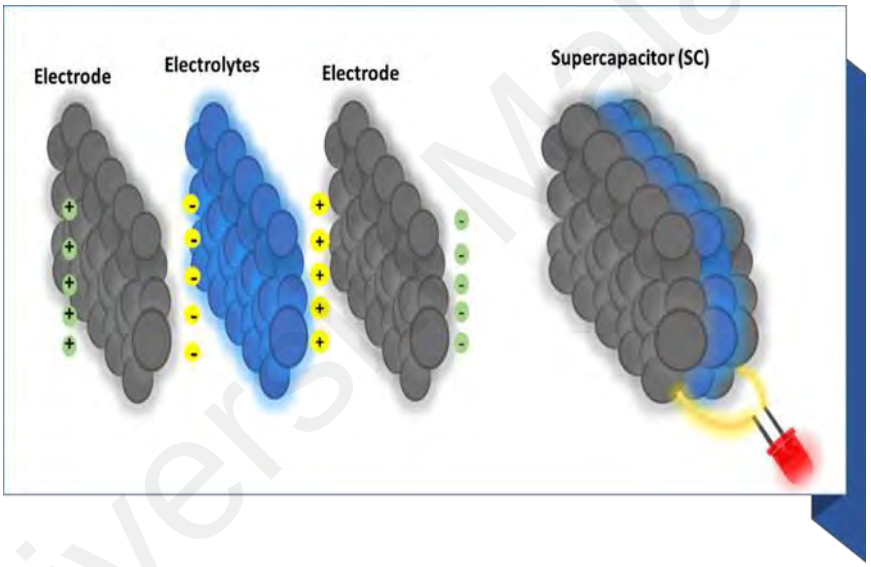

Figure 7.1: Supercapacitors Based on 3D solid-state Hydrogel electrolytes (pure Cotton /Graphene).

The critical performance parameters of a supercapacitor are measured using twomain electrochemical techniques, which include cyclic voltammetry (CV) and Galvanostatic Charge/Discharge (GCD).

University of Malaya

7.1.1 Cyclic voltammetry (CV) and Galvanostatic Charge/Discharge (GCD)

The CV measurement was performed to determine the potential of the prepared cells and the measurements were carried out in the potential range of 0-1.6 V, at a scanning rate of 10, 20, 50, and 100 mAg^{-1}, as shown in Figure 7.2 . The roughly rectangular CV curves show nearly perfect capacitive behavior, with no apparent peak, which indicates that the supercapacitor is charging and discharging at a constant rate (Xiao Q et al., 2019). It is worth noting that the CV region for the sample CGH2 is much higher than that of other samples for all scan rates, which could be reasoned because, with the soaking of samples in H_2SO_4, the number of freewater molecules decreases, and the electrolyte transforms into a gel state, where a small number of free ions can enter the micro-pores of the electrode.

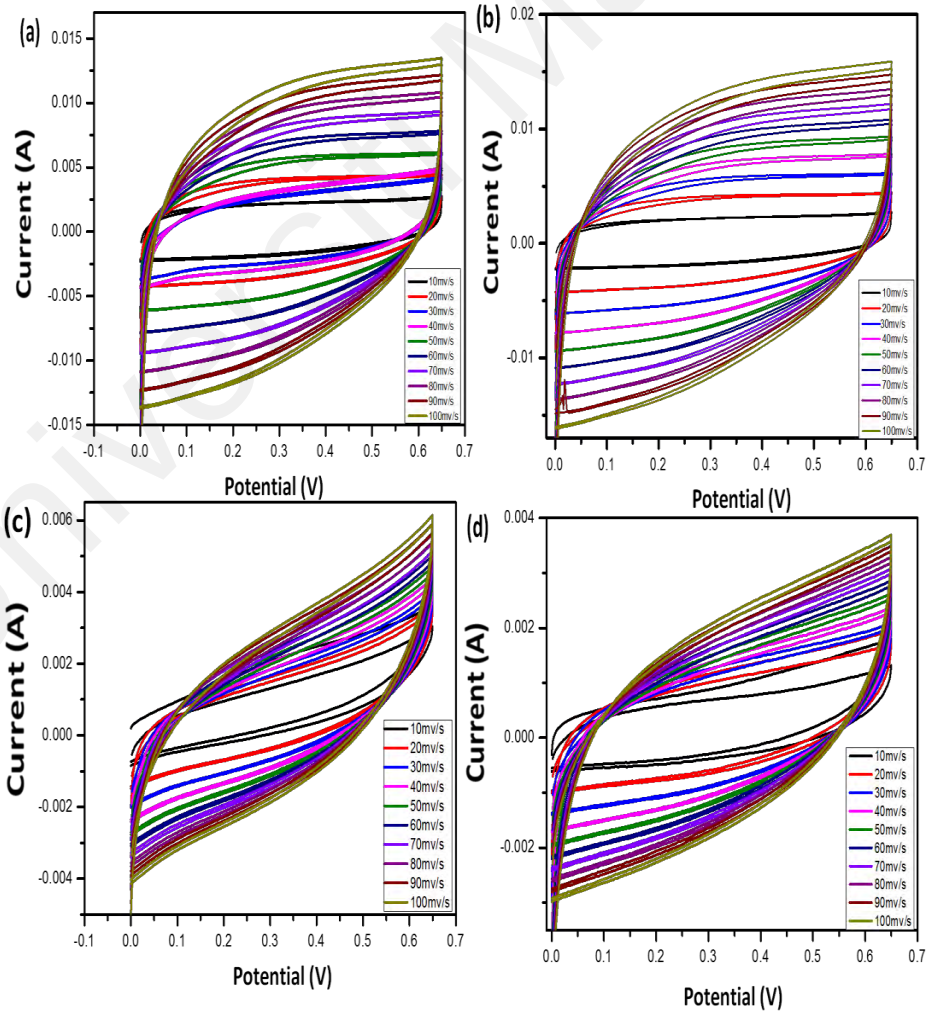

Figure 7.2 :(a-d) CV curves of all supercapacitors.

University of Malaya

This leads to an increase in capacitance mainly due to the presence of graphene. When the scanning rate is increased, the CV curves of the cotton-graphene-based hydrogel become close to rectangular shape even at 100 mAg^{-1} (Xie L et al., 2016;Wu X et al., 2020). There are no obvious oxidation peaks in the scanning range, which might indicate the superiority of the capacitive behavior (Alipoori S et al., 2019) as shown in Table 7.1, and the specific capacitance of the samples CGH1, CGH2, CGH3 and VGH4 are higher such as 312.88, 390.75, 250.30 and 333.50 F/g and also high energy density values of 48.79, 50.99, 35.18 and 52.25 $Whkg^{-1}$ at a power density of 478.50, 499.99, 100.00 and 100.10 W kg^{-1}, respectively. This is attributed to the high porosity, electrolyte absorption and hydrogen bonding with water molecules (Alipoori S et al., 2019). In the composite hydrogel sample CGH the effective electrode material makes the electrical conductivity low as observed byan ideal cyclic behaviour during CV measurement with the charge and discharge cycles tend to resemble those shown in Figure 7.2 (Chen Y and Zheng Chen G, 2019).

The hydrogel treated with KCl has a much smaller number of ionized ions compared to H_2SO_4 treated hydrogel since H^+ ions can easily and rapidly diffuse between the layers of graphene and cotton compared to the heavy K^+ ions. It is to be noted that only the oversized surface of the graphene electrode can be accessed during charging and discharging (Chen Y and Zheng Chen G, 2019). Meanwhile, H_2SO_4 can ionize more free ions than KCl at the same molar concentrations. In a double layer capacitor, the negatively charged (-) electrode attracts positively (+) charged ions and vice versa and the H_2SO_4 ions penetrate the electrode while the ionsin KCl cannot penetrate the electrode as shown in Figure 7.3. Thus, the supercapacitor using H_2SO_4 shows a specific capacitance higher than the basic capacitance (Wu X et al., 2020).

Universiti Malaya

Figure 7.3 describes the circuit model of a periodic voltmeter (Zhao C et al., 2013). The central idea is to represent a non-ideal circuit consisting of a capacitor (C) connected in parallel with a resistor (R_p) and a series resistor (R_s), respectively, to illustrate the role of each circuit parameter (inset Figure 7.4). Furthermore, weobserved a unique porous cotton fiber structure with the hydrogel blend. The heat treatment with H_2SO_4 and KCl can be used to control better the internal structure andto adjust the properties of the formed structures of the supercapacitor while the ESR can measure the transition between the electron spin energy levels. The rectangular- shaped plots turn out to be blunt CV due to the presence of ESR Figure 7.5 (a) whichare suitable for supercapacitors and become weak and italic with both electronparamagnetic resonance spectroscopy (EPR), also called electron spin resonance (ESR) as shown in Figure 7.5 (b) which indicates that the capacitive area decreases. Inmodels of electrolytic capacitors CGH3 and CGH4 the CVs appear slightly deviated from the ideal behavior due to the ESR and EPR, in which ESR represents the finite resistance of the graphene-treated cotton electrode material, whereas, the EPR represents the ohmic conduction through the capacitor via an electrolyte gel (Azman, N et al., 2018).

Table 7.1 : The Specific capacitance (F/g), Power density (W Kg^{-1}) and Energy density (Wh Kg^{-1}) of samples CGH1, CGH2, CGH3 and CGH4.

Cell	Specific Capacitance (F/g)	Power Density (WKg^{-1})	Energy density (Wh Kg^{-1})
CGH1	**312.88**	**478.50**	**48.79**
CGH2	**390.75**	**499.99**	**50.99**
CGH3	**250.30**	**100.00**	**35.18**
CGH4	**333.50**	**100.10**	**52.25**

Universiti Malaya

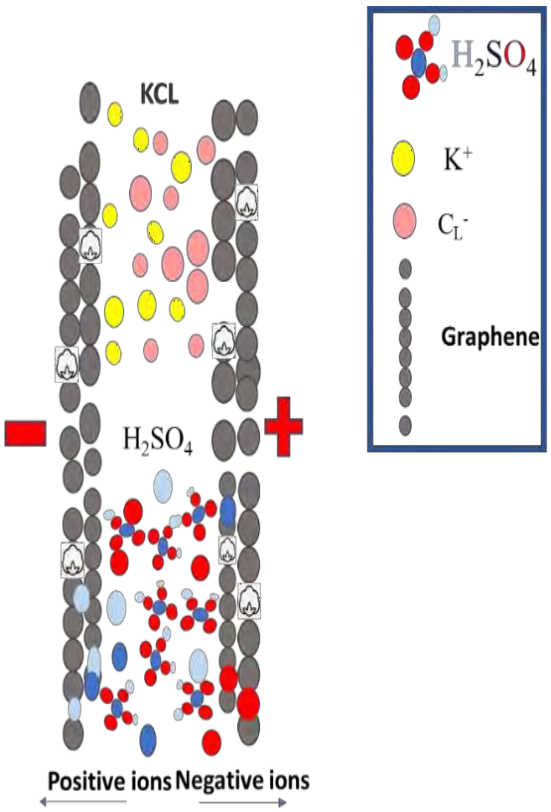

Figure 7.3 : Schematic illustration of ions diffusion in different electrolytes.

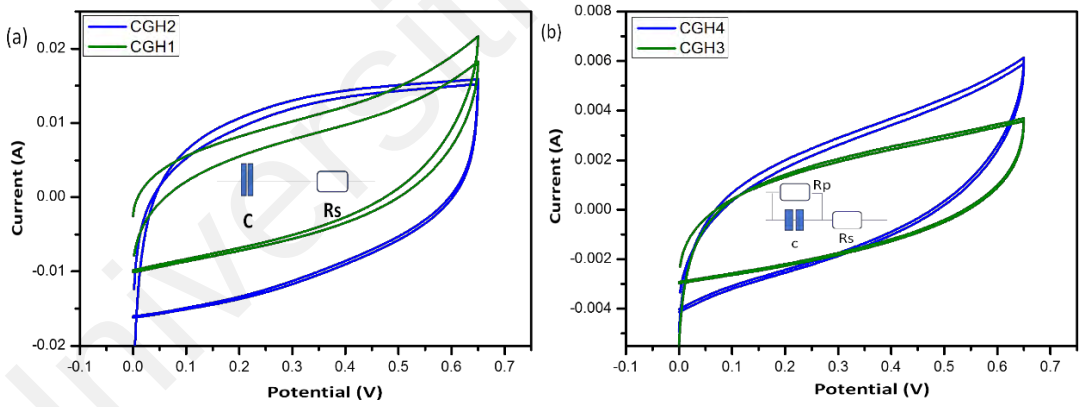

Figure 7.4 : Shape of CV curves represents the capacitive response for the samples CGH1, CGH2, CGH3 andCGH4 with inset showing the equivalent circuits representing the typical behavior of the samples.

University Malaya

In addition, GCD is implemented at current densities of 100 mA for the samples CGH1, CGH2, CGH3 and CGH4 which show symmetrical triangles with different current densities as seen in Figure 7.5 (a,d) indicating the energy storage mechanismis a typical capacitive type of EDLC. By applying a voltage, the ions are driven to the surface of the electrolytic double layer and the supercapacitor is charged.

Inversely, they move away when the supercapacitor is discharged and the hydrogel is also responsible for preventing or shortening the connection of the AC electrodes (Azman N et al., 2018). The curve is almost linear within the entire potential range, which shows an excellent performance of the four supercapacitors.

The symmetrical GCD curves indicate that the charge and discharge processes of the electrode materials are highly reversible (Azman N et al., 2018). Electrolytic double-layer capacitors (EDLCs) reveal higher capacity than previous generations of dielectric capacitors due to the composition of molecularly thin double Helmholtz layers throughout porous networks of cotton and graphene hydrogel electrodes where hydrogels have precisely defined surface areas. The electrical response generated by EDLCs is similar to dielectric capacitors. However, the surface functional groups on graphene can lead to parasitic electrochemical reactions, which lead to deviations fromthe ideal triangle for loading and unloading appearance (Wang G X et al., 2005).

It is noted that the four devices behave in an ideal manner similar to commercial capacitors where redox dopants store electrical charge via electron transfer or Faraday interactions and the charging time is the same as the discharging time since the currentis the same for charging and discharging but in the opposite direction.

Universiti Malaya

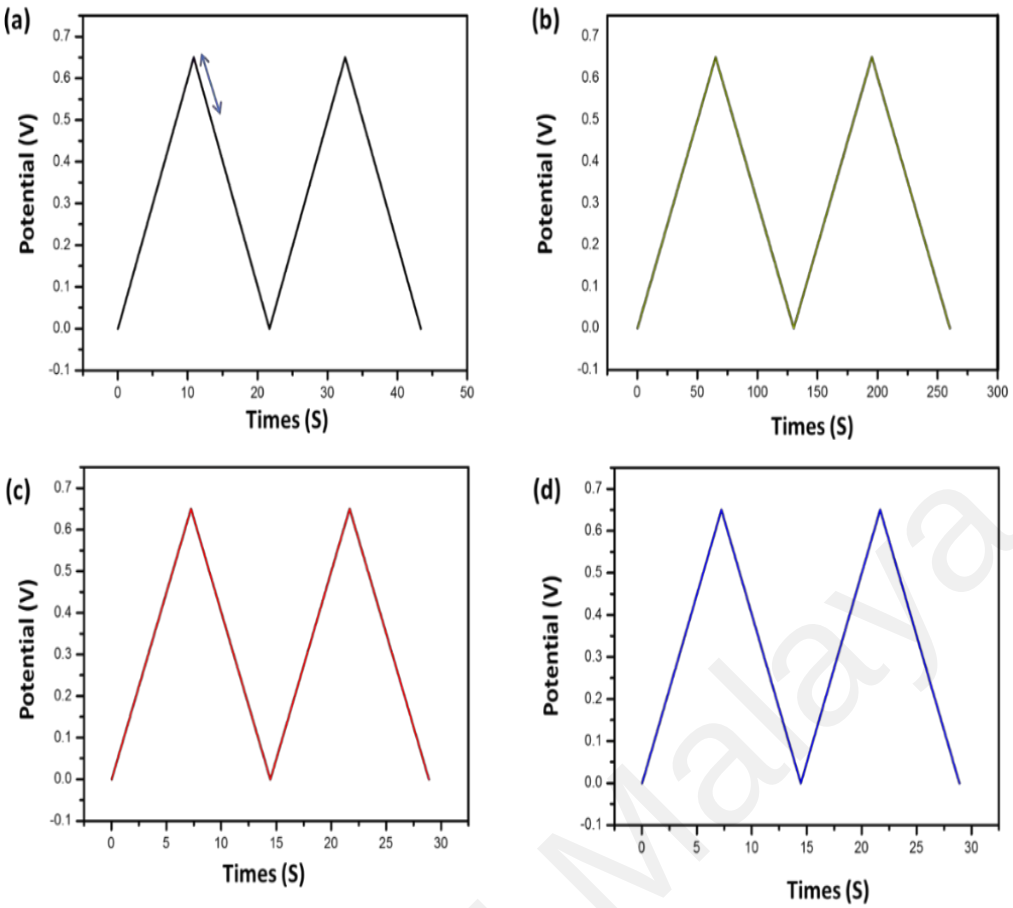

Figure 7.5 : (a-d) Galvanostatic charge–discharge (GCD) curves at 100 mA/g of the samples CGH1,CGH2, CGH3(c) and CGH4(d).

7.2 Proof of Concept

Electrolyte sample prepared using sodium alginate, starch and graphene and pure cotton were immersed in 4ml H_2SO_4 (CGH2) with an ionic conductivity of $13.9x10^{-3}$ S/cm and a thickness of 0.54 mm is shown in Figure 7.6. By configuring a fully flexible cotton-based supercapacitor with copper wire Figure 7.6 (b), it can light a red LED at full power as shown in Figure 7.6(c) by connecting to a voltage source of 9 volts. The samples acted as a supercapacitor acted by providing current to the LED and the LED was turned on with full intensity.

Universiti Malaya

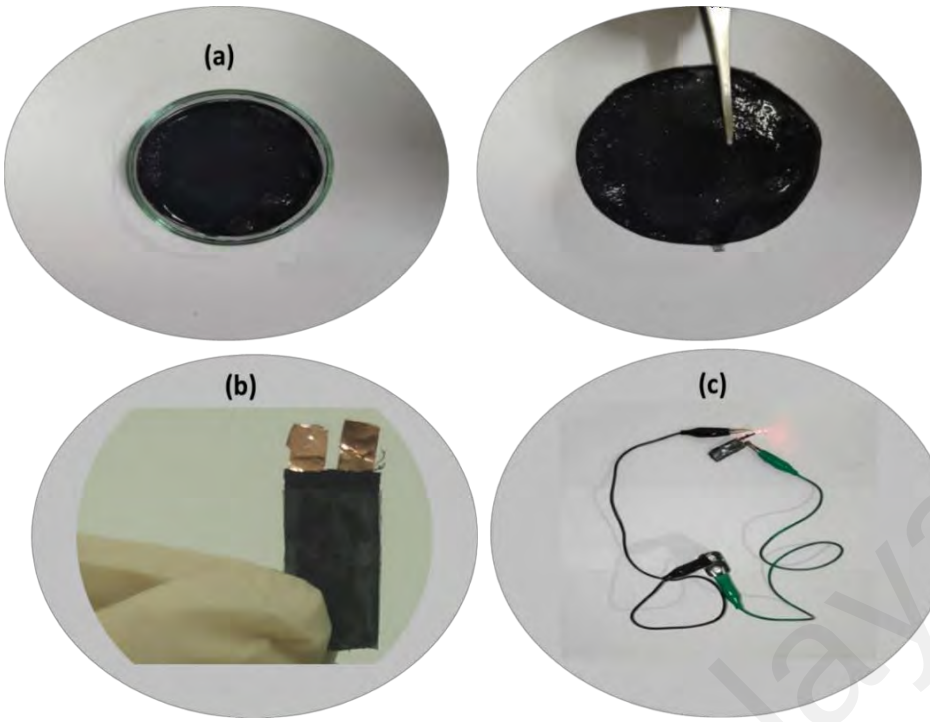

Figure 7.6 : (a) Sample CHG2, (b) Set up for device fabrication by connecting two coted cotton\graphene electrodes with CHG2 hydrogel electrolyte in series, (c) lighting of the LED lamp.

7.3 Summary

1. Developed hydrogel electrolytes with a highly open pore structure, allowing the effective interfacial interaction between the electrodes.
2. Cotton/graphene used successfully as an electrode in supercapacitors, due tothe rapid transport of the electrolyte ions or electrons throughout the sandwich structure.
3. The supercapacitors were successfully fabricated using CGH2 had highestenergy density and excellent electrochemical performance.

Universiti Malaya

CHAPTER 8: CONCLUSIONS

We have successfully prepared conductive cotton fabric (Gossypium herbaceum) as electrode by coating graphene using a layer-by-layer technique to convert the insulating character of pure cotton to a good electrical conductor by using a dip-coatingtechnique. The resistance values has obtained of (0.644 Ω/sq) at the 17th layer of graphene solution. The SEM, FTIR, and XRD confirm the formation of graphene bonding on the cotton surface while the EDX study elucidated the presence of any unwanted element. Moreover, the efficiency of the cotton sample was tested by connecting it to an electrical circuit in series and lighting a bulb of 12 W. Reasonablestability properties of the coating were obtained when the coated sample evaluated thestability factors, due to the electrostatic attraction between the cotton substrate and thegraphene particles. This technology is expected to have commercial potential as it hasa high potential for integration into applications especially in the design of electrical devices and conductive fabrics, especially in the electronic industry. However, the function of positive surfaces in graphene networks is still debatable and further studiesare warranted.

A novel cotton/graphene composite hydrogel electrolyte was developed using starch and Sodium alginate, to fabricate supercapacitor. X-ray diffraction analysis wasused to analyze the structure of the CGH complex electrolyte. The morphology studyrevealed the porous 3D lattice structure while the elemental mapping described the appropriate dispersion of graphene in the hydrogel. Electrochemical impedance analysis revealed that the ionic conductivity of CGH2 hydrogel significantly increasedup to 13.9 x 10^{-3} S/cm at 25 °C. The results suggest that the presence of graphene supports the increase in ionic conductivity and provides a smooth pathway for the transport of charge carriers and the polymer. Furthermore, CGH2 achieved the highest

Universiti Malaya

specific amplitude of 327 F/g at 3 mV s^{-1} during cyclic voltammetry (CV) and galvanostatic charge-discharge (GCD) analysis revealed 385.4 F/g at 100 mAg^{-1} current density. The electrochemical analysis demonstrated that CGH cotton- graphene-based electrolyte hydrogel is electrically stable and presents reversible responses to electrochemical catalysts. The assembled device was used to light up a red LED lamp. The composite CGH2 hydrogel will have a significant impact on the design of the next generation of supercapacitors for the development of cells due to itspromising capacitive properties, and excellent electrochemical stability. Therefore, composite hydrogel electrolytes will have wide applications in the field of energy storage.

Universiti Malaya

REFERENCES

Abdellatif, KF. Khidr, YA, El-Mansy, YM., El-Lawendey, MM., Soliman ,YA (2012). Molecular diversity of Egyptian cotton (Gossypium barbadense L.) and its relation to varietal development. *J Crop Sci Biotechnol* 15(2):93–99.

Abhishek ,Kumar, Mishra .(2018). Conducting Polymers: Concepts and Applications. *Journal of Atomic, Molecular, Condensed Matter and Nano Physics*, *5*(2), 159–193.

Abidi, N., Cabrales, L., &Hequet, E. (2010). Fourier transform infrared spectroscopic approach to the study of the secondary cell wall development in cotton fiber. *Cellulose,* 17(2), 309–320.

Abidi, N., Hequet, E., & Cabrales, L. (2010). Changes in sugar composition and cellulose content during the secondary cell wall biogenesis in cotton fibers. *Cellulose,* 17(1), 153–160.

Abidi, N., Hequet, E., Cabrales, L., Gannaway, J., Wilkins, T., & Wells, L. W. (2008). Evaluating cell wall structure and composition of developing cotton fibers using Fourier transform infrared spectroscopy and thermogravimetric analysis. *Journal of Applied Polymer Science,* 107(1), 476–486.

Ajalli, N., Alizadeh, M., Hasanzadeh, A., Khataee, A., & Azamat, J. (2022). A theoretical investigation into the effects of functionalized graphene nanosheets on dimethyl sulfoxide separation. *Chemosphere, 297*, 134183.

Akerholm M, Hinterstoisser B and SalmenL (2004). *Characterization of the crystalline structure of cellulose using static and dynamic FT-IR spectroscopy*. *Carbohydr. Res*. 339: 569–578.

Akram, S., Javid, A., & Ashraf, M. (2023). *Silver electroless plating on aminated graphene oxide-based cotton fabric for electromagnetic interference shielding and bioactivity.* Materials Science and Engineering: B, 288, 116159.

Alexander KS, Riga AT, Haines PJ(2009). *Thermoanalytical Instrumentation and Application. In: Ewing's Analytical Instrumentation Handbook.* Third edition: Marcel Dekker, p.462.

Alexandrov, G. N., Smagulova, S. A., Kapitonov, A. N., Vasil'eva, F. D., Kurkina, I. I., Vinokurov, P. v., Timofeev, V. B., & Antonova, I. v. (2014). *Thin partially reduced oxide-graphene films: Structural, optical, and electrical properties.* Nanotechnologies in Russia, *9*(7–8), 363–368.

Alhashmi Alamer, F., Badawi, N. M., & Alsalmi, O. (2020). Preparation and Characterization of Conductive Cotton Fabric Impregnated with Single-Walled Carbon Nanotubes. *Journal of Electronic Materials*, *49*(11), 6582–6589.

Alipoori, S., Torkzadeh, M. M., Moghadam, M. H. M., Mazinani, S., Aboutalebi, S. H., & Sharif, F. (2019). *Graphene oxide: An effective ionic conductivity promoter for phosphoric acid-doped poly (vinyl alcohol) gel electrolytes*. Polymer, 184.

Universiti Malaya

Antal MJ, Varhegyi G and Jakab E(1998). *Cellulose pyrolysis kinetics: The current state of knowledge.* Ind Eng Chem Res. 37: 1267-1277.

Argyropoulos, D. S. (2001). Wood and Cellulosic Chemistry. Second Edition, Revised and Expanded Edited by David N.-S. Hon (Clemson University) and Nubuo Shiraishi (Kyoto University). Marcel Dekker: New York and Basel. 2001. vii + 914 pp. $250.00. ISBN 0-8247-0024-4. *Journal of the American Chemical Society*, *123*(36), 8880–8881.

Arof, A. K., Amirudin, S., Yusof, S. Z., & Noor, I. M. (2014). A method based on impedance spectroscopy to determine transport properties of polymer electrolytes. *Physical Chemistry Chemical Physics,* 16(5), 1856–1867.

Azman, N. H. N., Mamat @ Mat Nazir, M. S., Ngee, L. H., & Sulaiman, Y. (2018). Graphene-based ternary composites for supercapacitors. *International Journal of Energy Research,* 42(6), 2104–2116.

Azzouz, B., ben Hassen, M., & Sakli, F. (2008). Adjustment of Cotton Fiber Length by the Statistical Normal Distribution: Application to Binary Blends. *Journal of Engineered Fibers and Fabrics*, *3*(3), 155892500800300.

Babu, K. F., Senthilkumar, R., Noel, M., & Kulandainathan, M. A (2009). Polypyrrole microstructure deposited by chemical and electrochemical methods on cotton fabrics. *Synthetic Metals,* 159(13),1353–1358.

Badawi, N. M., & Batoo, K. M. (2020). Conductive Nanocomposite Cotton Thread Strands for Wire and Industrial Applications. *Journal of Electronic Materials,* 49(11), 6483–6491.

Bai, R., Zhang, M., Zhang, X., Zhao, S., Chen, W., Chen, N., Ji, P., Kurbanov, M. S., Wang, H., Gou, H., & Wang, G. (2022). A Multidimensional Topotactic Host Composite Anode Toward Transparent Flexible Potassium-Ion Microcapacitors. *ACS Applied Materials and Interfaces,* 14(1), 1478–1488.

Bai, Y., Zhao, Y., Li, Y., Xu, J., Fu, X., Gao, X., Mao, X., & Li, Z. (2020). UV-shielding alginate films crosslinked with Fe3+ containing EDTA. *Carbohydrate Polymers,* 239:115480.

Balandin, A. A., Ghosh, S., Bao, W., Calizo, I., Teweldebrhan, D., Miao, F., & Lau, C. N. (2008). *Superior thermal conductivity of single-layer graphene*. Nano Letters, 8(3), 902–907.

Balter, M. (2009). Clothes make the (Hu) man. *Science*, *325*(5946), 1329.

Batoo, K. M., Badawi, N. M., & Adil, S. F. (2021). Highly sensitive coated cotton thread for applications in soft circuit. *Journal of Materials Science: Materials in Electronics,* 32(8), 10880–10889.

Bhattacharjee, S., Bahl, P., de Silva, C., Doolan, C., Chughtai, A. A., Heslop, D., & Macintyre, C. R. (2021). Experimental Evidence for the Optimal Design of a High-Performing Cloth Mask. *ACS Biomaterials Science and Engineering*, *7*(6), 2791–2802.

Universiti Malaya

Bochek, A. M. (2003). Effect of Hydrogen Bonding on Cellulose Solubility in Aqueous and Nonaqueous Solvents. *Russian Journal of Applied Chemistry 2003 76:11*, *76*(11), 1711–1719.

Boehm, H. P. (2010). Graphene—How a Laboratory Curiosity Suddenly Became Extremely Interesting. *Angewandte Chemie International Edition,* 49(49), 9332–9335.

Boonpakdee, D., Guajardo Yévenes, C. F., Surareungchai, W., & La-O-Vorakiat, C. (2018). Exploring non-linearities of carbon-based microsupercapacitors from an equivalent circuit perspective. *Journal of Materials Chemistry A*, *6*(16), 7162–7167.

Cao, B., Liu, H., Zhang, P., Sun, N., Zheng, B., Li, Y., Du, H., & Xu, B. (2021). Flexible MXene Framework as a Fast Electron/Potassium-Ion Dual-Function Conductor Boosting Stable Potassium Storage in Graphite Electrodes. *Advanced Functional Materials,* 31(32), 2102126.

Chang, C., Wang, S., Jiang, J., Gao, Y., Jiang, Y., & Liao, L(2022). Lithium-Ion Battery State of Health Estimation Based on Electrochemical Impedance Spectroscopy and Cuckoo Search Algorithm Optimized Elman Neural Network. *Journal of Electrochemical Energy Conversion and Storage*, *19*(3).

Chen, M., Chen, J., Zhou, W., Han, X., Yao, Y., & Wong, C. P (2021). Realizing an All-Round Hydrogel Electrolyte toward Environmentally Adaptive Dendrite-Free Aqueous Zn–MnO_2 Batteries. *Advanced Materials,* 33(9), 2007559.

Chen, R., & Jakes, K. A. (2002). Effect of Pressing on the Infrared Spectra of Single Cotton Fibers. *Applied Spectroscopy*,56(5), 646–650.

Chen, Y., & Zheng Chen, G. (2019). *New precursors derived activated carbon and graphene for aqueous supercapacitors with unequal electrode capacitance*s. WuliHuaxueXuebao/ Acta Physico - ChimicaSinica, 36(2).

Conway, B. E., & Pell, W. G. (2003). Double-layer and pseudocapacitance types of electrochemical capacitors and their applications to the development of hybrid devices. *Journal of Solid State Electrochemistry,* 7(9), 637–644.

Crawford, R. L. (1981). *Lignin biodegradation and transformation*. John Wiley and Sons.154.

Cui, Z., Kang, L., Li, L., Wang, L., & Wang, K(2022). *A hybrid neural network model with improved input for state of charge estimation of lithium-ion battery at low temperatures.* Renewable Energy, 198, 1328–1340.

Dai, P., Zhang, S., Liu, H., Yan, L., Gu, X., Li, L., Liu, D., & Zhao, X (2020). *Cotton fabrics-derived flexible nitrogen-doped activated carbon cloth for high-performance supercapacitors in organic electrolyte.* Electrochimica Acta, 354 , 136-717.

Dai, S., Guo, H., Wang, M., Liu, J., Wang, G., Hu, C., & Xi, Y (2014). *A Flexible micro-supercapacitor based on a pen ink-carbon fiber thread.* Undefined, *2*(46), 19665–19669.

Universiti Malaya

Dalton, A. B., Collins, S., Muñoz, E., Razal, J. M., Ebron, V. H., Ferraris, J. P., Coleman, J. N., Kim, B. G., & Baughman, R. H(2003) . Super-tough carbon-nanotube fibres. *Nature*, 423(6941),703–703.

Deng, F., Wang, X., He, D., Hu, J., Gong, C., Ye, Y. S., Xie, X., & Xue, Z. (2015). Microporous polymer electrolyte based on PVDF/PEO star polymer blends for lithium-ion batteries. *Journal of Membrane Science*,*491*, 82–89.

Denisa, H. J., Puziy, A. M., Poddubnaya, O. I., Fabian, S. G., Tascón, J. M. D., & Lu, G. Q (2009). Highly stable performance of supercapacitors from phosphorus-enriched carbons. *Journal of the American Chemical Society*, *131*(14), 5026–5027.

Du, P., Liu, H. C., Yi, C., Wang, K., & Gong, X (2015). Polyaniline-Modified Oriented Graphene Hydrogel Film as the Free-Standing Electrode for Flexible Solid-State Supercapacitors. *ACS Applied Materials and Interfaces,* 7(43), 23932–23940.

Dubey, R.; Guruviah, V(2019). Review of carbon-based electrode materials for supercapacitor energy storage. *Ionics , 25*, 1419–1445.

Eddahech, A., Briat, O., Bertrand, N., Delétage, J. Y., & Vinassa, J. M(2021). Behavior and state-of-health monitoring of Li-ion batteries using impedance spectroscopy and recurrent neural networks. *International Journal of Electrical Power & Energy Systems*, *42*(1), 487–494.

Ellis, J. (1995). Scouring, enzymes, and softeners. In C. M. Carr (Ed.), *Chemistry of the textile industry ,* C. M. Carr, Ed., Blackie Academic & Professional, London 249–275

Evseev, Z. I., Vasileva, F. D., Smagulova, S. A., & Dmitriev, P. S. (2023). Highly Washable and Conductive Cotton E-textiles Based on Electrochemically Exfoliated Graphene. *Materials 2023, Vol. 16, Page 958, 16(3), 958.*

Fang, J.; Zhang, X.; Miao, X.; Liu, Y.; Chen, S.; Chen, Y.; Cheng, J.; Wang, W.; Zhang, Y (2018). *A phenylenediamine-mediated organic electrolyte for high performance graphene-hydrogel based supercapacitors.* Electrochim. Acta , 273, 495–501.

Farrell, R. E., Adamczyk, T. J., Broe, D. C., Lee, J. S., Briggs, B. L., Gross, R. A., McCarthy, S. P., & Goodwin, S. (2009). *Estudio comparativo de rendimiento de bolsas biodegradables: un enfoque de múltiples niveles para evaluar la compostabilidad de los materiales plásticos*. 337–375.

Fitzgerald, M. M., Bootsma, K., Berberich, J. A., & Sparks, J. L. (2015). *Tunable stress relaxation behavior of an alginate-polyacrylamide hydrogel: Comparison with muscle tissue.* Biomacromolecules, 16(5), 1497–1505.

Gan, L., Shang, S., Yuen, C. W. M., Jiang, S. X., & Luo, N. M. (2015). *Facile preparation of graphene nanoribbon filled silicone rubber nanocomposite with improved thermal and mechanical properties*. Composites Part B: Engineering, 69, 237–242.

Ganguly, S., Ghosh, S., Das, P., Das, T. K., Ghosh, S. K., & Das, N. C. (2020). *Poly(N-vinylpyrrolidone)-stabilized colloidal graphene-reinforced poly(ethylene-co-*

Universiti Malaya

methyl acrylate) to mitigate electromagnetic radiation pollution. Polymer Bulletin, 77(6), 2923–2943.

Gao J., Pan N., and Yu WD(2010). *Compression behavior evaluation of single down fiber and down fiber assemblies.* J Text Inst; 101: 253–260.

Gao, D., Zhu, J., Ye, M., Li, Y., Ma, J., & Liu, J. (2022). Super wear-resistant and conductive cotton fabrics based on sliver nanowires. *Journal of Industrial Textiles*, *51*(5_suppl), 8227S-8245S.

Gao, Z., Song, N., Zhang, Y., & Li, X (2015). *Cotton-Textile-Enabled, Flexible Lithium-Ion Batteries with Enhanced Capacity and Extended Lifespan.* N. ano Letters, 15(12), 8194–8203.

Geim, A. K., & Novoselov, K. S. (2007). The rise of graphene. *Nature Materials, 6*(3), 183–191.

Gouda, M. (2012). Nano-zirconium oxide and nano-silver oxide/cotton gauze fabrics for antimicrobial and wound healing acceleration. *Journal of Industrial Textiles*, *41*(3), 222–240.

Gupta, S., Chang, C., Anbalagan, A. K., Lee, C. H., & Tai, N. H. (2020). *Reduced graphene oxide/zinc oxide coated wearable electrically conductive cotton textile for high microwave absorption.* Composites Science and Technology, 188, 107994.

Guragain, D., Zequine, C., Poudel, T., Neupane, D., Gupta, R. K., & Mishra, S. R (2019). Facile Synthesis of Bio-Templated Tubular Co 3 O 4 Microstructure and Its Electrochemical Performance in Aqueous Electrolytes. *Journal of Nanoscience and Nanotechnology,* 20(5)(2019)3182–3194.

Gurunathan, K.; Murugan, A.V.; Marimuthu, R.; Mulik, U.; Amalnerkar, D(1999). *Electrochemically synthesised conducting polymeric materials for applications towards technology in electronics, optoelectronics and energy storage devices.* Mater. Chem. Phys. *61*, 173–191.

Gürünlü, B., Taşdelen-Yücedağ, Ç., &Bayramoğlu, M. (2020). *Graphene Synthesis by Ultrasound Energy-Assisted Exfoliation of Graphite in Various Solvents*. Crystals 2020, Vol. 10, Page 1037, 10(11), 1037.

Han, C. G., Sheng, N., Zhu, C., & Akiyama, T (2017). *Cotton-assisted combustion synthesis of Fe_3O_4/C composites as excellent anode materials for lithium-ion batteries.* Materials Today Energy, 5, 187–195.

Han, J., Zhu, K., Liu, P., Si, Y., Chai, Y., & Jiao, L. (2019). N-doped CoSb@C nanofibers as a self-supporting anode for high-performance K-ion and Na-ion batteries. *Journal of Materials Chemistry A*, *7*(44), 25268–25273.

Hao, G. P., Hippauf, F., Oschatz, M., Wisser, F. M., Leifert, A., Nickel, W., Mohamed-Noriega, N., Zheng, Z., & Kaskel, S. (2014). *Stretchable and semitransparent conductive hybrid hydrogels for flexible supercapacitors.* ACS Nano, 8(7), 7138–7146.

Universiti Malaya

Hartzell, M. M., & Hsieh, Y.-L. (1998). Enzymatic scouring to improve cotton fabric wettability. *Textile Research Journal*, 68, 233–241.

Hass, J., de Heer, W. A., & Conrad, E. H. (2008). The growth and morphology of epitaxial multilayer graphene. *Journal of Physics Condensed Matter*, ***20*** *323202*.

Hattori, K., Cuculo, J. A., & Hudson, S. M. (2002). New solvents for cellulose: Hydrazine/thiocyanate salt system. *Journal of Polymer Science, Part A: Polymer Chemistry*, *40*(4), 601–611.

He, S., Xin, B., Chen, Z., & Liu, Y. (2019). Functionalization of cotton by reduced graphene oxide for improved electrical conductivity. *Textile Research Journal*, *89*(6), 1038–1050.

He, X., Liao, J., Tang, Z., Xiao, L., Ding, X., Hu, Q., Wen, Z., & Chen, C (2018). Highly disordered hard carbon derived from skimmed cotton as a high-performance anode material for potassium-ion batteries. *Journal of Power Sources,* 396, 533–541.

Heinze, T., el Seoud, O. A.,Omar A., & Koschella, A. (2010). *Cellulose derivatives : synthesis, structure, and properties*. 10,5485,3.

Hequet, E. F., Wyatt, B., Abidi, N., & Thibodeaux, D. P. (2016). *Creation of a Set of Reference Material for Cotton Fiber Maturity Measurements*. Http://Dx.Doi.Org/10.1177/0040517506064710, 76(7), 576–586.

Ho, D. H., Cheon, S., Hong, P., Park, J. H., Suk, J. W., Kim, D. H., Han, J. T., & Cho, J. H. (2019). *Multifunctional Smart Textronics with Blow-Spun Nonwoven Fabrics.* Advanced Functional Materials, 29(24), 1900025.

Hong, X., Fu, J., Liu, Y., Li, S., & Liang, B. (2021). *Strawberry-like carbonized cotton Cloth@Polyaniline nanocomposite for high-performance symmetric supercapacitors.* Materials Chemistry and Physics, *258*, 123999.

Hong, X., Li, S., Wang, R., & Fu, J (2019). Hierarchical SnO2 nanoclusters wrapped functionalized carbonized cotton cloth for symmetrical supercapacitor. *Journal of Alloys and Compounds,* 775,15–21.

Hosseini Ravandi, S.A. (2011). *Improving Comfort in Clothing || Properties of fibers and fabrics that contribute to human comfort,* 61–78.

Htwe, Y. Z. N., & Mariatti, M. (2022). Printed graphene and hybrid conductive inks for flexible, stretchable, and wearable electronics: Progress, opportunities, and challenges. *Journal of Science: Advanced Materials and Devices, 7(2).*

Hu, Z., Shao, Q., Moloney, M. G., Xu, X., Zhang, D., Li, J., Zhang, C., & Huang, Y. (2017). *Nondestructive Functionalization of Graphene by Surface-Initiated Atom Transfer Radical Polymerization: An Ideal Nanofiller for Poly(p-phenylene benzobisoxazole) Fibers.* Macromolecules, *50*(4), 1422–1429.

Huang J., Tang Y, Cen Z., Wang Z, Liu S., Fu R. (2022) . *A hierarchical porous carbon aerogel embedded with small-sized TiO2 nanoparticles for high-performance Li–S batteries,* 59–65.

Universiti Malaya

Huang, J., Chen, Y., Leng, K., Liu, S., Chen, Z., Chen, L., Wu, D., & Fu, R. (2020). *Morphology-persistent carbonization of self-assembled block copolymers for multifunctional coupled two-dimensional porous carbon hybrids.* Chemistry of Materials, 32(20), 8971–8980.

Huang, X., Feng, X., Zhang, B., Zhang, L., Zhang, S., Gao, B., Chu, P. K., & Huo, K(2019). Lithiated $NiCo_2O_4$ Nanorods Anchored on 3D Nickel Foam Enable Homogeneous Li Plating/Stripping for High-Power Dendrite-Free Lithium Metal Anode. *ACS Applied Materials and Interfaces,* 11(35), 31824–31831.

Igathinathane C, Tumuluru JS, Sokhansanj S, Bi. X, Lim CJ, Melin S and Mohammad E(2010). *Simple and inexpensive method of wood pellets macro-porosity measurement.* Bioresource Technol; 101: 6528–6537.

Jain, V. K., & Chatterjee, A. (2022). Graphene coated cotton nonwoven for electroconductive and UV protection applications. *Journal of Industrial Textiles*, *51*(3_suppl), 4390S-4409S.

Jee, C. E., Chow, M. K., & Yeap, S. P. (2023). Fabrication of flexible carbon dioxide gas sensor with conductive polymer/reduced graphene oxide hybrids: Effects of substrate type and mass ratio. *Journal of Applied Polymer Science*, *140*(5), e53415.

Jia, M., Li, Y., Cui, L., An, Y., Pan, C., &Jin, X. (2021). *An anthraquinone-decorated graphene hydrogel based on carbonized cotton fibers for flexible and high-performance supercapacitors.Sustainable Energy & Fuels*, *5*(3), 862–873.

Jinlong, L., Wang, Z., Tongxiang, L., Meng, Y., Suzuki, K., & Miura, H (2017). The effect of graphene coated nickel foam on the microstructures of NiO and their supercapacitor performance. *Journal of Electroanalytical Chemistry*, 799, 595–601.

Jost, K., Perez, C. R., McDonough, J. K., Presser, V., Heon, M., Dion, G., & Gogotsi, Y(2011). *Carbon coated textiles for flexible energy storage.* Energy & Environmental Science, 4(12),5060–5067.

Kabel, K. I., Farag, A. A., Elnaggar, E. M., & Al-Gamal, A. G. (2015). Improvement of graphene oxide characteristics depending on base washing. *Journal of Superhard Materials*, *37*(5), 327–334.

Kadir, M., Aspanut, Z., Majid, S., A, A. A.-S. A. P(2011), *undefined. (n.d.). FTIR studies of plasticized poly (vinyl alcohol)–chitosan blend doped with NH4NO3 polymer electrolyte membrane*. Elsevier. Retrieved April 5, 22.

Kasaw, E., Haile, A., & Getnet, M. (2020). *Conductive Coatings of Cotton Fabric Consisting of Carbonized Charcoal for E-Textile*. Coatings 2020, Vol. 10, Page 579, 10(6), 579.

Khalid, M. Y., al Rashid, A., Arif, Z. U., Ahmed, W., Arshad, H., & Zaidi, A. A. (2021). *Natural fiber reinforced composites: Sustainable materials for emerging applications.* Results in Engineering, 11.

Universiti Malaya

Kim, H., & Lee, S. (2021). *Effect of Relative Humidity Condition on Electrical Heating Textile Coated with Graphene-based on Cotton Fabric.* Fibers and Polymers 22(1)(2021) 276–284.

Klemm, D., Heublein, B., Fink, H. P., & Bohn, A. (2005). *Cellulose: fascinating biopolymer and sustainable raw material.* Angewandte Chemie (International Ed. in English), 44(22), 3358–3393.

Knittel, D., & Schollmeyer, E. (2009). *Electrically high-conductive textiles.* Synthetic Metals, 14(159), 1433–1437.

Köhler, A. R. (2013). *Challenges for eco-design of emerging technologies: The case of electronic textiles.* Materials and Design, 51, 51–60.

Kulkarni, P., Bhattacharya, S., Achuthan, S., Behal, A., Jolly, M. K., Kotnala, S., Mohanty, A., Rangarajan, G., Salgia, R., & Uversky, V. (2022). *Intrinsically Disordered Proteins: Critical Components of the Wetware. Chemical Reviews, 122*(6), 6614–6633.

Kursun Bahadir, S., Mitilineos, S., Symeonidis, S., Şahin, U. K., Vassiliadis, S., Kalaoglu, F., Goustouridis, D., Stathopoulos, N., & Savvaidis, S. P. (2020). Electromagnetic Shielding and Reflection Loss of Conductive Yarn Incorporated Woven Fabrics at the S and X Radar Bands. *Journal of Electronic Materials, 49(3), 1579–1587.*

Kvavadze, E., Bar-Yosef, O., Belfer-Cohen, A., Boaretto, E., Jakeli, N., Matskevich, Z., & Meshveliani, T. (2009). *30,000-year-old wild flax fibers*. Science, *325*(5946), 1359.

Lang, J. W., Yan, X. bin, Liu, W. W., Wang, R. T., & Xue, Q. J. (2012). Influence of nitric acid modification of ordered mesoporous carbon materials on their capacitive performances in different aqueous electrolytes. *Journal of Power Sources*, *204*, 220–229.

Lang, J., Li, J., Ou, X., Zhang, F., Shin, K., & Tang, Y. (2020). A Flexible Potassium-Ion Hybrid Capacitor with Superior Rate Performance and Long Cycling Life. *ACS Applied Materials and Interfaces,* 12*(*2), 2424–2431.

Larciprete, R., Gardonio, S., Petaccia, L., &Lizzit, S. (2009). *Atomic oxygen functionalization of double-walled C nanotubes*. Carbon, 47(11), 2579–2589.

Le, T. S. D., Park, S., An, J., Lee, P. S., & Kim, Y. J. (2019). Ultrafast Laser Pulses Enable One-Step Graphene Patterning on Woods and Leaves for Green Electronics. *Advanced Functional Materials, 29*(33).

Lee, G. H., Cooper, R. C., An, S. J., Lee, S., van der Zande, A., Petrone, N., Hammerberg, A. G., Lee, C., Crawford, B., Oliver, W., Kysar, J. W., & Hone, J. (2013). High-strength chemical-vapor-deposited graphene and grain boundaries. *Science*, 340*(*6136), 1074–1076.

Lee, K. Y., & Mooney, D. J. (2001). *Hydrogels for tissue engineering.* Chemical Reviews, 101(7), 1869–1879.

Universiti Malaya

Li, D., Müller, M. B., Gilje, S., Kaner, R. B., & Wallace, G. G. (2008). Processable aqueous dispersions of graphene nanosheets. *Nature Nanotechnology, 3*(2), 101–105.

Li, D., Yang, D., Li, L., Wang, L., & Wang, K(2022). Electrochemical Impedance Spectroscopy Based on the State of Health Estimation for Lithium-Ion Batteries. *Energies,* 15(18),6665.

Li, L., Jung, J., Ma, W., Wen, J., Ren, X., & Sun, Y (2022). Enhanced antimicrobial and antifungal property of two-dimensional fibrous material assembled by N-halamine polymeric electrolytes. *Materials Science and Engineering:* C, 115, 111-122.

Li, X., Zhuang, C., Xu, J., Li, L., Xu, T., Dai, S., Wang, X., Li, X., & Wang, Y. (2021). *Rational construction of K0.5V2O5 nanobelts/CNTs flexible cathode for multi-*functional potassium-ion batteries. *Nanoscale,* 13(17), 8199–8209.

Li, Y., & Hardin, I. R. (1997). *Enzymatic scouring of cotton: Effects on structure and properties.* Textile Chemist and Colorist, 29, 71–76.

Li, Y., Dong, B., Zerrin, T., Jauregui, E., Wang, X., Hua, X., Ravichandran, D., Shang, R., Xie, J., Ozkan, M., & Ozkan, C. S(2020). State-of-health prediction for lithium-ion batteries via electrochemical impedance spectroscopy and artificial neural networks. *Energy Storage,* 2(5).186.

Li, Y., Hu, Y. S., Titirici, M. M., Chen, L., & Huang, X (2016) . Hard Carbon Microtubes Made from Renewable Cotton as High-Performance Anode Material for Sodium-Ion Batteries. *Advanced Energy Materials,* 6(18), 1600659.

Li, Y., Zhang, Y., Zhang, H., Xing, T. L., & Chen, G. Q (2019). A facile approach to prepare a flexible sandwich-structured supercapacitor with rGO-coated cotton fabric as electrodes. *RSC Advances,* 9(8), 4180–4189.

Lin, J., Zheng, S. Y., Xiao, R., Yin, J., Wu, Z. L., Zheng, Q., & Qian, J. (2020). Constitutive behaviours of tough physical hydrogels with dynamic metal-coordinated bonds. *Journal of the Mechanics and Physics of Solids,* 139.

Lin, Y., Zhang, K., Chen, W., Liu, Y., Geng, Z., Zeng, J., Pan, N., Yan, L., Wang, X., & Hou, J. G. (2010). Dramatically enhanced photoresponse of reduced graphene oxide with linker-free anchored CdSe nanoparticles. *ACS Nano,* 4(6), 3033–3038.

Liu, C., Li, D., Wang, L., Li, L., & Wang, K(2022). Strong robustness and high accuracy in predicting remaining useful life of supercapacitors. *APL Materials,* 10(6), 061106.

Liu, C., Li, Q., Kang, W., Lei, W., Wang, X., Lu, C., & Naebe, M. (2021). Structural design and mechanism analysis of hierarchical porous carbon fibers for advanced energy and environmental applications. *Journal of Materials Chemistry A*, *10*(1), 10–49.

Liu, H., Lee, Y. Y., Norsten, T. B., & Chong, K. (2014). In situ formation of anti-bacterial silver nanoparticles on cotton textiles. *Journal of Industrial Textiles*, *44*(2), 198–210.

Universiti Malaya

Liu, W. W., Yan, X. bin, Lang, J. W., Peng, C., & Xue, Q. J(2012). Flexible and conductive nanocomposite electrode based on graphene sheets and cotton cloth for supercapacitor. *Journal of Materials Chemistry,* 22(33), 17245–17253.

Liu, X., Meng, Y., Li, R., Du, M., Zhu, F., & Zhang, Y(2019). Nitrogen-doped carbon-coated cotton-derived carbon fibers as high-performance anode materials for lithium-ion batteries. *Ionics* 25(12),5799–5807.

Liu, Y., Xiong, H., Yu, X., Huang, H., Li, L., Ji, J., Huang, Y., & Xu, M. (2018). Interfacial fabrication of polypyrrole/sulfonated reduced graphene oxide nanocomposites for electrochemical capacitors. *Polymer Composites,* 39*,* E378–E385.

López-Barroso, J., Martínez-Hernández, A. L., Rivera-Armenta, J. L., & Velasco-Santos, C. (2018). Multidimensional Nanocomposites of Epoxy Reinforced with 1D and 2D Carbon Nanostructures for Improve Fracture Resistance. *Polymers* 2018, Vol. 10, Page 281, 10(3), 281.

Lu, C., Tian, M., Zheng, X., Wei, C., Rummeli, M. H., Strasser, P., & Yang, R(2021). Cotton pad derived 3D lithiophilic carbon host for robust Li metal anode: In-situ generated ionic conductive Li_3N protective decoration. *Chemical Engineering Journal,* 430,132722.

Lu, S., Zhu, Y., Dong, L., Na, G., Hao, Y., Zhang, G., Zhang, W., Cheng, S., Yang, J., & Sui, Y(2022). Small-Signal Stability Research of Grid-Connected Virtual Synchronous Generators. *Energies* 15(19), 7158.

Lu, Y. H., Tang, Y. C., Tang, K. H., Wu, D. C., & Ma, Q. (2022). Controllable fabrication of superhierarchical carbon nanonetworks from 2D molecular brushes and their use in electrodes of flexible supercapacitors. *New Carbon Materials,* 37(5), 978–987.

Makowski, T., Svyntkivska, M., Piorkowska, E., Mizerska, U., Fortuniak, W., Kowalczyk, D., & Brzezinski, S. (2018). Conductive and superhydrophobic cotton fabric through pentaerythritol tetrakis(3-(3,5-di-tert-butyl-4-hydroxyphenyl)propionate) assisted thermal reduction of graphene oxide and modification with methyltrichlorosilane. *Cellulose,* 25(9), 5377–5388.

Marchessault, R. H. (1987). Cellulose structure modification and hydrolysis, Raymond A. Young and Roger M. Rowell, Eds., Wiley-Interscience, New York, 1986, 379 pp. *Journal of Polymer Science Part C: Polymer Letters*, *25*(3), 139–140.

Meng, J.-K., Wang, W.-W., Yue, X.-Y., Xia, H.-Y., Wang, Q.-C., Wang, X.-X., Zhou, Y.-N(2020). Cotton-derived carbon cloth enabling dendrite-free Li deposition for lithium metal batteries. *Journal of Power Sources*, 465, 228291.

Mingant, R., Bernard, J., Sauvant Moynot, V., Delaille, A., Mailley, S., Hognon, J.-L., & Huet, F(2011). EIS Measurements for Determining the SoC and SoH of Li-Ion Batteries. *ECS Transactions,* 33(39)(2011) 41–53.

Morton, W. E., & Hearle, J. W. S. (2008). *Physical Properties of Textile Fibres: Fourth Edition. In Physical Properties of Textile Fibres: Fourth Edition*. Elsevier Ltd.232,25.

Universiti Malaya

Murdan, S. (2003). Electro-responsive drug delivery from hydrogels. *Journal of Controlled Release : Official Journal of the Controlled Release Society*, *92*(1–2), 1–17.

Nair, R. R., Blake, P., Grigorenko, A. N., Novoselov, K. S., Booth, T. J., Stauber, T., Peres, N. M. R., & Geim, A. K. (2008). Fine structure constant defines visual transparency of graphene. *Science,* 320(5881), 1308.

Nakao, Y. (1992). Dissolution of noble metals in halogen–halide–polar organic solvent systems. *Journal of the Chemical Society, Chemical Communications*, *5*, 426–427.

Nevell, T. P., &Zeronian, S. H. (1985). Cellulose chemistry fundamentals. In T. P. Nevell, & S. H. Zeronian (Eds.), *Cellulose chemistry and its application* . 15–29.

Niyogi, S., Bekyarova, E., Itkis, M. E., McWilliams, J. L., Hamon, M. A., & Haddon, R. C. (2006). Solution properties of graphite and graphene. *Journal of the American Chemical Society*, *128*(24), 7720–7721.

Novoselov, K. S., Andreeva, D. v., Ren, W., & Shan, G. (2019). Graphene and other two-dimensional materials. *Frontiers of Physics,* 14(1).

Novoselov, K. S., Geim, A. K., Morozov, S. v., Jiang, D., Zhang, Y., Dubonos, S. v., Grigorieva, I. v., & Firsov, A. A. (2004). Electric field in atomically thin carbon films. *Science,* 306(5696), 666–669.

Oh, Y. J., Yoo, J. J., Kim, Y. il, Yoon, J. K., Yoon, H. N., Kim, J. H., & Park, S. bin. (2014). *Oxygen functional groups and electrochemical capacitive behavior of incompletely reduced graphene oxides as a thin-film electrode of supercapacitor.* Electrochimica Acta, *116*, 118–128.

Paleo, A. J., Staiti, P., Brigandì, A., Ferreira, F. N., Rocha, A. M., & Lufrano, F (2018). Supercapacitors based on AC/MnO2 deposited onto dip-coated carbon nanofiber cotton fabric electrodes. *Energy Storage Materials*, *12*, 204–215.

Park, S., An, J., Jung, I., Piner, R. D., An, S. J., Li, X., Velamakanni, A., & Ruoff, R. S. (2009). Colloidal suspensions of highly reduced graphene oxide in a wide variety of organic solvents. *Nano Letters,* 9(4), 1593–1597.

Park, S., An, J., Piner, R. D., Jung, I., Yang, D., Velamakanni, A., Nguyen, S. B. T., & Ruoff, R. S. (2008). Aqueous suspension and characterization of chemically modified graphene sheets. *Chemistry of Materials,* 20(21), 6592–6594.

Peng, H., Salmén, L., Jiang, J., & Lu, J. (2020). Contribution of lignin to the stress transfer in compression wood viewed by tensile FTIR loading. *Holzforschung, 74*(5), 459–467.

Peng, S., Wang, L., Zhu, Z., & Han, K. (2020). Electrochemical performance of reduced graphene oxide/carbon nanotube hybrid papers as binder-free anodes for potassium-ion batteries. *Journal of Physics and Chemistry of Solids*, *138*, 109296.

Pijpers MFJ, Mathot VBF(2008). Optimisation of instrument response and resolution of standard and high speed power compensation DSC. *J Therm Anal Calorim*. 93: 319–327.

Universiti Malaya

Pradyumna, T. K., Cho, K., Kim, M., & Choi, W(2022*).* Capacity estimation of lithium-ion batteries using convolutional neural network and impedance spectra. *JPEle, 22*(5),850–858.

Qiu, W., Xiao, H., Li, Y., Lu, X., & Tong, Y. (2019). Nitrogen and Phosphorus Codoped Vertical Graphene/Carbon Cloth as a Binder-Free Anode for Flexible Advanced Potassium Ion Full Batteries. *Small,* 15(23), 1901285.

Remadevi, R., al Faruque, M. A., Zhang, J., & Naebe, M. (2020). Electrically conductive honeycomb structured graphene composites from natural protein fibre waste. *Materials Letters,* 264.

Riaz, T., Iqbal, M. W., Jiang, B., & Chen, J. (2021). A review of the enzymatic, physical, and chemical modification techniques of xanthan gum. *International Journal of Biological Macromolecules,* 186, 472–489.

Rong, Q.; Lei, W.; Liu, M (2018). Conductive hydrogels as smart materials for flexible electronic devices*. Chem. A Eur. J.* 24, 16930–16943.

Roslan, M., Chaudhary, K., Doylend, N., Society, A. A. S. C .(2019), undefined. (n.d.). *Growth of wall-controlled MWCNTs by magnetic field assisted arc discharge plasma.* Elsevier. Retrieved December 20-21.

S. H. Lee, D. Lee, W. J. Lee and S. O. Kim,(2011) Tailored assembly of carbon nanostructures: tailored assembly of carbon nanotubes and graphene, *Adv. Funct. Mater.,* 21, 1329.

Sahito, I. A., Sun, K. C., Arbab, A. A., Qadir, M. B., & Jeong, S. H. (2015). Integrating high electrical conductivity and photocatalytic activity in cotton fabric by cationizing for enriched coating of negatively charged graphene oxide. *Carbohydrate Polymers,* 130, 299–306.

Santos, F. A. dos, Iulianelli, G. C. v., & Tavares, M. I. B. (2016). The Use of Cellulose Nanofillers in Obtaining Polymer Nanocomposites: Properties, Processing, and Applications*. Materials Sciences and Applications,* 07(05), 257–294.

Shah, J., & Brown, R. M. (2005). Towards electronic paper displays made from microbial cellulose. *Applied Microbiology and Biotechnology,* 66(4), 352–355.

Shaw, R. K., Long, B. R., Werner, D. H., & Gavrin, A. (2007). The characterization of conductive textile materials intended for radio frequency applications. *IEEE Antennas and Propagation Magazine, 49(3), 28–40.*

Shen, H., Zhou, X., Wang, Z., & Wang, J(2022). State of charge estimation for lithium-ion battery using Transformer with immersion and invariance adaptive observer. *Journal of Energy Storage*, 45.

Shi, Y., Pan, L., Liu, B., Wang, Y., Cui, Y., Bao, Z., & Yu, G. (2014). Nanostructured conductive polypyrrole hydrogels as high-performance, flexible supercapacitor electrodes. *Journal of Materials Chemistry A*, *2*(17), 6086–6091.

Shi, Y.; Peng, L.; Ding, Y.; Zhao, Y.; Yu, G (2015). *Nanostructured conductive polymers for advanced energy storage.* Chem. Soc. Rev. 44, 6684–6696.

Universiti Malaya

Shirakawa, H., Louis, E. J., MacDiarmid, A. G., Chiang, C. K., & Heeger, A. J. (1977). Synthesis of electrically conducting organic polymers: halogen derivatives of polyacetylene, (CH)x. *Journal of the Chemical Society, Chemical Communications,* 16, 578–580.

Si, Y., & Samulski, E. T. (2008). Synthesis of water soluble graphene. *Nano Letters, 8*(6), 1679–1682.

Siddiqua, U. H., Ali, S., Iqbal, M., & Hussain, T. (2017). Relationship between structure and dyeing properties of reactive dyes for cotton dyeing. *Journal of Molecular Liquids, 241, 839–844.*

Silva, A. K. A., Richard, C., Bessodes, M., Scherman, D., & Merten, O. W. (2009). Growth factor delivery approaches in hydrogels. *Biomacromolecules,* 10(1), 9–18.

Simon, P., &Gogotsi, Y. (2008). Materials for electrochemical capacitors. *Nature Materials,* 7(11), 845–854.

Sivaranjana, P., Nagarajan, E. R., Rajini, N., Ayrilmis, N., Rajulu, A. V., & Siengchin, S. (2021). Preparation and characterization studies of modified cellulosic textile fabric composite with in situ-generated AgNPs coating. *Journal of Industrial Textiles*, *50*(7), 1111–1126.

Snook, G.A.; Kao, P.; Best, A.S(2011). Conducting-polymer-based supercapacitor devices and electrodes. *J. Power Sources*, 196*,* 1–12.

Song, C.; Chen, B.; Hwang, J.; Lee, S.; Suo, Z.; Ahn, H (2021). *A printed highly stretchable supercapacitor by a combination of carbon ink and polymer network.* Extrem. Mech. Lett. 49*,* 101459.

Song, H., Jeon, S. Y., & Jeong, Y (2019). Fabrication of a coaxial high performance fiber lithium-ion battery supported by a cotton yarn electrolyte reservoir. *Carbon,* 147, 441–450.

Soundharrajan, V., Alfaruqi, M. H., Alfaruqi, M. H., Lee, S., Sambandam, B., Kim, S., Kim, S., Mathew, V., Pham, D. T., Hwang, J. Y., Sun, Y. K., & Kim, J (2020). Multidimensional Na4VMn0.9Cu0.1(PO4)3/C cotton-candy cathode materials for high energy Na-ion batteries. *Journal of Materials Chemistry A*, *8*(24) ,12055–12068.

Souri, H., & Bhattacharyya, D(2018). Highly Stretchable Multifunctional Wearable Devices Based on Conductive Cotton and Wool Fabrics. *ACS Applied Materials and Interfaces,* 10(24), 20845–20853.

Stoller, M. D., & Ruoff, R. S (2010). Best practice methods for determining an electrode material's performance for ultracapacitors. Energy & Environmental *Science*, 3(9), 1294–1301.

Su, M., Chen, X., Zhang, L., & Min, J. (2020). Synthesis of Active Graphene with Para-Ester on Cotton Fabrics for Antistatic Properties. *Nanomaterials* 2020, Vol. 10, Page 1147, 10(6), 1147.

Universiti Malaya

Sukor, M., Ait, S. , Yusri, M., Rahman, A., Su', M. S., Ahmad, & A., & Rahman, M. Y. A. (2009). Ionic conductivity studies of 49% poly (methyl methacrylate)-grafted natural rubber-based solid polymer electrolytes. *Springer,*15(4), 497–500.

Sun, C., Li, X., Cai, Z., & Ge, F (2019). *Carbonized cotton fabric in-situ electrodeposition polypyrrole as high-performance flexible electrode for wearable supercapacitor.* Electrochimica Acta, 296, 617–626.

Sun, D., He, L., Chen, R., Liu, Y., Lv, B., Lin, S., & Lin, B(2019). Biomorphic composites composed of octahedral Co_3O_4 nanocrystals and mesoporous carbon microtubes templated from cotton for excellent supercapacitor electrodes. *Applied Surface Science*, 465(2019) 232–240.

Sun, D., Liu, Q., Yi, C., Chen, J., Wang, D., Wang, Y., Liu, X., Li, M., Liu, K., Zhou, P., & Sun, G (2020). *The construction of sea urchin spines-like polypyrrole arrays on cotton-based fabric electrode via a facile electropolymerization for high performance flexible solid-state supercapacitors.* Electrochimica Acta, 354, 136746.

Sun, F., Tian, M., Sun, X., Xu, T., Liu, X., Zhu, S., Zhang, X., & Qu, L. (2019). Stretchable Conductive Fibers of Ultrahigh Tensile Strain and Stable Conductance Enabled by a Worm-Shaped Graphene Microlayer. *Nano Letters,* 19(9), 6592–6599.

Tanaka, T., Nishio, I., Sun, S. T., & Ueno-Nishio, S. (1982). Collapse of gels in an electric field. *Science,* 218(4571), 467–469.

Tang, L.; Wu, S.; Qu, J.; Gong, L.; Tang, J (2020). A review of conductive hydrogel used in flexible strain sensor. *Materials,* 13, 3947.

Tarabella, G., Villani, M., Calestani, D., Mosca, R., Iannotta, S., Zappettini, A., & Coppedè, N(2012). A single cotton fiber organic electrochemical transistor for liquid electrolyte saline sensing. *Journal of Materials Chemistry,* 22(45), 23830–23834.

Tian, M., Du, M., Qu, L., Chen, S., Zhu, S., & Han, G (2017). Electromagnetic interference shielding cotton fabrics with high electrical conductivity and electrical heating behavior via layer-by-layer self-assembly route. *RSC Advances,* 7(68), 42641–42652.

Tomiyasu, H., Shikata, H., Takao, K., Asanuma, N., Taruta, S., & Park, Y. Y. (2017). An aqueous electrolyte of the widest potential window and its superior capability for capacitors. *Scientific Reports*, 7.

Tsuji, W., Nakao, T., Hirai, A., & Horii, F. (1992). Properties and structure of never-dried cotton fibers. III. Cotton fibers from bolls in early stages of growth. *Journal of Applied Polymer Science,* 45(2), 299–307.

Tugrul OR and Serin MM(2012). *Total porosity, theoretical analysis, and prediction of the air permeability of woven fabrics.* J Text Inst; 103: 654–661.

Tunakova, V., Tunak, M., Bajzik, V., Ocheretna, L., Arabuli, S., Kyzymchuk, O., & Vlasenko, V. (2020). Hybrid knitted fabric for electromagnetic radiation shielding. *Journal of Engineered Fibers and Fabrics*, *15*.

Universiti Malaya

Ullah, F., Othman, M. B. H., Javed, F., Ahmad, Z., & Akil, H. M. (2015*).* Classification, processing and application of hydrogels: A review. *Materials Science and Engineering C,* 57, 414–433.

Wang, B., Li, J., Hou, C., Zhang, Q., Li, Y., & Wang, H (2020). Stable Hydrogel Electrolytes for Flexible and Submarine-Use Zn-Ion Batteries. *ACS Applied Materials & Interfaces*, 12(41), 46005–46014.

Wang, D., Wang, P., Lu, B., Ye, K., Zhu, K., Wang, Q., Yan, J., Wang, G., & Cao, D. (2021). Porous Carbon Tubes Constructing Freestanding Flexible Electrodes for Symmetric Potassium-Ion Hybrid Capacitors. *ACS Applied Energy Materials,* 4(12), 13593–13604.

Wang, F., Sun, S., Xu, Y., Wang, T., Yu, R., & Li, H (2017). (n.d.). High-performance asymmetric supercapacitor based on Cobalt Nickle Iron-layered double hydroxide/carbon nanofibres and activated carbon. *Scientific Reports* **,**7, 4707 .

Wang, G. X., Zhang, B. L., Yu, Z. L., & Qu, M. Z. (2005). Manganese oxide/MWNTs composite electrodes for supercapacitors. Solid State *Ionics,* 176(11–12), 1169–1174.

Wang, H., He, L., Sun, J., Liu, S., & Wu, F(2011). *Study on correlation with SOH and EIS model of Li-ion battery.* Proceedings of the 6th International Forum on Strategic Technology, *IFOST* , 1, 261–264.

Wang, K., Zhang, X., Sun, X., & Ma, Y (2016). M*atter Conducting polymer hydrogel materials for high-performance flexible solid-state supercapacitors*. *59*(6), 412–420.

Wang, Q. J., & Zhu, D(2013). Hertz Theory: *Contact of Spherical Surfaces.* Encyclopedia of Tribology*,* 1654–1662.

Wang, T., Li, Y., Zhang, J., Yan, K., Jaumaux, P., Yang, J., Wang, C., Shanmukaraj, D., Sun, B., Armand, M., Cui, Y., & Wang, G (2020). Immunizing lithium metal anodes against dendrite growth using protein molecules to achieve high energy batteries. *Nature Communications* 11(1), 1–9.

Wang, W., Lu, L., Zhang, D., Yao, Y., & Xie, Y. (2023). *Experimental and modeling study of laser induced silicon carbide/graphene on cotton cloth for superhydrophobic applications.* Optics & Laser Technology, 158, 108782.

Wang, X., Wei, X., & Dai, H(2019). Estimation of state of health of lithium-ion batteries based on charge transfer resistance considering different temperature and state of charge. *Journal of Energy Storage*, *21*,618–631.

Wang, Z., Li, Q., Qin, S., Liu, D., Zhang, P., Hegh, D., Zhang, J., Naebe, M., Lei, W., & Razal, J. M (2021) . Pore-assisted lithium deposition in hierarchically porous and hollow carbon textile for highly stable lithium anode. *Journal of Power Sources,* 489, 229-464.

Wang, Z., Wang, H., Ji, S., Wang, H., Brett, D. J. L., & Wang, R (2020). Design and synthesis of tremella-like Ni–Co–S flakes on co-coated cotton textile as high-performance electrode for flexible supercapacitor. *Journal of Alloys and Compounds,* 814.

Universiti Malaya

Wang, Z.; Zhu, M.; Pei, Z.; Xue, Q.; Li, H.; Huang, Y.; Zhi, C (2020). Polymers for supercapacitors: Boosting the development of the flexible and wearable energy storage. *Mater. Sci. Eng. R Rep*. 139*,* 100520.

Ward, M. A., & Georgiou, T. K. (2011). Thermoresponsive polymers for biomedical applications. *Polymers,* 3(3), 1215–1242.

Weiner , M. L. . K. (2019). *Excipient Toxicity And Safety.* CRC Press. https://www.routledge.com/Excipient-Toxicity-and-Safety/Weiner-Kotkoskie/p/book/9780367399313.

Wichterle, O., & Lím, D. (1960). Hydrophilic Gels for Biological Use. *Nature,* 185(4706), 117–118.

William WRJ and Norman BB (2004). Fibrous assemblies: modeling/computer simulation of compressional behaviour. *Int J Cloth Sci Tech*; 16: 108-118.

Wu, D. Y., & Shao, J. J. (2021). Graphene-based flexible all-solid-state supercapacitors. *Materials Chemistry Frontiers*, 5(2), 557–583.

Wu, T., Wen, Z., Sun, C., Wu, X., Zhang, S., & Yang, J (2018). Disordered carbon tubes based on cotton cloth for modulating interface impedance in β″-Al_2O_3-based solid-state sodium metal batteries. *Journal of Materials Chemistry A,* 6(26), 12623–12629.

Wu, X., Sun, H., Qin, Z., Che, P., Yi, X., Yu, Q., Zhang, H., Sun, X., Yao, F., & Li, J. (2020). *International Journal of Biological Macromolecules*, *149*, 707–716.

X. Wang, Y. Yang, Q. Zhang, X. Yang and Z. Hu, J. Phys. Chem. C, 2018, 122, 6526–6538.

Xi, Y., Liu, Y., Qin, Z., Jin, S., Zhang, D., Zhang, R., & Jin, M (2018). *Ultralong cycling stability of cotton fabric/LiFePO4 composites as electrode materials for lithium-ion batteries.* Undefined, 737, 693–698.

Xiao, Q., Deng, C., Wang, Q., Zhang, Q., Yue, Y., & Ren, S (2019). In Situ Cross-Linked Gel Polymer Electrolyte Membranes with Excellent Thermal Stability for Lithium-Ion Batteries. *ACS Omega*,*4*(1), 95–103.

Xie, L., Sun, G., Xie, L., Su, F., Li, X., Liu, Z., Kong, Q., Lu, C., Li, K., & Chen, C. (2016). A high energy density asymmetric supercapacitor based on a CoNi-layered double hydroxide and activated carbon. *Carbon*, 100, 710.

Xiong, J., Pan, Q., Zheng, F., Xiong, X., Yang, C., Hu, D., & Huang, C (2018). N/S *Co-doped carbon derived from cotton as high performance anode materials for Lithium ion batteries.* Frontiers in Chemistry, 6 , 78.

Xiong, R., Tian, J., Mu, H., & Wang, C(2017). A systematic model-based degradation behavior recognition and health monitoring method for lithium-ion batteries. *Applied Energy*, 207,372–383.

Xu, B., Qi, S., Li, F., Peng, X., Cai, J., Liang, J., & Ma, J (2020). *Cotton-derived oxygen/sulfur co-doped hard carbon as advanced anode material for potassium-ion batteries.* Chinese Chemical Letters, 31(1),217–222.

Universiti Malaya

Xu, J., Dou, S., Cui, X., Liu, W., Zhang, Z., Deng, Y., Hu, W., & Chen, Y. (2021). Potassium-based electrochemical energy storage devices: Development status and future prospect. *Energy Storage Materials*, 34*,* 85–106.

Xu, J., Zhang, S.-K., Wei, Z.-N., Yan, W.-R., Wei, X.-J., & Huang, K.-J. (2021). Orientated VSe2 nanoparticles anchored on N-doped hollow carbon sphere for high-stable aqueous energy application. *J. Colloid Interface Sci*., 585, 12–19.

Xu, Y., Yuan, T., Zhao, Y., Yao, H., Yang, J., & Zheng, S. (2020). Constructing Multichannel Carbon Fibers as Freestanding Anodes for Potassium-Ion Battery with High Capacity and Long Cycle Life. *Advanced Materials Interfaces*, 7(3), 1901829.

Yang, C., Xiong, J., Ou, X., Wu, C. F., Xiong, X., Wang, J. H., Huang, K., & Liu, M (2018). A renewable natural cotton derived and nitrogen/sulfur co-doped carbon as a high-performance sodium ion battery anode. *Materials Today Energy*, 8,37–44.

Yang, W., Zhou, J., Wang, S., Zhang, W., Wang, Z., Lv, F., Wang, K., Sun, Q., & Guo, S. (2019). Freestanding film made by necklace-like N-doped hollow carbon with hierarchical pores for high-performance potassium-ion storage. *Energy & Environmental Science,* 12(5), 1605–1612.

Yazdanshenas, M. E., & Shateri-Khalilabad, M. (2013). In situ synthesis of silver nanoparticles on alkali-treated cotton fabrics. *Journal of Industrial Textiles*, *42*(4), 459–474.

Yetisen, A. K., Qu, H., Manbachi, A., Butt, H., Dokmeci, M. R., Hinestroza, J. P., Skorobogatiy, M., Khademhosseini, A., & Yun, S. H. (2016). Nanotechnology in Textiles. *ACS Nano,* 10(3), 3042–3068.

Yin, B.-S.; Zhang, S.-W.; Ke, K.; Wang, Z.-B (2019). Advanced deformable all-in-one hydrogel supercapacitor based on conducting polymer: Toward integrated mechanical and capacitive performance. *J. Alloys Compd.* 2019, *805*, 1044–1051.

Yong, S., Hillier, N., & Beeby, S (2021). The influence of textile substrate on the performance of multilayer fabric supercapacitors. *Journal of Industrial Textiles*, *50*(9),1397–1408.

Yong, S., Owen, J. R., Tudor, M. J., & Beeby, S. P (2013). Fabric based supercapacitor. *Journal of Physics: Conference Series,* 476(1), 012114.

You, Y., Qu, K., Shi, C., Sun, Z., Huang, Z., Li, J., Dong, M., & Guo, Z. (2020). Binder-free CuS/ZnS/sodium alginate/rGO nanocomposite hydrogel electrodes for enhanced performance supercapacitors. *International Journal of Biological Macromolecules*, *162*, 310–319.

Yun, Y. J., Ah, C. S., Hong, W. G., Kim, H. J., Shin, J. H., & Jun, Y. (2017). Highly conductive and environmentally stable gold/graphene yarns for flexible and wearable electronics. *Nanoscale,* 9(32), 11439–11445.

Zang, L.; Liu, Q.; Qiu, J.; Yang, C.; Wei, C.; Liu, C.; Lao, L (2017). Design and Fabrication of an All-Solid-State Polymer Supercapacitor with Highly

Universiti Malaya

Mechanical Flexibility Based on Polypyrrole Hydrogel. *ACS Appl. Mater. Interfaces ,* 9, 33941–33947.

Zeng, C., Xie, F., Yang, X., Jaroniec, M., Zhang, L., & Qiao, S.-Z. (2018). Ultrathin Titanate Nanosheets/Graphene Films Derived from Confined Transformation for Excellent Na/K Ion Storage. *Angewandte Chemie,* 130(28), 8676–8680.

Zhang h., ,Alamer A., F. A .,H, F (2018). Structural and electrical properties of conductive cotton fabrics coated with the composite polyaniline/carbon black. *Cellulose* 25(3), 2075–2082.

Zhang, L., Xia, J., Zhao, Q., Liu, L., & Zhang, Z. (2010). Functional Graphene Oxide as a Nanocarrier for Controlled Loading and Targeted Delivery of Mixed Anticancer Drugs. *Small*, 6(4), 537–544.

Zhang, Q., Huang, C. G., Li, H., Feng, G., & Peng, W. (2022). Electrochemical Impedance Spectroscopy Based State-of-Health Estimation for Lithium-Ion Battery Considering Temperature and State-of-Charge Effect. *IEEE Transactions on Transportation Electrification,* 8(4), 4633–4645.

Zhang, X., Ding, W., Zhao, N., Chen, J., & Park, C. B(2018). Effects of Compressed CO_2 and Cotton Fibers on the Crystallization and Foaming Behaviors of Polylactide. *Industrial and Engineering Chemistry Research,* 57(6), 2094–2104.

Zhang, X., Li, J., Liu, D., Liu, M., Zhou, T., Qi, K., Qian, Y (2021). Ultra-long-life and highly reversible Zn metal anodes enabled by a desolvation and deanionization interface layer. *Energy & Environmental Science,* 14(5), 3120–3129.

Zhao, C., He, X., Sheng, N., & Zhu, C. (2023). Directional fiber framework wrapped by graphene flakes for supporting phase change material with fast thermal energy storage properties. *Journal of Energy Storage, 57, 106304.*

Zhao, C., Wang, C., Yue, Z., Shu, K., & Wallace, G. G. (2013). Intrinsically stretchable supercapacitors composed of polypyrrole electrodes and highly stretchable gel electrolytes. *ACS Applied Materials and Interfaces,* 5(18), 9008–9014.

Zhao, Y., Liu, B., Pan, L., & Yu, G. (2013). 3D nanostructured conductive polymer hydrogels for high-performance electrochemical devices. *Energy and Environmental Science,* 6(10), 2856–2870.

Zhao, Z., Huang, Y., Ren, W., Zhao, L., Li, X., Wang, M., & Lin, Y. (2021). Natural Biomass Hydrogel Based on Cotton Fibers/PVA for Acid Supercapacitors. *ACS Applied Energy Materials,* 4(9), 9144–9153.

Zheng, C., Yuan, A., Wang, H., & Sun, J(2012). Dyeing properties of novel electrolyte-free reactive dyes on cotton fibre. *Coloration Technology*, 128(3), 204–207.

Zhou, M., Zhang, H., Qiao, Y., Li, C. M., & Lu, Z. (2018). A flexible sandwich-structured supercapacitor with poly (vinyl alcohol)/H_3PO_4-soaked cotton fabric as solid electrolyte, separator and supporting layer. *Cellulose* 2018 25:6, 25(6)(2018) 3459–3469.

Universiti Malaya

Zhou, Q., Ye, X., Wan, Z., & Jia, C. (2015). A three-dimensional flexible supercapacitor with enhanced performance based on lightweight, conductive graphene-cotton fabric electrode. *Journal of Power Sources*, 296, 186–196.

Zhou, W., Chen, M., Tian, Q., Chen, J., Xu, X., & Wong, C. P (2022). Cotton-derived cellulose film as a dendrite-inhibiting separator to stabilize the zinc metal anode of aqueous zinc ion batteries. *Energy Storage Materials*, 44, 57–65.

Zhou, W., Zhou, K., Liu, X., Hu, R., Liu, H., & Chen, S (2014). Flexible wire-like all-carbon supercapacitors based on porous core–shell carbon fibers. *Journal of Materials Chemistry A*, *2*(20),7250–7255.

Zhu, R., Zhu, C., Sheng, N., Rao, Z., Aoki, Y., & Habazaki, H (2020). A widely applicable strategy to convert fabrics into lithiophilic textile current collector for dendrite-free and high-rate capable lithium metal anode. *Chemical Engineering Journal,* 388, 124-256.

Zhu, Y., Cai, W., Piner, R. D., Velamakanni, A., & Ruoff, R. S. (2009). Transparent self-assembled films of reduced graphene oxide platelets. *Applied Physics Letters,* 95(10), 103104.

Zhu, Y., Murali, S., Cai, W., Li, X., Suk, J. W., Potts, J. R., & Ruoff, R. S. (2010). Graphene and graphene oxide: Synthesis, properties, and applications. *Advanced Materials,* 22(35), 3906–3924.

Zhu, Y., Yang, M., Huang, Q., Wang, D., Yu, R., Wang, J., Zheng, Z., & Wang, D (2020). V_2O_5 Textile Cathodes with High Capacity and Stability for Flexible Lithium-Ion Batteries. *Advanced Materials,* 32(7) 190-6205.

Zou, Y.; Chen, C.; Sun, Y.; Gan, S.; Dong, L.; Zhao, J.; Rong, J (2021*).* Flexible, all-hydrogel supercapacitor with self-healing ability. *Chem. Eng. J.* 418, 128616.

Universiti Malaya